

DEVELOPMENT AND TEST OF MODERN CONTROL TECHNIQUES APPLIED TO SOLAR BUILDINGS

Dr. D. Christoffers, U. Thron

**Institut für Solarenergieforschung GmbH Hameln/Emmerthal
Am Ohrberg 1, D-31860 Emmerthal, Germany**

Contract JOE3-CT97-0076

FINAL REPORT – Draft

01.01.1998 to 31.12.1999

Research funded in part by
THE EUROPEAN COMMISSION
in the framework of the
Non Nuclear Energy Programme
JOULE III

Contents

1	Executive summary	7
2	Objectives of the project	8
3	Introduction and control concept	11
4	Work performed by ISFH	13
4.1	The ISFH control algorithm	13
4.1.1	The control and measurement concept	13
4.1.2	The controlled system	14
4.1.3	The concept of predictive control	15
4.1.4	Model identification	19
4.1.5	Prediction of the indoor temperature	21
4.1.6	The weather forecast	21
4.1.7	The structure of the algorithm	22
4.2	Simulation tests of the ISFH-algorithm	25
4.2.1	The simulation environment used by ISFH	25
4.2.1.1	Simulation of the reference control	26
4.2.2	Results of the simulation tests	27
4.2.2.1	Control behaviour without influence of disturbances	27
4.2.3	Control behaviour with influence of disturbances	29
4.2.3.1	Control behaviour with influence of unmeasured disturbances	36
4.3	Experimental investigations at ISFH	40
4.3.1	Description of the test facility	40
4.3.1.1	Sensors and data acquisition	41
4.3.2	Results of the experimental investigations	43
4.3.2.1	The control behaviour of the PC control	43
4.3.2.2	The behaviour of the microcontroller	50

5 Work performed by FUL	55
5.1 Specifications (Task 1)	55
5.2 Development of algorithms by FUL (Task 2)	57
5.2.1 Predictive control	57
5.2.1.1 Development of an adequate mathematical model of the system to be controlled	58
5.2.1.2 Development of a predictive/optimal controller	59
5.2.1.3 Implementation in a simulation environment	62
5.2.2 Expert controller	63
5.3 First testing phase of the different controllers at FUL (Task 3)	64
5.3.1 Predictive control (passive solar building)	64
5.3.1.1 Simulation tests	64
5.3.1.2 In-situ testing	72
5.3.2 Expert control (active solar building)	73
5.4 Second testing of the control programs at FUL (fall'99), Task 5	73
5.4.1 FUL's predictive controller	73
5.4.2 Changes operated to the experimental site	73
5.4.2.1 Improvement of the controller	75
5.4.2.2 Experimental results	75
5.4.3 FUL's expert controller	75
5.5 Experimental results and conclusions of FUL (tasks 3 and 5)	75
5.5.1 Tests on FUL building	75
5.5.1.1 Data sets description	75
5.5.1.2 Controllers description	76
5.5.1.3 Controllers global performance	78
5.5.1.4 Typical daily profiles	80
5.5.1.5 Comparison on shorter periods	84
5.5.1.6 Comparison using simulation	86
5.5.1.7 The user's point of view	87
5.5.1.8 Some lessons from experimental testing	87
5.5.2 Experiments on Passys testcell	88
5.5.2.1 Data sets description	88
5.5.2.2 Measured controller performance	88
5.5.2.3 Comparison using simulation	91
5.5.3 Conclusions of experimental tests on Passys testcell and FUL building . . .	95

6 Work performed by NOA	96
6.1 Introduction to NOA work	96
6.2 NOA ANN-Controller - initial phase and E_{AVE} demand predicting	96
6.2.1 ANN-Controller initial setup	97
6.2.2 ANN-controller development	98
6.3 NOA ANN-Controller - first controller for $E_{ON/OFF}$	101
6.3.1 Weather forecasting ANN-modules	102
6.3.2 Heating energy switch predicting ANN-module (inverse model)	103
6.3.3 Indoor temperature defining ANN-module (internal model)	104
6.3.4 ANN-controller for online and simulation tests - <i>nnpred</i>	106
6.3.5 ANN-modules development with MATLAB	106
6.3.6 ANN-modules development with own C-program <i>ann-learn</i>	108
6.4 NOA ANN-Controller - final controller for T_{SUP}	109
6.4.1 ANN-modules development with SNNS	109
6.4.2 ANN-controllers for FUL and for ISFH buildings	113
6.5 Experimental facility – PASSYS test cell of NOA	114
6.6 Controller implementation in PASSYS test cell of NOA	115
6.7 NOA Online testing results - ANN-Controller for $E_{ON/OFF}$	117
6.8 Off-line performances assessment – ANN-Controller for $E_{ON/OFF}$	117
6.9 Tests of the FUL partner $E_{ON/OFF}$ controller by NOA	119
6.10 Tests of the NOA ANN-Controller for T_{SUP} at FUL	120
6.11 Conclusion	122
7 Work performed by INSA	123
7.1 Introduction to INSA work	123
7.2 INSA controller	123
7.2.1 General constraints	123
7.2.2 Global architecture of INSA controller	124
7.2.3 INSA Model of the building	125
7.2.4 Meteorological forecasts	128
7.2.4.1 Temperature forecasts	128
7.2.4.2 Solar gains forecasts	128
7.3 Optimization module	130
7.3.1 Idle mode	130
7.3.2 Research for starting-up hour	130
7.3.3 Pre-heating period	131
7.3.4 Regulation mode	131
7.4 Comfort level	132

7.5	Tests performed by INSA	133
7.5.1	Tests in simulation with FUL data	133
7.5.1.1	Model of FUL building	133
7.5.1.2	Control of FUL building	133
7.5.2	INSA tests in simulation with ISFH data	135
7.5.2.1	Model of ISFH building	135
7.5.2.2	Control of ISFH building	137
7.5.3	Experiments in Rennes	138
7.5.3.1	Model of Rennes building	138
7.5.3.2	Control of Rennes building	139
7.5.3.3	Evaluation of energy saving	139
7.6	Experimental hardware	141
7.7	Limits of the INSA approach	143
7.7.1	Meteorological forecasts	143
7.7.2	Training data	144
7.8	Simula: a thermal simulation tool	144
7.9	Available softwares from INSA	146
7.9.1	Design of the model	146
7.9.2	The model	146
7.9.3	The controller	146
7.10	Conclusion	147
7.10.1	What is new ?	147
7.10.2	Future work	147
8	Work performed by UNN	148
8.1	Introduction	148
8.2	Simulation environment	148
8.3	Performance assessment	150
8.4	Controllers parameters	150
8.5	Schedules	150
8.5.1	Occupancy schedule	150
8.5.2	Heating fixed schedule	151
8.6	Compared controllers	151
8.6.1	Conventional controller	151
8.6.2	Ideal thermostatic controller	152
8.6.3	Optimal controller	153
8.6.4	ANN controller	153
8.6.5	Predictive controller	153

8.7	Tested cases	153
8.8	Results	154
8.8.1	Global performance	154
8.8.2	Parameters influence	156
8.8.3	Typical profiles	159
8.8.3.1	Cold period	159
8.8.3.2	Sunny mid-season period	163
8.9	Conclusions	167
8.9.1	Energy - comfort performance	167
8.9.2	Implementation aspects	167
8.9.3	Summary of controllers characteristics	168
9	Work performed by INGA	170
9.1	General specifications	170
9.2	Hardware and software development by INGA	170
9.3	Market analysis performed by INGA	174
9.4	Other activities of INGA	175
10	Comparison of initially planned objectives and work actually accomplished	181
11	Conclusions	183
A	List of outcomes of the project	185
A.1	Publications and conference presentations	185
A.2	Internal Working Documents	186
A.3	Doctoral thesis	186
A.4	Prototypes	186

Participants

The contractors of the project are

- Institut für Solarenergieforschung GmbH Hameln/Emmerthal,
Am Ohrberg 1, D-31860 Emmerthal, Deutschland (ISFH), (Coordinator)
- Fondation Universitaire Luxembourgeoise,
185, Avenue de Longwy, B-6700 Arlon, Belgium (FUL)
- Institut National des Sciences Appliquées, Département d’Informatique,
20, Avenue des Buttes de Coësmes, F-35043 Rennes CEDEX (INSA)
- University of Northumbria at Newcastle, School of Engineering,
Ellison Place, Newcastle upon Tyne NE18ST, Great Britain, (UNN)
- Institut of Meteorology and Physics of the Atmospheric Environment,
National Observatory of Athens,
Lofos Nymfon- Thission, P.O. 20048, GR-11810 Athens (NOA)

and the "Ingenieurgesellschaft für Gebäudeautomation mbH, Wehler Weg 14, D-31785 Hameln, Deutschland, (INGA)" as associated contractor of the ISFH.

Chapter 1

Executive summary

Buildings with a high insulation standard show an increased fraction of solar and internal gains influencing the building energy balance. The reaction of conventional heating controls is often not satisfying especially for buildings with a high thermal mass. An intelligent heating control with a knowledge about additional gains and the buildings reaction on it is able to anticipate these gains leading to both a reduced energy consumption and a comfort improvement.

The "Development and Test of Modern Control Techniques Applied to Solar Buildings" with the mentioned properties was the objective of the project which is described in this report. Four algorithms using different mathematical approaches were developed by the partners FUL, INSA, NOA and ISFH. They have in common the use of the climatic conditions not only at present but with a short time prediction for the control.

The developed algorithms were investigated in simulation environments and test buildings. Partner UNN was responsible for the comparative evaluation of the algorithms with the help of simulation tests. A special simulation environment was developed by partner FUL and UNN in the frame of this project. Experimental tests have been carried out by the developing institutes each of them providing a test building. The buildings differ with regard to their use, climatic conditions and thermal properties.

The tests showed that all approaches are suitable in principle for an intelligent heating control leading to energy savings of up to 15% during the in-between season and comfort improvements compared to conventional controls. The investigations showed further, that an evaluation only on the basis of energy consumption and a comfort indicator is not sufficient to reflect the different properties necessary also for practical application. The computational load, the possibility to adapt to different buildings and changes of the building behaviour and the suitability for an implementation into a standalone microcontroller have been regarded as well.

One algorithm has been chosen to be implemented into the final hardware which was provided by the industrial partner INGA. It is a microcontroller which works as stand-alone device. Experimental tests on a real building showed that the microcontroller is able to control the heating with almost the same quality as a PC with the implemented software. The hardware is now available for demonstration objects.

Chapter 2

Objectives of the project

The objective of this project was to develop, test and compare modern innovative control techniques for energy (HVAC) systems applied to buildings presenting a relatively high solar fraction. This means not only the so called "Solar Buildings" but every building with reduced transmission and ventilation losses, such as newly built low energy buildings as well as old refurbished buildings. Since the trend goes to these types of buildings, an adapted control of the energy system becomes an important factor for a further reduction of the fossil energy consumption.

The efficiency of energy systems for such buildings is indeed heavily relying on the operation of an adequate control system, taking into account the characteristics of the building, the external climate and the internal loads not only in the present state but with a short time prediction. This may lead to considerable energy savings while preventing the overheating risk.

Within this project, new control paradigms have been investigated:

- Predictive and adaptive control,
- Expert systems,
- Fuzzy logic,
- Neural networks.

The scientific institutes ISFH, FUL, INSA and NOA each had to develop control algorithms based on one of the named methods.

Expected scientific and technical achievements of the project were:

- Development of 4 algorithms using the mentioned approaches for the heating control of solar buildings,
- test of the algorithms in simulation and experiment
- comparative evaluation of the 4 different modern control strategies,
- implementation of a selected algorithm into a standalone hardware,
- test and optimization of the hardware in experiment.

The algorithms should have the following properties:

1. consideration of solar radiation in the control strategy,

2. selfadaptation of the controller to building and climatic parameters or an user-friendly possibility for their input making the control system transparent to the user,
3. prediction of the climatic conditions for at least 24 hours,
4. wide applicability of the controller to the building type and the climate.

These properties should lead to a saving of fossil fuel energy while improving the thermal comfort. The development should be carried out from the beginning with respect to the required properties of the hardware:

1. cheap computing unit and sensors usable
2. easy installation and configuration by an expert
3. easy operation also by a layperson
4. applicable to the most common heating systems and buildings without remarkable structural changes

To ensure, that the algorithms are developed according to the requirements, specifications had to be made in the beginning of the project. During the project the specification had to be checked and corrected if necessary. The industrial partner (INGA) had to accompany the development continuously and give advice if necessary.

The algorithms should be tested in a simulation environment to be developed in the framework of the project. After the optimization with the help of simulation the algorithms should be tested in the experimental environments of the partners. Each of the developing institutes (ISFH, FUL, INSA,NOA) has a test building available which should be used to validate the functionality of the algorithms also in practice.

The comparative evaluation of the 4 different modern control strategies should show advantages and disadvantages, optima and limits of application for the most common building types and typical climates in Europe. It should be carried out in simulation by UNN.

According to the test results an algorithm should be selected to be implemented in a standalone controller hardware to be provided by the industrial partner. The test was to be carried out in an experimental environment. Results of the test should be communicated to the industrial partner to be implemented in an optimized controller prototype.

The project was divided into the following tasks (see table 2.1)

Table 2.1. Tasks planned in the project

Task	Activity
1	Specifications
2	Developement and implementation of control algorithms
3	First testing phase
4	Realization of first stand-alone prototype
5	Second testing phase
6	Realization of the final version of the prototype

Fig. 2.1 shows the interdependance between the different tasks and the project partners.

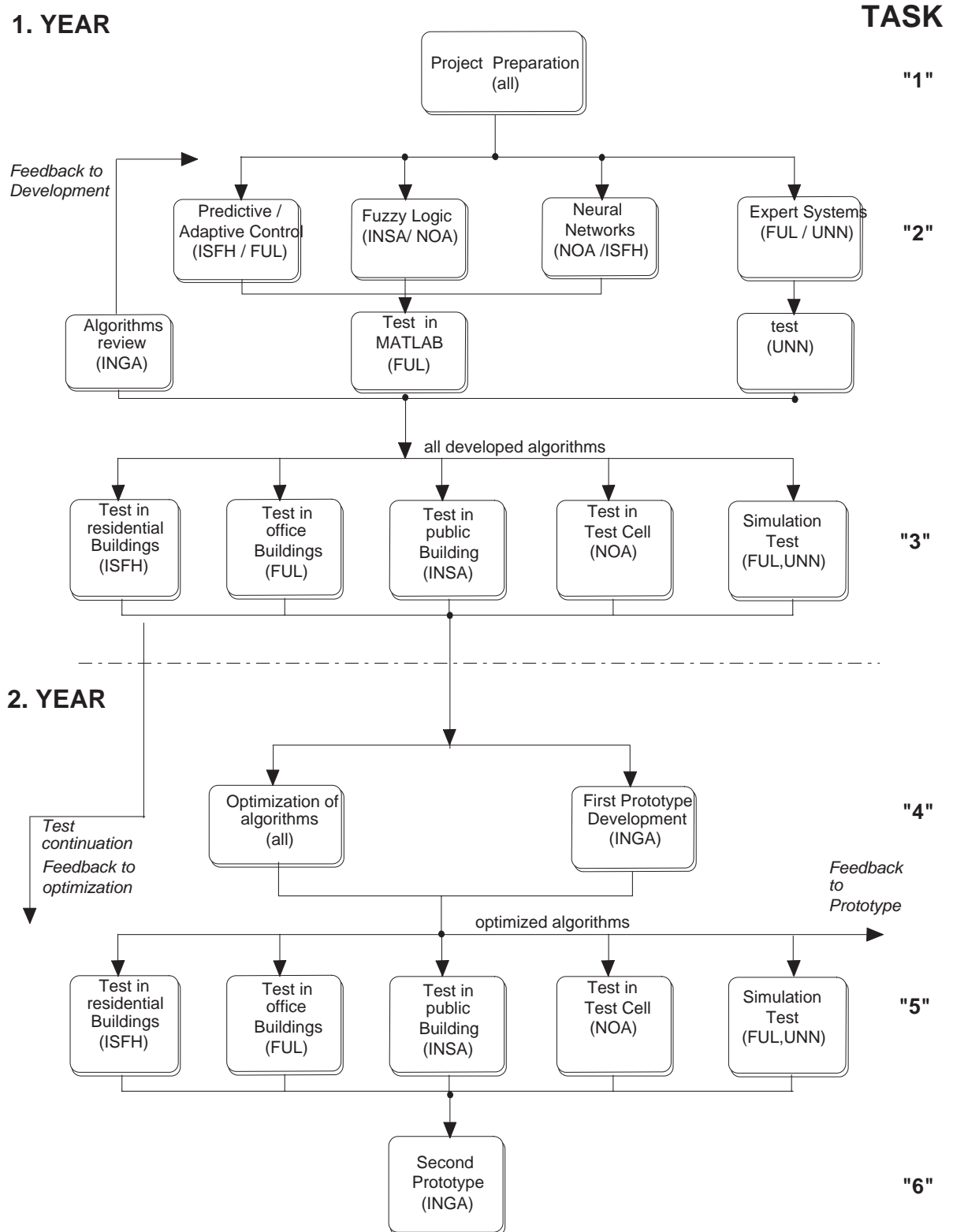


Figure 2.1. Interdependance between the tasks and the project partners

Chapter 3

Introduction and control concept

In this part of the report, firstly the problem and the concept for its solution is described. After that the contributions of the partners to the project and their results are presented. Four different algorithms have been developed by each of the institutes ISFH, FUL, NOA, INSA. A comparative evaluation by simulation have been carried out by partner UNN. The hardware for a standalone device was provided by the industrial partner INGA. The corresponding sections firstly describe the concept used by this partner to fulfill his part of work, followed by the results.

The indoor climat in buildings can be influenced by different technical building equipment. Heating-, ventilation and air-conditioning systems must hold temperature and indoor humidity on an acceptable level for the user. The control of the equipment is however difficult because of proportionally long dead times and time constants of the controlled system .

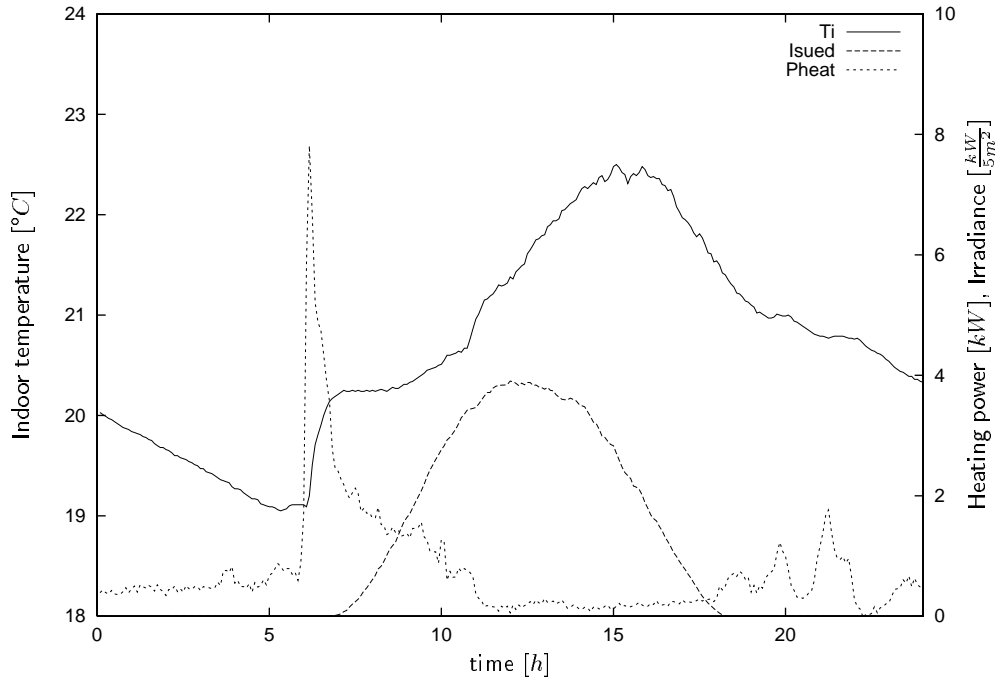


Figure 3.1. Measured course of indoor temperature (Ti), irradiance (Isued) and heating power (Pheat) on 5th March 1996 in the experimental house of ISFH

The control of the supply temperature of the heating system after the room temperature is for example rare in use at the hot-water central heating with radiators. Rather one tries to supply the radiator with a sufficient heating power. This power is then limited by an additional fast

controller in the room (e.g. radiator thermostatic valve). The necessary heating power is determined into dependence of the outside temperature and her provision made by a feedforward control. Advantages of this method are the comparatively fast reaction to heating demand or overheating appearances in the room. It is adverse that the supply temperature to be provided must lie in general over the actually necessary value to ensure the controlability and to satisfy different user demands. This can lead to unnecessary heat losses of the pipes. High temperatures further affect negatively the possibility of the imbedding of burning value boilers or thermal solar plants in the heating circuit.

Furthermore can be observed (Fig. 3.1) that conventional controls react unsatisfactorily to additional energy inputs by internal gains or solar irradiation, especially for buildings or heating systems with high time constants. The problem is due to the way of the control which takes only current measurands into account. A conventional control for example only then reacts to the solar irradiation, if it causes an overheating.

At this time a large part of the energy already is however in the building since the entries affect the indoor temperature time delayedly. Both the solar irradiation and internal gains can frequently be predicted. It seems reasonable therefore to take the predicted influences into account already in advance. A suitable approach consists in the use of the model based predictive control.

Target of the project, whose results are explained in the report on hand was the development of a predictive heating regulator which in addition self-adapts to the building and the heating system. The indoor temperature is regulated with help of the supply temperature of the heating system of the building. The controller acts on the supply temperature via the 3-way valve for the mixture of heating water of the return pipe and heating water of the heating device. The kind of heat supply is not part of the considerations. Condition for the control of the indoor temperature with the supply temperature is a nearly constant mass flow in the heating system.

The indoor temperature is measured in a reference room. Criteria for the choice of this room and considerations of the applicability of the concept are given in the report. The approach chosen allows furthermore the adaption of the control algorithm to other heating systems without problems (e.g. air heating systems, floor heating systems, heating systems with the heating power as manipulated variable).

The definition of the specifications in task 1 was mainly a collective work that took place during the kick-off meeting in Brussels and that was definitely concluded at the first co-ordination meeting in Hameln. A description of the results of this task can be found in chapter 5. The following chapters give reports of the work performed by each of the collaborating institutes.

Chapter 4

Work performed by ISFH

Authors: Ute Thron and Dr. Dirk Christoffers

4.1 The ISFH control algorithm

The ISFH control algorithm was developed in a first version in Task 2. A number of tests have been performed to check the behaviour of single parts of the algorithm, that led to a design used for the first tests. The results of the simulation and experimental tests performed in task 3 and 5 were used for a further optimisation. The problems that occurred at the implementation into the standalone hardware again required an optimisation of the algorithm especially concerning the memory and the calculation time, which influenced also the mathematical base that could be used. The concept of the algorithm presented in this section is the result of all optimizations within the project.

4.1.1 The control and measurement concept

In the control algorithm for predictive and adaptive heating control developed by partner ISFH, the indoor temperature is regulated by means of the supply temperature of the heating system. The developed algorithm calculates a set value of the supply temperature for the next time step (15 min). A fast PID conventional control algorithm regulates a 3 way valve to adjust the supply temperature according to this set value. It is assumed that the required heating power is provided by the heater. The kind of heat supply and its efficiency is not regarded here. The only requirement was, that the necessary maximum power is not higher than for a conventional control. With the used control concept, there is already an advantage compared to conventional control. The concept requires to provide the building only with no more heating power as necessary to reach the indoor set value. A conventional control with a heating curve always needs a surplus of heating power to be delivered to the building. The necessary power for a heating-up depends on the user-defined indoor temperature set points. A limitation of the heating power is possible by fixing the maximum allowable supply temperature step in the algorithm.

The indoor temperature is measured in a reference room. This room must meet the following requirements:

- it must be one of the main living rooms,
- the window direction must correspond to the main solar aperture of the building,
- disturbances, e.g. by high internal gains or frequent window or door openings, should be small

The two first conditions have to be fulfilled absolutely. The indoor temperature sensor must be attached radiation protected and distant from electrical equipments. The thermostatic valve is removed from the radiator in the reference room, since otherwise it changes the effect of the supply temperature on the indoor temperature in an undefined way. All other rooms keep their thermostatic valves. This variant presupposes that the estimated supply temperature provides all rooms with sufficient heating power. This can be guaranteed by adjusting the mass flow in the reference room radiator.

The solar irradiation is measured in the direction of the main receiving areas of the passiv solar components of the building.

For larger buildings with various orientations of the living rooms, or occasional shading of some rooms, it is useful to define several zones. The indoor temperatures of these zones are controlled separately, by corresponding algorithms. An extra mixing valve is then necessary for every zone. However, for larger buildings several circiuts are already available in most cases.

Seasonal dependences, such as a shading by neighbour buildings in winter time, can be learned by the parameter identification procedure, using the database from the last days, with the largest weighting on current mesurements. The outdoor temperature sensor must be fixed at the northern side of the building. A radiation protected place is absolutely necessary, since otherwise the outside temperature and irradiation, i.e. the input values for the model identification, would interfere.

4.1.2 The controlled system

Fig. 4.1 shows a general system with different inputs and one output. In our case the output, i.e. the indoor temperature, is the controlled variable.

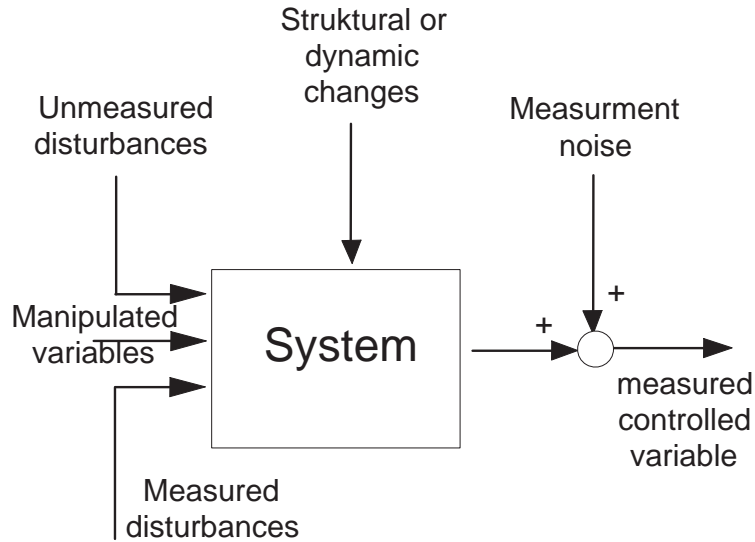


Figure 4.1. Influences on the controlled variable [MR95]: besides the manipulated variables, there act a number of disturbances, which are partly measurable. Furthermore, the dynamic behaviour of the system can change during the control process. Additionally, measurement noise interferes with the signal of the controlled variable.

The system inputs are often called driving forces. Inputs which can be changed are called manipulated variables, the others are disturbances. The disturbances can partly be measured. A model of the system describes the relation between the main driving forces (the manipulated variables and the most important disturbances) and the system output.

The system is the building with its structure and the heating system with pipes and radiators. The system output (controlled variable) is the indoor temperature. To be able to control the indoor temperature, it is necessary to know the system behaviour, i.e. the consequences of the different system inputs to the system output. The system behaviour is described with a model, which takes into account the most important influences. As measured driving forces for the indoor temperature are regarded:

- the supply temperature of the heating system (manipulated variable)
- the ambient temperature (measured disturbance)
- the irradiance (measured disturbance).

Actually, the temperature differences act as driving forces. The supply temperature or the outdoor temperature can change the indoor temperature only if they are not equal to it. Tests showed that the best control behaviour is achieved, when taking the differences to the mean value of the set indoor temperature, instead of the temperatures themselves.

All other influences (e.g. wind speed, air humidity, internal gains etc.) are regarded as unmeasured disturbances. The confinement to the main three driving forces is due to several reasons: every further input requires another sensor and increases the price of the device, furthermore it increases the number of model parameters to be identified, and therefore the model error and the calculation time are enlarged. The reaction of the control algorithm to unmeasured disturbances has been investigated in simulation tests, described in section 4.2.3.1.

According to the project goals, the controller to be developed, should be applicable to a large variety of buildings and heating systems. Therefore the creation and validation of a special model for every possible building is not practical. It is more promising to leave the model identification to the controller itself, after installation. Since the building behaviour may change with time, (e.g. due to seasonal depending wall humidity) the model estimation should be repeated from time to time. Before starting the process, the controller should only know a very general model structure that can cover the dynamic behaviour of many building types and heating systems. Both, physical or black box models are suitable. During the process the parameters of the model are identified.

In the application described here - the predictive adaptive heating control of a solar building- step response models are used to predict the system output. The step responses are calculated from a transfer function model (ARX), since the direct identification of the step response coefficients was too inaccurate. The parameters of the ARX-model are identified each time step. For the identification a recursive least squares method is used. The model and the identification is described in more detail in section 4.1.4.

4.1.3 The concept of predictive control

From a number of approaches which are covered by the name "predictive control" the Generalized predictive control (GPC) has been chosen [Cla94].

A conventional feedback control only takes into account the current measured value of the controlled variable and the current setpoint. On the other hand, GPC considers a discrete function $e(k+j|k)$ which is formed by the difference between the future set values $y_r(k+j|k)$ and the future controlled variable $\hat{y}(k+j|k)$ (see fig. 4.2).

$$e(k+j|k) = y_r(k+j|k) - \hat{y}(k+j|k) \quad . \quad (4.1)$$

That means that a prediction of the controlled variable (indoor temperature) is necessary. A model M with the parameter vector θ serves for the prediction of the future behaviour of the

system. The model must be estimated before the calculation of the manipulated variable is started. The prediction can be divided into 2 components, the free and the forced system response. The free system response $\hat{y}_o(k+j|k)$ is the expected behaviour of the controlled variable $\hat{y}(k+j)$ if no future control moves are applied. That means the free system response only results from past system inputs (manipulated variable and measured disturbance). The forced system response is the additional term due to a given sequence of future control moves. The predictions are made at time k for a prediction horizon $k+j = P$.

For linear systems the total prediction of the system output or controlled variable can be determined by superposition:

$$\hat{y}(k+j|k) = y_f(k+j|k) + y_o(k+j|k) \quad . \quad (4.2)$$

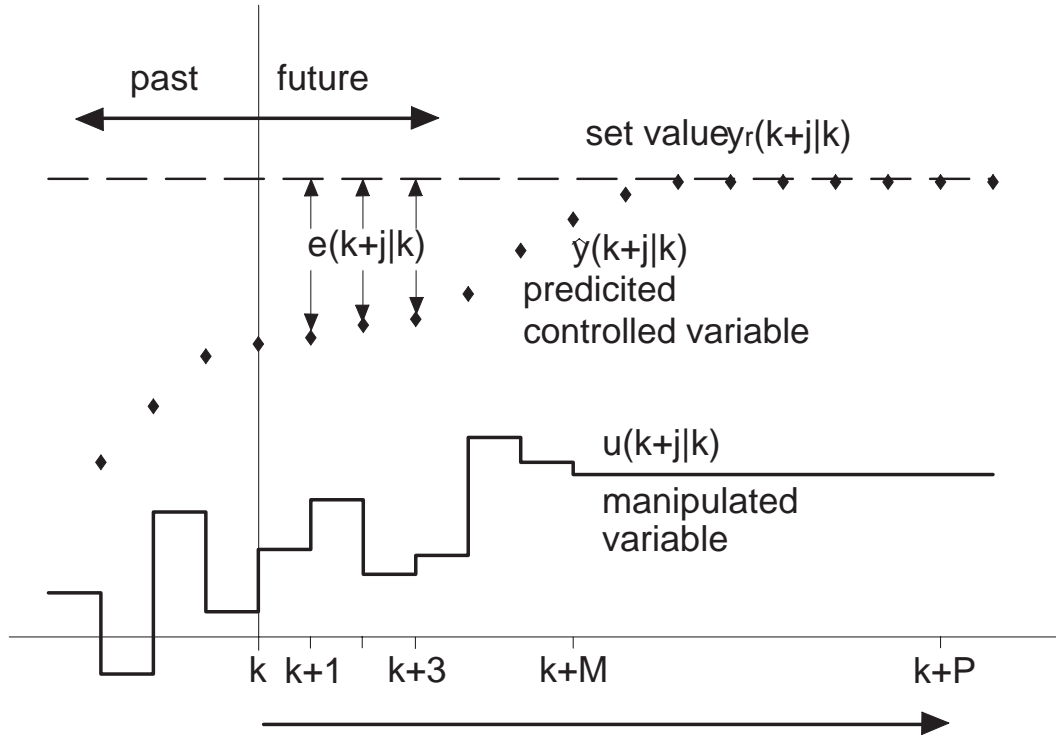


Figure 4.2. Example for the course of manipulated and controlled variable for predictive control [MR95]. At the current time k the difference between predicted controlled variable $\hat{y}(k+j|k)$ and future set value $y_r(k+j|k)$ is calculated up to the prediction horizon P . The future course of the manipulated variable $u(k+j|k)$ up to the control horizon M is calculated to achieve a good approximation of the set value

A schematic representation of the calculation procedure is shown by illustration 4.3 [Cla94].

The difference between set value and free system response is calculated using eq. 4.1. The forced system response should be an optimal future course of the manipulated variable which is calculated by the control algorithm. The future sequence of control moves should be chosen in a way that the set values are reached fast, but without too much control effort. This is achieved by the minimization of a cost function of the form:

$$J = \sum_{j=N1}^P Q_j (y_r(k+j) - \hat{y}(k+j|k))^2 + \sum_{j=1}^M R_j \Delta u(k+j-1)^2 \quad . \quad (4.3)$$

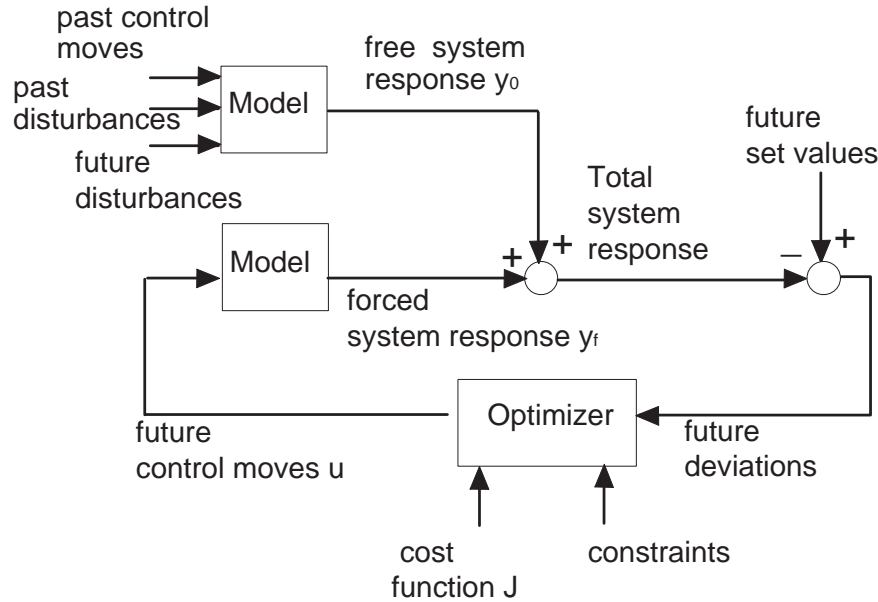


Figure 4.3. Calculation procedure for the manipulated variable. A model of the system serves for the prediction of the free system response (controlled variable). It is compared to the set value. The deviations are used in the optimizer to calculate the future sequence of the manipulated variable.

The first term of the cost function contains the future deviation from the set value, the second the future changes of the manipulated variable. The terms can be weighted by altering the parameters Q_j und R_j , which can be time dependent.

Cost functions, which take the actual height of the control variable into account, can be defined as well. This seems to be very interesting, especially with regard to the application presented here. The manipulated variable is the supply temperature or the heating power. The optimizer would weight between comfort and energy demand then.

An investigation with the simulation environment was carried out to check the applicability of both cost functions for the predictive heating control. It was an aim of the development introduced here, that the user votes whether he prefers more comfort or saving energy. Therefore a comfort parameter cl was introduced. By changing this parameter the user can adjust the weighting in the cost function:

$$R = \frac{9-cl}{\mu} \text{ und } Q = 1 = \text{const}$$

The user is allowed to change the comfort parameter cl in the limits 0...9 (9: maximum comfort, 0: maximum energy saving). For $cl = 9$ only the deviation of the indoor temperature from its set value plays a role in the cost function. Then the controller tries to reach the set value as fast as possible. The parameter μ determines the upper limit of R and is different for the two cost functions examined here. The choice of the upper limit R was derived from simulations of the test building. It was evaluated, what comfort losses can be expected from a user in the mode "maximum energy saving".

Figure 4.4 shows the behaviour of the control with a cost function, which weights between the deviation from set value (indoor temperature) and the manipulated variable (supply temperature) itself. A remaining deviation with increasing weighting of the manipulated variable can be clearly seen. On the other hand, a low weighting of the manipulated variable leads to oscillations of the heating power. For this reason the cost function weighting the control *increment* was used for the

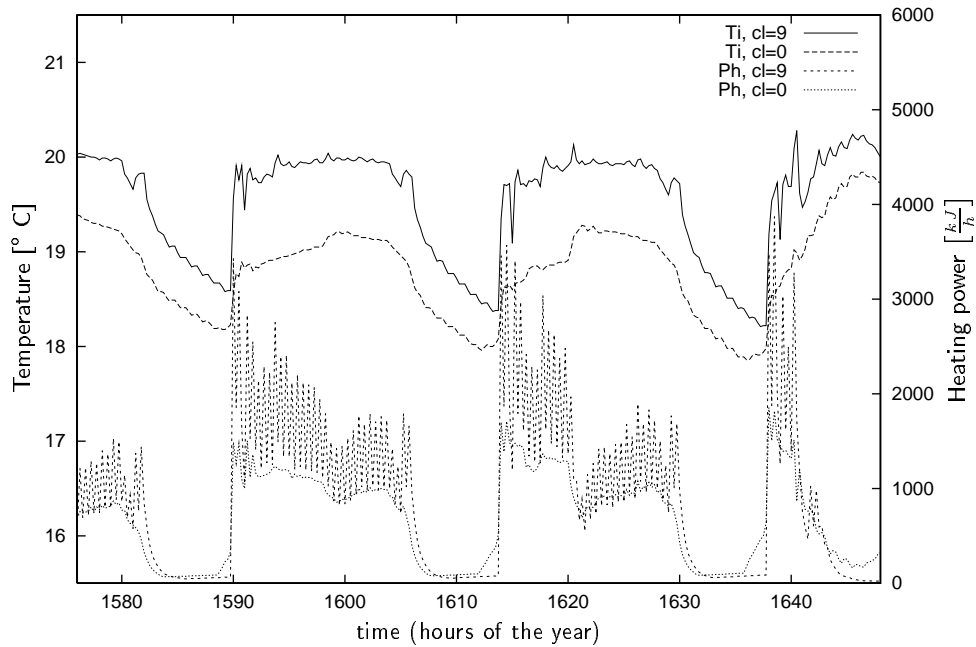


Figure 4.4. Simulated heating power and indoor temperature for different weights between the deviation of the indoor temperature from its set value and the *level* of the supply temperature. Using the comfort parameter $cl = 9$ ($R = 0$ and $Q = 1$) only the deviation from the set value of the indoor temperature is effective. For $cl = 0$ is $R = 0.05$ and $Q = 1$.

control algorithm.

Applied to the control of the indoor temperature via the supply temperature, this means that the parameter R reduces the control moves of the supply temperature rather than the supply temperature itself. This avoids temperature oscillations but no savings in heating energy are caused yet. Therefore the energy reduction mode was implemented into the control algorithm as follows: The user changes the parameter $cl = 0..9$ to choose a weighting between comfort and energy reduction mode. Then, R and Q are calculated, if the current measured indoor temperature is smaller than the set point. If the indoor temperature exceeds the set point, $R = 0$ and $Q = 1$ results, with the effect of reducing the supply temperature as fast as possible.

The simulated indoor temperature and the heating power are shown in figure 4.5, for the same period as in figure 4.4. Concerning the deviations from the set value and the stability of the heating power an improved behaviour can be stated here. Both the maximum values of the heating power and the consumed heating energy are reduced significantly at the mode "maximum energy saving", in contrast to the comfort mode. In the energy saving mode the set point of the indoor temperature is reached substantially slower. This also allows a contribution of the passiv solar gains to the room temperature rise with reduced overheating danger.

From the minimisation of the cost function, a calculation procedure of the so called controller gain is to be derived. Similar as in conventional control, the multiplication of the controller gain with the set point deviation of the controlled variable (the sequence of future values) gives the optimal sequence of the manipulated variable. Only the first value of the optimal sequence is applied and the calculation is repeated at the next time step.

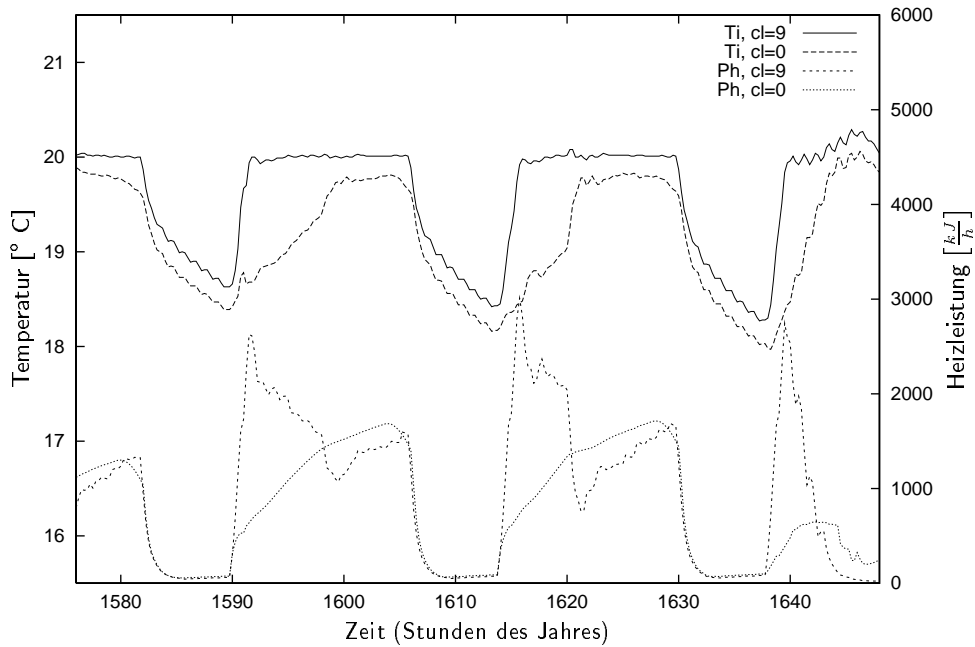


Figure 4.5. Simulated heating power and indoor temperature for different weights between the deviation of the indoor temperature from its set value and the *increment* of the supply temperature. $cl = 9 \Rightarrow R = 0, Q = 1$ and $cl = 0 \Rightarrow R = 1, Q = 1$

4.1.4 Model identification

Investigations on the model identification method showed that the direct determination of the impulse or step response coefficients from the measurements with the least squares method is not suitable. Because of the large number of the coefficients to be determined, large errors arise, which often cause uninterpretable step response coefficients. Therefore other models were examined with regard to their suitability to describe the dynamic system behaviour.

The model should contain as little information about the building as possible, so that the general validity and the transferability to other buildings is unrestricted. In addition, the number of the parameters to be identified should be minimized. Transfer function models fulfil both conditions, provided that they are not of too high order.

Suitable transfer function models are the ARX and the ARMAX model with the mentioned driving forces as inputs and the indoor temperature as output.

Since an instantaneous effect of the inputs on the output is physically not possible for a building, a model is chosen with a delay time step. Both ARX and ARMAX models of different order were identified using measurements from the test building. The tests showed, that an ARX model of 2nd order with one delay is excellent for the system description. Models of higher order do not lead to any noticeable improvement.

The used ARX model can be written as:

$$\begin{aligned}
 y(n) + a_1 y(n-1) + a_2 y(n-2) = & b_{11} u_1(n-1) + b_{12} u_1(n-2) + \\
 & + b_{21} u_2(n-1) + b_{22} u_2(n-2) + \\
 & + b_{31} u_3(n-1) + b_{32} u_3(n-2)
 \end{aligned} \tag{4.4}$$

where y is the indoor temperature, u_1 the difference between outdoor temperature and mean set

indoor temperature, u_2 the solar irradiance and u_3 the difference between supply temperature and mean set indoor temperature.

The identification of the model parameters is carried out with the help of the least squares method. Because of the considerably reduced memory need, a recursive identification method (RLS) was chosen. In case of the recursive model identification, the parameters of the previous time step and the actual input quantities are used to get a one step forecast of the system output. The forecast value is compared with the measured output value. If differences occur, the model parameters are corrected.

Only the parameter set of the preceded time step and the input quantities for the model of the last n time steps must be kept in memory (n order for the ARX model, here $n=2$). For this application with slowly varying parameters a RLS with exponential forgetting is suitable. With help of measurements of the experimental houses of the ISFH the behaviour of identified parameters and the calculated system output was examined in dependence of the chosen forgetting factor. In [Lju95] forgetting factors $\lambda = 0.95 \dots 0.995$ are recommended. Smaller factors indicate that old measurements get less weighted. Therefore the choice of the forgetting factor must depend on how fast the parameters of the system change.

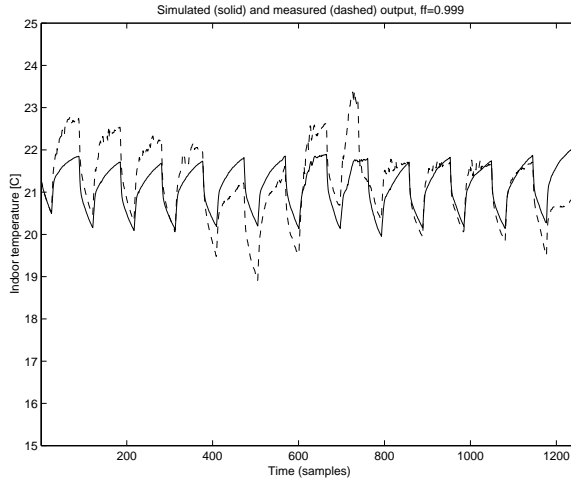


Figure 4.6. Measured and simulated indoor temperature for $\lambda = 0.999$

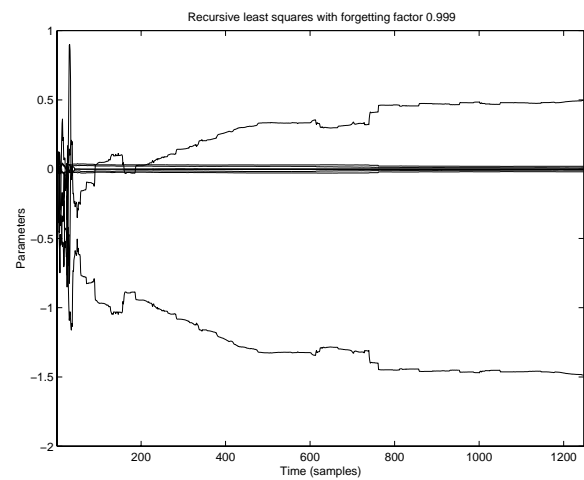


Figure 4.7. Parameters of the ARX-model for $\lambda = 0.999$

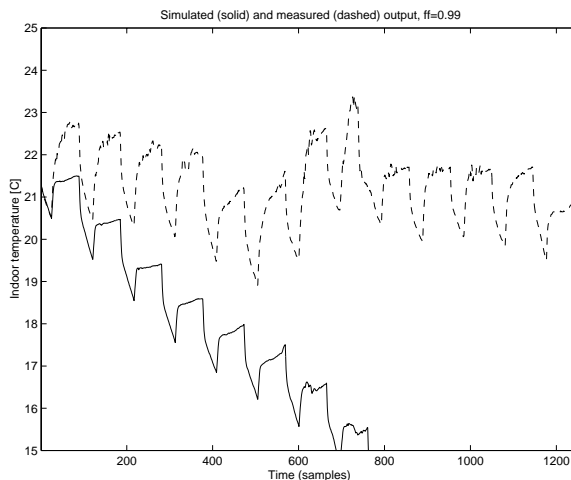


Figure 4.8. Measured and simulated indoor temperature for $\lambda = 0.99$

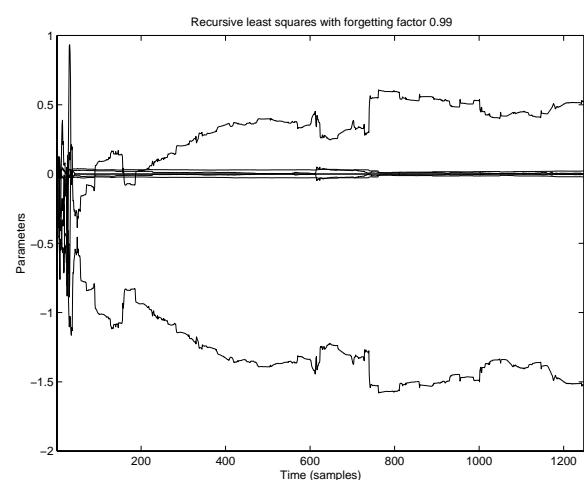


Figure 4.9. Parameters of the ARX-model for $\lambda = 0.99$

The figures 4.6 to 4.9 show that the choice of a high forgetting factor is suitable. Small forgetting factors lead to unstable model parameters, since the data base is small. The indoor temperature course correspondingly gets bad reconstructed. A forgetting factor $\lambda = 1$ weights all past measurements equally – this isn't desired either since certain seasonal fluctuations are expected. Because of the results shown here a forgetting factor of 0.999 was selected for the algorithm. Such factor weights e.g. the measurements of 9 days ago still with about 42% in the identification.

With the identified model parameters the step responses necessary for the indoor temperature prediction can be calculated by setting the respective input vector to the unity vector and the other inputs to zero.

4.1.5 Prediction of the indoor temperature

The prediction of the indoor temperature is calculated by a superposition of the convolution sums of the inputs with their step responses

$$\begin{aligned} \hat{T}_i(k+j|k) = & \sum_{i=1}^j \hat{s}_i \Delta \hat{u}(k+j-i|k) + \sum_{i=j+1}^{N-1} \hat{s}_i \Delta u(k+j-i) + \hat{s}_N u(k+j-N) + \\ & + \sum_{i=j+1}^{N-1} \hat{f}_{1i} \Delta d_1(k+j-i) + \hat{f}_{1N} d_1(k+j-N) + \\ & + \sum_{i=j+1}^{N-1} \hat{f}_{2i} \Delta d_2(k+j-i) + \hat{f}_{2N} d_2(k+j-N) \end{aligned} \quad (4.5)$$

f is the dynamic matrix of the step responses of the disturbances indicated by the first index. The disturbance variable changes are given with Δd . This is the standard approach at predictive control: the prediction takes past control variables and disturbance variables however only future control variables (still to be determined) into account.

In the development presented here this principle is extended, that also future predicted disturbance steps are included:

$$\begin{aligned} \hat{T}_i(k+j|k) = & \sum_{i=1}^j \hat{s}_i \Delta \hat{u}(k+j-i|k) + \sum_{i=1}^j \hat{f}_{1i} \Delta \bar{d}_1(k+j-i|k) + \sum_{i=1}^j \hat{f}_{2i} \Delta \bar{d}_2(k+j-i|k) + \\ & + \sum_{i=j+1}^{N-1} \hat{s}_i \Delta u(k+j-i) + \hat{s}_N u(k+j-N) + \\ & + \sum_{i=j+1}^{N-1} \hat{f}_{1i} \Delta d_1(k+j-i) + \hat{f}_{1N} d_1(k+j-N) + \\ & + \sum_{i=j+1}^{N-1} \hat{f}_{2i} \Delta d_2(k+j-i) + \hat{f}_{2N} d_2(k+j-N) \end{aligned} \quad (4.6)$$

The future disturbance steps are calculated from the predicted course of the outside temperature and the solar irradiation (see section 4.1.6).

4.1.6 The weather forecast

The weather forecast provides the future disturbance variable courses required in eq. 4.6. The courses of outside temperature and irradiation must be prognosticated depending on the choice of

the prediction horizon for different horizons. An external supply (e.g. over a meteorological service) or an internal forecast of data measured on base stood by the choice. At present an external forecast isn't available in a corresponding timing resolution for Germany yet. The German meteorological service (Deutscher Wetterdienst) offers 3 h interval forecasts only with a verbal description of the clouds degree which can be used to quantify the irradiance. The costs for the connection arising at present moreover are still relatively high in comparison with the savings to heating cost. Because of that for the development presented here an internal forecast was integrated in the algorithm. In the future probably however an external forecast in corresponding quality will be at the disposal. The modular structure of the algorithm then makes straightforwardly an exchange of the forecast routine possible. Therefore the effort for the development of the weather forecast was held smallly.

Practical conditions were the available measurements and the request for short computing time and low memory need. To keep the costs of the regulator little the necessary sensors equipment was reduced as much as possible, i.e. for the prediction of irradiance and outdoor temperature only the measurements of these values themselves were available.

For the calculation of the courses of the predicted outside temperature and irradiance an approach described in [Sta95] has been used and developed. The courses are approximated by cos-functions which are multiplied by the amplitude (the expected maximum irradiance of the day). The period of the function is adapted by a time function.

The time function for the irradiance is zero at 35 min before sunrise and 35 min after sunset and has its maximum at 12 h solar time. The expected maximum irradiance of the day is calculated by fitting previous measurements of the last 75 min with a decreasing weighting of older measurements. So irradiation fluctuations resulting from clouds are smoothed (these don't make themselves noticeable anyway because of the integrating system behave) and the prediction can follow weather trends. Before sunrise, the maximum irradiance of the past day is used.

The time function of the outdoor temperature has its minimum on sunrise and its maximum on 14:30 h solar time. The cos-function for the approximation is added to a constant value equal to the last measured minimum outdoor temperature. The difference between maximum and minimum used is the result of a weighted mean of the present and the past day.

Results of the forecast of the irradiance and outside temperature can be found in section 4.3.2.1. A program flowchart is enclosed in the appendix.

4.1.7 The structure of the algorithm

The illustration 4.10 shows the structure of the complete developed algorithm as well as his integration into hard and software.

The software can be subdivided into two levels which are called with various time step. The outer loop contains the measurement (i.e. recording of sensors, AD-conversion, data saving) as well as the control of the supply temperature with a PID algorithm. This loop is called every 10 s. The inner loop is called to every whole quarter of an hour. It contains the real predictive adaptive algorithm that calculates a set value supply temperature set value for the coming 15 min.

During every call of the inner loop at first the mean average values of the measurements of the former 15 min are calculated. They are saved to the later evaluation on the harddisk in the case of the PC control. Then the data are given to the data storage which keeps the 15-min mean average values of the respectively last 98 time steps. These are needed for the weather forecast. For the model identification only the current and the measurements of the past 2 time steps are necessary (see eq. 4.4).

To every whole quarter of an hour after start of the process a counting index n is increased by one. As soon as $n > 2$ is valid, the model identification is started since data are sufficiently available then.

A check of the quality of the determined model parameters is carried out within the subroutine of the model identification (**recident**). If the difference between the model output (indoor temperature) and the measured indoor temperature of the last 24 hours lies within predefined tolerances, the model can be used for the predictive algorithm. The currently predefined tolerance is 5 K per time step, i.e. 120 Kh for 96 time steps. The model check is executed for the first time after 24 hours after start of the controller. At sufficient model quality the predictive part of the algorithm is started. If the model check should turn out negative, then the classic supply temperature calculation with the heating curve is activated for the next 24 hours. This gives the algorithm time to learn the system behaviour with a larger database. After failing the model check three-times repeatedly (at the earliest after 72 hours) the parameter matrices are set to their starting values and the complete identification process is started of the front.

For the start of the predictive part of the algorithm three conditions must be fulfilled.

- the counting index n must be larger than 96, so that data are sufficiently available for the weather forecast
- the model quality must be sufficient
- the current measured indoor temperature may not lie below the set point any more than 4 K

The latter condition is primarily a protection against a malfunction of the algorithm of any manner, to prevent from a too strong undercooling of the building.

In the predictive algorithm at first the weather forecast procedure (**weatpred**) is called, which updates the the matrix of the predicted irradiation and outside temperature. The call of the procedure for the calculation of the controller gain (**cgain**) is then carried out. Weather forecast and controller gain are given to the procedure **predalg**. In this procedure, at first the indoor temperature forecast is updated on base of the new measurements and the predicted irradiation and outside temperature (measured disturbance variables). The multiplication of the difference between set point and predicted indoor temperature with the controller gain gives the sequence of the manipulated variable (set value of the supply temperature for the time intervall 15 min).

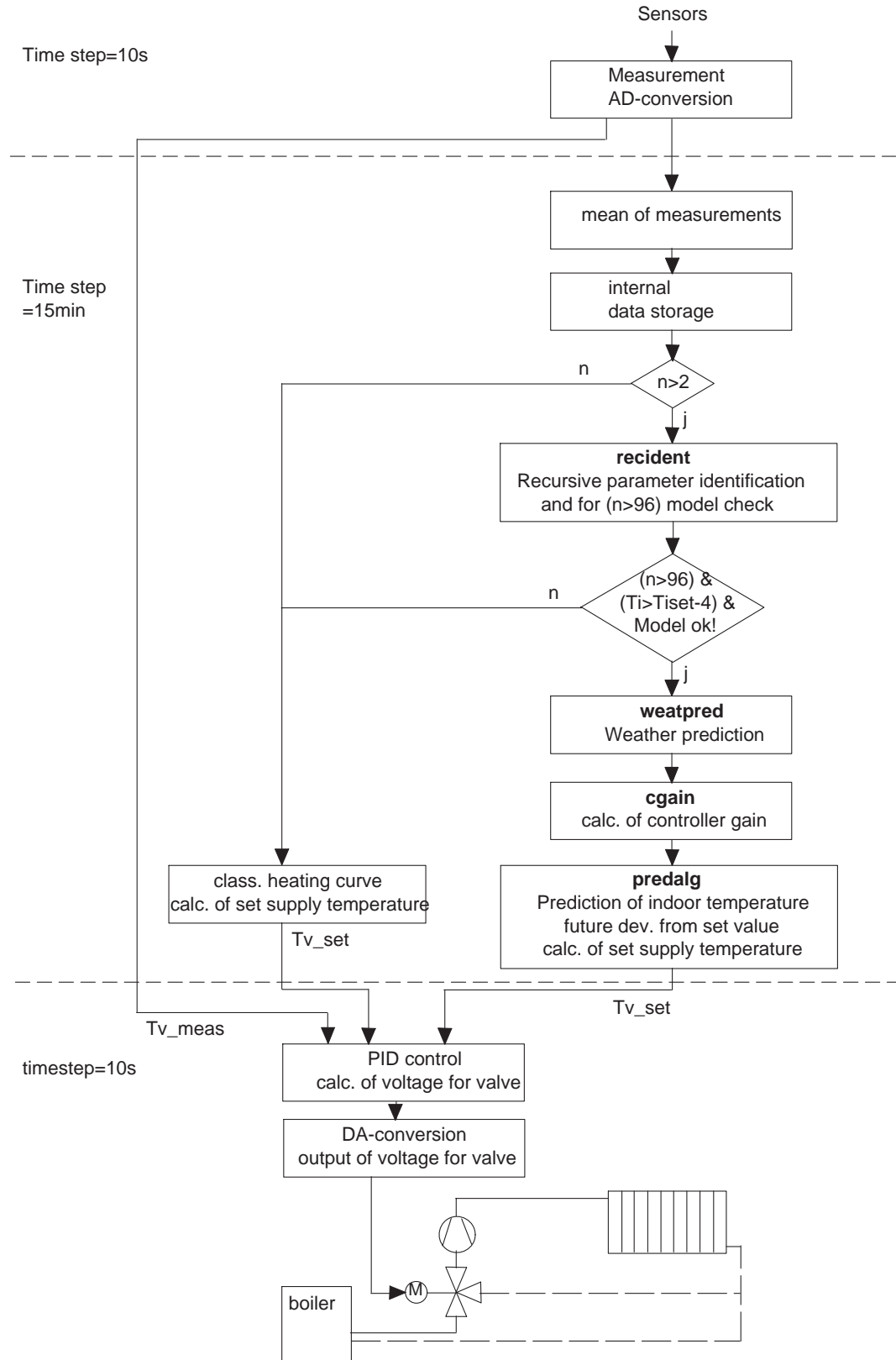


Figure 4.10. Program flowchart of the algorithm for predictive adaptive heating control developed by ISFH and his integration into hard and software. The time steps for the call of he program parts are given on the left hand side. The names of subroutines are bold.

4.2 Simulation tests of the ISFH-algorithm

First the developed algorithm was thoroughly examined with the help of simulations. The effects of different parameters on the control response could this way be tested and the results could be used for resettings in the experimental tests. On the other hand comparisons with a classic control strategy could be made under the same conditions. The additional unmeasured disturbances occurring in the practical operation were simulated in a sensitivity analysis and her effects on the control response were estimated.

In this chapter, at first the environment used for the simulations is explained. In the result part at first a parameter study is described where no disturbances act on the system. After this the control response was examined with measured and unmeasured disturbances.

4.2.1 The simulation environment used by ISFH

The simulations have been carried out with the program TRNSYS in combination with MATLAB. The simulation environment consists of 3 main parts:

1. a building description file,
2. a file for the description of the simulation components and their combinations,
3. the algorithm for the calculation of the supply temperature in MATLAB.

Two building models were used for the tests: The first is a model of a test room of the Bâtiment Académique of project partner Fondation Universitaire Luxembourgeoise (FUL) in Arlon/ Belgium. This model was provided by the project partner. This model only was used to check the operation of the control algorithm also in other buildings.

The second model which was created by ISFH was used for the parameter variations. This is a model of the experimental house of the ISFH. It consists of 11 thermal zones. The indoor temperature is controlled by the algorithm only in the reference room. All other rooms are controlled by the TRNSYS-internal perfect heating. A component to describe a radiator which was provided by partner FUL was used to calculate the heating power into the reference zone from the supply temperature given by the control algorithm. It was assumed, that the supply temperature is perfectly controlled by the valve and that no heat losses in pipes do occur.

The model quality was checked by a comparison for the ISFH building with measurements. The mean deviation of the simulated and measured heating energy during a heating period is 9.7%. While a very good agreement was found during the winter months, the differences are relatively high during the in-between season. Since the in principle dynamic behaviour of the building was well simulated however the model is suitable for the simulation tests.

Results of a comparison between different simulations are transferable to the real case. A direct comparison between and simulated building and control behaviour isn't however sensible because of the variety of not ascertainable influences in a real building.

A TRNSYS description file has been written to combine all components necessary for the simulation. Figure 4.11 shows a block diagram of the components (types) and its combination. As time step of the simulation 15 minutes was used since this corresponds to the time step for the call of the control algorithm.

The types 151 and 182 as well as the were provided by partner FUL. For the simulations measured weather data from the meteorological station of ISFH from the year 1995 have been used.

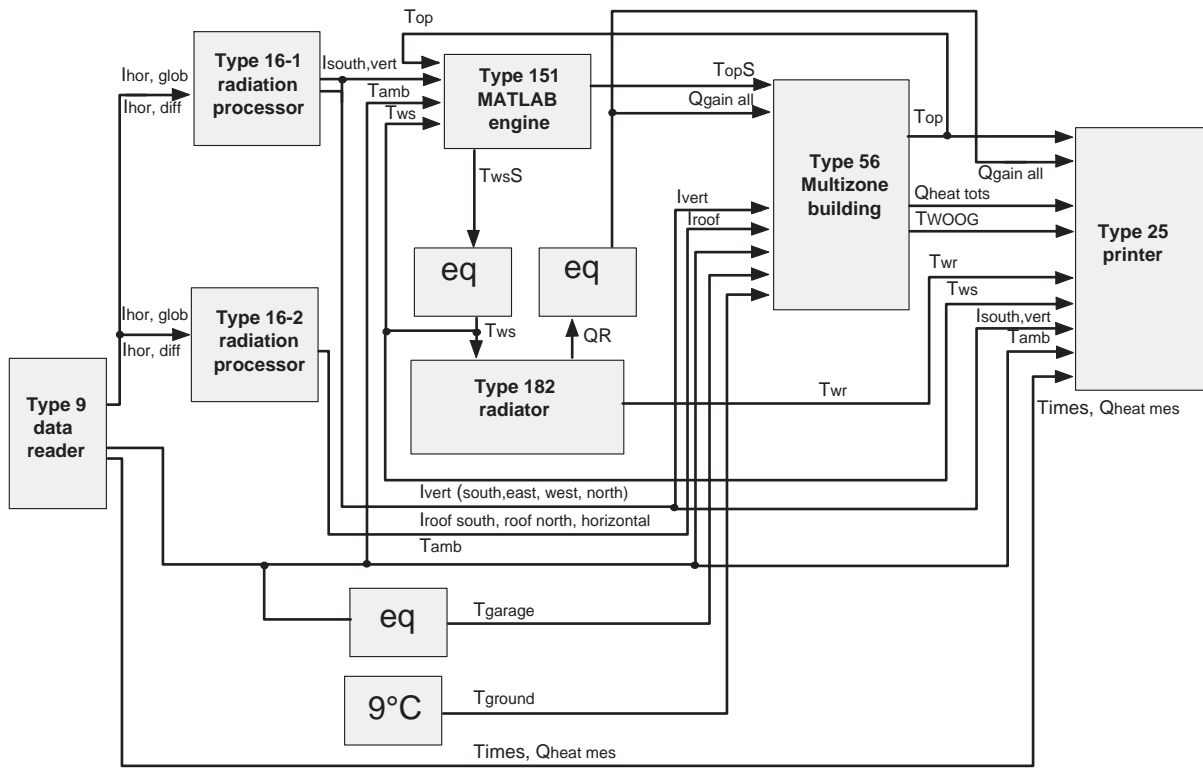


Figure 4.11. Block diagram of the TRNSYS definition file for the simulation of a building with different heating control strategies

4.2.1.1 Simulation of the reference control

The control which was installed in the experimental buildings before the installation of the new control was taken as a reference (conventional or classical control). It is the calculation of the supply temperature set point with a heating curve and a control of the room temperature with thermostatic valves on the radiators. For the classical heating control, the supply temperature is a linear function of the outdoor temperature, whose parameters are time-dependent. For the experimental houses, the following heating curve was in practical use:

$$T_{Vorlauf} = 20 + bw - T_a \quad (4.7)$$

where $bw = 35$ during day (6-22 h) and $bw = 15$ during night. The thermostatic valves were set by the user. It was assumed that the indoor temperature setpoint is at 20 °C during day and 18 °C during night. The mass flow was set constant, because the radiator type did not allow a mass flow variation. The function of the radiator thermostatic valve is therefore simulated by a variation of the supply temperature entering the radiator. It is assumed, that for a completely closed valve the supply temperature is equal to the indoor temperature and for a fully open valve the supply temperature remains unchanged. Between the closing and opening point, a linear course is assumed. The closing point is 1.5 K above the indoor temperature set point the opening point 0.5 K below. Furthermore a hysteresis of 1 K between opening and closing has been simulated.

Both mechanical and electronical thermostatic valves are on the market. Electronical valves offer

the possibility to define an indoor temperature set point for day and night. Then the indoor temperature is controlled also during night. A mechanical thermostatic valve, which is not manipulated by hand, opens during night completely. This leads to more heat transfer to the room. Between the different valves it was distinguished with the indoor temperature set value which was used to calculate the supply temperature entering the radiator.

4.2.2 Results of the simulation tests

In this section the results of the simulation experiments are presented. It was target of the examinations to test the consequence of different parameters in the algorithm and to determine the influence of single elements of the control on the overall result. The comparison with a simulated classical control serves to judge the qualities of the new control with regard to energy savings and thermal comfort. A sensitivity analysis serves for the estimate of the influence of unmeasured disturbances which can occur in real operation.

4.2.2.1 Control behaviour without influence of disturbances

The influence of irradiation, outside temperature and additional energy sources can be removed in the simulation in simple way. In the case of the climate for example, one uses weather data at which the outside temperature is constant and the irradiation in all directions is zero. In that way one can test, whether and under which conditions the algorithm in principle is able to follow a setpoint. Parameter studies have been carried out by varying the comfort parameter cl , the number of step response coefficients used for the free system response SAK , the prediction horizon P and the control horizon M . Figure 4.12 shows the control behaviour without disturbances for

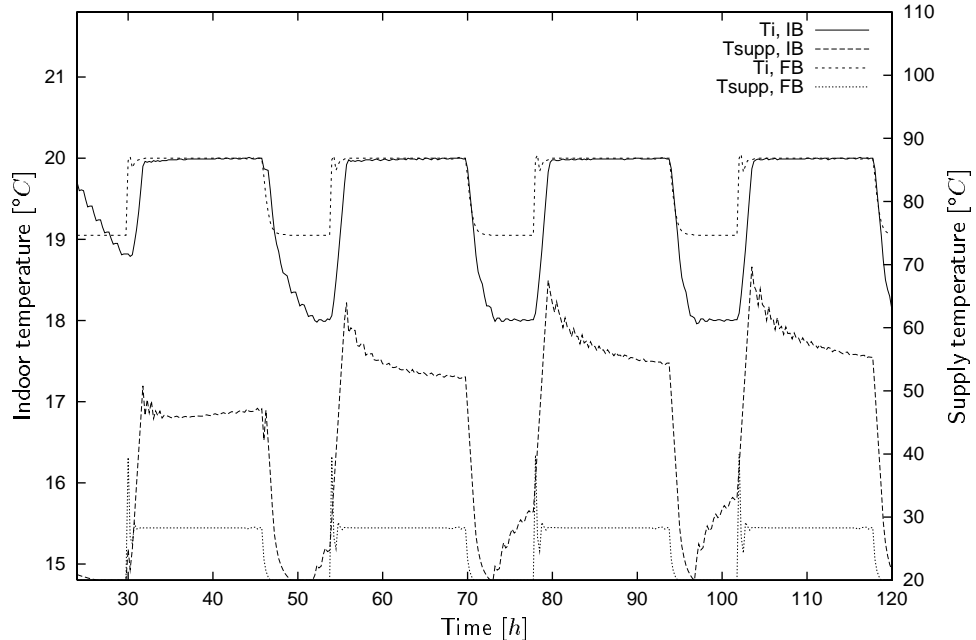


Figure 4.12. Simulated control behaviour for constant climatic conditions and variable indoor temperature set point, T_{supp} : supply temperature, T_i : Indoor temperature, IB: ISFH-building model, FB: FUL-building model, $cl = 9$, $P = 10$, $M = 5$, $SAK = 100$, the first 4 days after start of the predictive adaptive control at hour 25

an indoor temperature set value of 20°C during day (6-22 Uhr) and a night setback to 18°C . The algorithm needs a learning phase of about 80 hours for the ISFH building model till he has included

the dynamic reaction of the inside temperature to the supply temperature completely. After that period the algorithm regulates exactly on the set point. After hour 80 identical trapezium profiles of the inside temperature course are created every day since due to the constant weather conditions and the missing of disturbances no more information is added to the data.

For the FUL building model is the studying phase substantially shorter (already finished before hour 25) since it has a considerable smaller time constant. The non-reaching of the night set point results from the constant boundary conditions of the reference zone, that lead to a thermal equilibrium at about 19 °C for the chosen constant weather conditions.

In the following the influence of different parameters of the algorithm is examined at constant weather conditions.

The comfort parameter cl controls the weighting of set point deviation and control variable change in the cost function.

It can be changed in predefined limits $cl = 0..9$ to choose a weighting between comfort and energy reduction mode by the user (9: maximum comfort, 0: maximum energy saving). The course of the indoor temperature and the heating power for different comfort parameters simulated with the ISFH bulding model is shown in figure 4.13. Constant climatic condition have been assumed for this simulation.

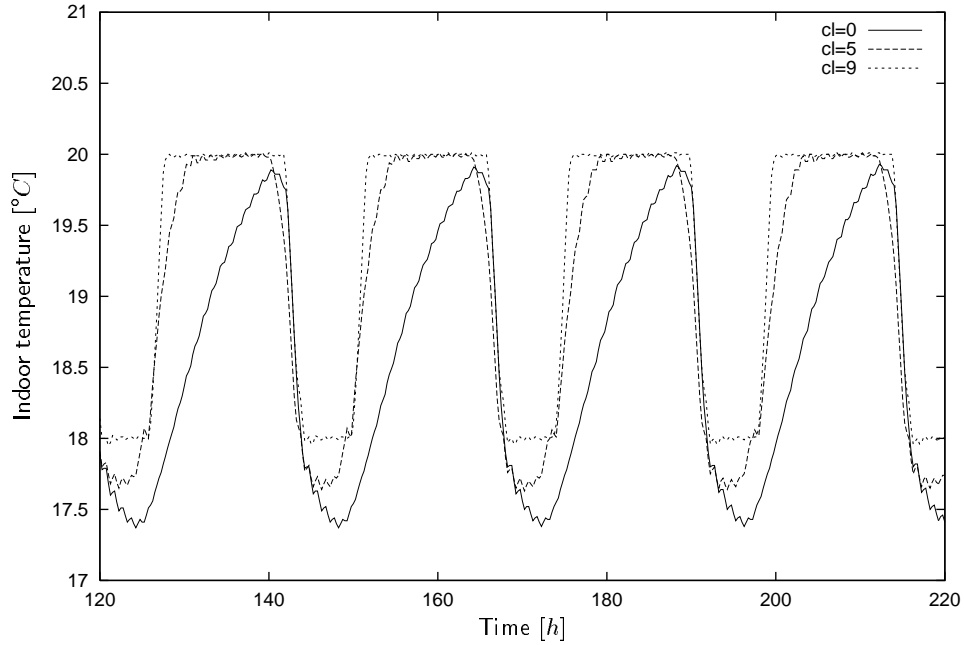


Figure 4.13. Simulated control bahaviour of the predictive adaptive control algorithm without influence of disturbances – indoor temperature, $P = 10$, $M = 5$, $SAK = 100$

The various weighting affects in the cost function the control response can be recognized clearly. If the change of the control variable doesn't get weighted at all ($cl = 9$), the set point trajectory is followed almost ideally. Merely the limitations of the control variable and the building sluggishness prevent an ideal rectangle profile. At high comfort parameter the resulting control variable changes are corresponding high. The agreement of the inside temperature with the set point deteriorates at increasing weighting of the control variable change. As explained above, the weighting of the control variable change is reduced on zero at transgression of the set point. This is the reason for the fast temperature drop when the night setback is switched on. The lower limit for the weighting of the deviation from set value (or the upper limit of the weighting of the control variable change)

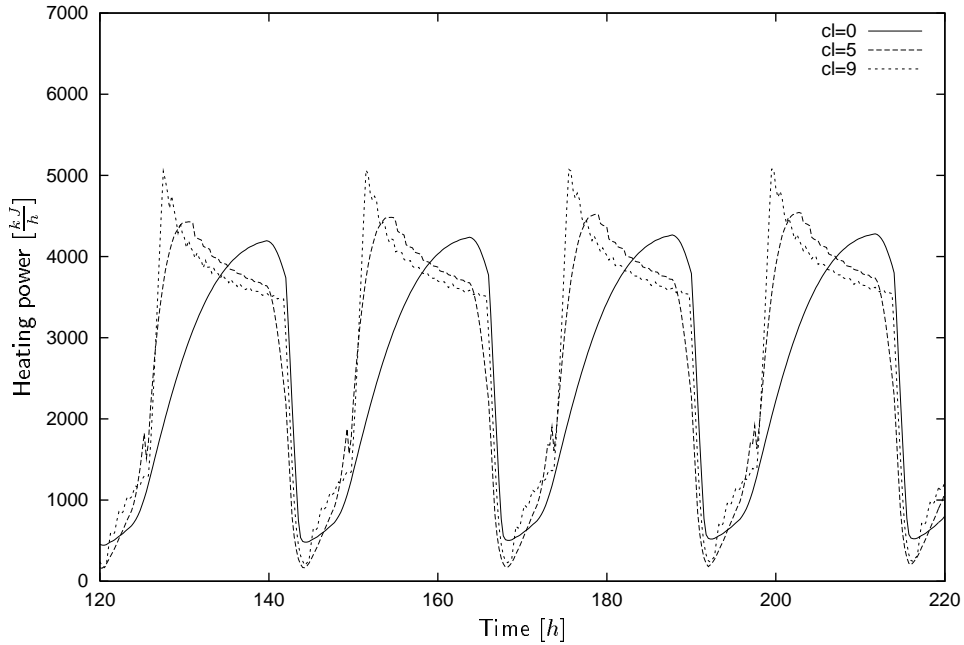


Figure 4.14. Simulated control behaviour of the predictive adaptive control algorithm without influence of disturbances – heating power, $P = 10$, $M = 5$, $SAK = 100$

was fixed arbitrarily. For this was assessed, which comfort losses still have to be expected of an energy reduction willing user.

The influence of the other parameters is discussed in section 4.2.3.

4.2.3 Control behaviour with influence of disturbances

Influence of the comfort parameter

The simulated influence of the comfort parameter is shown here in a period for weather data of march 1995 (hours 1945-2045). The figures 4.15 and 4.16 show the simulated course of the indoor temperature and the corresponding heating power for different comfort parameters. The figure show that the heating power is reduced for a smaller comfort parameter. The small weighting of deviations from the set point leads to a more sluggish reaction on changes in the set value. On days with a high irradiance, the overhaeting risk is reduced considerably. Though on days with low irradiance the agreement of set value and real value is worse. The heating power is reduced correspondingly at smaller comfort parameters.

A simulation for a full year for different comfort parameters was carried out with the weather data of the year 1995. Figure 4.17 shows the monthly mean values of the heating energy inputs into the reference zone for different control strategies. For a classical control with electronical thermostatic valve as a reference, the monthly heating energy can be represented as a percentage (Figure 4.18). The simulations show, that the new control in comparison with the classic control leads to energy savings. The savings are the lowest within the winter months and at the highest within the in-between season. By reducing the comfort parameter one can reduce the heating energy consumption further. The height of the diminution has the same seasonal dependence. For a comparison, also the TRNSYS-internal ideally fast control is drawn. Due to the way of calculation, the seasonal dependence differs from those of the other controls shown.

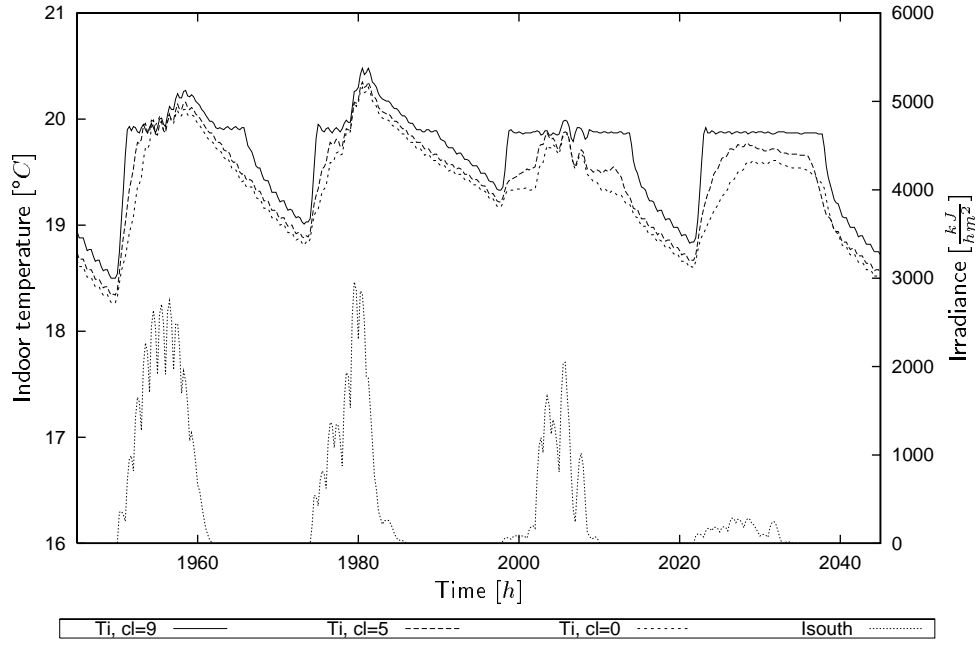


Figure 4.15. Simulated zone temperature for different comfort parameters cl , for weather data of 23.3.-26.3.1995, furthermore the irradiance on the south facade is drawn

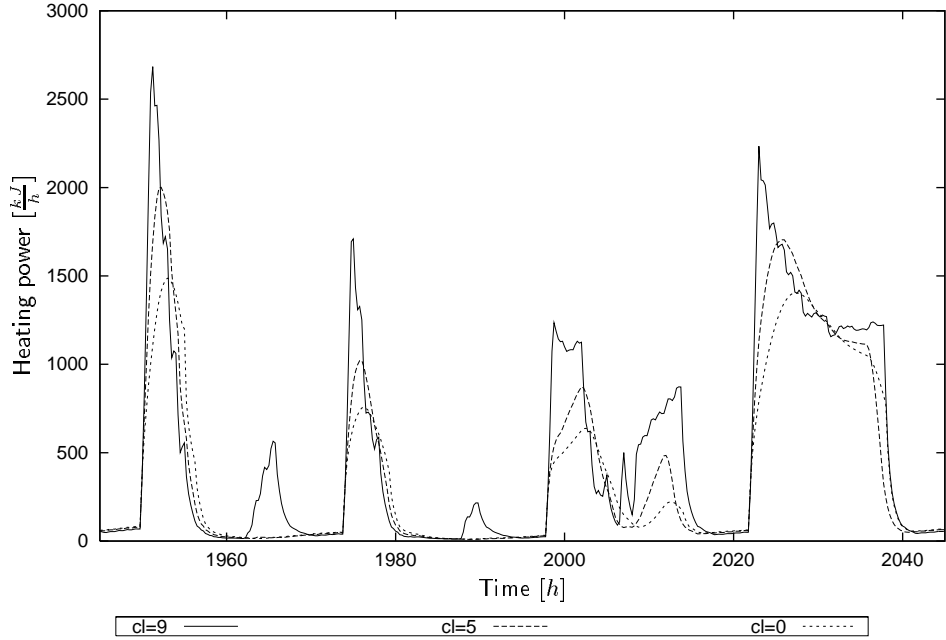


Figure 4.16. Simulated heating power for different comfort parameters cl , for weather data of 23.3.-26.3.1995

Illustration 4.18 shows, that the quantitative assessment of the possible energy savings strongly depends on the reference and the select comparison period. For a whole heating period the simulation with the ISFH building model gives the results indicated in table 4.1.

To the assessment of the thermal comfort the time integral of the difference between simulated

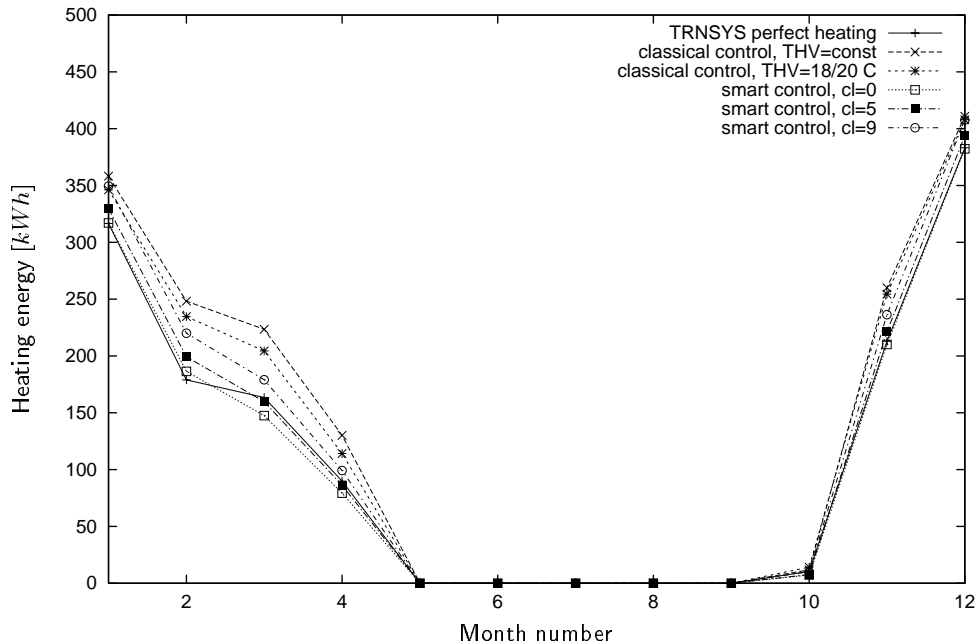


Figure 4.17. Monthly mean values of the heating energy input into the reference zone for different control strategies simulated with the ISFH building model (weather data 1995)

Table 4.1. Simulated heating energy savings for the reference zone of the ISFH building model in a heating period (weather data 1995)

Comfort parameter	reference: thermostatic valve $T_{set}=20\text{ }^{\circ}\text{C}$	reference: thermostatic valve $T_{set}=18/20\text{ }^{\circ}\text{C}$
$cl = 0$	17.8	12.9
$cl = 5$	13.6	8.5
$cl = 9$	7.2	1.7

indoor temperature and set point was used.

$$Abw = \int_{t_a}^{t_e} T_i - T_{i,soll} \ dt \quad (4.8)$$

The calculation was executed for a negative and positive deviation from the set point separately, only for the timesteps in which there was a heating on energy requirement. In addition, only the times on which the day set point was sedate were judged.

The sums of the complete heating period are written down on table 4.2. Overheatings naturally occur more within the in-between season while sub-temperatures have to be more frequently found within the winter months. For the new control algorithm substantially less temperature transgressions occur than for the control with radiator thermostatic valve. The transgressions are hardly different for different comfort parameters of the new control. This has to be explained with the predictive mode of operation of the new control with which future overheatings are recognized and turned away already in advance by a corresponding control strategy. In comparison sub-temperatures occur more frequently at the new control.

In the cost function the change of the control variable is judged more strongly at small comfort parameter, what leads that the indoor temperature is increased more slowly.

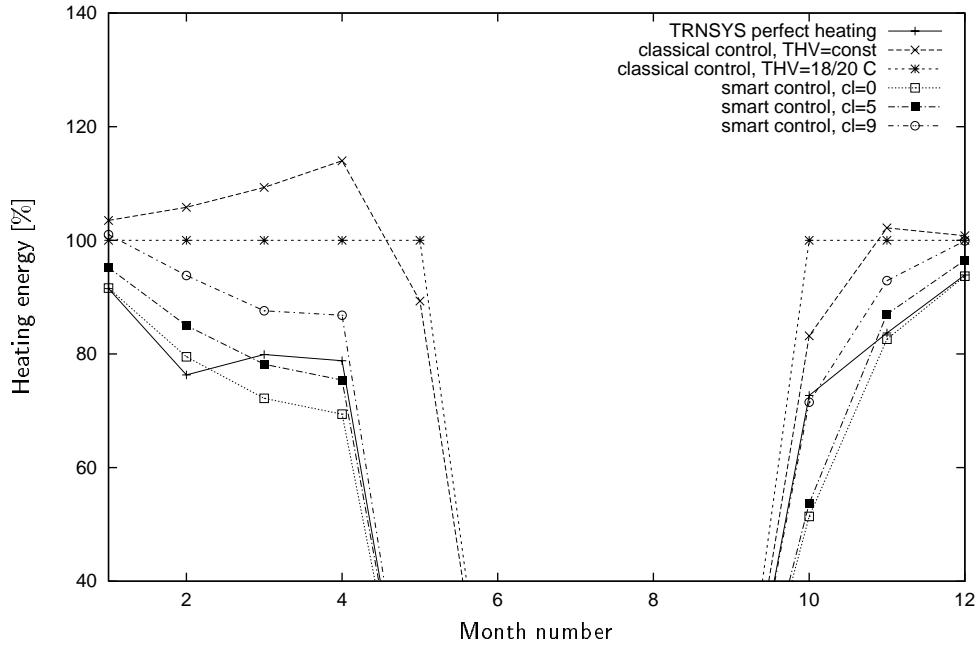


Figure 4.18. Monthly mean values of the heating energy input into the reference zone for different control strategies simulated with the ISFH building model (weather data 1995) referred to a classical control with electronical thermostatic valve as a reference

Table 4.2. Time integral of the deviation of the simulated indor temperature from its set value in a heating period (weather data 1995). Only the times on which the day set point was sedate were judged.

Control strategy	Abw for $T_i < T_{i, set}$ [Kh]	Abw für $T_i > T_{i, set}$ [Kh]
classical, mech. thermostatic valve	-267	514
classical, elektron. thermostatic valve	-404	468
new $cl = 0$	-1574	319
new $cl = 5$	-1077	328
new $cl = 9$	-447	345

Influence of the number of step response coefficients

The number of step response coefficients used for the calculation of the free system response must be fixed before the start of the control. Since it influences the calculation time considerably, it should be reduced as much as possible, without loosing to much information about the dynamic behaviour of the system. The tests showed that the influence within the range $SAK = 20..1000$ is low for the ISFH building model for a high comfort parameter. The reason is the correction of the free system response on every time step with current measured data which compensates for an erroned modelization. A further reason is the fact that the most information about the dynamic system behave is contained in the first part of the step response, which hasn't been influenced by the variation. At high comfort parameters, the current deviations from the set value are more important than future ones, that's why the influence of SAK remains low. For smaller comfort parameters, the influence is a little higher. A value of $SAK = 100$ has been chosen for the control program used in experimental testing as a compromise between precision and calculation time.

Influence of control and prediction horizon

The control horizon M and the prediction horizon P must also be fixed before the control process. The prediction horizon estimates the number of timesteps in the future for which the difference between predicted value and set value is taken into account by the cost function. The control horizon is the number of timesteps in the future for which the control moves are taken into account by the cost function.

The figure 4.19 shows the comparison of the control response with different prediction horizons P for a comfort parameter $cl = 5$.

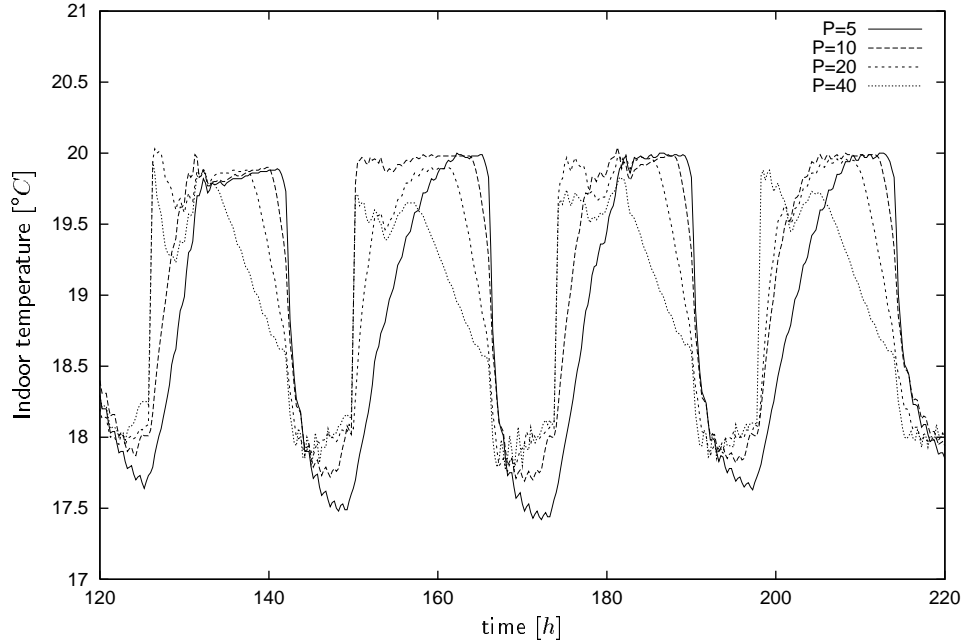


Figure 4.19. Simulated indoor temperature of the reference zone for different prediction horizon P with influence of measured disturbances (weather data: 6.1.-9.1.1995), control horizon $M = 5$, comfort parameter $cl = 5$ number of step response coefficients $SAK = 100$, set value of indoor temperature = 20/18 °C, control horizon $M = 5$

As shown in the graph, the choice of the prediction horizon has a considerable influence on the quality of the control. If the control horizon is too long, the control reacts to early on future steps of the set value. If it is too short, only a few time steps are considered in the cost function. Then the weighting of the control moves gets more important.

The variation of the control horizon M in the limits of 1...5 didn't show significant dependence of the control response of this parameter.

For the control program used in experimental testing $P = 10$ and $M = 5$ has been used.

Influence of the weather prediction

The effect of the weather forecast on the control response was determined with help of the simulation of the two extreme cases in the forecast quality. An ideal weather forecast doesn't have any differences on the weather terms occurring actually. Such forecast was created in the simulation by reading the weather data into the forecast algorithm. In the other extreme case the algorithm has no information about the future outdoor temperature fluctuations or energy inputs by irradiation.

This case was simulated by setting the future course of the outdoor temperature constant to the last value measured and the future irradiation to zero. Figure 4.20 shows the simulated indoor tem-

peratures for both cases and weather prediction used in the developed algorithm (see section 4.1.6). The heating power for the correspondig days are drawn in figure 4.21. For the estimation of the

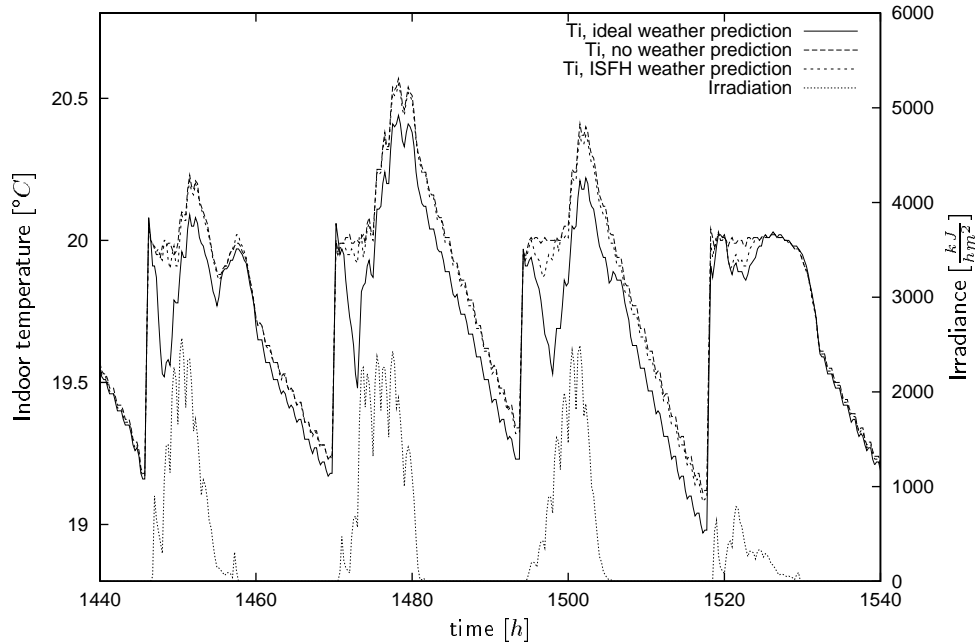


Figure 4.20. Simulated indoor temperature for different weather predictions, ISFH building model with floor heating $cl = 8$, weather data 2.3.-5.3.1995, in addition the irradiance on the south facade is plotted for the simulation period

influence of the quality of prediction, a simulation with the ISFH building model was used. The heat capacity of the radiator was set to $5722 \frac{kJ}{K}$. This is the thermal capacity of a 15 cm thick concrete floor, which was set to simulate a floor heating. The heat capacity of the pipes and the water was neglected here.¹

Since the available heating system reacts comparatively fast in the experimental house, a more sluggish system was used for this simulation. Overheating phenomena occur substantially more often and affect more the advantages of the inclusions of future disturbance variables in the control strategy.

Table 4.3. Heating energy input into the reference zone and time integral of deviation from set value of indoor temperature (weather data 1.1.-31.3.1995), number of step response coefficients $SAK = 100$, control horizon=prediction horizon=20, $cl = 8$, set value of indoor temperature = 18/20 °C

weather prediction	heating energy in reference zone [kWh]	Abw für $Ti < Ti_{set}$ [Kh]	Abw für $Ti > Ti_{set}$ [Kh]
no	820	-129	153
ideal	796	-238	108
ISFH	816	-152	148

If one compares the two forecast extreme cases then it can be observed that the control with ideal forecast of gains by irradiation reduces the heating power early. Through this the indoor temperature elevation caused by irradiation isn't as high as without forecast. The indoor temperature courses for the internal weather forecast by the ISFH control lie between the two extreme cases.

¹In comparison the estimated heat capacity of the radiator used for the other simulations was $60 \frac{kJ}{K}$

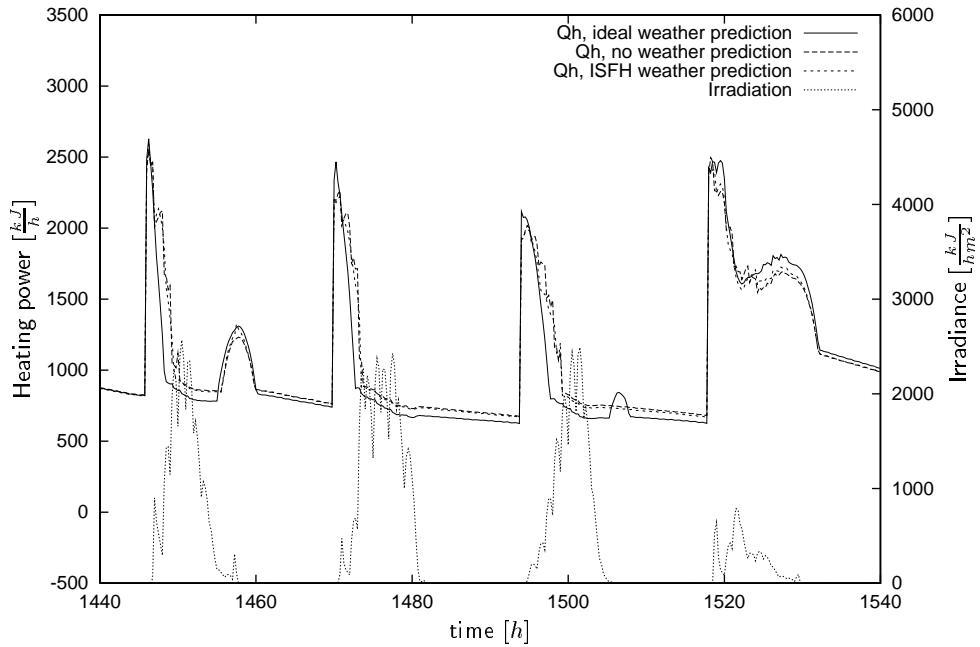


Figure 4.21. Simulated heating power for different weather predictions, ISFH building model with floor heating $cl = 8$, weather data 2.3.-5.3.1995

It has to be remarked that the absolute height of the overheatings caused by irradiation depends of further building parameters like solar aperture and thermal mass. The obtainable savings also are dependent on building parameters and parameters of the control. The consumption on heating energy mentioned in table 4.3 and comfort assessments refer therefore to the chosen building model and the presettings in the control.

With the data is obvious that a considerable potential of the energy savings lies in an improvement of the weather forecast of the developed algorithm. The determined results also make clear, that with the developed predictive adaptive heating control comfort improvements particularly for very sluggish heating systems are possible.

The effect of the weather forecast on the control response also depends on the prediction and control horizon (see figure 4.22). For a larger prediction horizon and expected solar energy input the heating power is reduced earlier, what makes itself noticeable in an earlier reduction of the indoor temperature. The following overheating is also lower since the indoor temperature is already far reduced when the irradiation has an effect. It is remarkable that the difference between the indoor temperatures at a control and prediction horizon of 10 and 20 (corresponds to 2.5 h und 5 h) is substantially higher than for a control and prediction horizon of 20 and 40 (corresponds to 5 h und 10 h).

Influence of the change of building parameters

With these examinations it shall be checked, if the developed algorithm is also working for a different solar aperture of the building (see figure 4.23) On the first day of the simulation the supply temperature is adjusted with the heating curve. This leads to overheatings since no radiator thermostatic valve is available in the simulated reference room. The predictive adaptive heating control is switched on on hour 25. It can be recognized, that on the fifth day after the start of the simulation overheatings occur. The larger the window area is, the higher are the overheatings.

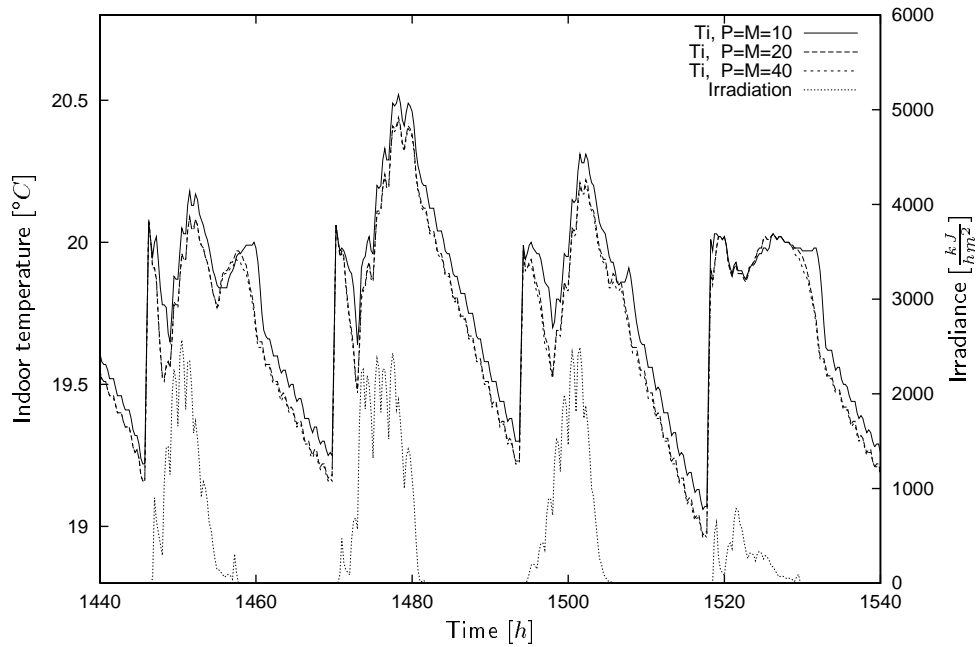


Figure 4.22. Simulated indoor temperature for the ideal weather prediction for the ISFH building model with floor heating $cl = 8$, variation of control and prediction horizon, weather data 2.3.-5.3.1995

The early reduction of the supply temperature doesn't suffice for the avoidance either. A larger prediction horizon could cause improvements here. On days with low irradiation the indoor temperature is very well controlled on the set point. The consequence of model errors is shown on some days with middle irradiance. The larger the window area is the more the consequence of the irradiation was overestimated. The room temperature therefore is reduced more than necessary for the compensation.

4.2.3.1 Control behaviour with influence of unmeasured disturbances

In the real application measured and unmeasured disturbances act on the system. The most important possible influences are examined with help of the simulation in this section. It is assessed, how the developed algorithm is able to work well under these non-ideal conditions.

Influence of additional energy inputs and losses

Additional energy inputs are caused by heat emission of persons and electrical equipment for example. Additional losses can for example arise from window ventilation. The effect of additional internal energy sources on the indoor temperature course shows figure 4.24. If a constant additional energy input of $P_{int} = 2000 \text{ kJ/h}$ is applied to the reference zone, then the resulting high heating power leads to overheatings already in some periods. This makes the control of the indoor temperature more difficult. However during the periods where there is a heating energy demand, the control is working well. The start phase with the classic control during the first 24 hours can be seen. After the transient period the day set value is controlled as well as without additional energy inputs.

For internal gains varying with time it can be recognized that after the morning add-on of the input (at 9 o'clock) a short-time temperature elevation results which is however intercepted by

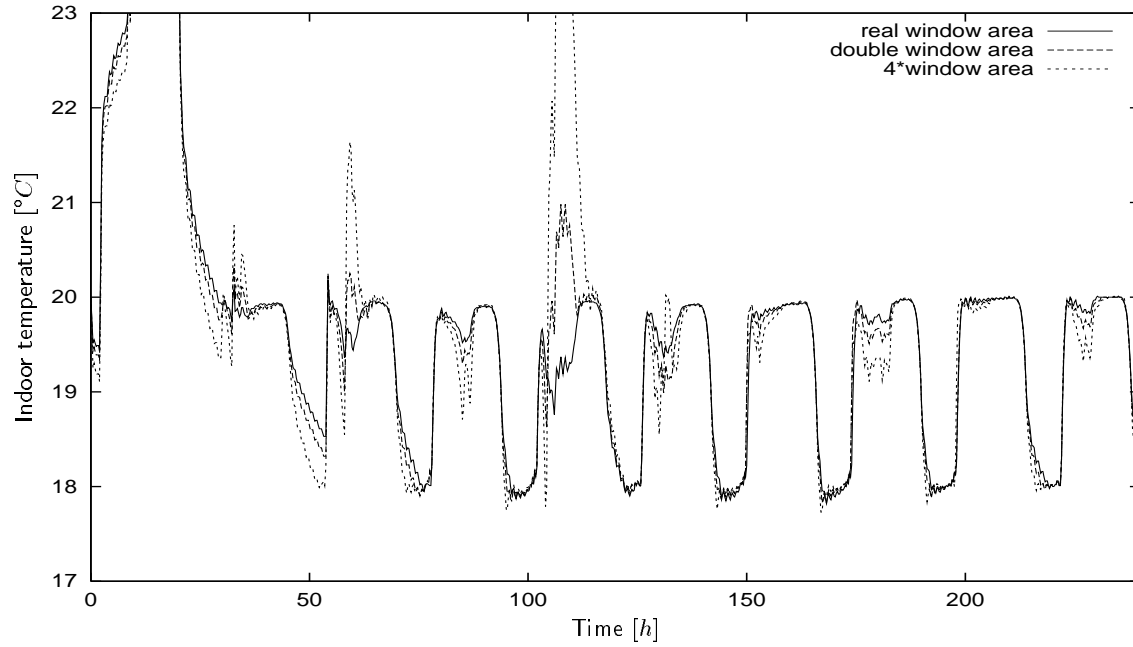


Figure 4.23. Simulated indoor temperature for different window area in the south facade of the ISFH building model, set value of indoor temperature 20/18 °C, weather data 1.1.-10.1.1995, $cl = 8$

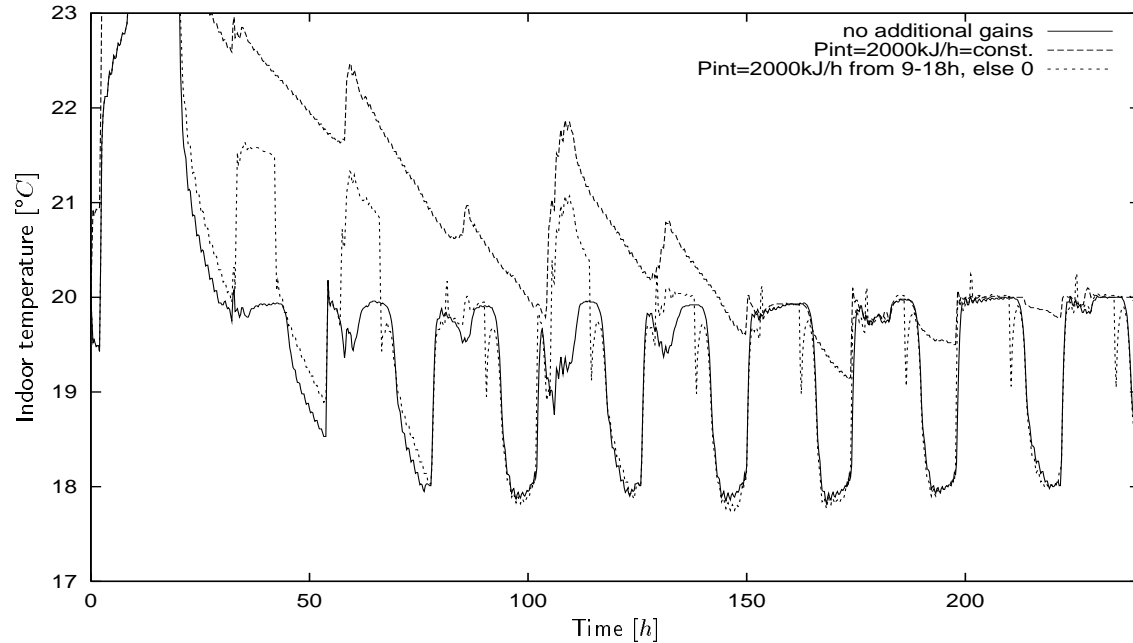


Figure 4.24. Simulated indoor temperature for the reference room of the ISFH building model for additional energy input, set value of the indoor temperature 20/18 °C, weather data: 1.1.-10.1.1995, $cl = 8$

the reaction of the control algorithm after short time. An indoor temperature reduction which is corrected by the control of the heating system also after short time analogously occurs when switching the load off at 18 hours. The algorithm therefore is able to react to not measured disturbances adequately.

It is pointed out again that the internal gains can be included in the control in addition or instead of solar gains as measured disturbance variables.

Especially in office buildings the quota of internal gains to the energy balance is often considerable. Moreover the temporal course there can be predicted usually with a good precision. The decision depends in the end which gains are relevant in the corresponding building and which additional costs arise from a further sensor.

Influence of sensor inaccuracies

In this section the consequence of random and systematic errors at the measurement recording is examined. A random error was simulated by adding random numbers with a variance of 10% of the measured value to it. A systematic error was created by addition of 10% of the measured value to it. In figures 4.25 and 4.26 the corresponding simulated indoor temperatures influences by the errors.

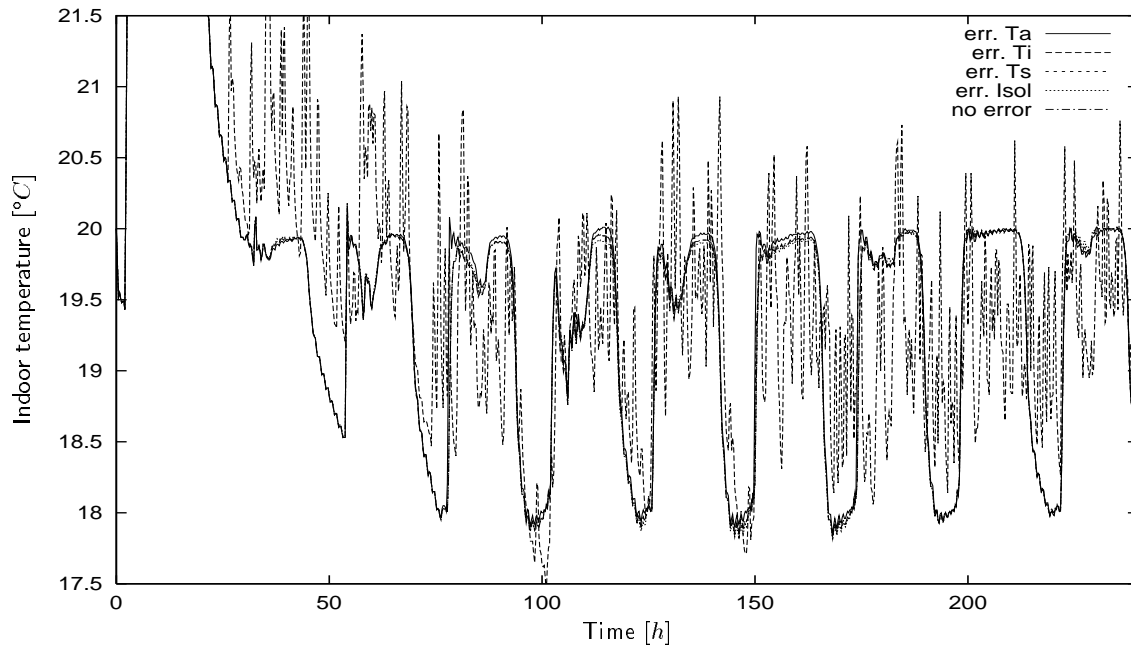


Figure 4.25. Simulated indoor temperature for a random error of the corresponding measured value (Ta: outdoor temp., Ti: indoor temp. Ts: supply temp. Isol: insolation) for the ISFH building model, the real simulated temperature without error is shown, set value of the indoor temperature 20/18 °C, weather data: 1.1.-10.1.1995, $cl = 8$, only for an error in the indoor temperature measurement a noticeable deviation occurs

The controlled variable (the indoor temperature) is most sensitive to a random error of the measured value. Random errors of the measured values of the driving forces also have an influence, but much lower and without any influence on the operation in principle. This is due to the delayed and damped effect of all driving forces on the output quantity.

The system has an effect on the input quantities like a lowpass so that high-frequency fluctuations around the mean average value have hardly influence on the output quantity. A large random error however at the measuring of the controlled indoor temperature leads to considerable problems in the control. Because of the necessary correction of the predicted output quantity with the respectively current measurement the future course of the indoor temperature is either about- or underestimated in frequent change. The supply temperature is correspondingly de- or increased.

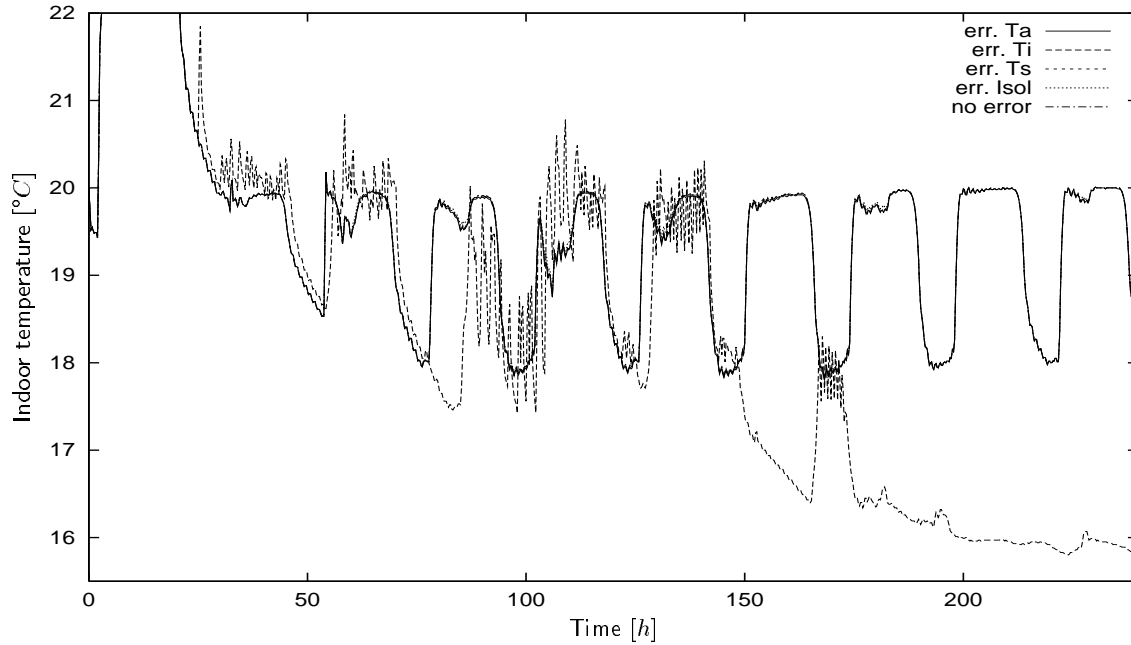


Figure 4.26. Simulated indoor temperature for a systematic error of the corresponding measured value (Ta: outdoor temp., Ti: indoor temp. Ts: supply temp. Isol: insolation) for the ISFH building model, the real simulated temperature without error is shown, set value of the indoor temperature 20/18 °C, weather data: 1.1.-10.1.1995, $cl = 8$, only for an error in the indoor temperature measurement a noticeable deviation occurs

For the addition of an offset of 10% of the driving forces, no deviation occurs compared to the case without error. The offset is simply learned and then compensated by the control algorithm. However problems for the control arise for the addition of an offset to the controlled variable. The fluctuations of the model which arise from the identification cause the fluctuations of the indoor temperature to be seen. The identified model gets completely useless approximately on hour 150. Then the identification gives the result that an increase of the supply temperature leads to a decrease of the indoor temperature. Compared to this errors in the model output quantity (indoor temperature) affect very negatively the control response. The sensors for a practical use must be chosen according to this facts.

4.3 Experimental investigations at ISFH

The experimental examinations served primarily the proof that the control algorithm works under practical conditions. Furthermore the operation of subroutines could be tested to get ideas about possibilities for an optimisation. A comparison between the predictive adaptive and a conventional control is possible only qualitatively, since the experimental condition cannot be reproduced exactly. A quantitative comparison has been presented in section 4.2.3.

In this section, at first the test facility for the experimental investigation of the developed algorithm is described and then the results are presented.

4.3.1 Description of the test facility

The tests were executed in the experimental houses of the ISFH Emmerthal. These are two buildings with a reflectedly built up ground plan and 160 m² living space. The eastern building (experimental house) and the western building (reference house) are separated by the garage section from each other 4.27. The heating energy is supplied to the buildings by separated heating circuits but one



Figure 4.27. The ISFH test buildings

boiler. The low temperature gas boiler (20 kW) provides a primary circuit with hot water. The primary circuit supplies the three heating circuits. For every circuit a three way valve mixes the hot water with the water from the return pipe to hold the desired supply temperature. Before the developed control was put into operation, a heating curve was used to calculate the set value for the supply temperature (see section 4.2.1.1). If not indicated different, the indoor temperature set point was fixed to 21 °C from 6-22 hours, during the night to 19 °C.

Both houses are used as office buildings. This indicates that disturbances by internal gains or door opening occur primarily in the time on Mondays till on Fridays from 8 to 18 hours. The use of the buildings restricts the possibilities of variation of certain parameters like indoor temperature set points and comfort parameter during the experimental tests.

For the experimental examinations an independent data acquisition and sensors had to be installed since the available devices weren't compatible with the used software. Moreover, the ongoing experiments with the already available device shouldn't be disrupted. For the tests with PC

control the experimental house was used, for the tests of the independent controller (prototype) the reference house was used. Both controllers use however the same principle which was explained in section 4.1.1.

4.3.1.1 Sensors and data acquisition

The sensors and data acquisition are different at the PC control and the control with the microcontroller. The choice of the sensors was determined by precision, price and market availability. Background was the target to develop a marketing capable controller. The function ability had therefore to be made sure also with cheap and more inaccurate sensors.

Control with personal computer

Table 4.4 gives a list of the sensors used for the PC control. The first four mentioned sensors are actually used for the control. The other sensors served the system supervision. Air temperature

Table 4.4. Sensors used for the PC control

measured quantity	sensor type	precision	supplier
Indoor temperature	PT100 class A	$\pm(0.15 + 0.002[t])^{\circ}C$	Heraeus Sensor Hanau
Outdoor temperature	PT100 class A	$\pm(0.15 + 0.002[t])^{\circ}C$	Heraeus Sensor Hanau
Supply temperature	PT100 class A	$\pm(0.15 + 0.002[t])^{\circ}C$	Heraeus Sensor Hanau
Irradiance	Si-01TC	$\pm 8.9\% \text{ v.M.}$	Ingenieurbüro Mencke & Tegtmeyer
Heating power	VMT 1.5 / T1	$\pm 1\% \text{ v.E. [RKE]}$	Raab Karcher Energieservice
return temperature	PT100 class A	$\pm(0.15 + 0.002[t])^{\circ}C$	Heraeus Sensor Hanau
supply temperature at the radiator	PT100 class A	$\pm(0.15 + 0.002[t])^{\circ}C$	Heraeus Sensor Hanau
return temperature at the radiator	PT100 class A	$\pm(0.15 + 0.002[t])^{\circ}C$	Heraeus Sensor Hanau

sensors are not ventilated but provided with a radiation protection. Temperature sensors for the measurement of temperatures in the heating circuit have been fixed outside of the pipe with a good thermal contact. The radiation sensor is a silicon solar cell with temperature correction. It has been fixed on the south facade of the test building. The sensor for the measurement of the heating power consists of a sensor for the mass flow and 2 temperature sensors for the supply and return pipe. A Microcomputer calculates the corresponding heating power and creates a proportional electrical signal, which is registered by the data acquisition.

The measurement and the AD-conversion is carried out by a Hewlett Packard data logger (see fig. 4.3.1.1). The data acquisition device consists of a mainframe and three cards. The command module serves for the control of all processes in the device. With the multiplexer all channels are switched in succession to the multimeter, which is the actual measuring device. The data are converted to a digital signal and then transferred to the computer. A library allows to control the data acquisition from a C or C++ program.

The measuring program in C++ collects the data every 10 s. After 15 min the mean value is calculated and saved to the hard disk. Then the developed algorithm is called which calculates the optimal supply temperature (set value) for the next 15 min. In a first version the algorithm was running in MATLAB, in the second version the algorithm had been translated to C language.

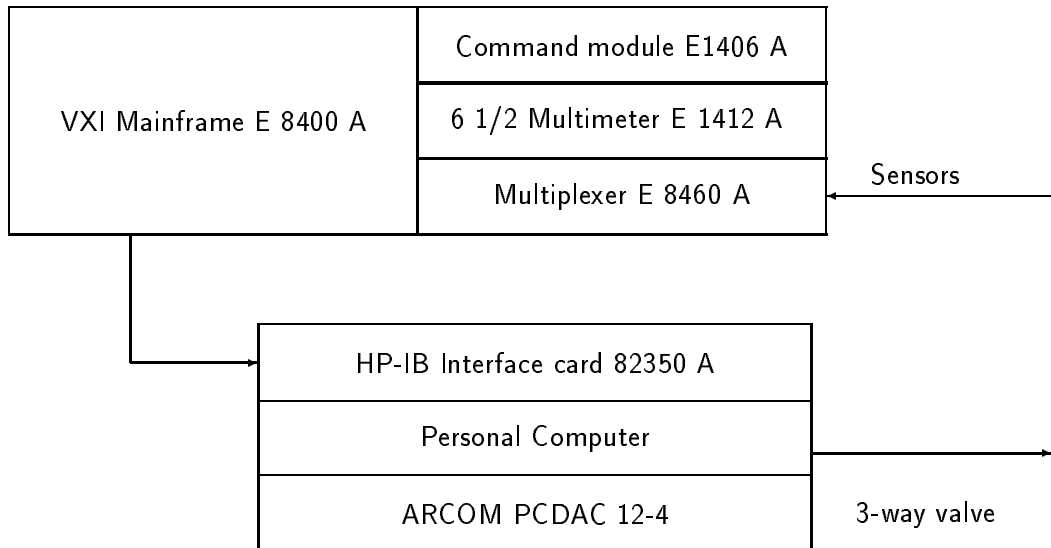


Figure 4.28. Data acquisition system and analog signal output for the PC control

The calculated optimal supply temperature is the set value for a fast PID-control of the 3-way-valve which mixed water of the primary circuit and the return pipe. The PID-Control is called by the measuring program every 10 s. Output value is a voltage (0-10 V), which is given as digital value to a DA-conversion card in the computer.

Control with microcontroller

All tasks carried out by the PC and the data acquisition is transferred to a Microcontroller in this variant. An already existing hardware of the company Brauns Control GmbH was used and modified. The basic device consists of a microcontroller, a communication panel and a board for the connection of sensors.

The hardware performance (e.g. calculation velocity, available memory) is considerably reduced compared to the PC. The control algorithm therefore had to be optimized according to the hardware limits.

Table 4.5. Sensors used for the control with microcontroller

measured quantity	sensor type	precision	supplier
Indoor temperature	BCTF-205RF	± 1.5 K	Brauns Control GmbH
Outdoor temperature	BCTF-205W	± 1.5 K	Brauns Control GmbH
Supply temperature	BCTF-R2	± 1.5 K	Brauns Control GmbH
Irradiance	Si-01TC	±8.9% v.M.	Ingenieurbüro Mencke & Tegtmeyer

The attachment of the sensors followed the same principles as for the PC control. For an assessment of the control behaviour measurements of the already available data aquisition system of the experimental houses have been used.

4.3.2 Results of the experimental investigations

In this section, at first the results of the experimental tests of the control algorithm with a personal computer are presented. After an assessment of the general control behaviour the results of single program modules are described. They were determined from the results of select variables stored to every time step. The representation of the measurement results for the microcontroller confines itself to the general control response since the values of the variables couldn't be stored.

4.3.2.1 The control behaviour of the PC control

Figure 4.29 and figure 4.30 show the measured indoor and supply temperature (controlled and manipulated variable) and the measured weather data for an example period. At first can be

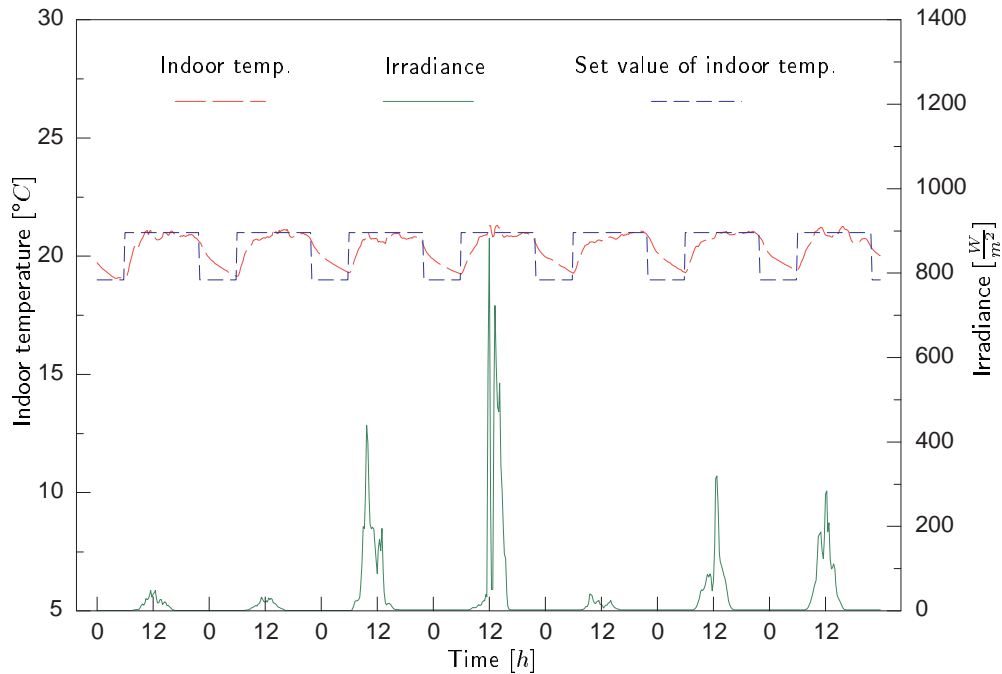


Figure 4.29. measured indoor temperature and irradiance for the period 23.11-29.11.99 for the PC control, the measured values are 5-min mean values, furthermore the course of the indoor temperature set value is shown, comfort parameter $cl = 8$

recognized that the course of the measured indoor temperature follows the set point very well. With the chosen comfort parameter $cl = 8$, the deviation of the indoor temperature from its set value is weighted relatively high, the control moves relatively low. During the night the control moves are not weighted at all in the shown period, since the indoor temperature lies above the set value. The supply temperature is set to the minimum value. That means that the night set value is not reached only because of the slow building cooling. At the presence of solar irradiation and danger of overheating the supply temperature is reduced. In the period showed no considerable overheating was registered. The reaction of the manipulated variable to changes in the insolation and outdoor temperature can be seen in the graph too.

A comparison between the calculated optimal supply temperature set value and the set value given by the classical heating curve is shown in figure 4.31. The set value calculated by the developed algorithm lies below the classical set value in most cases. From that it can be deduced that at least

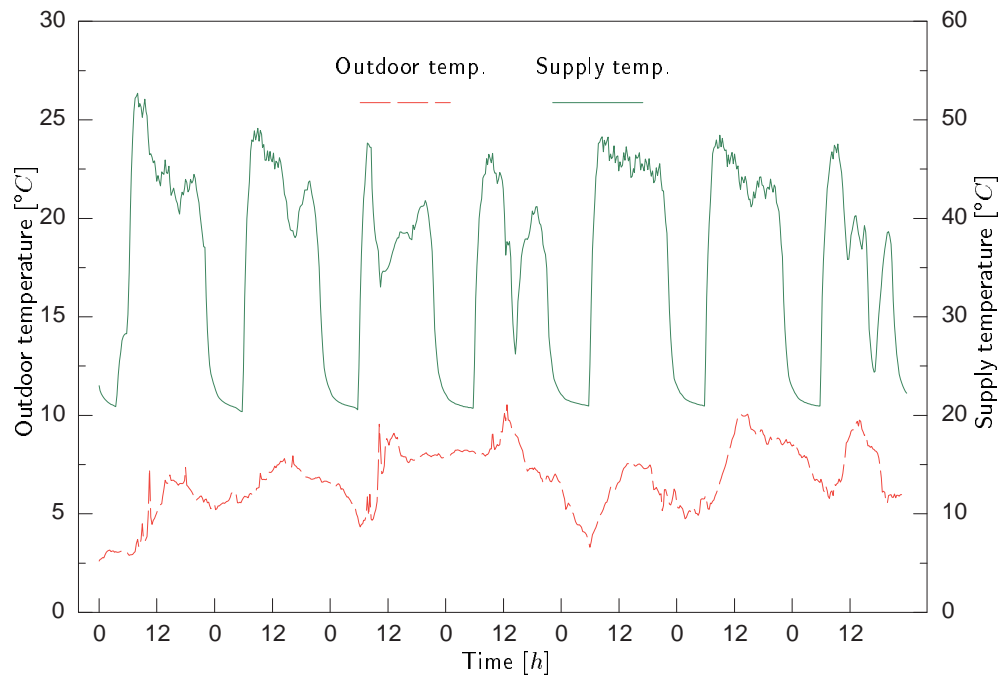


Figure 4.30. Measured supply and return temperature and outdoor temperature for the period 23.11-29.11.99 for the PC control

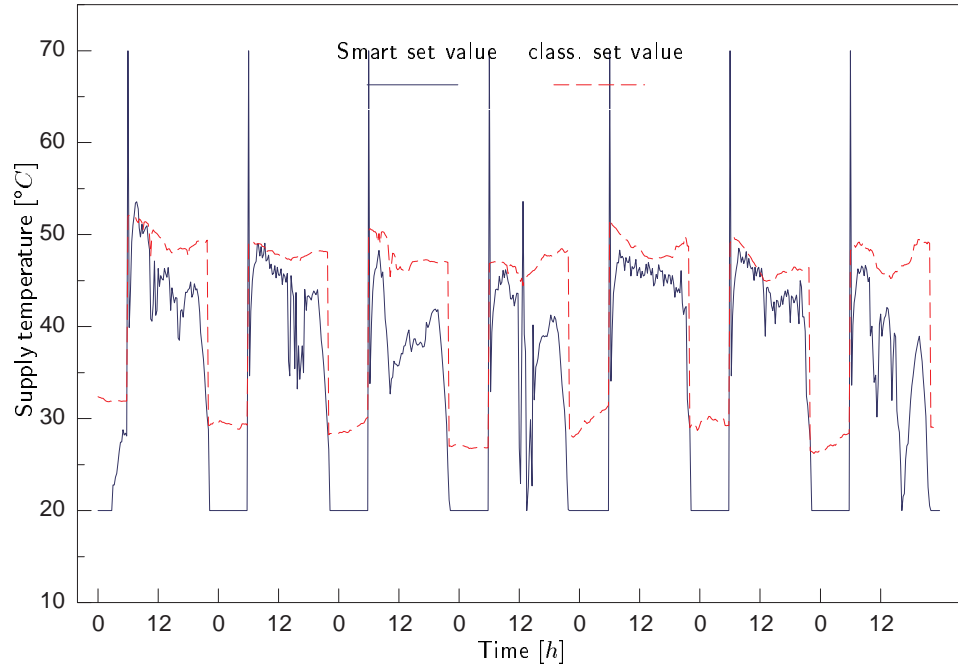


Figure 4.31. Supply temperature set value calculated by the predictive adaptive algorithm and calculated with the classical heating curve for the period 23.11-29.11.99

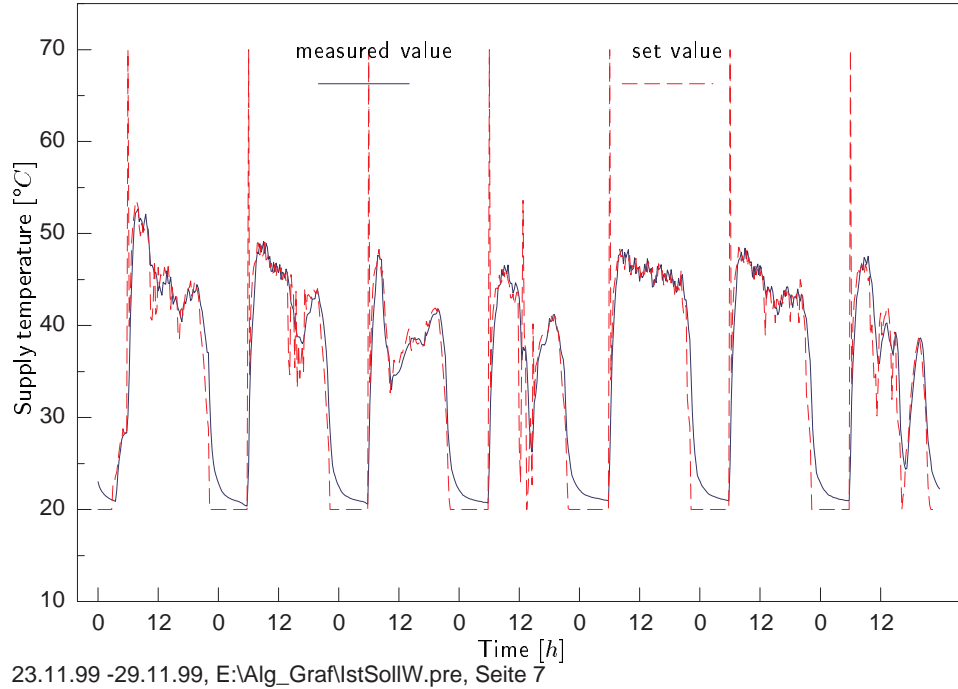


Figure 4.32. Measured supply temperature and supply temperature set value for the period 23.11-29.11.99

the distribution are lower than in the classical case. Comparative statements about the energy consumption concerning the room heating can be given with the simulations (see section 4.2.3). The graph also shows that during the night the classical supply temperature is considerably higher than the optimal one. If the radiators are equipped with mechanical thermostatic valves this would cause a considerable not necessary energy input into the building. The indoor temperature can be kept on the night set value of 19 °C with a much lower supply temperature.

The peaks during the morning heat-up result from the relatively high comfort parameter and the fact that the control increment wasn't limited for these tests. This served for the determination of the maximum control moves the algorithm demands in the extreme case.

A limitation of this value can be made by the setting of the at most permissible control increment, which has to be fixed before the start of the control. So, a to high demand for the boiler can be avoided. The plot of the supply temperature set value and the measured supply temperature shows, that the load is to high with the calculated increment (see fig. 4.32). However, this has no further consequences except the one that the indoor temperature is not reached as fast as required.

The evaluation of the measurements of the whole test period showed that on days with high wind-speed ($>5 \frac{m}{s}$) the calculated optimal supply temperature lies above the one calculated with the classical heating curve. Nevertheless the indoor temperature set value was not exceeded. This means that the indoor temperature set value would not have been reached with a classical control. However, the predictive adaptive control did compensate the higher losses due to the wind speed, although the quantity was not included in the model. This shows, that a comfort improvement is possible with the new control not only by preventing the overheating. Furthermore this results show that the heating curve of the experimental buildings which was used to evaluate the possible energy savings is already a very "energy saving" standard.

Results of the online-model identification

The used ARX model was selected by physical considerations and tests with help of measurements. In this section is checked, how good the model and the chosen identification method work in real operation. Figure 4.33 shows the course of the indoor temperature measured and the one calculated from the determined model parameters. The course of the determined parameters of the ARX model for the same time period is represented in figure 4.34. Only still insignificant changes of the model

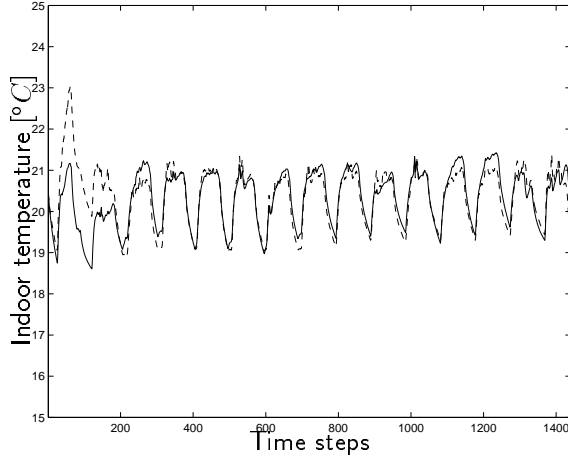


Figure 4.33. Measured (---) and simulated (—) indoor temperature for the period 16.11-30.11.99

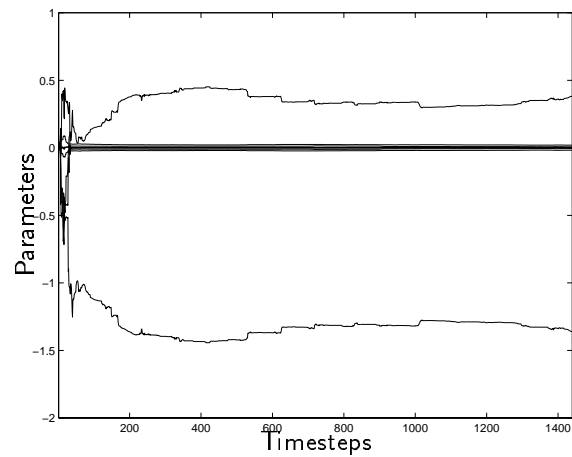


Figure 4.34. Temporal course of the identified model parameters for the period 16.11-30.11.99

parameters occur after approx. 200 time steps (approximately 2 days). The indoor temperature course is reproduced with the parameters got at the end of the identification time period with a high precision.

The free system response offers also a possibility for the check of the model quality. The second value of the vector must equal the measured value of the following time step for an exact model and a recording of all influences. The two courses are represented exemplarily for a day with middle irradiation (26.11.99) in figure 4.35.

Because of model errors and a number of non-recorded disturbance variables differences occur which however remain below 0.3 K.

The differences are particularly high at noon. This indicates that the irradiation is underestimated in the step responses. Only a respectively small irradiation was actually measured on the preceded days which have influence on the identification with largest weighting on last measurements. Due to that the signal to noise relation deteriorates. A corresponding model inaccuracy can be justified with that. Differences also occur during the night. The model expected a faster cooling than actually arised. Additional internal energy inputs can be excluded for the reference room for this time.

It is suspected that the step response of the outside temperature represents an essential cause, since it has the largest uncertainty. In addition, the system reaction can be different because of non-recorded climate sizes like the wind speed and the air humidity at the same outside temperature steps.

Summarizing one can say that the on-line model identification has proved its suitability in the practice test. The tests have shown however that the identification at small signal to noise relations leads to a larger error of the model parameters. For this reason the identification only then should be executed, if a having the heating energy requirement exists. Furthermore, it would be possible to make the weighting of the measurements for the identification dependent on the signal to noise

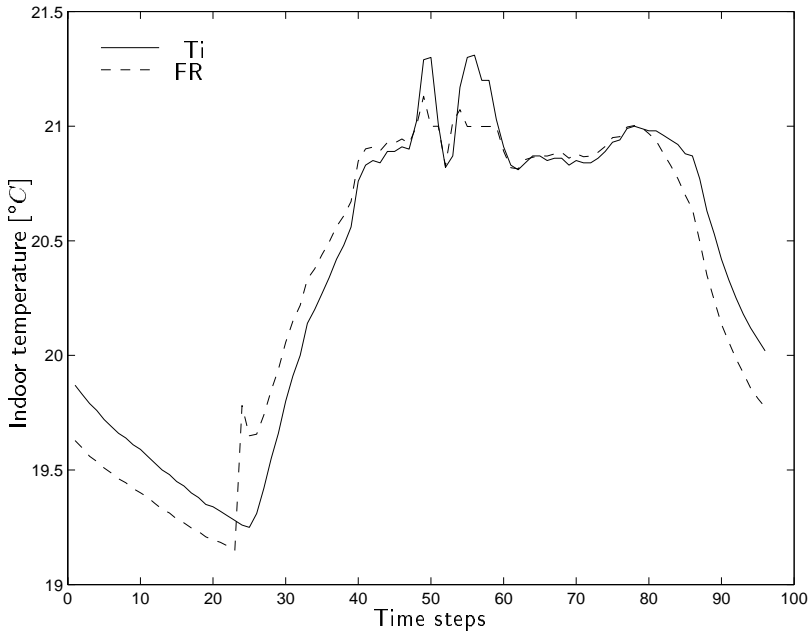


Figure 4.35. Comparison of the measured indoor temperature (Ti) and the indoor temperature of the next time step predicted by the free system response (FR) on 26.11.99

relationship. The forgetting factor could for example be increased during the in-between season (that means the period relevant for the identification is increased) but be reduced in winter. At present a forgetting factor of 0.999 is used.

Results of the internal weather forecast

For the assessment of the quality of the weather forecast the predicted courses of outside temperature and irradiation were stored on the hard disk on every time step of the measurement. Since the building has an integrating effect, the irradiated energy instead of the performance is compared.

$$Abw = \int_{t_0}^{t_0 + \Delta t} (I_{pred} - I_{meas}) dt \quad (4.9)$$

where Δt is equal to respectively 1, 2 and 4 hours. For the assessment of the outside temperature forecast the standard deviation of the difference between measured and predicted value is calculated. Figure 4.36 shows exemplary the calculated values for the period 26.11.99-28.11.99

The outside temperature forecast works in most cases very well. Also for a forecast period of 4 hours the standard deviation lies below 1 K, normally. Larger differences occurred, if the "natural" course of the outdoor temperature was changed by disturbing influences. Though, these temperature elevations are mostly locally limited and therefore hardly relevant for the energy losses over the whole building envelope. However, such influences should be considered at the sensor placement.

The irradiation forecast with the chosen attempt still shows a high inaccuracy. Particularly at strongly fluctuating irradiance, differences up to several 100% can be observed at single time steps. When pursuing the courses of the predicted irradiation one notices, that strong fluctuations occur between single time steps. These are caused by irradiation peaks which strongly affect the prediction with the respectively current measurement due to the weighting with forgetting effect.

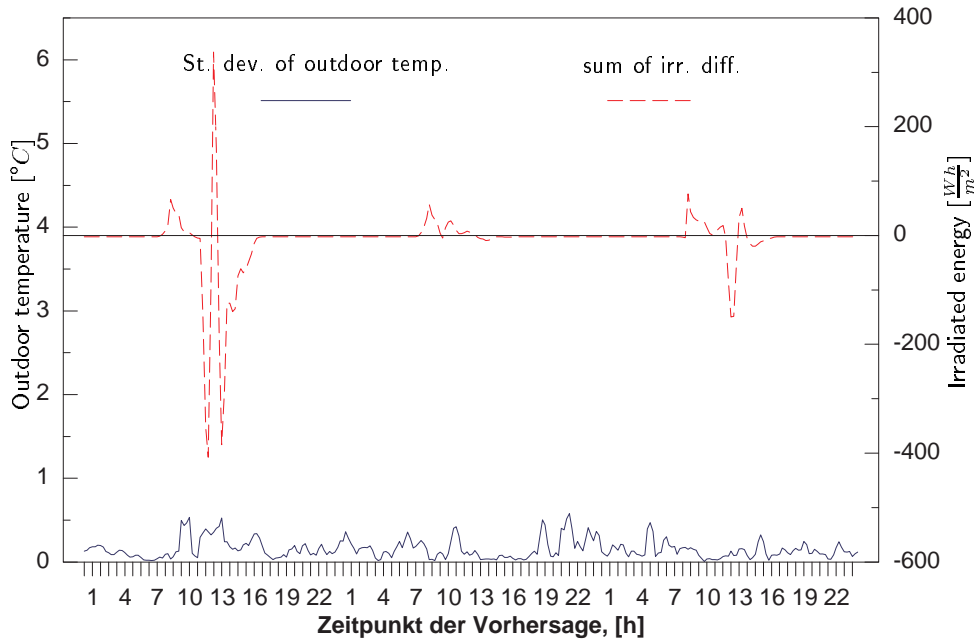


Figure 4.36. Standard deviation of the difference between predicted and measured outdoor temperature and difference between predicted and measured irradiated energy for a prediction period of 1 hour, shown for the period 26.11-28.11.99

As investigated in the simulation tests already, a considerable energy reduction potential lies in the improvement in the weather forecast. Further optimizations of the introduced approach or also other approaches would have exceeded the frame of the project however. In the context of the approach here an optimization in the weighting function could lead to improvements. In addition, a coupling between measured irradiation and outdoor temperature as it also corresponds to the general experience could be included in the forecast. Since the strength of the coupling can vary in various climatic zones it is suggested to determine it by a self-learning algorithm.

Besides the approach used here, transfer function models could be applied for an internal prediction only on the basis of measurements of the quantities to be predicted. It is however foreseeable, that in the not too far future a suitable weather service will be available about via internet, which doesn't exceed the financial possibility for the control of the heating either in single family houses. For large buildings or settlements the arising costs are so low compared other costs already, that a use would already be possible today. The modular structure of the algorithm then makes possible straightforwardly a replacing the present forecast procedure by an external forecast.

Temperatures in other rooms for the PC control

By the investigation of the temperatures in other rooms of the building during the test period the proof of the suitability of the used control concept should be furnished (see section 4.1.1). The course of the indoor temperatures in all four south oriented rooms of the experimental house is shown in figure 4.37.

The difference of the indoor temperatures of the rooms reaches more than 1 K only in rare cases during the period shown. The reference room is the room with the on an average lowest temperature.

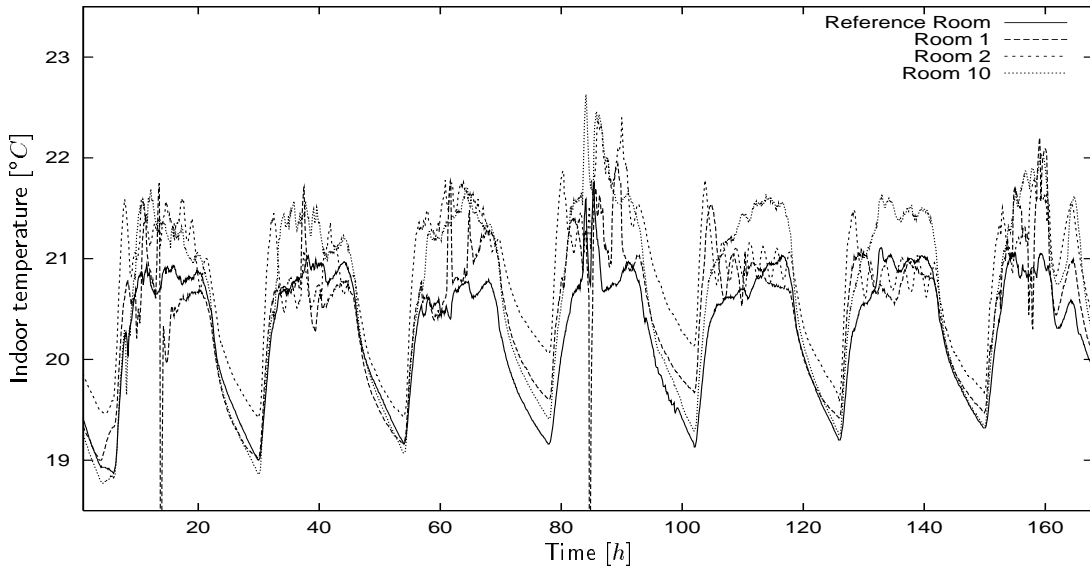


Figure 4.37. Measured indoor temperatures in the south-facing rooms of the experimental house for a control of the indoor temperature of the reference room (small room in the upper floor) by adjusting the supply temperature, period 23.11-29.11.99, Room 1: big room in the ground floor, Room 2: small room in the ground floor, Room 10: big room in the upper floor

Temperature peaks result from solar radiation or window opening.

Despite the mostly lower supply temperature compared to the classic control sufficient heating power is delivered to the whole building. In addition the results show that the reference room was well chosen. The higher temperatures in the other rooms result from the users presettings of the radiator thermostatic valves. If the indoor set point would not have been reached there would be still the possibility to correct this by reducing the mass flow in the radiator of the reference room.

4.3.2.2 The behaviour of the microcontroller

The microcontroller has been taken in operation on 21-12-99. The indoor and supply temperature as well as the irradiance during the starting phase show figures 4.38 and 4.39. After the start, the

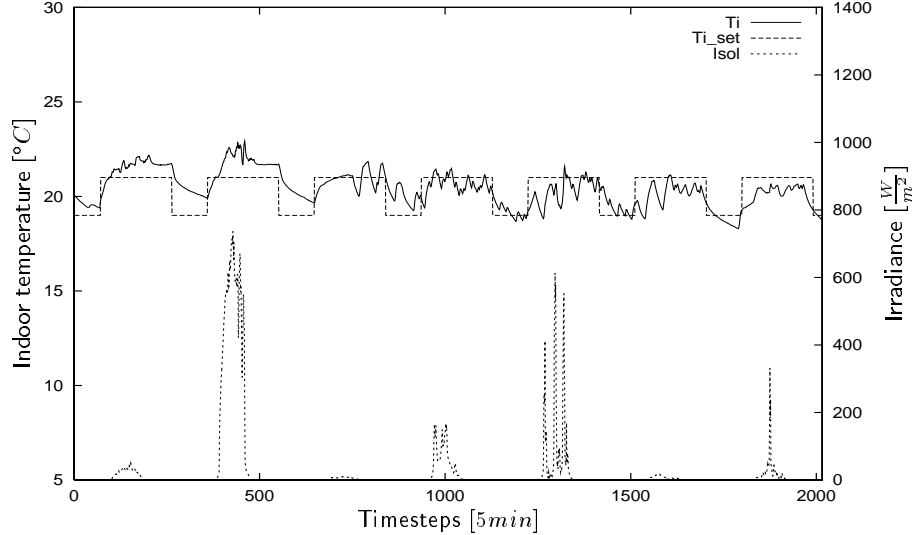


Figure 4.38. Measured indoor temperature (T_i) and vertical global irradiance on the south facade (I_{sol}) for the period 21.12-27.12.99 for the microcontroller, the shown measurements are 5-min mean values, furthermore the set value is drawn comfort parameter $cl = 8$

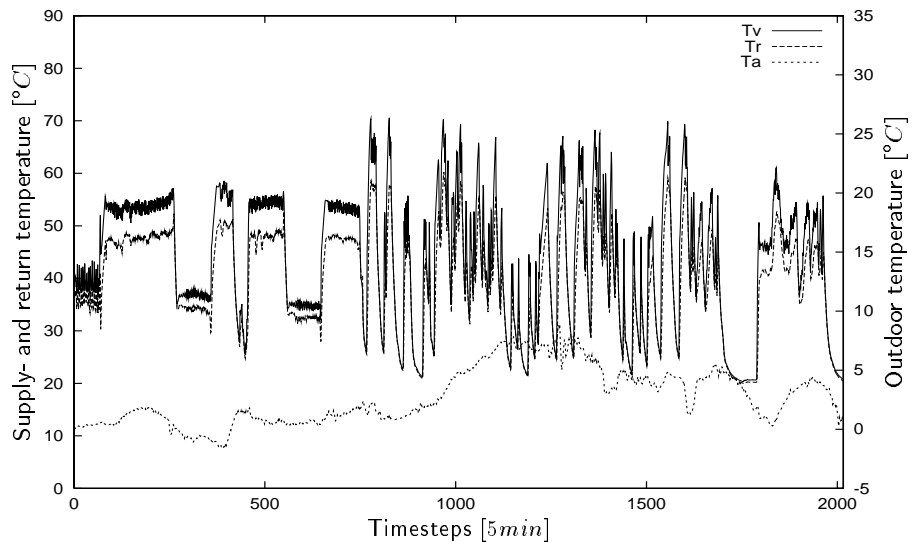


Figure 4.39. Measured supply (T_v) and return temperature (T_r) and the outdoor temperature (T_a) for the period 21.12-27.12.99 for the microcontroller

supply temperature was calculated with the classical heating curve for the next 24 h. The difference between supply and return temperature is nearly constant. Although the thermostatic valve has been removed the indoor temperature in the reference room only reaches 22 °C. This is due to the low parameters of the heating curve. 24 h after the start, the model quality was proofed. This test was successful, so the predictive adaptive control with the microcontroller started on 22nd

December at 10:30 h (Timestep 414).

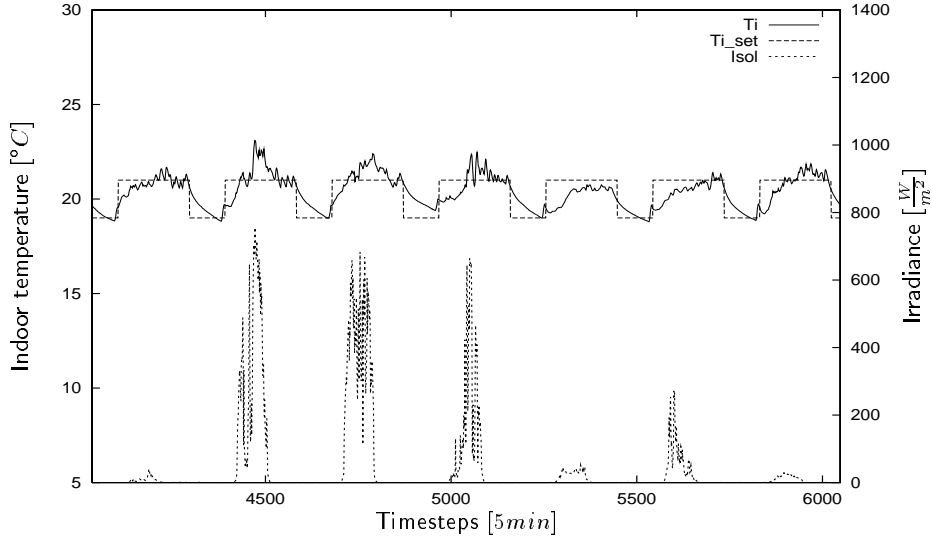


Figure 4.40. Measured indoor temperature (T_i) and vertical global irradiance on the south facade of the test building for the period 4.1.-10.1.2000 for the control with microcontroller, the measured values are 5-min mean values, furthermore the course of the indoor temperature set value is shown, comfort parameter $cl = 8$

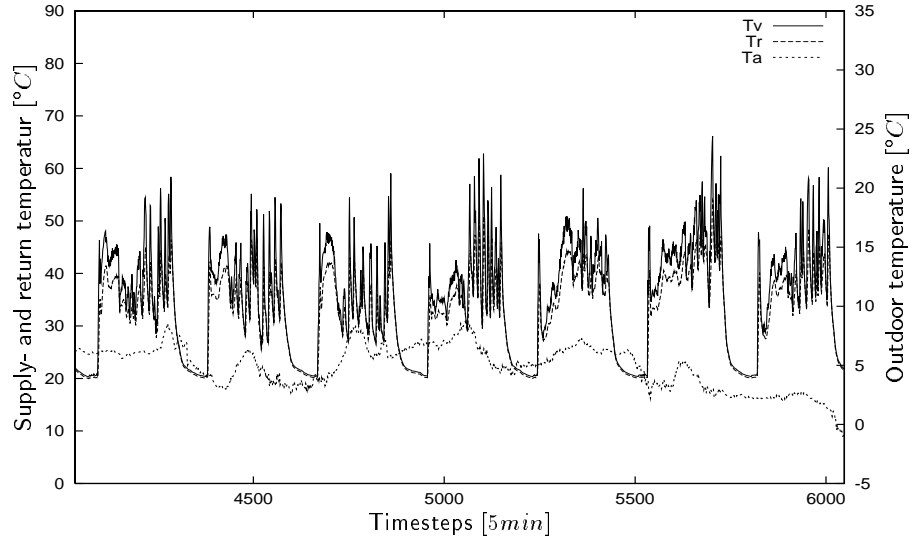


Figure 4.41. Measured supply (T_v) and return temperature (T_r) and outdoor temperature (T_a) for the period 4.1-10.1.2000 for the control with microcontroller

During that day at about 14:00 h (timestep 456) the model test turned out negative, so that the controller used the heating curve for the following 24 h. Then, from 23rd December, 14:00 h the predictive adaptive heating control worked continuously.

From the strong oscillations of the supply temperature one can see that the model parameters are still very unstable during the first days. From the 6th day on after the start of the control (26.12.99) the oscillations become less strong. Figure 4.40 shows measured indoor temperature and irradiance in the period 5.1.-7.1.2000. During this time relatively high irradiance occurred, which led to a transgression of the set indoor temperature. The corresponding courses of the supply, return and

outdoor temperature shows figure 4.41.

Already 7 days after the start, a significant reduction of the oscillations arises, since the model parameters are relatively stable then. However, the remaining oscillations are higher as in the PC control, despite of the same pre-setting of the comfort parameter. Several reasons are possible for this behaviour. As shown in the simulation tests, the control is relatively robust at measuring errors of the model inputs but sensitive at errors of the model output. As shown in tables 4.4 and 4.5, the indoor temperature sensor used for the microcontroller is less precise than the one for the PC control. Another reason could be that more disturbances through door opening occur in the reference room used for the microcontroller. Furthermore the internal calculation in the microcontroller uses floating point variables of single precision instead of double precision in the PC.

Summary and discussion of ISFH results

The report on hand presents the work carried out in the frame of the project "Development and Test of Modern Control Techniques Applied to Solar Buildings" funded by the European Commission. The aim was the development of an algorithm for the predictive and adaptive heating control in buildings with high solar gains. The developed algorithm has been investigated in a simulation environment and test buildings. The tests showed that the chosen procedure is suitable in principle. Despite of the high dead times and time delays, which represent a big problem for conventional controls, the developed algorithm is acting excellently because of the prediction of the system behaviour.

An implemented model identification learns the dynamic building behaviour during the control process. So, no pre-information about the building structure is necessary. Different investigations were executed concerning the model and the identification procedure. An ARX-model and an identification of the parameters with the recursive least squares method with forgetting factor was found to be most suitable for this application. This has been proven in experiment during a 5 month test period with very different conditions. The chosen limitation to three model inputs results from the demand on low costs for the necessary hardware. The tests into simulation and experiment showed however that the algorithm reacts correctly also at existence of considerable unmeasured disturbance variables.

With the help of simulation tests the influence of different parameters act on the control behaviour. These parameters must either be predefined or can be changed during operation by the user. In addition to the set value of the indoor temperature a comfort parameter has been introduced. With this parameter, the user can choose whether he wishes to have more comfort or to save energy.

The calculation of the supply temperature with a heating curve and the control of the indoor temperature with thermostatic valves on the radiators served as reference system for a quantitative assessment. This system was installed in the test buildings before. The experiments showed that this reference is already on the lower limit of the energy consumption. Despite of this high standard, the developed control leads to energy savings, even at a high comfort requirement. The savings result primarily from the prediction of the indoor temperature from past measurements of the supply and outdoor temperature and the irradiance. So, an earlier reaction to the danger of overheating could be achieved. The height of the savings depends on the chosen reference (type of thermostatic valve) and the dynamic behaviour of the heating system and the building.

The method of predictive control was extended by the consideration of future disturbances (irradiance and outdoor temperature) in the indoor temperature prediction. The aim was a better use of passive solar gains and the prevention of overheating due to an earlier reaction. For the test buildings with their heating system the contribution of this extension is relatively small. The simulation tests showed advantages concerning energy saving and comfort improvement particularly for buildings with more sluggish heating systems and larger window areas.

A comparison between different weather prediction possibilities showed that the approach used in the algorithm should be improved. The prediction of the outdoor temperature works very well. However its prediction is of less importance for the energy saving. The prediction of the insolation still remains a difficult task. Simulations with an "ideal" prediction showed a considerable potential to save energy when the insolation prediction is improved. The modular structure of the algorithm allows to replace the weather prediction by a more efficient algorithm or external data later.

The experimental investigations have firstly been carried out with a personal computer in one of the test houses of the ISFH in Emmerthal/ Germany. They showed an excellent control behaviour of the algorithm also under the more difficult practical conditions. A direct comparison between the developed and a conventional heating control for an experimental quantitative assessment was

not possible, however. Qualitatively, one can state that the developed control leads to energy saving because of the reduced distribution losses, which result from the mostly lower supply temperatures. Furthermore, comfort improvements could be stated qualitatively, too. Peaks in the heating power can be avoided by limiting the allowable supply temperature step.

The developed and optimized algorithm has been implemented in a microcontroller. The device was already available on the market with a conventional control. So, general tasks like the data management and the user communication could be solved with existing software. An experimental test has been carried out in one test building of the ISFH. The controller showed that it is working in principle. However, the control behaviour was a little worse than for the PC-control. It is assumed that the precision of variables in the microcontroller is the reason for that behaviour. Furthermore the positioning of the indoor temperature sensor plays an important role.

The tested microcontroller is available as prototype. It fulfills the requirements concerning a low price and a simple operation. The costs of the complete device are increased by the cost for the irradiance and the indoor temperature sensor, compared to a conventional controller. As shown in the simulation tests, no precise sensor is necessary to measure the irradiance. The used control concept does not require substantial structural changes in the heating system. It can also be transferred to large buildings. Furthermore, the control can be extended to include a ventilation or shading system.

Chapter 5

Work performed by FUL

Authors: Michaël Kummert, Philippe André

5.1 Specifications (Task 1)

As explained in the project programme, the research was based upon a development and cross-comparison of innovative controllers applied to solar buildings. In order to allow an effective exchange of controllers in view of their application on several buildings by the different partners, it was considered as crucial to define, at the early phase of the project, the necessary specification that should make possible the prescribed exchange.

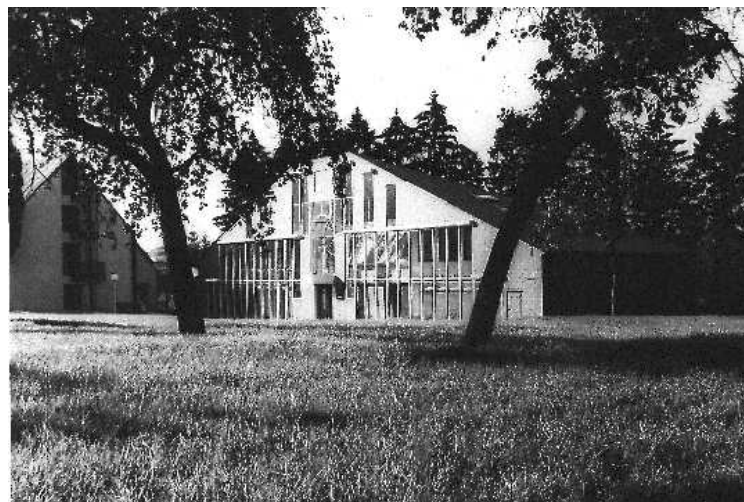


Figure 5.1. General view of FUL's passive solar building

The definition of the specifications was mainly a collective work that took place during the kick-off meeting in Brussels and that was definitely concluded at the first co-ordination meeting in Hameln. Specific input of FUL partner to the discussion and propositions concerned the following items:

- Agreement on programming language and simulation tools. Building, HVAC and control simulation would be based upon TRNSYS [KB⁺94] (either as such or through encapsulation

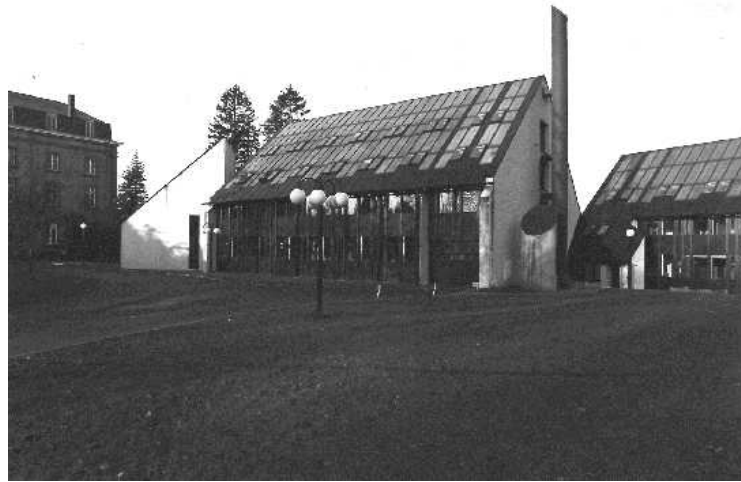


Figure 5.2. General view of FUL's active solar building

within Simulink [Inc97] blocks). Experience of FUL in the use of TRNSYS simulations was presented and offered to the other partners.

- Agreement on optimisation procedure. It was agreed between the partners to develop the innovative algorithm using the Matlab [Mat96] program. Again, experience of FUL with this programming language was offered to the partners.
- It was also decided among the partners to develop the control algorithm by means of an efficient communication between the TRNSYS simulation program and the Matlab optimisation tool. This specific problem was analyzed by FUL and a synthesis of the communication possibilities as well as an example are given in a report produced during the project.
- Test facilities and building system to be tested. The test facilities offered by the different partners were presented during the kick-off meeting. FUL presented the two buildings which were the objects of the project:
 - a passive solar building on which the application of predictive control possibly associated to the use of neural networks had to be tested.
 - an active solar building on which the application of expert systems (possibly associated with fuzzy logic) to the supervisory control of solar system was looked for. Concerning this second building, and after discussion with the partners, it was felt difficult to use it as a testing bed for other algorithms if staying at the supervisory level. Consequently, it was decided to restrict the application of the expert system paradigm to "local" control loops. Later it was proposed that the expert control would be applied to the optimisation of the short -term heat storage device management in mid-season.
- Interface characteristics and communication protocols. In order to allow an efficient exchange of algorithm between the partners, the input/output characteristics of the controller routines were to be specified. This was discussed at the kick-off meeting and the selection of inputs/outputs was definitively approved at the second meeting in Hameln. As shown below, development of FUL's algorithm was carried out according to these specifications. At the hardware level, it was decided between the partners that the communication problem be-

tween the developed controllers (Matlab routine) and the system to be controlled should be solved by each partner on his side. FUL solution includes the following features (fig. 5.3):

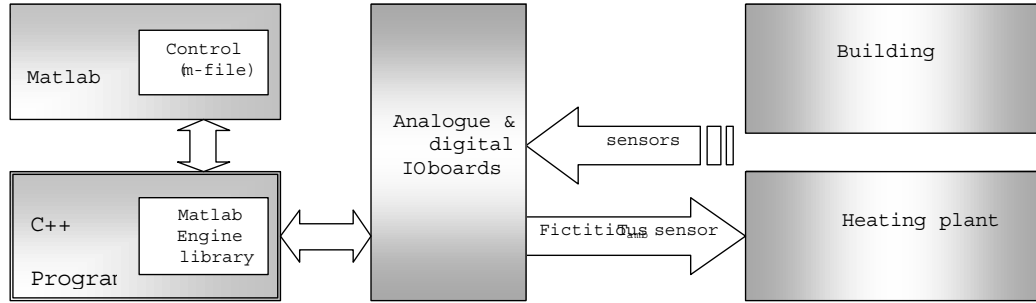


Figure 5.3. Block diagrams of the hardware / software communication procedure. FUL passive solar building.

- calculation (by the controller) of the optimised water supply temperature
- using the building heating curve in reverse mode, calculation of the fictitious ambient temperature which is corresponding to the optimised supply temperature
- replacement of the existing ambient temperature sensor by an voltage controlled resistor which mimics the fictitious ambient temperature
- connection of the fictitious temperature sensor to an electronics board connected to the data acquisition board located inside the PC.
- Evaluation criteria during the testing phases. The proposal for a cost function to compare different controllers performance was prepared by FUL and presented to the partners during the Hameln meeting. The proposed cost function combines the energy consumption of the conventional heating, ventilation and air conditioning system and the cost of discomfort. The latter is based upon Fanger's theory (PPD and PMV indices). Those quantities are computed with a variable clothing, which is equivalent to suppose that the mean building occupant can adapt his/her clothing in a given range. A Matlab file was produced to compute the PPD index with a variable clothing.

5.2 Development of algorithms by FUL (Task 2)

According to the work programme, FUL was responsible for the development of two paradigms:

- predictive control algorithm
- expert control algorithm

5.2.1 Predictive control

One activity of FUL in Task 2 was concerning the development of a specific predictive controller applied to the HVAC control system of solar buildings. The development was carried out according to the following steps:

1. development of an adequate mathematical model of the system to be controlled,

2. development of a predictive/optimal controller,
3. implementation in a simulation environment.

5.2.1.1 Development of an adequate mathematical model of the system to be controlled

The development was carried out in two steps:

- model of the building
- model of the heating system

For both approaches, a state-space approach was selected because of the better suitability with the predictive/optimal control formalism. On the other hand, the development was of course led by the experimental object which would serve as the test-bed for the controller i.e. FUL's passive solar building. A (relatively small) part of the building (a series of two offices) was selected for the experimental phase. Later on, the model was adapted to other buildings.

Building model [KAN96]

The building model considers a second order representation of the walls and the parameters of the model are calculated according to an analytical procedure. The development of the model proceeded in two steps:

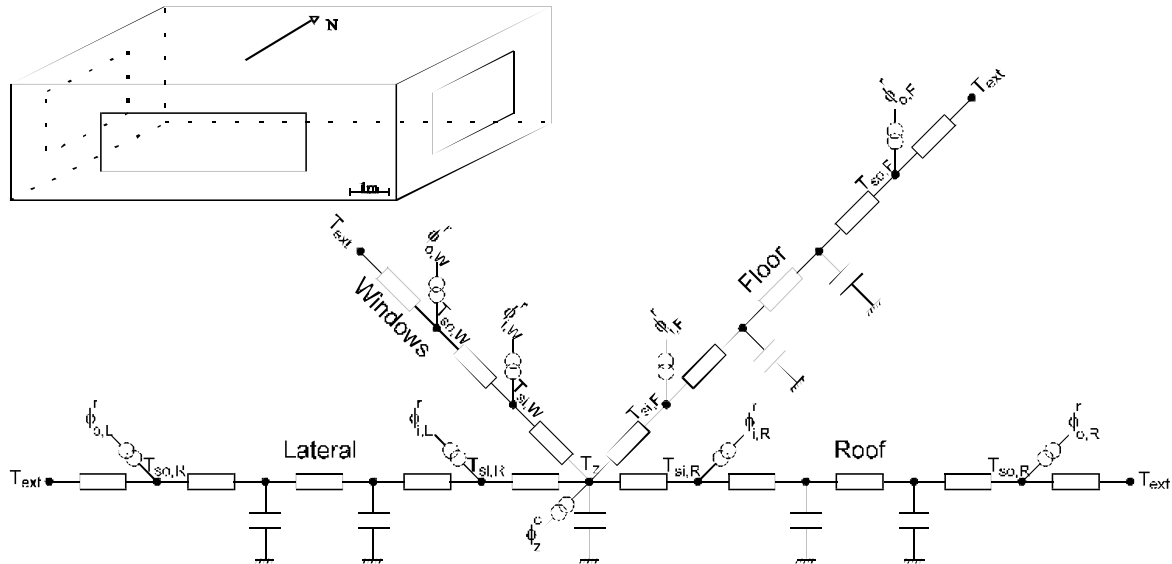


Figure 5.4. Example of a one zone model

1. Development of low-order model for capacitive walls.

Low-order was an objective for the model to remain sufficiently parsimonious in view of integration within an industrial controller. Different configurations (1 node, 2 nodes, and

3 nodes) were compared. Models with fictitious (or "algebraic" i.e. without any thermal capacitance walls) were also introduced. As a conclusion, a two-node model appears to offer the best compromise in view of the application.

2. Development of a low-order building zone model.

The approach considered here involved the connection of the different wall models calculated in the previous step around a "central" node representing the thermal capacitance of the air of the zone. At the end, the building model is made of a "star" network with one branch for each individual wall. Each wall is represented by two state variables and two additional nodes, which represent the wall surfaces. These have no associated thermal capacity and are used to introduce the radiation heat fluxes, which are distributed according to area-absorptance weighted ratios. Fig. 5.4 shows the resulting model for a one-zone test-cell model.

HVAC model

The University of Liège was commissioned for the development of specific HVAC models. The development considered the following components: pipe (optional), radiators and thermostatic valve. The boiler was not considered in the scheme as it is supposed to deliver a constant supply temperature, as far as its maximum power is not used. On/off control of the boiler was supposed not to affect the optimisation of the supply temperature.

Development was carried out using the EES software [KA98a]. Afterwards, translation of EES routines into TRNSYS types was engineered. Simplified versions were produced for integration within the optimal controller.

The radiator is modelled as a single node and heat emission characteristics are linearised. The average temperature between radiator (T_R) and water supply (T_{ws}) is used to compute the power emission. Heat flux is directed to air and to wall surfaces according to a fixed ratio. The radiator equation is written as:

$$C_R \frac{dT_R}{d\tau} = UA_{R,c} \left(T_a - \frac{T_R + T_{ws}}{2} \right) + UA_{R,r} \left(T_{ms} - \frac{T_R + T_{ws}}{2} \right) + \dot{Q}_w (T_{ws} - T_R) \quad (5.1)$$

With

C_R	... radiator thermal capacity $\frac{J}{K}$
$UA_{R,c}, UA_{R,r}$... radiator radiative and convective heat exchange coefficients $\frac{W}{K}$
T_R	... radiator temperature, considered equal to water return temperature (T_{we}) $^{\circ}C$
T_a, T_{ms}	... resp. air and mean surface temperature of the zone $^{\circ}C$
T_{ws}	... water supply temperature $^{\circ}C$
\dot{Q}_w	... water capacitive flow rate $\frac{W}{K}$

5.2.1.2 Development of a predictive/optimal controller

The controller was developed according to a combination of the predictive and optimal control theory:

Optimal control:

a "cost" function is minimised over a period (typically 12...24h) called the "optimisation horizon". The result of the calculation is a sequence of optimal control signals, in this case the water supply (to the radiators network) set-point.

Predictive control:

To reduce the influence of modelling and forecasting errors, a receding horizon is used, i.e. the optimisation is repeated with a period smaller than the optimisation horizon (typically one hour). Consequently, only the first value of the optimal control hourly sequence is applied and optimisation is re-evaluated every hour. Constraints are related to physical limits on the supply temperature and to the set-points on the building internal temperature.

The controller is made of a number of components (fig. 5.5):

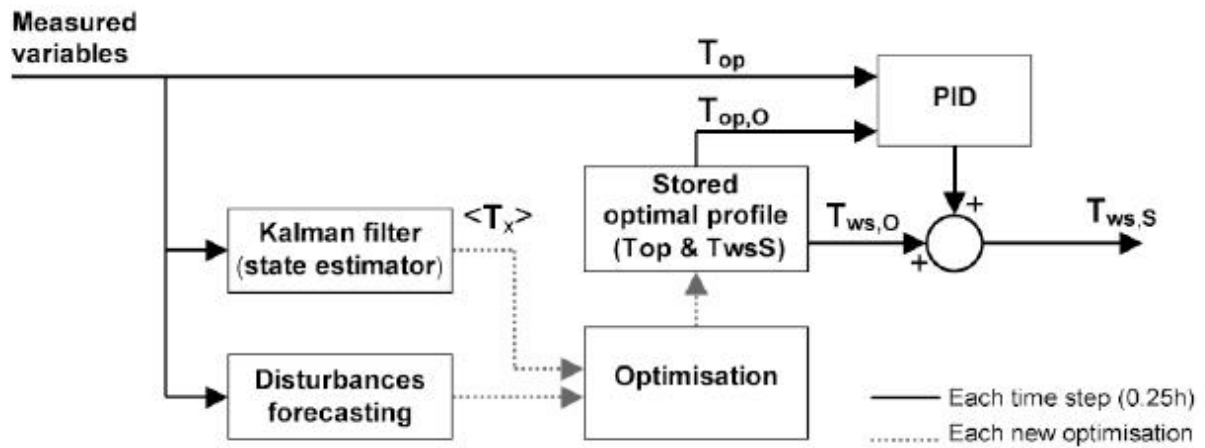


Figure 5.5. Block-diagram of the proposed control scheme

State estimator:

As information about the value of the different state variables of the model (specially wall temperatures) is not likely to be available in a realistic implementation of the controller, a Kalman Filter algorithm (state reconstruction) was prepared in order to provide an estimation of the state space model variables at the beginning of each optimisation period.

Cost function:

Controllers will be evaluated using a cost function, which express their global performance. This cost function must be an expression of the trade-off between comfort and energy consumption. The chosen indicator of thermal comfort is Fanger's PPD [Fan72], while energy cost is considered to be proportional to the boiler energy consumption (Q_b).

In the discomfort cost, PPD is computed with default parameters for non-simulated aspects (air velocity, humidity and metabolic activity). Furthermore, it is assumed that occupants can adapt their clothing to the zone temperature. This method allows modelling a comfort range in which occupants are satisfied. With the chosen value for parameters, the comfort zone covers operative temperatures from 21 °C to 24 °C. PPD is also shifted down by 5%, to give a minimum value of 0. This modified PPD index will be referred to as PPD'. Discomfort cost is represented Fig 5.6. This gives, respectively for discomfort cost and energy cost (J_d and J_e):

$$J_d = \int (PPD[\%] - 5) \quad (5.2)$$

$$J_e = \int \dot{Q}_b \quad (5.3)$$

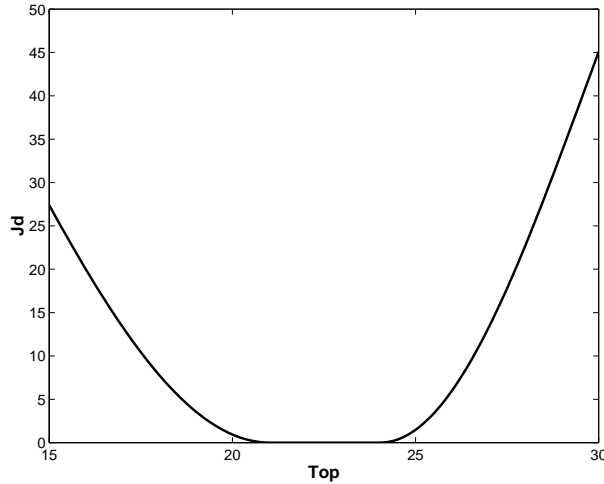


Figure 5.6. Discomfort cost

The global cost (J) is a weighted combination of both:

$$J = \alpha J_d + J_e \quad (5.4)$$

The principle of minimising a cost function is the basis of optimal control theory. It seems natural to use the same cost function in the controller than the one that will be used to evaluate its performance afterwards. The cost function implemented in the controller is a quadratic-linear function, where the quadratic term is an approximation of PPD' and the linear term is exactly J_e . It is detailed in an earlier paper [KAN97].

Disturbances forecasting:

optimal/predictive control requires the knowledge of the disturbances profile over the optimisation horizon. Two major sources of disturbances affect the behaviour of the controller: meteorological data and internal gains.

- Internal gains are related to occupancy schedules, which are well known in office buildings. The situation would be more difficult in residential dwellings, but the use of past observed daily and weekly schedules can still be used.

- Meteorological data:

The first retained approach attempted to use a neural network-based algorithm [KAGN98] to obtain meteorological forecasting, using locally measured data. However, the performance did not justify the computational power involved compared to the simple use of previous day recorded data.

In simulation, perfect forecasting and the use of the previous day were compared to allow an evaluation of the lower and upper bounds of the controller performance with respect to the quality of available forecasting.

During the experimental tests, the previous day was the default applied solution. However, an innovative solution was also implemented using weather forecasts from Belgian Royal Meteorological Institute. This information is currently used for agricultural activity. These forecasts are available twice a day (morning and afternoon) and concern the 36 hours to come. They provide the following information: ambient temperature, solar radiation, humidity, wind average and maximum speed, rain fall, atmospheric pressure. The time step is 3 hours and

forecasting are given for 14 different regions in Belgium. The use of this forecasting during the last experimental phase has shown that such meso-scale information can greatly improve the quality of forecasting, even if the perfect forecasting is still far from the reality.

Optimisation algorithm:

The problem of finding the control sequence minimising a linear-quadratic cost function for the given linear system can be rewritten as a quadratic-programming problem [KAN97]. This guarantees the existence of a solution and allows the use of efficient projected gradient algorithm. This algorithm was implemented in Matlab Optimisation Toolbox, which was used for the optimal control computation [Gra96]. The system includes 11 state variables. For a 24 steps-ahead optimisation, the total number of variables in the QP-problem is 325, and 397 linear constraints are necessary. Typical computational time is about 40 sec on a Pentium II-350 PC, using Matlab (a C++ equivalent code should run much faster). Memory requirements are not too high since most matrices are sparse.

In the case of perfect modelling and perfect disturbances forecasting, the optimisation should be repeated only at the end of the period on which the cost function was minimised. However, to reduce the influence of modelling and forecasting errors, a "receding horizon" is used, i.e. the optimisation is repeated with a period smaller than the prediction horizon. The prediction horizon and the time step for new optimisation will respectively be referred to as N_H and N_C . Both are expressed in [h].

In this study, optimisation horizons (N_H) ranging from 12 to 24 h were considered, and this optimisation was repeated up to every 6 hours (N_C range : 6..12h). In the case of a 24h-ahead prediction repeated every 6 h, for example, only the first six values of optimal control signals are applied.

PID controller:

When a new optimisation is computed, a feedback from the real system is present, since the estimated state of the system based on measured outputs is used. During the period between two optimisations, the computed optimal control profile is applied without any feedback from the real system. In the case of large forecasting errors, this can lead to a system evolution being far from the predicted one and hence far from "the optimum". To compensate for these errors, a feedback controller is cascaded with the optimisation. This controller is a conventional PID with anti-windup and uses the base time step (0.25h).

5.2.1.3 Implementation in a simulation environment

A controller developed according to the scheme presented here above has first to be tested in numerical simulation. Therefore, a common "test shell" was developed with the objective of providing a common environment allowing to:

- test the controller developed by the different partners
- ensure the controller developed will be exchangeable, even when connected to the specific hardware of each Institute.

The simulation environment was developed in the TRNSYS modular software and made use of the following components:

- Type 151: special component developed for the purpose of establishing the connection with the controller, developed using Matlab

- Type 56: multizone building. This is the classical model of TRNSYS
- Type 182: radiator
- Type 183: thermostatic valve
- Type 201: user behaviour and natural ventilation controller. The purpose of this component is to make the simulation more realistic as most buildings have windows that can be opened by occupants. To take this possibility into account, a rough model of the user behaviour and natural ventilation was developed (TYPE 201). The user is supposed to open windows when the temperature rises above the maximum comfort temperature (24°C). She/he is supposed to close them when the temperature falls below the lower comfort bound (21°C). The natural ventilation is modelled by a variable infiltration rate in TYPE 56. This type is optional in the simulation and can be removed if no windows can be opened by occupants.

A general view of the simulation scheme is given by fig. 5.7

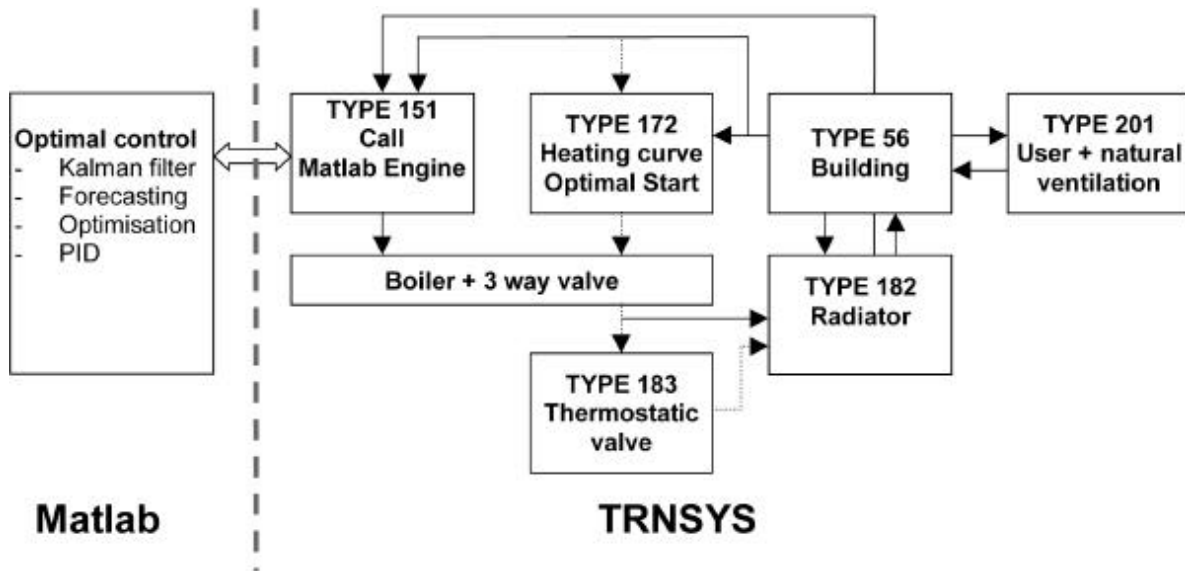


Figure 5.7. Controller simulation scheme

5.2.2 Expert controller

Another activity of FUL within task 2 concerned the development of a solar controller based upon the expert system paradigm. This development was closely linked with the testing activity to be carried out on the FUL active solar building. Because of the very particular nature of this building, it was decided very early in the project not to focus on this building as a whole but, rather, to test the applicability of the expert control approach on specific subsystems of the building, namely the management of the short-term storage device in mid-season.

The development of the controller included the following steps :

- Development of a software environment to host the controller. This software made use of the C++ language and is based upon an object-oriented data structure.

- Development of a simulation environment in order to test different control strategies and paradigms.
- Development of the expert control knowledge base. Expert control consists of a set of rules which are "fired" when specific conditions are fulfilled. Continuous evaluation of rules is performed by an inference engine connected to the central data structure. Extraction of realistic rules was made possible through interviews of the technical manager of the building.
- Connection of the expert control knowledge base to an inference engine. Therefore, an existing C++ based inference engine, specially developed for building control applications was used (RICE [Jag], developed by TNO, The Netherlands).
- Implementation of the expert controller, first in the simulation environment, then in the in-situ testing environment.

5.3 First testing phase of the different controllers at FUL (Task 3)

The first testing phase was scheduled to take place, first in the simulation environment, then in the real buildings. The common testing in the simulation environment was made easier by the use of the flexible test-shell described here above. Later on, the test-shell was improved in order to provide a calling sequence to the controller (developed in Matlab) compatible with a real time call. This ensured the exchangeability of controllers, not only in simulation but also for the testing in-situ.

5.3.1 Predictive control (passive solar building)

5.3.1.1 Simulation tests

During the development of the algorithm, extensive tests were carried out at different stages:

- test of the building model, in order to check the ratio accuracy/parsimony of the model. This ended up with a 2nd order model for the walls representation
- test of the HVAC models required for integration within the global model. This testing took place by means of the EES software [KA98a] and was carried out by the University of Liège
- test of the controller against the thermal behaviour of the building calculated by a simulation program (TRNSYS). This testing was realised in three steps :
 - test of the optimal controller applied to the building alone, assuming a "perfect" HVAC system

The optimal controller was first applied to the test-cell presented here above [KAN97] and then to a part of FUL's passive solar building [KAN98]. Fig. 5.8 shows the result of the optimisation for 3 typical days (winter, summer, mid-season) : temperature and optimal heating/cooling profiles (perfect HVAC system).

- test of the optimal controller applied to the building and heating system. In this case, the following components were included within the heating system [KAN99]:
 - * radiator and thermostatic valve
 - * three way valve and boiler
 - * PID controller to provide a feedback correction to the supply temperature.

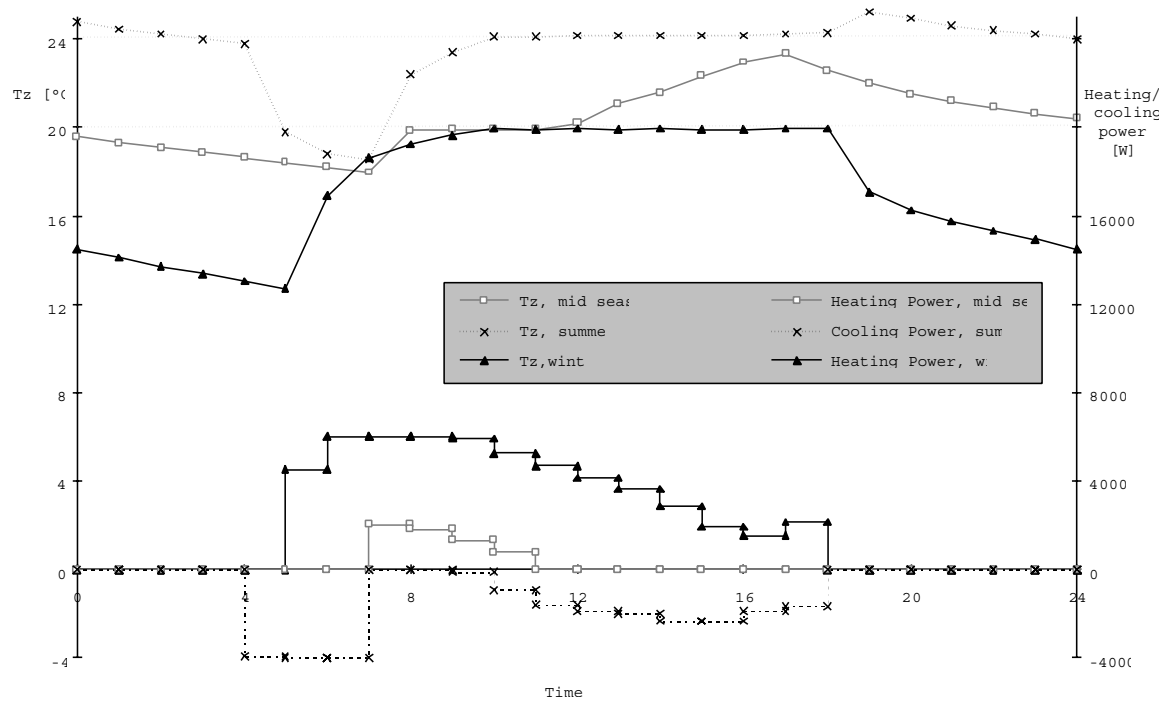


Figure 5.8. Optimisation results for three typical days. Building simulation.

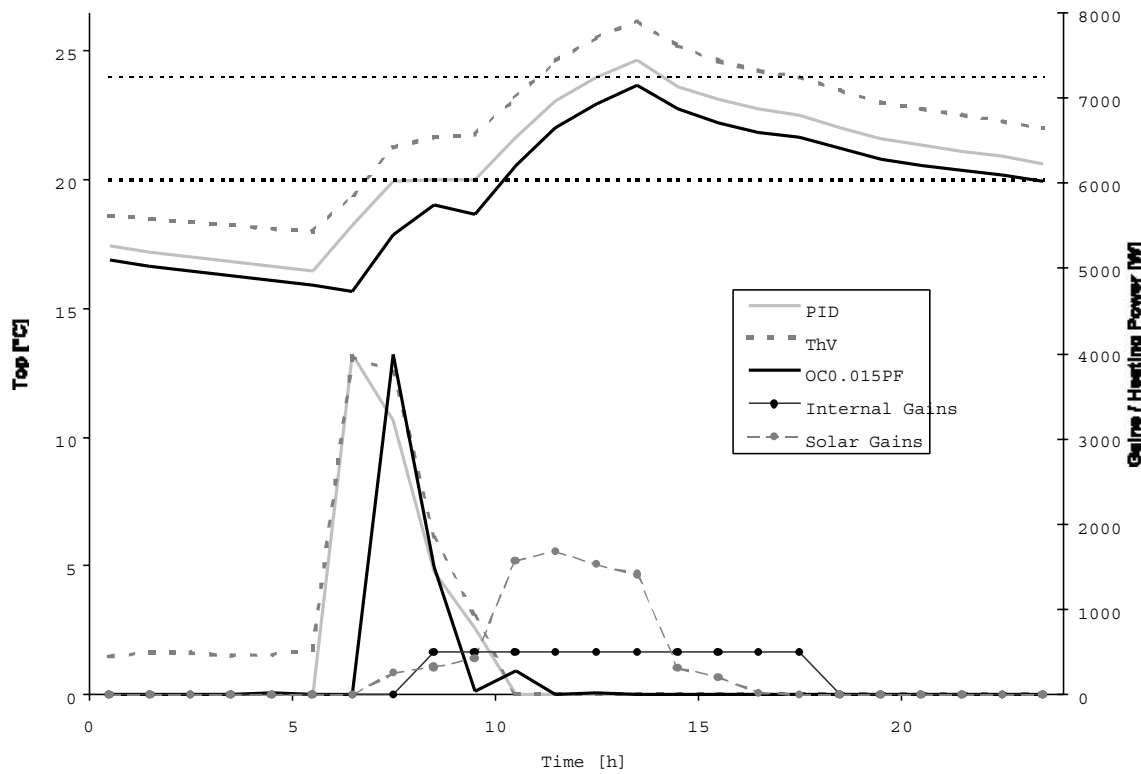


Figure 5.9. Optimisation results for a typical warm mid-season day. Building and HVAC simulation

Fig. 5.9 shows the optimal profiles (heating) for a warm mid-season day: heating is needed in the morning, but internal and solar gains induce overheating during the afternoon. The optimal controller allows to anticipate the phenomenon and this leads to both comfort improvement and energy savings (OCO0.015PF means optimal controller, perfect forecasting).

- Systematic comparison of the optimal controller with a classical control system.

Several simulations were realised using both controllers (conventional and optimal) with different parameters. All simulations were realised with real measured meteo data from Uccle (Brussels), in the years 1985-1986.

Meteorological data

First, a "typical meteo set" for heating period was constructed. This data set contains four typical weeks concatenated. It served to test different settings of the optimal controller and to study its behaviour in more details. In a second phase, a whole heating season (30 weeks) was used, to assess the optimal controller performance and to compare it with the conventional controller. Data sets characteristics are presented Table 5.1. (G_h is the global horizontal solar radiation)

Table 5.1. Meteo data sets

Description		Meteo variables			
Temperature	Sunshine	$T_{amb,min} [^{\circ}C]$	$T_{amb,max} [^{\circ}C]$	$T_{amb,avg} [^{\circ}C]$	$G_{h,avg} [\frac{W}{m^2}]$
cold	cloudy	-16.0	-1.7	-8.0	31
cold	sunny	-9.9	6.8	-1.8	88
warm	sunny	7.2	21.7	14.0	177
warm	cloudy	4.8	15.2	11.5	61
Typical set		16.0	21.7	3.8	89
Heating season		-10.4	26.2	4.2	67

Conventional controller

Traditional heating control strategies include a feed-forward action on water supply temperature by the so-called "heating curve" and a feedback action on water flow rate by a thermostatic valve. Moreover, up-to-date controllers use an optimal start algorithm. Our reference control strategy combines these three features. The heating curve consists actually of two different curves, giving the required water supply temperature to maintain desired setpoints (night and day) in the reference zone. In this case, setpoints were fixed to 15 °C (night) and 21 °C (day). Furthermore, the "day" heating curve is slightly over-estimated to take into account the dynamic evolution of the building. Indeed, these curves are calculated in steady-state regime, which is never the case in practice. The building structure is always colder than in the corresponding steady-state, since a night set-back is applied. The thermostatic valve has a proportional band of 2 °C, and different settings of the thermostat are compared.

The optimal start algorithm uses a non-linear function proposed by Hittle and O'Connor ([SAH89]) to estimate the recovery time from night set-back. This relation uses the current temperature of the zone, the ambient temperature, and the desired final temperature. Parameters for this building were identified by a regression using TRNSYS simulation results. Two different parameters sets were kept (the second one gives a more conservative estimate of the return time).

Different conventional solutions are referred to as 'Cc' for the conservative parameter set, and 'Cr' for the "risky" one.

Comfort/Energy trade-off

The cost function implemented in the optimal controller is presented in eq. 5.2, 5.3 and 5.4. α is a parameter which allows to give more or less importance to comfort versus energy consumption.

As above-mentioned, the discomfort cost (J_d) implemented in the controller is an approximation of PPD' (PPD shifted to give a minimum of 0 and not 5% and computed with variable clothing). This value is integrated and can be expressed in [%h]. If we express the energy cost (J_e) in kWh, α units are $[\frac{kWh}{\%h}]$. α can thus be interpreted as **"the energy quantity (expressed in kWh) that can be consumed to reduce the percentage of dissatisfied people in the building by 1% during 1h"**. Despite this fact, the ratio between total energy consumption and integrated value of PPD' on a long period will not be equal to α . This is illustrated in Table 5.2 and Fig. 5.10, which compare the total energy consumption and integrated PPD for the typical meteo data set, and for different α values in the range [1;10].

Table 5.2. J_e and J_d for different α values

$\alpha[\frac{kWh}{\%h}]$	$\frac{J_e}{J_d}$	$J_e[kWh]$	$J_d[\%PPD'h]$
10	68.6	550	8
5	62.0	539	8.7
4	54.2	537	9.9
3	39.2	533	13.6
2	22.3	526	23.6
1	7.9	511	65

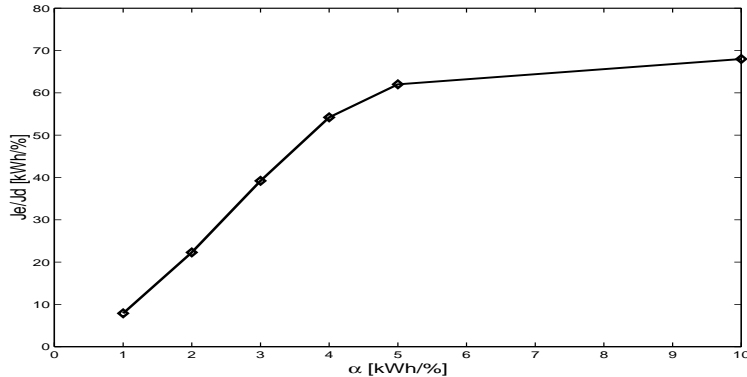


Figure 5.10. J_e and J_d for different α values

It is clear that α is linked to $\frac{J_e}{J_d}$, but the value of this ratio on a long period (e.g. one heating season) is not easily predictable. The relation between these two variables is even not linear: a "saturation" happens for high α values, when the upper limit of comfort achievable with the heating plant is reached. Furthermore, the curve is different if other controller settings are changed (e.g. N_H and N_C).

Optimisation horizon and "new computation" time step

Every N_C hours, a new optimisation is computed, minimising the cost function on N_H hours. This implies that only the first N_C optimised setpoints are applied. This principle, known as "receding horizon", is commonly applied in predictive control.

The selection of N_H and N_C depends on the building and on the model and forecasting quality. N_H must be long enough to allow an effective anticipation of disturbances. This means for example that N_H must be larger than the recovery time from night set-back in the worst case. It should be

possible as well to under-heat the building during the morning in the case of afternoon overheating. This requires to reduce heating before 7 AM because of an overheating which can occur after 4 PM case, which implies a N_H value greater than 9 hours.

We tested different values for N_H (24;20;18;16;12;8) and N_C (24;12;8;6). In the case of perfect weather forecasting, no difference was noted between different N_C values smaller than 12 h. Relatively small modelling errors can explain this: linearisation of the radiator power, reduced order of wall models and constant infiltration rate. When imperfect forecasting was used, N_C values larger than 8 hours give a poor behaviour of the optimal controller, 6 hours giving even better results.

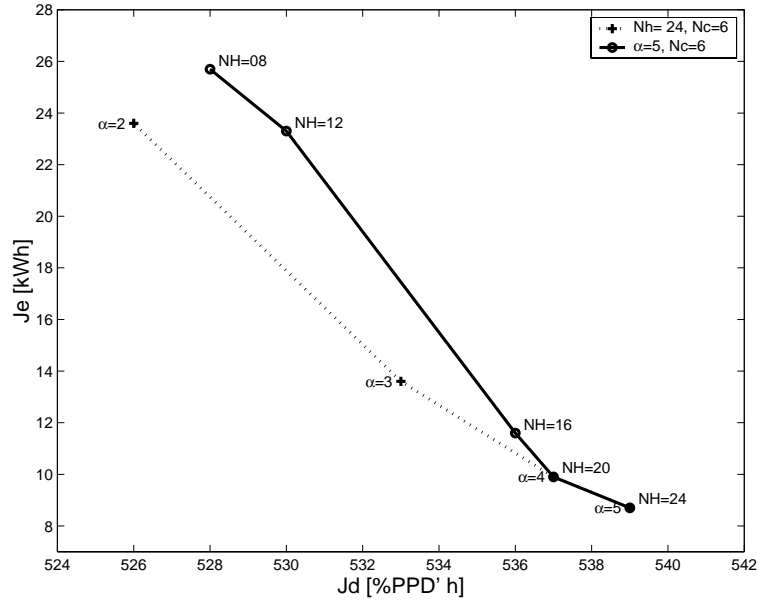


Figure 5.11. Performance decrease, when N_H is reduced

Fig.5.11 shows the decrease in controller performance caused by a reduction of the optimisation horizon, for a constant N_C value of 6 h ($\alpha = 5 \frac{kWh}{\%h}$). This plot represents J_d versus J_e . The closer a controller is to the lower left corner, the better its performance is. The dotted line shows the trajectory followed by results when varying α for constant N_H and N_C . For constant N_C and α , when N_H is reduced, the trajectory is different and shows a poorer performance. N_H values greater than 18 h seem to be suitable, but the performance of the controller decreases rapidly when N_H falls below this value. The difference may seem insignificant (e.g. for a similar discomfort of 20, the increase in energy consumption is about 1%), but the comparison with a conventional controller must be taken into consideration. If savings of the optimal controller are 5%, this 1% absolute loss represents 20% of possible savings.

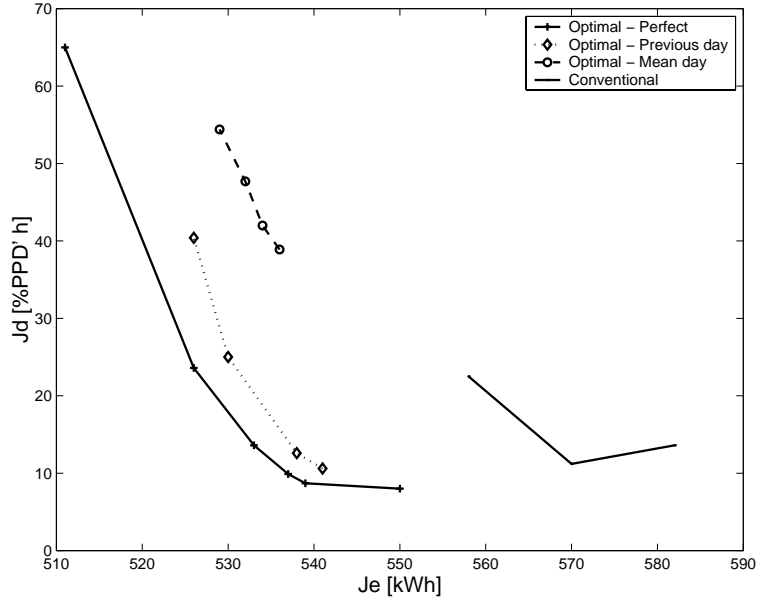
Forecasting quality

Three meteo forecasting types were investigated for the typical meteo data set: Perfect forecasting, use of the previous day and use of a "mean day". The latter is constructed by averaging all days on a hour-by-hour basis. This forecasting is of poorer quality, as shown in Table 5.3. This table presents statistics on two relevant variables: the ambient temperature (T_{amb}) and the total solar radiation entering the sunspace (G_{SS}). Statistics on forecasting errors show that the error standard deviation reaches 80% of the variable standard deviation for G_{SS} , and about 100% for T_{amb} .

Fig. 5.12 shows the effect of forecasting errors on the controller performance. Different values of α are used (1 to 5) for each forecasting case. The performance decrease resulting from the use of "previous day" forecasting is not too important: for a discomfort about 12, the energy consumption

Table 5.3. Forecasting error statistics

	Variables		Error (previous day)		Error (mean day)	
	$T_{amb}[^{\circ}C]$	$G_{SS}[W]$	$T_{amb}[^{\circ}C]$	$G_{SS}[W]$	$T_{amb}[^{\circ}C]$	$G_{SS}[W]$
min	-16	0	-7.9	-8960	-17.3	-3884
max	21.7	12016	10	10767	16.6	8226
avg	3.8	1062	0.3	4.26	0.3	-28
std dev	9.3	2327	3.44	1760	9.1	1886
	$stddev_{error}/stddev_{series}$		0.37	0.76	0.98	0.81

**Figure 5.12.** Influence of meteo forecasting quality

rises from 533 to 538, which represents a 1% increase. The difference increases for lower α values (higher part of the plot). This can be explained by the greater freedom left to the controller for small α values: achievable gains are more important in this case, but the optimal zone temperature profile is very dependent on meteo conditions. In this case, a forecasting error has a larger influence. The comparison with the conventional controller shows that the optimal controller still gives a better performance despite imperfect forecasting.

In the case of "mean day" forecasting, the controller performance is quite poor, and low discomfort cost values cannot be attained. This comparison shows that the quality of meteo forecasting is an important factor for the controller. The use of the previous day seems to be a satisfying solution, which is rather surprising. This conclusion has to be confirmed on a longer data set (this graph concerns the "typical set", but next section will confirm these results for the whole heating season).

The PID plays a determinant role in the case of imperfect forecasting. Table 5.4 gives statistics on the PID action for the three forecasting types. Three variables are considered: T_{op} , T_{ws} and \dot{Q}_b (zone temperature, water supply temperature and boiler power). First, the mean value and standard deviation are presented for each variable. For T_{op} , the error between the desired value by the optimal controller and the real value is analysed. For T_{ws} and \dot{Q}_b , the PID correction (between the setpoint given by the optimisation itself and the final setpoint given to the three-way valve) is considered. Values given for \dot{Q}_b are estimated, since the real control signal is T_{ws} (the controller has no direct influence on \dot{Q}_b).

Table 5.4. PID action (entire typical data set). T_{op} and T_{ws} are in $^{\circ}\text{C}$, in \dot{Q}_b Wh

	Perfect forecasting			Previous day			Mean day		
	T_{op}	T_{op}	\dot{Q}_b	T_{op}	T_{op}	\dot{Q}_b	T_{op}	T_{op}	\dot{Q}_b
avg	19.5	36.1	830	19.5	36.2	831	19.5	36.1	833
Stddev	2.5	25.2	1252	2.5	25.1	1249	2.6	25.3	1273
Stddev of error	0.06			0.25			0.26		
Stddev of PID correction		2.84	171		6.3	336		9.0	469

The PID correction remains relatively small for the first case, but the results for imperfect forecasting show clearly that the PID is important.

Fig. 5.13 illustrates the PID behaviour on two days for which the "previous day" forecasting was rather incorrect. It must be noted that the PID is bounded by some "common sense" rules. T_{ws} is for instance not corrected if T_{op} is lower than the expectations but still higher than the lower comfort limit. This happens during the first day, when the expected sunshine is higher than real one. The PID is allowed to correct the temperature to $21.5 ^{\circ}\text{C}$, but not higher. Actually, a PID correction is only possible if the zone temperature is lower than the lower bound of the comfort zone and if the building is occupied or in the "morning pre-heating" phase. In all other cases, the PID can only decrease T_{ws} .

Comparison on an entire heating season

Fig. 5.14 uses the representation introduced here above. (J_d vs. J_e) to compare optimal and conventional controllers. As mentioned in conventional controller description, two different parameter sets are used for the optimal start algorithm. They give the two curves labelled 'Cc' and 'Cr'. Different settings for the thermostatic valves explain the variations along these curves. For the optimal controller, previous day forecasting is used and different α values are compared. Energy savings for a similar discomfort reach 7 to 9%, which is close to the performance obtained by Nygard-Fergusson [NF90] for stochastic optimal control of floor-heated offices.

These simulation results show that optimal control could be one solution to achieve EC's objective mentioned in the introduction, which is to reduce energy consumption by 7% in 2010 through improved BEMS.

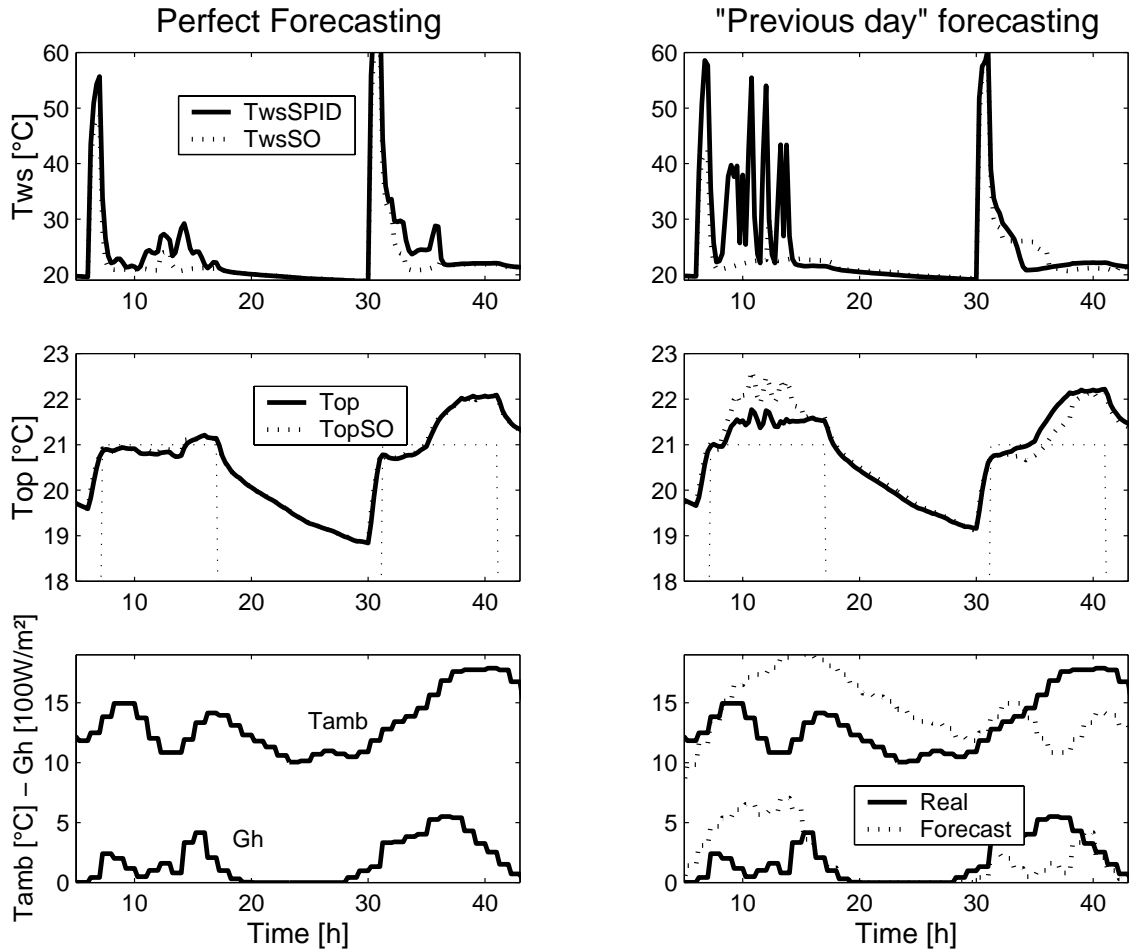


Figure 5.13. PID correction for two typical days, perfect and previous day forecasting

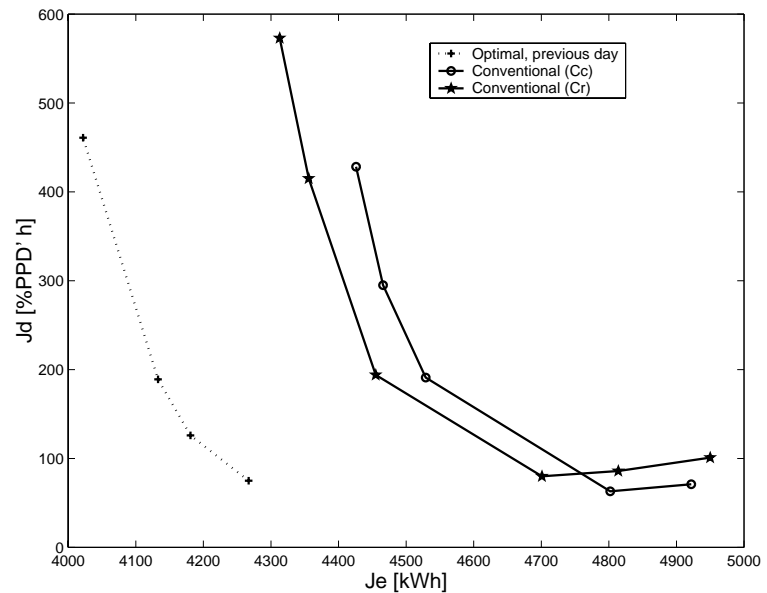


Figure 5.14. Controllers comparison on the entire heating season

5.3.1.2 In-situ testing

In parallel with the simulation test, the building was prepared in order to receive the infrastructure for in situ testing. The building is described in details in a technical report circulated during the project as well as the existing HVAC and associated control systems. The existing controller is a classical feed-forward controller based upon the ambient temperature, which adapts the supply temperature by means of a three-way valve according to a value calculated by the "heating curve". In order to connect the optimiser without introducing too much modification to the existing control system, only the ambient temperature sensor was removed and replaced by a software sensor which represents the fictitious ambient temperature corresponding to the optimised supply temperature. This fictitious temperature is calculated from a reverse use of the heating curve (fig. 5.15).

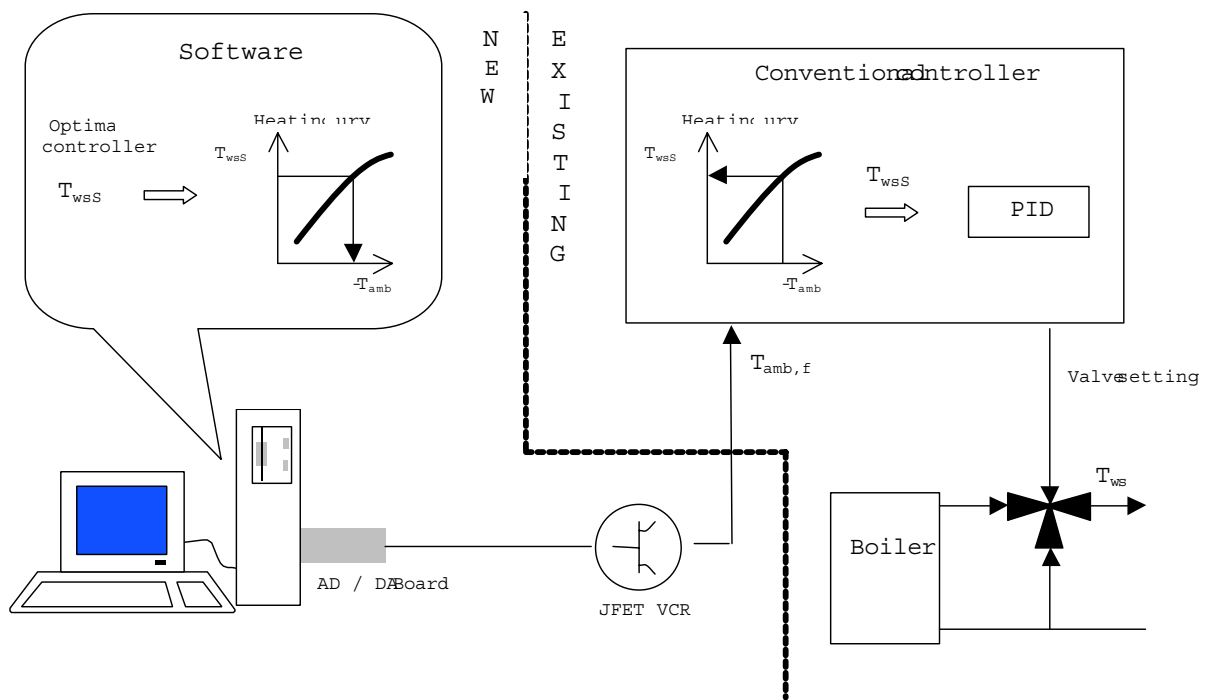


Figure 5.15. Realisation of the optimisation procedure.

The optimal controller is implemented as a Matlab routine interfaced with a C++ control program, which manages the data acquisition sequence. This program is implemented in an industrial PC. Electronic interface to the sensors and actuators is described here above.

The testing phase on the FUL passive solar building started at the end of 1998. The testing procedure was carried out according to the following steps:

- Test of the building with the existing (classical) controller in operation (december 98-january 99)
- Test with the new hardware system (industrial PC) but with a controller equivalent to the classical one (february-march 99)
- Test with the new hardware system AND the implementation of the predictive control algorithm (april-may 99)

The testing was concentrated on two test rooms of the building. The exact determination of the heating power delivered to those rooms was made possible by the installation of flow meters on each radiator present in the rooms.

This first testing phase allowed to identify the remaining software and hardware problems. It showed that the monitoring and control programs were working properly. The different problems observed during the first testing phase were solved during summer'99 and this allowed a second testing phase to take place.

5.3.2 Expert control (active solar building)

First testing of an expert controller to be applied on FUL active solar building was carried out only in simulation. The objectives of the testing were the following:

- to assess the feasibility of connecting an expert system controller, making use of a third-party inference engine, to a conventional simulation program like TRNSYS
- to compare the operation of a conventional controller to that of an expert controller with respect to the following criteria: performance of the system, reliability and robustness, ease of modification of the control rules.

On the other hand, a lot of time was devoted to the preparation of the building in view of the testing phase :

- a new industrial computer was installed together with a new interface board which, allows to communicate with the existing I/O boards
- all sensors and measurements chains were checked. Temperature sensors are Platinum resistance sensors ("Pt 100") which are connected to converters which transfer the resistance value into a current (4...20 mA). All converters were checked for accuracy and stability
- a C++ control program was implemented in the industrial PC. This program encapsulates the object-oriented data structure and establishes a connection with the interface boards. Testing of this program has started with a reduced set of rules, which makes this new controller equivalent to the previous controller.

5.4 Second testing of the control programs at FUL (fall'99), Task 5

After the first testing phase, the different control algorithms were improved together with some modifications on the testing environments to make them better suit with the control program.

5.4.1 FUL's predictive controller

5.4.2 Changes operated to the experimental site

The first testing phase allowed us to identify the remaining hardware problems. These problems were the following:

- Flow-meter measurements show that, even when thermostatic valves are maintained in the fully open position, the flow rate through the 2 radiators in the representative thermal zone are not constant. This has no influence on the controller performance assessment as real flow rates are measured. However, this situation can lead to a decrease in the optimised controller performance as it assumes the flow rate is constant.

- during overheating periods or during night and week-end set back, it appears impossible to achieve a low supply temperature (roughly below 35 °C). This problem affects both conventional and optimised controller and it is a strong limitation to experimental testing, as it prevents a really efficient night set back. Furthermore, as no thermostatic valves are present in the case of optimised control, this relatively high water supply temperature can lead to building overheating with the aggravating circumstance that users cannot act on the system when it happens.

Flow rate variations

A systematic study of the flow rate in radiators was carried out. First, the thermostatic part of the valves were removed from the two radiators in the representative thermal zone to insure that these valves remained fully open. Then, valves of all the other radiators (11 total) in the circuit were opened or closed in sequence. The pressure regulator was set to the highest sensitivity. The Table 5.5 shows the flow rate in each radiator of the reference zone in different situations. Flow rate values are normalised by the nominal flow rate given in technical specifications (45 l/h).

Table 5.5. Flow rate in each radiator of the reference zone in different situations

Situation	q_{vol} BA3	q_{vol} BA4
All valves open	1.2	1.4
Ref room, Hall, meeting rooms and amphi's open - other offices closed	1.35	1.6
Ref room, Hall and amphi's open. Other offices and meeting rooms closed	1.45	1.65
Ref room open, all other closed	2.44	2.53

It is clear that the assumption of a constant flow rate is not true in our installation despite the presence of a pressure regulator. Note that if this regulator is set to the lowest sensitivity, the normalised flow rate in reference radiators can reach 3.5. Considering the above results, it was decided to remove most of thermostatic valves of the concerned circuit during testing of an optimised controller. Only the valves of two offices which are very likely to overheat will be maintained in place. This will insure flow rate variations lower than 13%. In the case of a conventional controller, thermostatic valves will be put back in place on every radiator.

Lower limit on T_{ws}

This problem was exposed during the Athens meeting and the solution of controlling the heating pump in addition to the water supply temperature was discussed. This solution allows the controller to reduce efficiently the heating power to the zone. It has the advantage to suppress electrical consumption when no heating power is needed, which is the case during quite long periods for night setback.

An on/off control of the heating pump was implemented on the experimental building and a simple strategy was established to control the pump. This strategy uses the only output of the optimised controller (T_{wsS} , setpoint for water supply temperature). The pump is switched off if the desired water supply temperature is too low (<35 °C). When it is off, it is only switched on if the desired water supply temperature is high (>35 °C) and if the heating power for next 0.25 h is significant. This power is simply estimated with nominal water flow rate, current room and radiator temperatures. This simple strategy allows to prevent on/off oscillations that could speed up the pump wear. Later during the experimental period, the three-way valve controlling the water supply temperature was replaced, suppressing this problem.

5.4.2.1 Improvement of the controller

The optimal predictive controller uses of a building and heating plant model. Parameters of this model have to be continuously adapted to compensate modelling errors (e.g. linearisation) and real system variations (e.g. windows opening). Furthermore, the application of the controller to a building for which no estimates of the parameters are known would require an initial parameter identification. The task of identifying a state-space model of a relatively high order (11 state variables) "from nothing" is a difficult problem and the priority was given to an adaptation of pre-computed parameters in a first step. The retained approach was to choose some key parameters easily related to system disturbances or inputs and to identify these only parameters, leaving other ones unchanged. In a first step, 3 parameters were considered: windows transmittance, infiltration rate and radiator heat exchange coefficient. First tests show that a significant improvement of the model's accuracy can be achieved by modifying only these 3 parameters. Furthermore, these parameters are associated to different influences on the same output (zone temperature): influence of solar radiation, external temperature and water supply temperature.

5.4.2.2 Experimental results

All experimental results coming from tasks 3 and 5 are described in section 5.5.

5.4.3 FUL's expert controller

First experimental testing made use of a "classical" control strategy consisting of the following elements:

- control of the solar collection is operated by ON/OFF control with respect to a global average solar radiation threshold
- control of storage charge is identical to solar collection control
- control of storage discharge is "manual" and executed by the building operator

5.5 Experimental results and conclusions of FUL (tasks 3 and 5)

Experimental work took place during tasks 3 (1998-1999 winter) and 5 (1999-2000 winter). The experimental tests made essentially use of FUL's passive solar building, where the predictive optimal controller was implemented. Experimental results obtained during both tasks allow a performance comparison of the optimal controller with a conventional and a "reference" controller. During Task 5, a controller exchange was realised with NOA. FUL's controller was implemented in NOA's Passys testcell and NOA's ANN controller was tested on FUL's passive solar building. This document describes the obtained results during both experiments.

5.5.1 Tests on FUL building

5.5.1.1 Data sets description

The data set recorded at FUL during the heating period currently includes about 170 days, mostly during the year 1999. The 1998-1999 heating season ended on 26th of April 1999 and the 1999-2000 heating season started on the 10th of October 1999. Cold winter periods as well as warm mid-season periods are represented in the data set. Table 5.6 sums up the main daily characteristics

of meteorological variables for the retained data set. T_{min} , T_{avg} and T_{max} are respectively the minimum, average and maximum ambient temperatures during the day and $\int G_{south}$ is the daily integrated solar radiation on $1m^2$ of the southern vertical facade.

Table 5.6. Daily Meteo data summary

	$T_{min} [^{\circ}C]$	$T_{avg} [^{\circ}C]$	$T_{max} [^{\circ}C]$	$T_{max} - T_{min} [^{\circ}C]$	$\int G_{south} \frac{MJ}{m^2}$
min	-8.3	-6.8	-5.4	1.3	0.1
Max	11.0	12.7	18.7	14.5	18.6
avg	1.4	4.2	7.1	5.7	5.3
std dev	3.6	3.8	4.4	2.6	5.4

It can be seen that the average temperature of the coldest day (1999/12/22) was $-6.8^{\circ}C$. This day was also the one with the lowest minimum temperature ($-8.3^{\circ}C$) and the lowest maximum temperature ($-5.4^{\circ}C$). The warmest day in average ($12.7^{\circ}C$ on the last day of the heating period, 1999/04/26) also presented the absolute maximum temperature ($18.7^{\circ}C$), while the day with the warmest minimal temperature was 1999/10/10.

The darkest day was 8th of December 1999, while the brightest day was the 25th of February.

During this period, four controllers were alternatively implemented : The conventional controller (Conv), a "reference" controller (Ref), NOA's ANN controller (ANN) and FUL's optimal controller (Opti). Some boiler problems and transitional periods reduce the number of usable days to 50 for the conventional controller, 18 for the reference controller, 17 for NOA's ANN controller and 41 for the optimal controller. The 4 controllers characteristics are described in section 5.2.

Table 5.7 shows the summary of meteo data separately for the 3 periods corresponding to different controllers.

This table shows slightly different characteristics for the temperature, but a significant difference in mean solar radiation between the 4 periods: the sunshine was higher when the ANN controller was tested and mainly when the conventional controller was tested. This is mainly due to the historical succession of different controllers: the first tested controller was the conventional one (reproducing the behaviour of the existing controller). Then the optimal controller was implemented, but the retained data was recorded when the final version of the controller was implemented, in November and December 1999. The reference controller was added in order to provide a "conventional but improved" solution and was tested in December 1999 only, while the ANN controller was tested in early 2000 and benefited from very bright days after a snowfall.

5.5.1.2 Controllers description

Conventional controller

The implemented algorithm mimics the existing heating control scheme in the building. The water supply temperature is controlled by a heating curve varying according to a fixed schedule. The heating curve is designed to maintain $21^{\circ}C$ during day and $15^{\circ}C$ during night (or week-ends). Thermostatic valves are placed on each radiator and set by building occupants according to their preferences.

The good practice when choosing the heating curve in such installations is to overestimate the "day" curve in order to allow a quicker warm-up of the building, leaving to the thermostatic valves the role to maintain indoor temperature below their setpoint. The night heating curve can be slightly underestimated since the building will almost never meet steady-state "night" conditions, but this is not often done.

Table 5.7. Daily Meteo data summary for the 4 controllers

	Conventional controller				
	$T_{min} [^{\circ}C]$	$T_{avg} [^{\circ}C]$	$T_{max} [^{\circ}C]$	$T_{max} - T_{min} [^{\circ}C]$	$\int G_{south} \frac{MJ}{m^2}$
min	-4.1	-0.6	0.8	1.3	0.7
Max	11.0	12.7	18.7	14.5	18.6
avg	2.4	5.4	9.0	6.6	7.4
std dev	3.2	3.3	4.0	3.1	6.3
	Reference controller				
	$T_{min} [^{\circ}C]$	$T_{avg} [^{\circ}C]$	$T_{max} [^{\circ}C]$	$T_{max} - T_{min} [^{\circ}C]$	$\int G_{south} \frac{MJ}{m^2}$
min	-4.1	-2.3	-0.2	2.0	0.1
Max	5.1	6.1	9.3	7.4	9.5
avg	0.1	2.1	4.2	4.1	2.0
std dev	3.2	3.2	3.4	1.6	3.0
	Optimal controller				
	$T_{min} [^{\circ}C]$	$T_{avg} [^{\circ}C]$	$T_{max} [^{\circ}C]$	$T_{max} - T_{min} [^{\circ}C]$	$\int G_{south} \frac{MJ}{m^2}$
min	-8.3	-6.8	-5.4	2.3	0.1
Max	8.1	12.1	17.2	9.1	14.4
avg	1.1	3.8	6.3	5.2	3.5
std dev	4.4	4.4	4.9	1.8	3.9
	ANN controller				
	$T_{min} [^{\circ}C]$	$T_{avg} [^{\circ}C]$	$T_{max} [^{\circ}C]$	$T_{max} - T_{min} [^{\circ}C]$	$\int G_{south} \frac{MJ}{m^2}$
min	-3.6	-0.1	2.5	2.7	0.5
Max	4.5	7.6	10.5	9.8	14.6
avg	0.2	2.8	5.6	5.4	5.9
std dev	2.6	2.2	1.9	1.8	5.0

Reference controller

This controller is a purely thermostatic control acting on the water supply temperature to maintain the desired temperature in the reference room. The thermostatic valves are removed in this room. A fixed schedule is used to allow a pre-heating time before occupancy. The main advantage of this controller, compared to the conventional one, is that it does not assume a steady-state of the building. This will result in the maximum usage of boiler power for pre-heating, which allows for a less conservative fixed schedule, and this will effectively switch off the heating during night, as long as the night setpoint is exceeded. Combining a more efficient night setback and a later start of the heating, this controller can lead to significant energy savings compared to the conventional one, without requiring much intelligence in the algorithm. In practice, the thermostatic control is realised by a PID algorithm acting on the water supply temperature.

ANN controller

This controller was developed by NOA using artificial neural networks. It is described in other sections of this report. The current version of ANN controller uses a fixed schedule to allow a pre-heating period before occupants arrive in the building. It is not optimised to realise quick changes from one setpoint to another one, which was the reason to choose a very conservative heating schedules during the experimental testing of this controller. This schedule has a large effect on the energy performance of the controller, as shown by simulation results.

Optimal controller

This controller has been described in details in previous sections. A mid-range comfort level (6-7) was applied most of the time. Some tests were made with higher values, but no significant difference

was noted. Lower comfort settings values were not implemented to maintain the temperature in an acceptable range for building occupants, who considered the retained "comfort temperature" (21°C) as "rather cold". Meteorological forecasts provided by IRM (Royal Meteorological Institute of Belgium) were used during half of the optimal controller testing period instead of local-based forecasting. The latter actually consisted to use previous day data as forecasts, as the neural network approach did not give satisfying results. The possible benefit of these forecasts were not investigated on experimental results, but a similar comparison has been made in simulation (see here above), which showed that the quality of forecasting had an effect on the controller's performance but that the use of the "previous day" was still a good solution.

5.5.1.3 Controllers global performance

Table 5.8 shows a global summary of climatic conditions, energy consumption and comfort during both periods. This crude summary hides many discrepancies in the behaviour of different controllers, but some interesting information can still be gained from this data. J_d is the discomfort cost and is computed as $\text{PPD}'[\%]-5$ on 15 min values (PPD is Fanger's Predicted Percentage of Dissatisfied computed with variable clothing. PMV' is Fanger's Predicted Mean Vote computed in the same way. These indices are represented in Fig. 5.16 versus the zone operative temperature (Top).

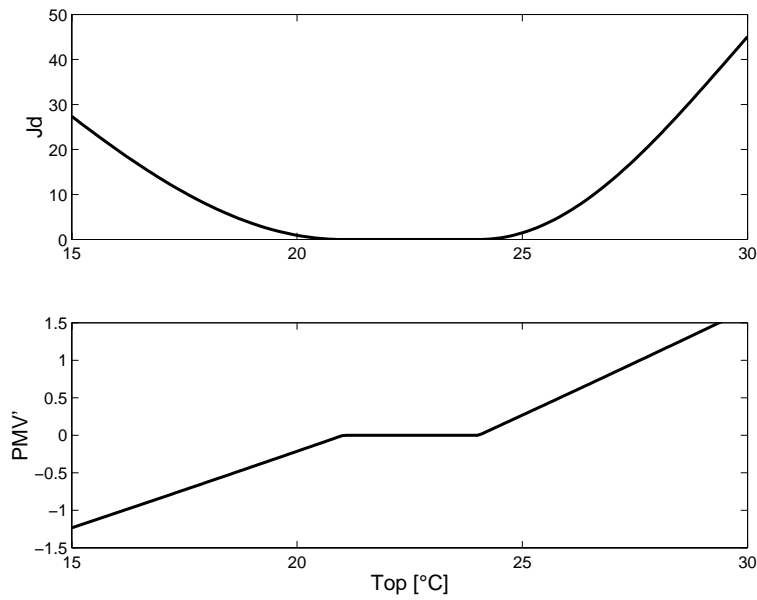


Figure 5.16. Comfort indices

J_e is the energy cost, which is simply the energy consumption expressed in kWh. To allow the comparison of periods of different lengths, the mean value of the energy cost is considered. It is equivalent to the average heating power, Avg PHeat, which is expressed in kW.

As mentioned here above, the conventional controller benefited from a higher solar radiation and from a slightly higher average ambient temperature. Despite this fact, the global heating energy consumption for the reference zone (consisting of two offices) is higher for this controller. The global comfort indices indicate no obvious superiority of the conventional controller in this respect. Note however that the comfort performance cannot be compared directly for these periods since the building is very sensitive to overheating. The poorer comfort performance of the conventional controller must be considered with care.

Table 5.8. Climatic conditions, energy consumption and comfort for the 3 controllers

		Conventional	Reference	ANN	Optimal
Tamb [°C]	Avg	5.4	2.1	2.8	3.8
Gsouth [$\frac{W}{m^2}$]	Avg	86	23	68	41
J_d [%PPD']	Max	14.3	6.1	2.5	5.3
	Avg	0.3	0.15	0.04	0.13
PMV' [-]	Min	-0.38	-0.55	-0.35	-0.51
	Max	0.86	0.0	0.0	0.0
	Avg	0.03	-0.03	-0.01	-0.03
Pheat [kW]	Avg	0.338	0.405	0.339	0.315

The reference controller was tested during a cold period only and shows a comfort performance very close to the optimal controller. The energy consumption is higher, but the average ambient temperature and solar radiation were lower, which could partly explain this difference.

The ANN controller, tested during a cold and sunny period, shows an energy consumption identical to the one of the conventional controller, but with a far better comfort. However again, the poor comfort performance of the conventional controller was mainly due to overheating during warm mid-season days.

Due to the large discrepancies in meteorological parameters describing the 4 testing periods, a refined analysis is necessary to draw some conclusions on the relative performance of tested controllers.

5.5.1.4 Typical daily profiles

The next figures represent typical profiles of the following variables:

Top	... Operative temperature in the reference offices
Tws	... Water supply temperature
Twr	... Water return temperature
Qr	... Radiator emission power
$Tamb$... Ambient temperature
$GSouth$... Solar radiation on southern facade

Grey rectangles represent the comfort temperature range ($21-24^{\circ}\text{C}$) when building is occupied (from 8 AM to 6 PM) or supposed to be occupied (some tests were realised during week ends, e.g. 25/12). The discomfort cost is zero in this zone. Light grey rectangles next to them indicate the zone where comfort is still very low (i.e. 0.5°C below the lower limit and 0.5°C above the upper limit).

Tws and Twr are represented for the reference and optimal controller because they show the controlled variable (Tws), while Qr is used for the conventional controller. Thermostatic valves control the flowrate in radiators, so this power would not be accurately represented by the temperature profile alone.

Conventional and reference controllers

Fig.5.17 shows the behaviour of the reference controller during two cold winter days. The fixed

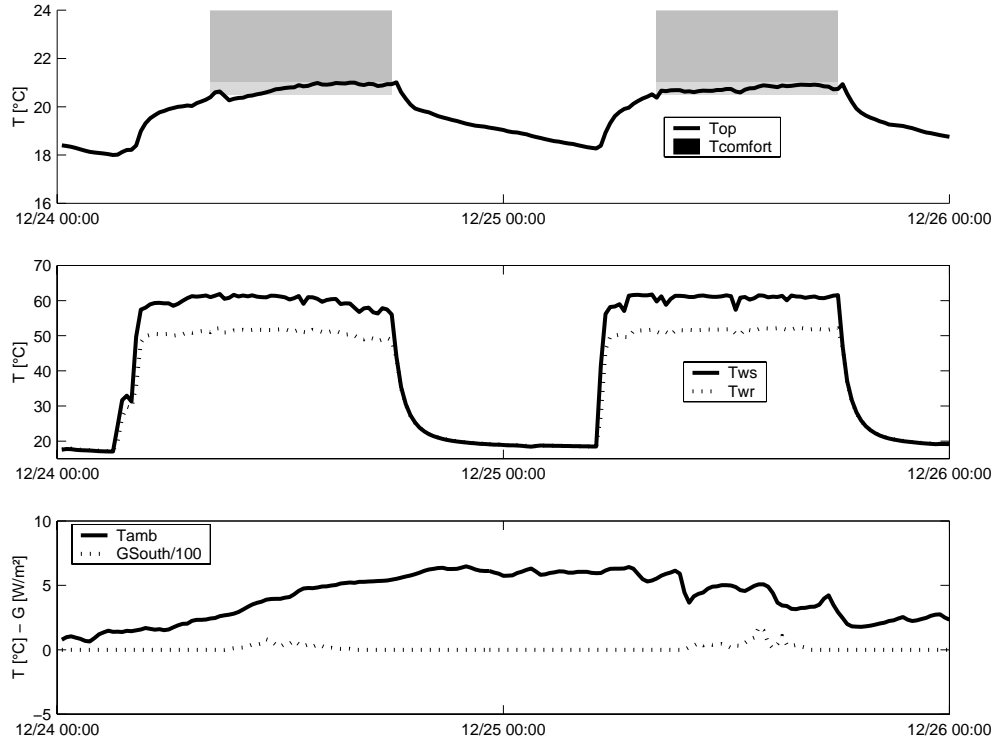


Figure 5.17. Cold and cloudy days, Reference controller

heating schedule is not very conservative and the building temperature is not reached before occupation start. However, the temperature in the building is very close to the setpoint and leads to a small discomfort cost. The sudden temperature drop which happens just after the occupants enter the building is actually due to the doors and windows opening (despite the cold outside temperature, occupants very often open the windows when they arrive due to the relatively poor indoor air quality inside the building).

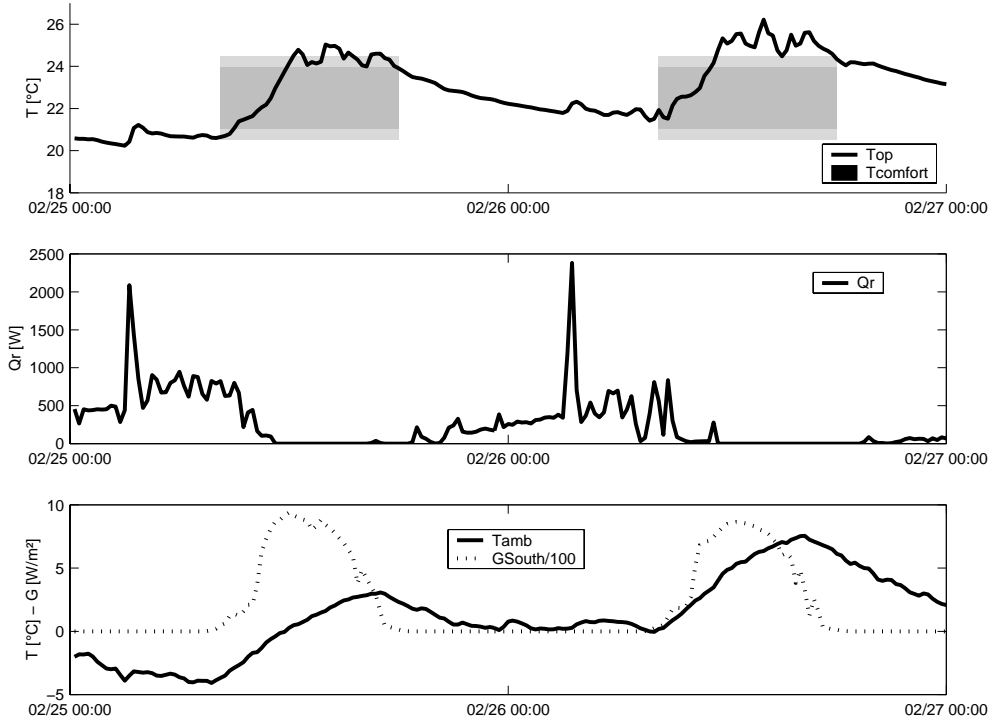


Figure 5.18. Sunny days, Conventional controller

Fig. 5.18 illustrates that important overheating can occur in the building when the conventional controller is implemented. The fixed heating schedule cannot be adapted to all conditions and is too conservative if the building has been submitted to high solar radiation during some successive days. It is the case for this period: heating is started at 3 AM, which is a good compromise for this time of the year (February). However, the building is very warm already. The thermostatic valves close quite quickly (reacting not only to the zone temperature but also to the radiator temperature itself), but the zone is nevertheless heated to about 21 $^{\circ}\text{C}$ before occupants arrive. During the day, internal and solar gains lead to overheating and to discomfort. Note that overheating occurs even if the windows are open. It can be seen on the graph that the increase of temperature is suddenly slowed down around 13:00 or 14:00, due to windows opening. It is also very interesting to note that users open the windows when the temperature is already significantly outside the comfort range, in other words when it is too late.

Optimal controller

Fig. 5.19 shows temperature profiles for two typical winter days (Monday and Tuesday). It can be seen that the optimal controller starts heating at the latest moment to reach an acceptable temperature when occupants are supposed to enter the building. During occupation, the heating is reduced earlier than in the case of conventional heating (thermostatic valves or PID) because internal and solar gains are anticipated.

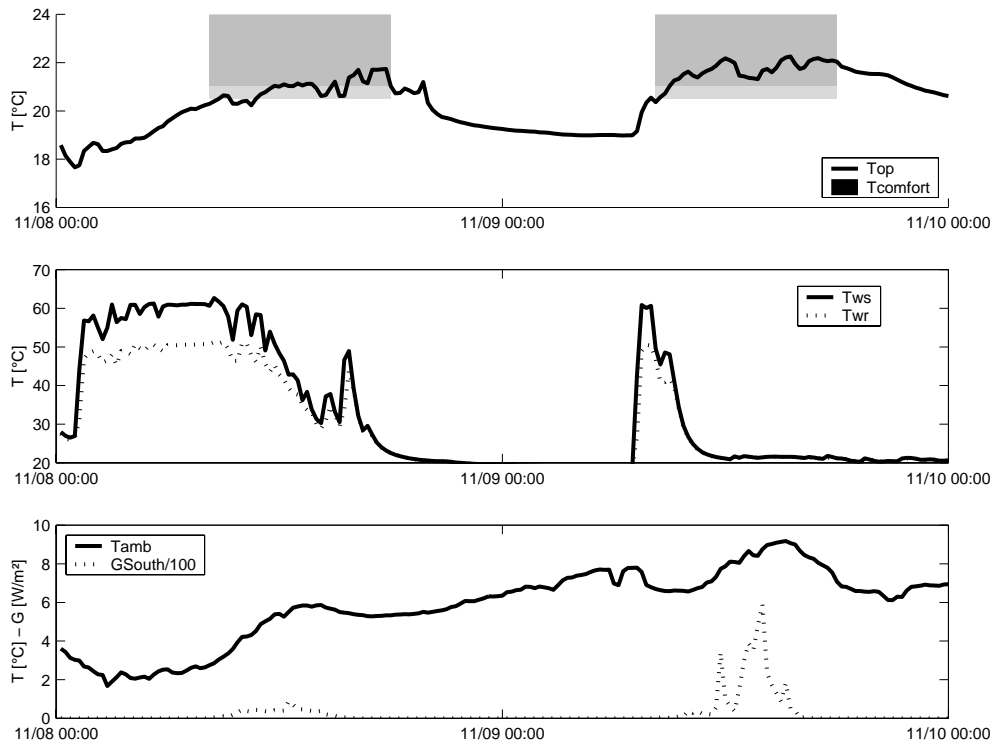


Figure 5.19. Typical building behaviour. Cold Monday and Tuesday, optimal controller

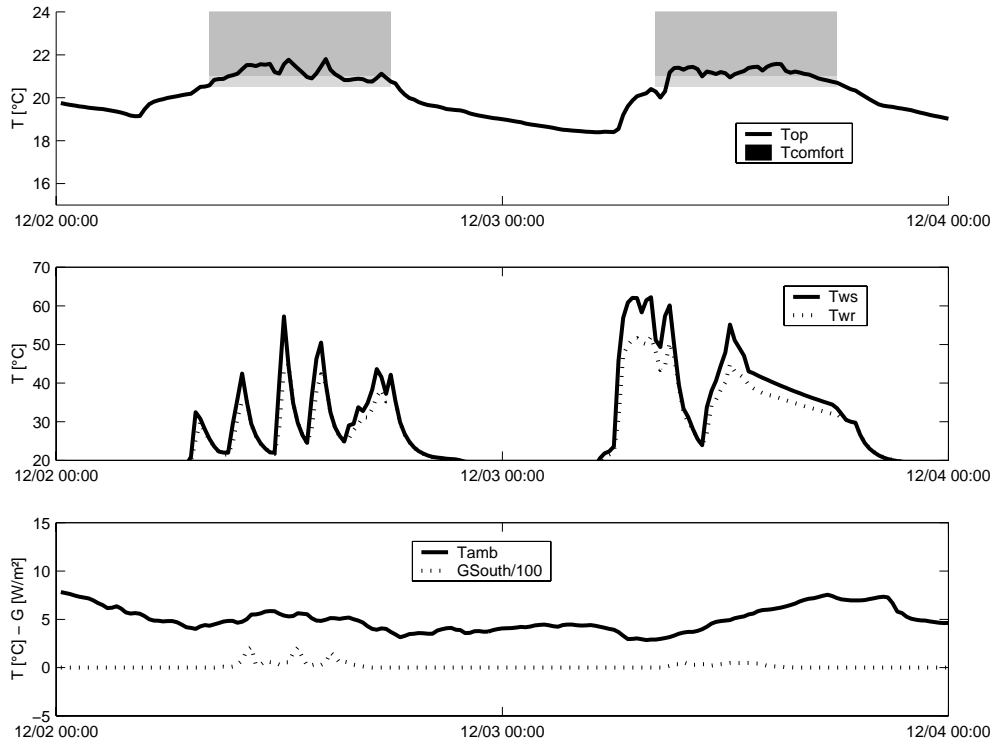


Figure 5.20. Cold and cloudy days. Optimal controller

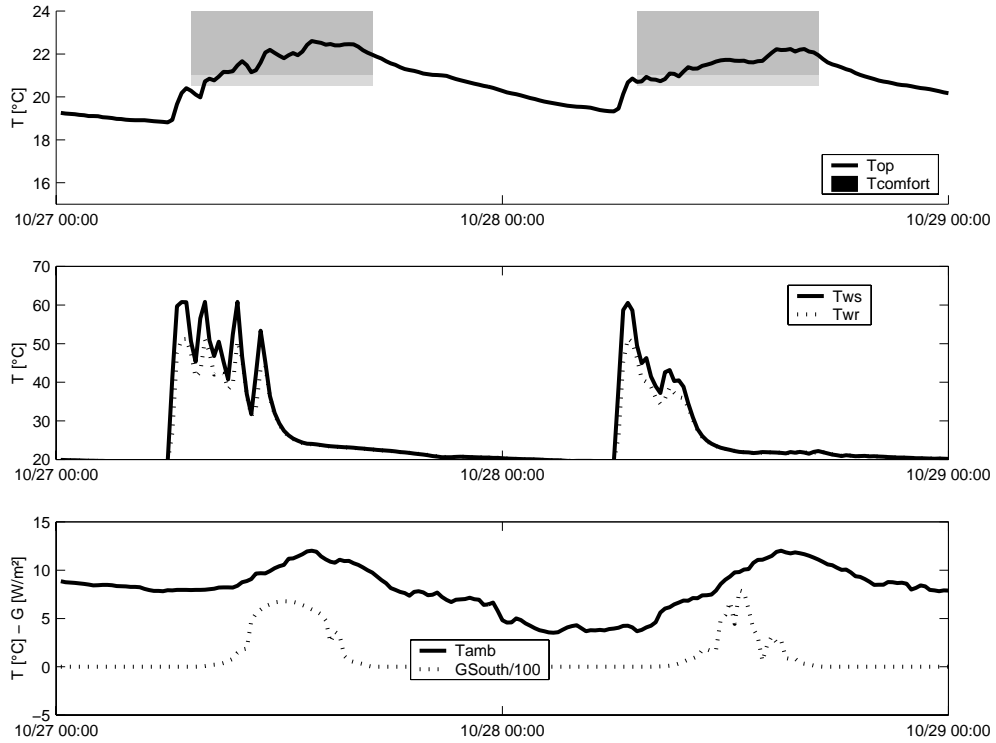


Figure 5.21. Sunny mid-season days. Optimal controller

Fig. 5.20 shows Temperature profiles for two cold and cloudy days. The first day shows an influence of the PID correction. If the forecasted zone temperature is not maintained with the foreseen water supply temperature, a correction is applied to maintain the desired zone temperature. To prevent unnecessary overheating, this correction is not applied if the temperature lies between comfort bounds. During this day, the foreseen temperature was higher than the real one, because of overestimated solar radiation forecasts. The PID does not track this temperature if the real temperature lies within the comfort range, but well if it lies outside. This can lead to oscillations in the water supply temperature if the zone temperature is close to the lower comfort bound.

The second day shows a typical "end of day" profile: the radiator temperature drops since 12 PM and the zone temperature falls just below the comfort level at the end of the occupation period. This allows to save heating energy, but it is sometimes not appreciated by buildings occupants (see the "users point of view" section).

Finally, the building behaviour during relatively warm and sunny days is presented in Fig. 5.21. This figure can be compared to Fig. 5.18. The optimal controller allows to save both energy and discomfort in the case of high solar gains leading to overheating.

ANN controller

Fig 5.22 shows temperature profiles for two days taken in the ANN testing period. The typical T_{ws}

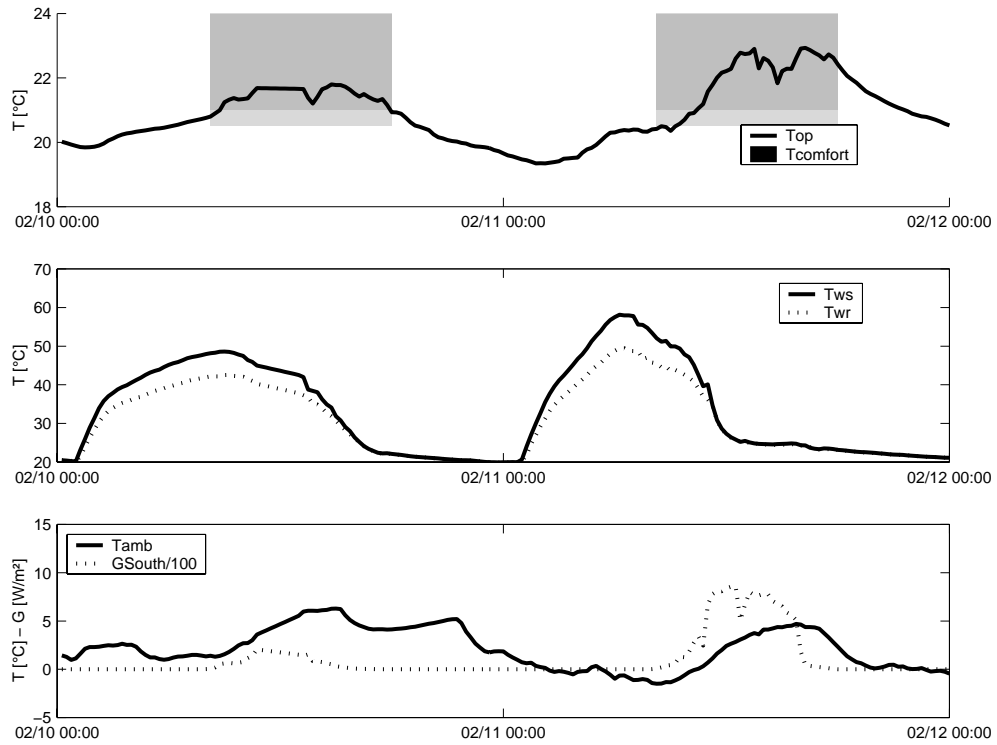


Figure 5.22. Typical profiles, ANN controller

profiles are shown, with a rounded shape due to the smooth increase in water supply temperature setpoint. Due to this smooth profile, the comfort range (darker gray rectangle) is not always reached when occupants enter the building, despite the use of a rather conservative heating schedule. However, the temperature remains in the zone where discomfort cost is very low, which is confirmed by global controller performance. The second day shows that the controller is able to react to sunshine to prevent overheating, but this reaction is rather slow. This would probably lead to overheating in the case of successive warm mid season days, as shown Fig. 5.18 for conventional controller.

5.5.1.5 Comparison on shorter periods

In order to refine the comparison between different controllers, shorter periods were investigated to find similar meteorological conditions in available data sets.

The first comparison concerns the conventional controller and the optimal controller, for which two similar 2-weeks periods are considered (table 5.9).

These results are obtained on relatively short periods, but can still give a good idea of the relative performance of both controllers.

The conventional controller uses a fixed schedule. During relatively warm periods, this schedule is too conservative, which leads to waste energy to pre-heat the building too long in advance. Furthermore, this warm building is more subject to overheating. This last point is still reinforced by the proportional band of the thermostatic valves, which reduce the power when the temperature

Table 5.9. Climatic conditions, energy consumption and comfort for conventional and optimal controllers. Similar periods (mid season)

		Conventional	Optimal
Tamb [°C]	Min	2.0	3.5
	Max	18.7	17.2
	Avg	10.0	9.3
Gsouth [$\frac{W}{m^2}$]	Avg	67	62
J_d [%PPD']	Max	3.8	2.4
	Avg	0.25	0.07
PMV' [-]	Min	-0.13	-0.34
	Max	0.43	0.0
	Avg	0.04	-0.02
Pheat [kW]	Avg	0.175	0.152

reaches the setpoint but do not really stop the heating until the temperature is about 0.5 °C above this setpoint.

In this kind of situation, the optimal controller is able to reduce the energy consumption while reducing the discomfort. Energy savings on the considered period reach 13%, for a significantly reduced discomfort ("optimal" discomfort cost is 28% from "conventional" cost) .

The second comparison concerns the optimal and the reference controller (table 5.10).

Table 5.10. Climatic conditions, energy consumption and comfort for reference and optimal controllers. Similar periods (cold)

		Reference	Optimal
Tamb [°C]	Min	-4.1	-8.3
	Max	9.1	8.2
	Avg	1.1	1.3
Gsouth [$\frac{W}{m^2}$]	Avg	27	26
J_d [%PPD']	Max	6.1	3.1
	Avg	0.25	0.14
PMV' [-]	Min	-0.55	-0.39
	Max	0.0	0.0
	Avg	-0.04	-0.03
Pheat [kW]	Avg	0.405	0.356

During this cold period, the fixed schedule leads to energy waste on some days because the pre-heating time is too long, but to high discomfort on other days because the pre-heating time is too short. The optimal controller sometimes underestimates the pre-heating time as well, leading to relatively high discomfort, but it adapts this pre-heating time to the building state. On the whole period, this allows here again to reduce the discomfort while saving energy (about 12% energy savings with 44% discomfort cost reduction).

Table 5.11 shows meteo data summary and controller performance for two 2-weeks periods during the conventional and ANN controllers tests.

On similar cold and sunny periods, the ANN controller achieves 18% energy savings compared to the conventional controller, while reducing the average discomfort cost by 20%.

Table 5.11. Climatic conditions, energy consumption and comfort for conventional and ANN controllers. Similar periods (cold and sunny)

		Conventional	ANN
Tamb [°C]	Min	-4.1	-3.6
	Max	8.7	10.5
	Avg	2.3	2.8
Gsouth [$\frac{W}{m^2}$]	Avg	56	68
	Max	1.6	2.5
	Avg	0.05	0.04
PMV' [-]	Min	-0.21	-0.35
	Max	0.28	0.0
	Avg	0.01	-0.01
Pheat [kW]	Avg	0.422	0.345

5.5.1.6 Comparison using simulation

Two controllers performance on the same building can be compared using simulation results. The principle is as follows:

During a first period, the controller one is tested on the building.

During a second period, the controller two is tested on the building.

The simulated performance of controller one on the first period and the simulation of controller two during the second period are used to validate a building model for the considered meteorological data set.

In a second step, the performance of controller one during the second period and the performance of controller two during the first period are simulated and serve to establish a virtual comparison on the same periods.

This method can be used to refine the comparison between different controllers implemented on FUL's academic building. However, up to now, the simulation of really implemented controllers did not reproduce accurately their performance, due to building modelling errors in the reference model (TRNSYS TYPE 56). Some "hard" hypotheses about boundary conditions of the reference zone can explain encountered problems: other rooms in the building are supposed to have a temperature almost identical to the reference zone. The only other simulated zone is the adjacent sunspace. However, the reference room is thermally linked to other building parts for which this assumption proved to be incorrect. Moreover, very important heat losses from the boiler room and from pipes cause high unmeasured heat gains to the reference zone. This has been clearly pointed out by the difference between summer and winter performance and by two boiler failures. Indeed, the building response is far more accurately simulated when the boiler is not in operation.

To solve this problem, a multi-zone model including a larger part of the building should be developed and heat gains should be identified using simplified models and then used as a simulation input. However, this task was not possible in the frame of this project.

The currently available model allows to reproduce energy consumption within 15%. Errors on discomfort cost can reach 40%, due to the non-linear cost function. can be with the currently available model. This is actually a fairly good modelling accuracy compared to "good practice" in building simulation, but it is not sufficient to study performance discrepancies in the range of 10-20%.

Nevertheless, previous work such as IEA Annex 21 / Task 12 [L+94] showed that most building simulation programs often better reproduce the influence of design changes on energy and comfort

performance than the absolute performance. The results obtained in the "pure" simulation phase can then be considered as giving a realistic idea of controllers performance when compared to each other.

The passys testcell can be simulated more easily (isolated building, no occupants) and the methodology described here above has been successfully applied to the experimental data recorded by NOA. The results are described later in this paper.

5.5.1.7 The user's point of view

A real user survey about the comfort in the test building was out of the scope of this project. However, the two regular occupants of the building were given survey forms were they could write their complaints when they felt uncomfortable. They were also surveyed on a regular basis to give their opinion on the thermal and general comfort in the building. Some information can be gained from these surveys and from the few complaints that occurred.

The first conclusion of this small survey is that the comfort feeling is not always directly related to the temperature that is measured by the controller. Many objective and subjective factors can have an influence : humidity, draughts, occupants mental / physical state, etc. In this respect, a controller achieving perfect thermal comfort for all occupants is not realistic.

However, some typical user behaviours could be considered in the development of a commercial controller: If building occupants feel uncomfortable, their first reaction is to verify that the radiators are cold/warm according to what they desire. It is also very often the case that they verify if the radiators are warm when they arrive in the building on a cold winter morning. In this respect, the optimal controller was appreciated because the heating is started as late as possible and the water temperature is very often high when the occupants arrive.

On the other hand, it happened quite often that the occupants were feeling cold on a cloudy afternoon and did not appreciate the fact that radiators were cool. With a conventional heating curve control associated with thermostatic valves, they always have the possibility to increase the radiator temperature and the lack of such a possibility was probably the major disadvantage of the optimal controller. The comfort temperature setting does not play exactly the same role, as the real need of the occupants often is to feel the warmth from the radiator rather than to have a warmer office.

Concerning the overheating problem, the optimal controller showed a very good behaviour. Moreover, simulation results confirm that this controller could be suitable even during very warm mid-season periods (when no heating is really needed), while the conventional controller would probably always heat the building in the morning. The need for user adjustment of the heating curve is completely suppressed.

5.5.1.8 Some lessons from experimental testing

Encountered boiler problems allowed us to verify some properties of the optimal controller:

- The presence of a model allows to quickly detect a boiler partial failure (in our case, one of the two burners was not always working). The automatic detection of such events has not been implemented yet but it could contribute to the success of optimised controllers.
- The optimal controller starts the heating at the latest minute in the morning. This can lead to substantial energy savings, and has a favourable effect on the comfort ("warm radiators", see here above), but it makes the controller more sensitive to some events. First, in case of boiler loss of power, the setpoint cannot be reached at due time and even if the model allows

to detect a malfunctioning, it is too late. Secondly, if the occupants arrive earlier or have a "non-reasonable" behaviour (e.g. opening the windows when they arrive), this can lead to a relatively high discomfort.

- The feedback action on the control signal is necessary to compensate for modelling and forecasting errors. In this respect, it improves the thermal comfort of the occupants. However, the PID also reacts to occupants actions such as windows openings, which could lead to energy waste if the occupants are not educated to save energy. This is a drawback of all feedback control systems.

5.5.2 Experiments on Passys testcell

5.5.2.1 Data sets description

Experiments on Passys testcell in order to test FUL's optimal controller started in November 1999. The first period was devoted to the implementation of a conventional reference controller in order to test software compatibility and to obtain a first data set with the current testcell configuration. Two weeks of usable data were recorded for this first phase.

A second period was used to test FUL's optimal controller. One month data was recorded by NOA, but 2 weeks are left after preliminary tuning of the controller and periods with too much missing data are removed.

Table 5.12 sums up the characteristics of meteorological parameters for both periods. T_{amb} is the ambient temperature and Gh is the solar radiation on a horizontal surface. Period 1 was recorded with conventional controller implemented, period 2 with optimal controller. Table 5.12 clearly

Table 5.12. Meteorological parameters for first tests on Passys testcell

	Period 1		Period 2	
	$T_{amb}[^{\circ}C]$	$Gh[\frac{W}{m^2}]$	$T_{amb}[^{\circ}C]$	$Gh[\frac{W}{m^2}]$
Minimum	3.6	0.0	0.6	0.0
Maximum	18.4	668	10.7	653
Average	10.3	106	3.9	65
Std. deviation	2.92	169	1.66	177

points out that both periods are not comparable from the meteorological point of view : period 1 was significantly warmer and sunnier. The global performance indices of both controller will then not be directly comparable.

5.5.2.2 Measured controller performance

Fig 5.23 and 5.24 show two typical weeks respectively taken in the first period (conventional controller implemented) and the second period (optimal controller implemented).

Table 5.13 and 5.14 show respectively the measured performance of the reference conventional controller during period 1 and the measured performance of optimal controller during period 2. The zone temperature (T_{in}) statistics concern occupation period only, as for PMV and Jd (which are naturally equal to 0 when the building is not occupied).

As mentioned here above, a "raw" comparison of these results is not possible due to the very large meteorological discrepancies between both periods.

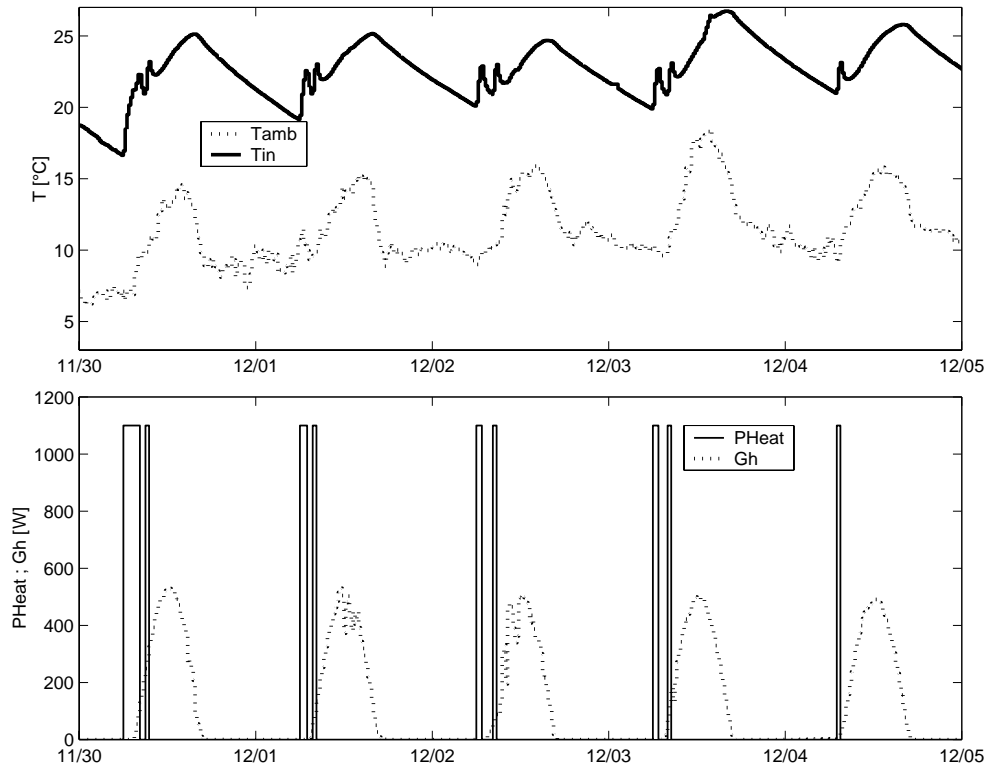


Figure 5.23. Typical week, Period 1 (Conventional controller)

Table 5.13. Measured Conventional Controller performance, Passys testcell - Period 1

	$Pheat[W]$	$Tin[^\circ C]$ (Occ.)	$PMV[-]$	$Jd[\%PPD']$
Minimum	0.0	20.6	-0.097	0.0
Maximum	1100	26.7	0.755	11.19
Average	78.1	23.4	0.097	0.88
Std. deviation	282.7	1.46	0.186	2.25

Table 5.14. Measured Optimal Controller performance, Passys testcell - Period 2

	$Pheat[W]$	$Tin[^\circ C]$ (Occ.)	$PMV[-]$	$Jd[\%PPD']$
Minimum	0.0	19.3	-0.36	0.0
Maximum	1100	23.1	0.0	2.6
Average	244	21.19	-0.045	0.16
Std. deviation	457	0.74	0.077	0.41

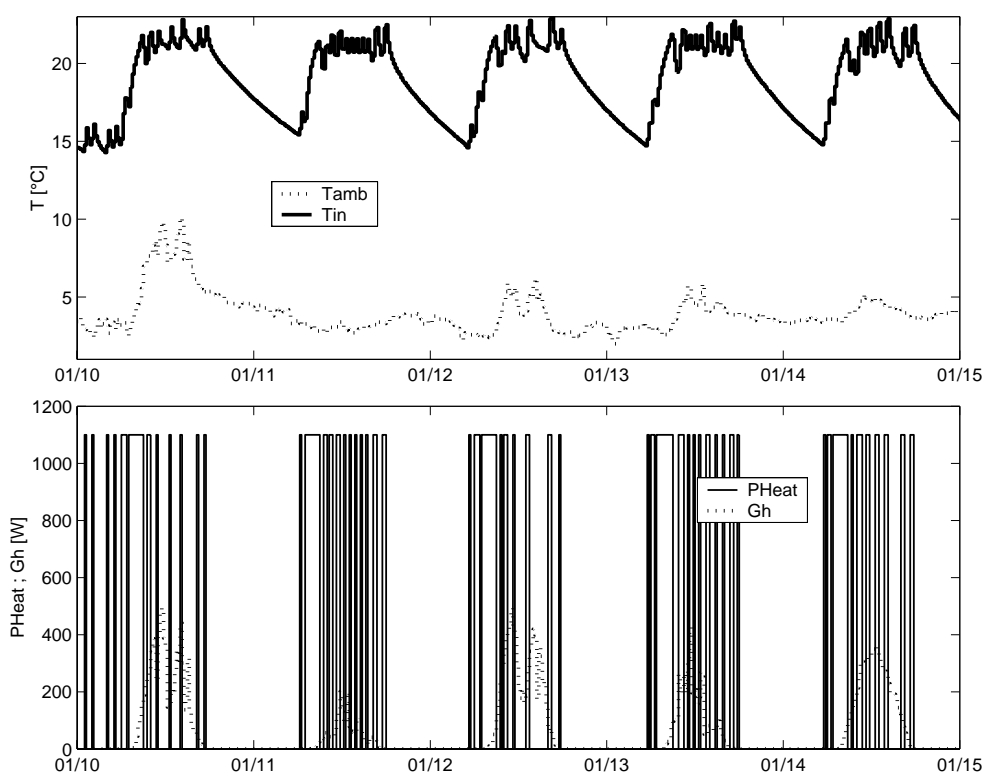


Figure 5.24. Typical week, Period 2 (Optimal controller)

5.5.2.3 Comparison using simulation

The methodology described in section 5.5.1.6 has been applied to the first experimental period. A first attempt using the TRNSYS model of the testcell led to a fairly good agreement between simulated results and measured values. However, the difference of performance (e.g. energy consumption) between two controllers is relatively small compared to the absolute value (order of magnitude : 10%). For this reason, small errors on absolute energy consumption can lead to a large error on the comparison results.

A simplified model based on a second order structure suggested by NOA was used in a second approach. The parameters of this simplified model were identified using the whole data set (periods 1 and 2). Constant values were identified for all parameters except for air infiltration and solar transmittance. The infiltration rate was allowed to vary in a range from 0.1 to 1 vol/h to take into account the influence of wind speed. The solar transmittance (i.e. the ratio of incident solar radiation entering the testcell) was allowed to vary in a range from 0.12 to 0.6 to take into account the variation of glass transmittance with incidence angle and the effect of un-modelled shading. This attenuation factor corresponds to a transmittance ranging from 0.1 to 0.5 for a 1.2 m² glazed area.

First, the controllers that were actually implemented were simulated on the corresponding periods to validate the "building+controller" model. The results presented in table 5.15 and 5.16 show a good agreement with measured performance (tables 5.13 and 5.14). Important measured values are also mentioned in these tables to allow a direct comparison.

The energy consumption is reproduced within 2.6% in the worst case. The more important error for discomfort cost is mostly due to the non-linear shape of Jd : very small errors on maximum or minimum temperatures during the day have a large effect on the discomfort cost. However, the agreement is still very good.

Table 5.15. Simulated Conventional Controller performance, Passys testcell - Period 1, bold: Measured quantities on the same period

	<i>Pheat</i> [W]	<i>Tin</i> [°C]	<i>PMV</i> [-]	<i>Jd</i> [%PPD']
Minimum		0.0	20.6	20.5
Maximum		1100	26.7	26.8
Average	78	76	23.4	23.2
Std. deviation		279		1.43
				-0.11
				0.77
				11.2
				11.2
				0.88
				0.73
				0.174
				2.08

Table 5.16. Simulated Optimal Controller performance, Passys testcell - Period 2, bold: Measured quantities on the same period

	<i>Pheat</i> [W]	<i>Tin</i> [°C]	<i>PMV</i> [-]	<i>Jd</i> [%PPD']
Minimum		0.0	19.3	18.9
Maximum		1100	23.1	23.4
Average	244	245	21.19	21.12
Std. deviation		458		0.77
				-0.11
				0.0
				2.6
				3.8
				0.16
				0.23
				0.091
				0.55
				-0.055
				0.045

Fig. 5.25 shows the indoor temperature profile for simulated and measured indoor temperature, for one typical week of each period. The low thermal capacitance of the building and the ON/OFF nature of the heating system lead to instantaneous discrepancies, but the behaviour of the "building+controller" couple is very well reproduced by the simulation.

In a second phase, the controllers performance is simulated for the period when the other controller was implemented. Table 5.17 and 5.18 present respectively the performance of the optimal controller

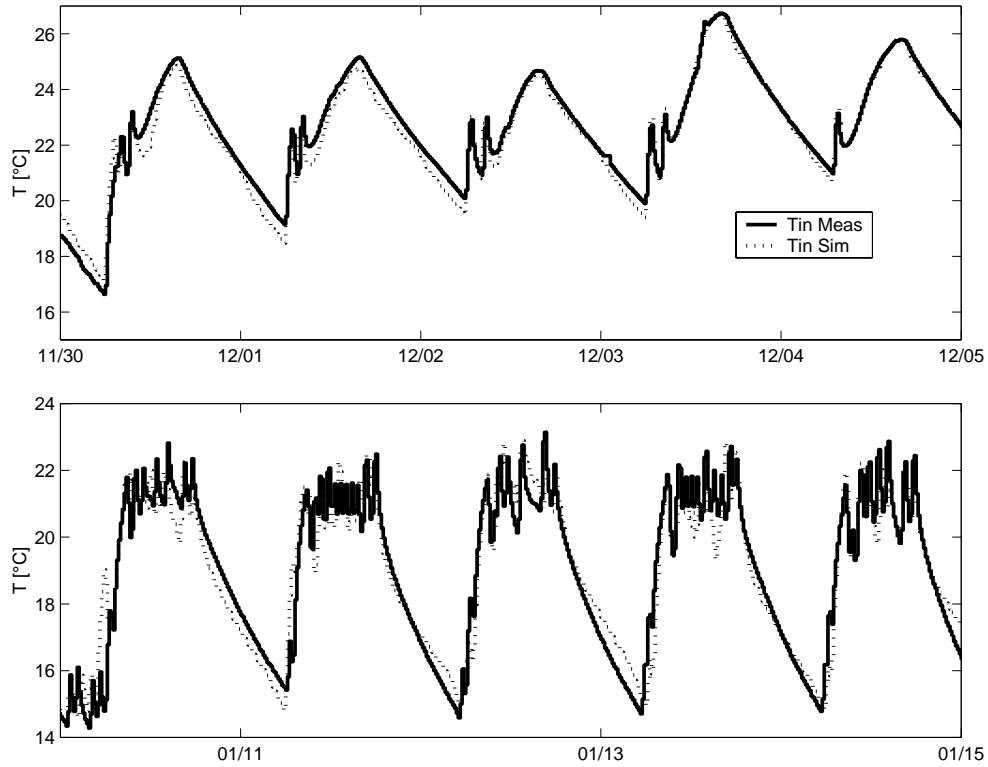


Figure 5.25. Simulated and Measured indoor temperature: typical week Period 1, Conventional (upper) – Period 2, Optimal controller (lower)

during period 1 and the performance of the conventional controller simulated on period 2.

Table 5.17. Simulated optimal Controller performance, Passys testcell - Period 1

	<i>Pheat[W]</i>	<i>Tin[°C]</i>	<i>PMV[-]</i>	<i>Jd[%PPD']</i>
Minimum	0.0	19.0	-0.42	0.0
Maximum	1100	26.0	0.54	5.8
Average	58.0	22.58	0.020	0.36
Std. deviation	246	1.42	0.132	1.02

Table 5.18. Simulated conventional Controller performance, Passys testcell - Period 2

	<i>Pheat[W]</i>	<i>Tin[°C]</i>	<i>PMV[-]</i>	<i>Jd[%PPD']</i>
Minimum	0.0	20.0	-0.21	0.0
Maximum	1100	23.4	0.0	0.89
Average	260	21.66	-0.015	0.032
Std. deviation	468	0.728	0.036	0.105

Total energy and discomfort costs are also represented Fig. 5.26

The comparison shows that important energy savings (25%) can be achieved with an improved comfort during period 1 (warm and sunny). Even if the implemented conventional controller was not optimised for these conditions (it used a rather conservative fixed schedule), this confirms that most of the savings and comfort improvement can be achieved during mid-season.

For the cold period, the optimal controller with implemented settings (mid-range comfort level)

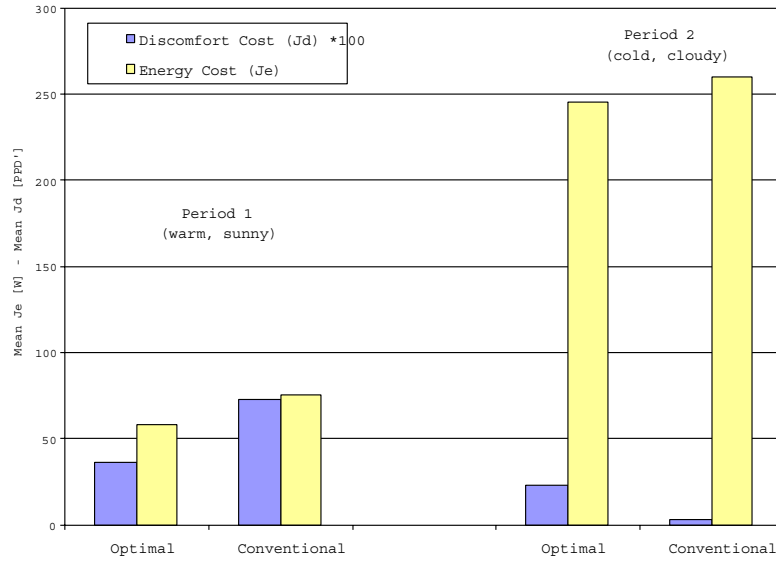


Figure 5.26. Optimal and conventional controllers comparison using simulation results

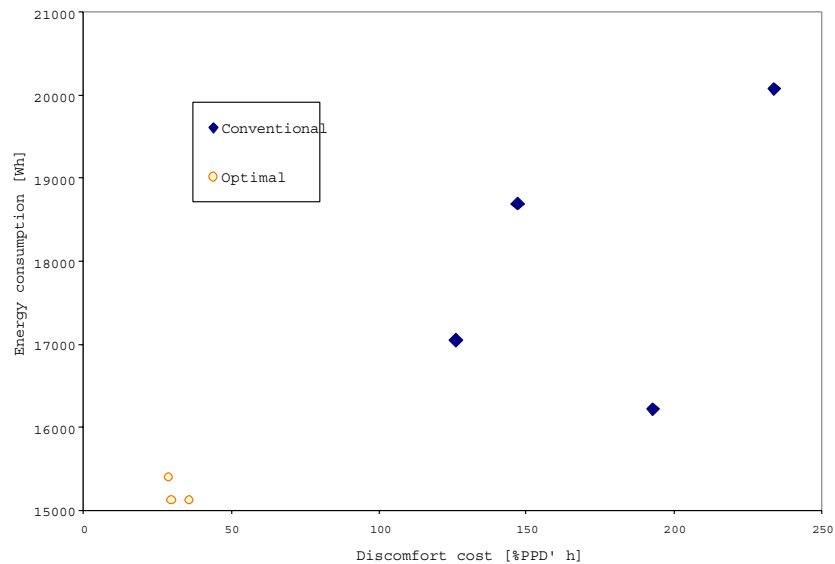


Figure 5.27. Controllers Comparison for different settings. Period 1

gives 6% energy savings, but at the cost of a higher discomfort. A look to Fig. 5.25 (lower part) allows to understand why the discomfort cost is so high. On the second day, the temperature goes down to 19 °C during the occupation period, while the setpoint was already reached before. The cause is that the ON/OFF control of heating is poorly handled by the optimal controller, and especially by the feedback compensation.

The comparison using simulation can be useful to compare different controllers on the same building, but also to test different settings of the same controller. The conventional controller uses for example a fixed schedule, which was roughly estimated before the start of the tests. Simulations could be used to assess the validity of these settings and study their influence on the results of the comparison with the optimal controller.

Different comfort level settings of the optimal controller and different schedules for the conventional controller were simulated for the period 1 using the identified building model. Fig. 5.27 represents the total discomfort cost and the total energy consumption for different controllers. In this graph, the closer a controller is to the lower left corner, the better it is.

By modifying the setpoint and the fixed heating start schedule of the conventional controller, it is possible to reduce the energy consumption and, for some parameters combinations, furthermore reduce the discomfort by preventing overheating. However, the "best settings" solution for this conventional controller is still far from the performance of the optimal controller on this sunny and relatively warm period.

5.5.3 Conclusions of experimental tests on Passys testcell and FUL building

Experiments realised on both buildings allow to draw some general conclusions:

The methodology of performance comparison by combining simulation and experiments has been applied successfully to the Passys testcell. On this special building, without user or adjacent rooms influence, simulation allowed to reproduce the measured behaviour of tested controllers very accurately. This simulation environment can afterwards be used to simulate different controllers with different settings and study their performance in various meteorological conditions, as illustrated in section 5.5.2.3. On this building, the optimal controller can achieve up to 25% energy savings during sunny mid season periods, with an improved thermal comfort (reduced overheating). During these periods, the optimal controller can start heating later or under-heat the building during the morning to reduce overheating. In absence of overheating, during very cold periods, the optimal controller can still achieve about 5% energy savings with a similar discomfort, thanks to the optimal start of heating.

For the Passive solar building of FUL, which is an occupied building with complex architecture, the currently available model is not accurate enough to use the simulation-experiments cross-comparison. Indeed, even small errors usually achieved by "good practice" modelling tools can be larger than the performance difference between two controllers. Note that this is a limitation of the model that could be developed during this project and not a limitation of the methodology itself. However, a comparison of different controllers for this building was possible in two ways : comparison of short similar experimental periods, and "full simulation" comparison. The latter uses a model giving absolute errors in the range of performance differences, but the relative performance of two controllers can be considered as representative from the reality. The comparisons show that ANN and optimal controllers can achieve energy savings from 6% to 20% energy savings for similar or improved comfort, depending on the period. It must be stressed that no single period was found giving a worst performance for "advanced" controller. Larger energy savings can be obtained during cold and sunny periods.

Building occupants also gave their impressions during experimental tests. The main disadvantage of "advanced" controllers in this respect was the lack of "immediate" action possibility, which is present in the case of conventional control with thermostatic valves. Users sometimes want to control the temperature of the heat source rather than the operative temperature of the zone. This is particularly the case at the end of some cloudy days, when advanced controllers stop heating before the real end of occupancy period. This proves again that the comfort feeling of buildings occupants will never be represented by an equation, even if it is based on well established scientific standards. On the other hand, no major complaint was noted when advanced controllers were implemented and no real overheating occurred during the testing of advanced controllers, while it is a quite common phenomenon when the conventional controller is operated.

It must be stressed that the limitations of advanced controllers that were highlighted by experimental tests are not limitations of the applied methodology but rather limitations of the developed and implemented controllers. Further developments of control algorithms could take these lessons into account without compromising their basic advantage on conventional controllers: solar gains consideration and building behaviour anticipation.

Chapter 6

Work performed by NOA

Authors: Dr. A. Argiriou, Dr. I. Bellas-Velidis

6.1 Introduction to NOA work

This chapter of the report describes the activities of the National Observatory of Athens (NOA). NOA participated via the Institute for Environmental Research and Sustainable Development (former Institute of Meteorology) and the Institute of Astronomy and Astrophysics (former Astronomical Institute). NOA was responsible for the theoretical development and experimental testing of an Artificial Neural Network (ANN) controller. The theoretical task of the development of the ANN-based controller is described in the first part of this Report. Presented are the three stages towards the development of the controller. The initial setting up and the simple energy-demand-predicting controller are described in the Section 6.2. This first task allowed us to analyze the suitability and performance of particular ANN architectures for such one controller. The development of a multi-module controller for heating energy on/off switching is presented in the next, Section 6.3. We had to prepare a controller that we could test on-line in our experimental facility during the winter season. We applied a modular architecture separating the particular functions of the controller. This allowed us to create a flexible base for the final controller and to experiment it in real conditions. The final ANN-based controller for the supply temperature of a hydronic heating system is presented in Section 6.4. It was developed in two versions, one for the ISFH-partner system (building/heating), and the other for the FUL-partner. In the second part the experimental task is presented. Sections 6.5 and 6.6 describe the experimental facility in NOA used to test the ANN-controller, the PASSYS Test Cell and the testing environment based on VEE. The heating on/off controller implementation and the results from real tests during the winter season 98/99 are given in Section 6.7. An off-line performance assessment of the same controller is presented in the next session. The NOA's experimental facility was used for online testing an adapted version of the optimal controller provided by FUL-partner. The results are shown in Section 6.9. Finally, in Section 6.10 we present the results, provided to us by the FUL-partner, from online and simulation tests of the version of ANN-controller for supply temperature, prepared for the FUL system.

6.2 NOA ANN-Controller - initial phase and E_{AVE} demand predicting

The major steps in setting up the ANN-based controller were initially fixed (Figure 6.1). This setup was applied in the development of all the three versions of the controller presented in the

Report. The main activities during the initial phase were to define the basic parameters of an ANN controller, the inputs and outputs, the controller action, and to test the ability of ANN-based modules to perform heating control functions.

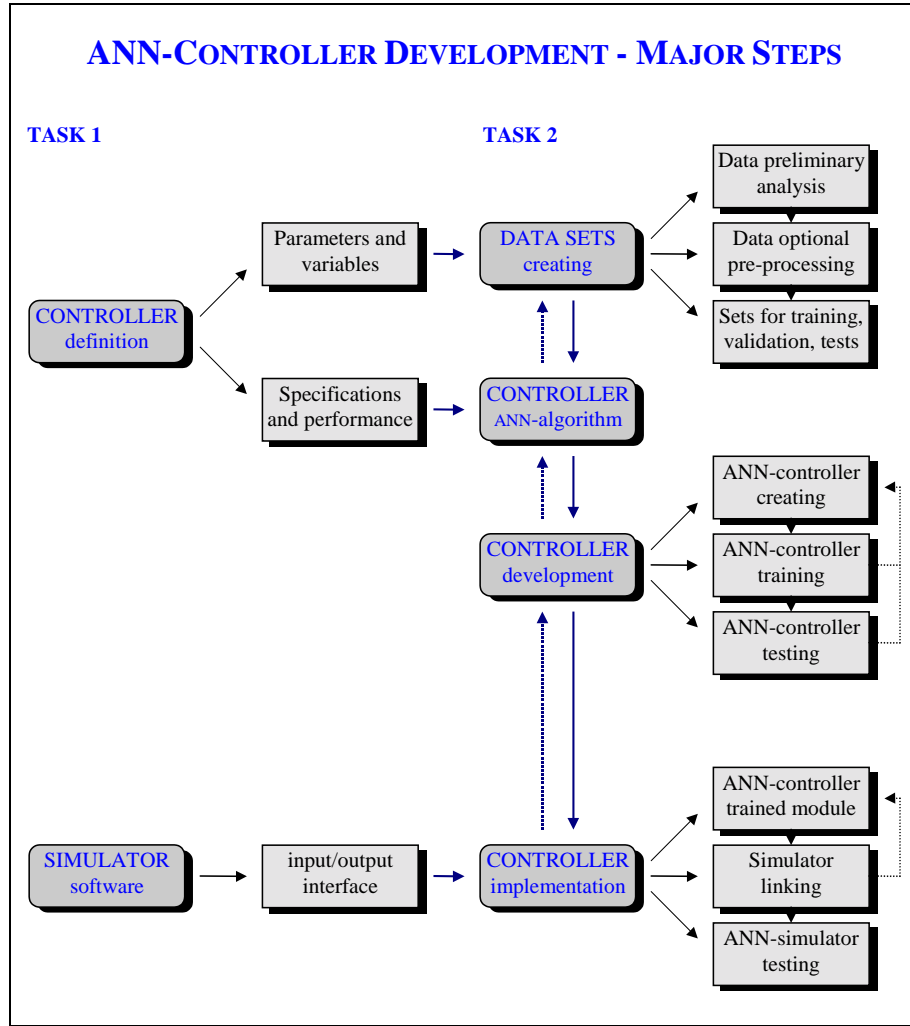


Figure 6.1. The main steps in the development of the ANN-based controller

6.2.1 ANN-Controller initial setup

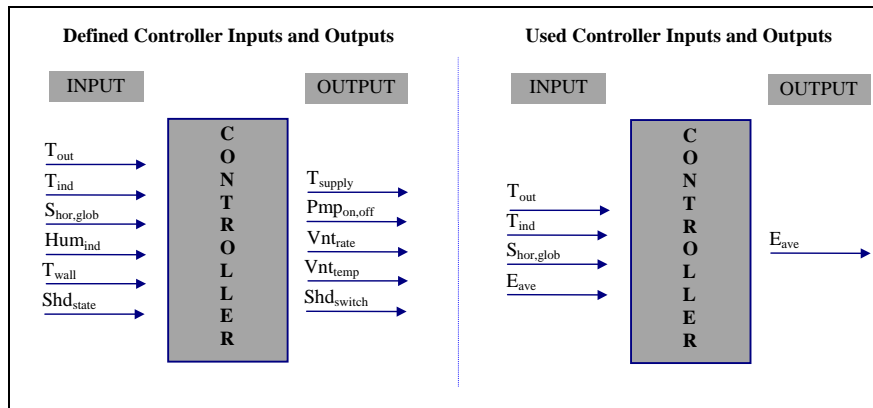
The heating controller parameters were defined (Table 6.1) by all the partners during the first meeting. These parameters defined a maximal set of inputs & outputs of a general controller.

A simplified subset (Figure 6.2) was used in the task of ANN-controller development. Two reasons led to this simplification. The main reason was the decision to develop a simple and cheap controller. The other reason was the available data set provided by ISFH-partner from his experimental solar house.

The necessary literature survey was carried out during this phase of the task. The problems of ANN application to control systems (Clouse et al, 1997 [CGHC97]; Han et al, 1997 [HXW⁺97]; Hunt et al, 1992 [HSZG92]; Khotanzad et al, 1997 [KARL⁺97]) and particularly to HVAC systems

Table 6.1. Initially defined parameters set for the controller

Parameter	Description
T_{out}	Ambient Temperature
T_{ind}	Indoor Temperature
$S_{hor,glob}$	Global Horizontal Solar Irradiance
Hum_{ind}	Indoor Relative Humidity
T_{wall}	Indoor Wall Surface Temperature
Shd_{state}	Status of the Shading Devices
T_{supply}	Supply Temperature
$Pmp_{on,off}$	Status of the Pump
Vnt_{rate}	Mechanical Ventilation Rate
Vn_{temp}	Ventilation Air Temperature
Shd_{switch}	Shading Device Switch
E_{ave}	Heating Energy Demand

**Figure 6.2.** The input/output as defined and as are used in the initial development

(Curtis et al, 1993 [CKB93]; Kreider, 1995 [Kre95]) were analyzed. Special attention was given to the task of ANN development (Nelson and Illingworth, 1990 [NI91]; Masters, 1993 [Mas93]; Yale, 1997 [Yal97]; Chen, 1997 [Che97]), to adaptive control systems and to the problem of optimal control (Mills et al, 1996 [MZT96]; Cichocki and Unbehauen, 1993 [CU93]).

6.2.2 ANN-controller development

The well-known SNNS (Stuttgart Neural Network Simulator, Zell et al, 1996 [Z⁺96]) was used to develop and test ANN models suitable for this task. It works both on UNIX (RISC- processors) and on PC systems providing a graphical user environment and a number of helpful tools for ANN development. A FORTRAN program **nn-pat.for** (widely used during the controller development) was created to prepare data sets for training, verification and testing the ANN models under SNNS. Two different classes of ANN architectures (Figure 6.3), that are well suited for the task of predicting the heating energy demand, the Time Delay Neural Network (TDNN) and the Feed Forward Back Propagation (FFBP) were tested.

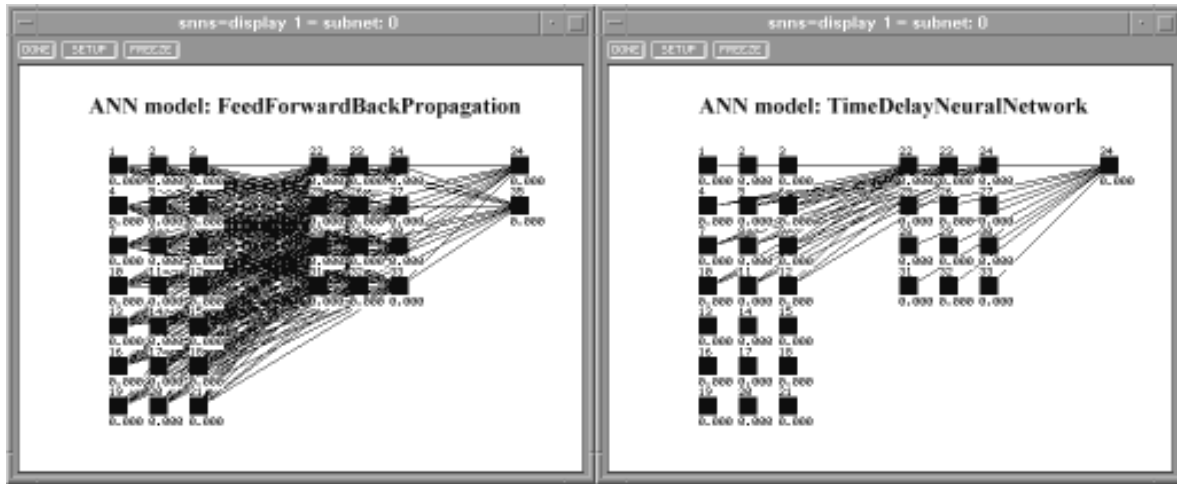


Figure 6.3. Illustration of ANN-models. Left: a FFBP with input layer of 21 neurons, hidden layer of 12, and output layer with two neurons. Right: a TDNN with the same input and hidden layer and with one output neuron (a time delay of 4 lines is fixed from the input and the total delay length is seven, but only the connections to the first hidden line are shown).

A set of models was tested with these two architectures (Table 6.2). These tests allowed us to investigate the performance of the TDNN and FFBP, the influence of the hidden layer and the type of input data. **The results showed the better performance of FFBP models, lower error in prediction the heating energy demand and more stable error development in ANN training.**

Table 6.2. The ANN architectures used in the two groups of tests. In the model's name the two letters indicate the ANN class (FFBP or TDNN) and the indices "i", "h", and "o" with the corresponding numbers fix the ANN layers and neurones topology.

input (n=23,22,...,1)	$T_{out}, S_{hor}, T_{ind}, E_{ave}$	$T_{out}, S_{hor}, T_{ind}, E_{ave}$	$T_{out}, S_{hor}, T_{ind}, E_{ave}^1, E_{ave}^2, E_{ave}^3$	$T_{out}, S_{hor}, T_{ind}, E_{ave}$	$T_{out}, S_{hor}, T_{ind}, N_{seq}$
output (n=24)	E_{ann}	(output splitting) $E_{ann}^1, E_{ann}^2, E_{ann}^3$	(input/output splitting) $E_{ann}^1, E_{ann}^2, E_{ann}^3$	(1,..., k steps ahead) $E_{ann}^n, \dots, E_{ann}^{n+k-1}$	(1,..., k steps ahead) $E_{ann}^n, \dots, E_{ann}^{n+k-1}$
ANN	FF i92h24o1	FF i92h24o3	FF i138h24o3	FF i92h24o3	FF i92h24o3
models	TD i92h24o1	TD i92h24o3	TD i138h24o3	FF i92h24o6	FF i92h24o6

In the following group of tests only FFBP architecture was used. These tests were necessary to analyze the performance of an ANN-module when working in opened vs. closed control loop and the error (root-mean-square, mean-absolute, and mean error) development when predicting more steps ahead (Table 6.3). A representative result is illustrated below (Figure 6.4).

The results showed clearly that Artificial Neural Networks can be successfully used for predicting the heating energy demand of single solar houses based on only small number of input variables. The FFBP models are preferable over the TDNN. The choice between the closed and the opened loop models should be based on the particular task objectives and the wished forecasting accuracy. Individual, dedicated ANN modules should be used for the particular steps ahead forecasting (one module for one step prediction ahead, other for two steps, etc.). **Such ANN-based subsystems will be very effective when implemented as a predictive module in a heating control system.** The results from the development of

Table 6.3. The performance of closed loop and opened loop ANN models in forecasting the heating energy demand of a single solar house for a number of 5-min steps ahead (RMSE – root mean square error, MAE – mean absolute error, ME – mean error)

Artificial Neural Networks Performance							
Prediction (steps ahead)		1 step	2 steps	3 steps	4 steps	5 steps	6 steps
closed loop ANN model: FF i92h24o3 input: T_{out} , S_{hor} , T_{ind} , E_{ave}	RMSE	221.6	385.9	554.6			
	MAE	124.9	213.5	315.7			
	ME	-1.5	57.7	120.6			
closed loop ANN model: FF i92h24o6 input: T_{out} , S_{hor} , T_{ind} , E_{ave}	RMSE	371.5	454.4	589.1	757.6	915.0	1021.7
	MAE	284.1	303.2	360.3	437.4	506.3	569.0
	ME	-225.5	-162.4	-107.5	-48.9	109.0	187.5
opened loop ANN model: FF i92h24o3 input: T_{out} , S_{hor} , T_{ind} , N_{seq}	RMSE	807.1	848.1	879.0			
	MAE	570.6	599.7	612.2			
	ME	-137.6	-187.5	-173.5			
opened loop ANN model: FF i92h24o6 input: T_{out} , S_{hor} , T_{ind} , N_{seq}	RMSE	832.9	852.6	876.7	894.1	924.0	941.8
	MAE	576.6	587.9	601.0	611.0	634.3	647.9
	ME	215.5	229.7	247.7	255.9	261.1	276.6

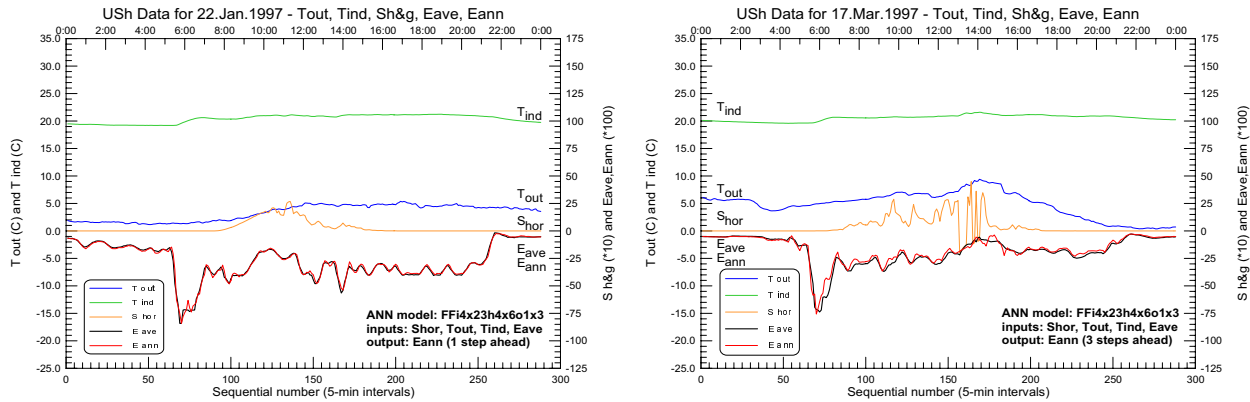


Figure 6.4. Results for closed loop FFBP model trained using input data T_{out} , S_{hor} , T_{ind} , E_{ave} . The input data and the predicted E_{ann} heating energy demand of the single-family solar house are shown. Left: One step prediction ahead model results for 22/01/97. Right: Three steps prediction ahead model results for 17/03/97.

ANN-predictor for E_{ave} controller were presented to the EUFIT'98 Congress in Aachen, Germany (Bellas-Velidis et al, 1998 [BVABK98]).

6.3 NOA ANN-Controller - first controller for $E_{ON/OFF}$

The development of ready-for-test ANN-based controller was carried out having in mind the objectives and the initial set-up of the controller function and the possibility to test it in the NOA PASSYS Test Cell. A limited input information is passed to the controller. It includes date & time (N_d, N_h), the user-set internal temperature preference T_s , the outdoor temperature T_o and global horizontal solar irradiation S_r , and the state of the controlled system, its indoor temperature T_i . In regular time intervals, fixed to $\Delta t = 15\text{min}$, the controller should output the heating energy value E_a necessary to apply during the next interval. The controller should optimally (e.g. based on some cost function C_f) maintain the T_i within the wished comfort zone. The developed ANN-controller has a modular structure, where separate modules perform particular internal functions necessary for the controller (Figure 6.5).

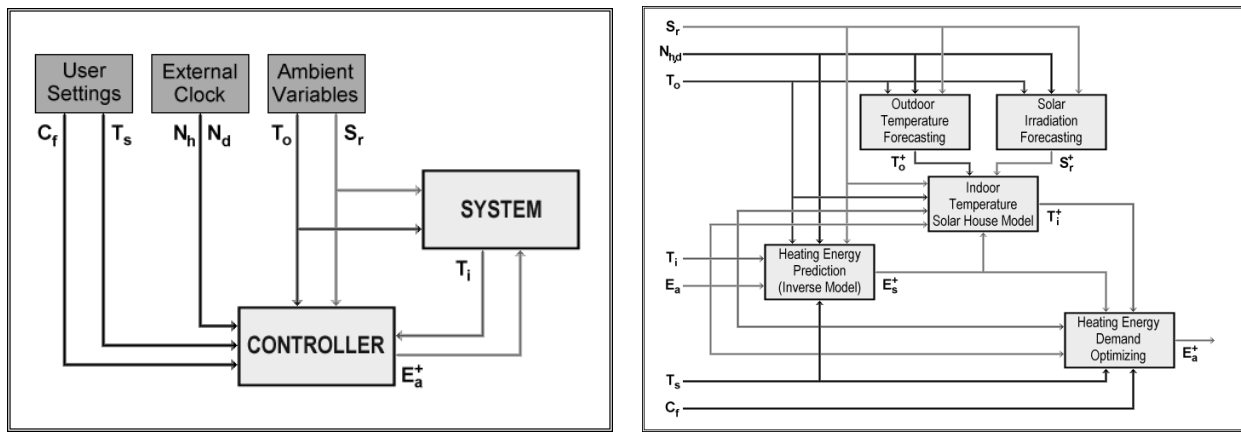


Figure 6.5. PASSYS Test Cell heating system controller set-up

Two modules perform weather forecasting, one predicting the S_r and the other the T_o , using the previous values of these parameters and the corresponding time and day parameters (N_d, N_h). Another module predicts the switching on/off the heating energy E_s using the previous values of the weather parameters (S_r, T_o), of the system and the controller (T_i, E_a), and the user set T_s . This module can be characterized as inverse model of the system. The three predicted parameters (S_r, T_o, E_s), the corresponding past values and the past T_i are parsed to the next module that outputs an estimate of the T_i for the following time interval. This module is an internal model of the system. These four modules are created applying Feed Forward Back Propagation (FFBP) Artificial Neural Networks algorithm. Supervised training with the method of Back Propagation with Momentum Term and Flat Spot Elimination was used. The SNNS software tool, was used for the four ANN modules development.

The final output from the controller to the heating system, the E_a on/off switch position, is fixed by the last module, a simple optimiser. The module uses the last and the predicted values (T_i, E_s, E_a) for the system and the controller to decide about the next action. This module applies simple logic rules based, additionally, on the user set T_s and the requirements for energy savings. There is one more module (not shown) that performs the necessary I/O functions and internal buffering of the parameters. The input gives the last time interval parameters, whereas the buffer keeps the six previous intervals values, and the output is the next control action (Figure 6.6).

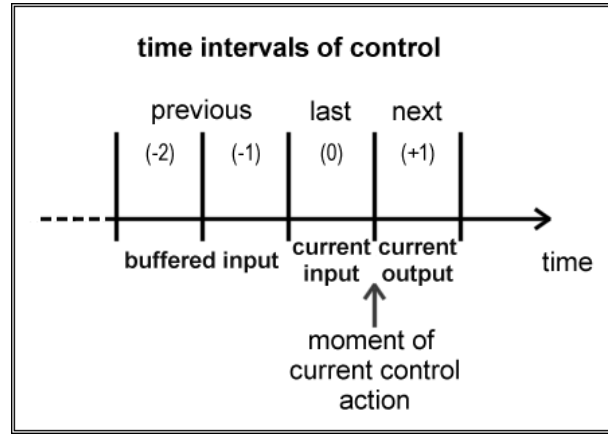


Figure 6.6. Definitions of the I/O data sequences

6.3.1 Weather forecasting ANN-modules

The module forecasting the outdoor temperature uses a simple ANN. It has ten input neurons, one hidden layer of 8 and another of 4 neurons, and one output neuron (**FF.i10h8h4o1**). This ANN was trained using part of real meteorological data for 1993 for the Athens. The rest of the data were used for verification during the training. Data for 1994-1996 were used in offline tests. The inputs and the output are listed in table 6.4.

Table 6.4. Inputs and outputs for the ANN forecasting the outdoor temperature

Input	$N_h^{(+1)}$	the (daily normalized) time value for the next interval
Input	$T_o^{(0,-1,-2,-3)}$	the last and three previous values of the outdoor temperature
Input	$N_d^{(+1)}$	the (yearly normalized) day number for the next interval
Input	$S_r^{(0,-1,-2,-3)}$	the last and three previous values of the solar irradiation
Output	$\Delta T_o = T_o^{(+1)} - T_o^{(0)}$	the outdoor temperature difference for the next interval

The solar irradiation forecast module uses similar FFBP architecture and training procedure, but the number of neurons is greater due to more complicated behavior of this parameter. The training/verification/testing of this ANN were carried out using the same data as in the previous module. The ANN has 28 input neurons, one hidden layer of 16 and another of 8 neurons, and one output neuron (**FF.i28h16h8o1**). The inputs and the output are listed in table 6.5.

Table 6.5. Inputs and outputs for the ANN forecasting the solar irradiation

Input	$N_h^{(0,-1,-2,-3,-4,-5,-6)}$	the daily time value for the next interval
Input	$T_o^{(0,-1,-2,-3,-4,-5,-6)}$	the last and six previous values of the outdoor temperature
Input	$N_d^{(0,-1,-2,-3,-4,-5,-6)}$	the yearly day number for the next interval
Input	$S_r^{(0,-1,-2,-3,-4,-5,-6)}$	the last and six previous values of the solar irradiation
Output	$\Delta S_r = S_r^{(+1)} - S_r^{(0)}$	the solar irradiation difference for the next interval

A small part of the results from testing the two modules is presented below (Figure 6.7). The difference between the real and the forecasted (one step ahead) outdoor temperature is shifted artificially to 250 °C. In rear cases this difference arises up to one degree. The situation with the solar irradiation prediction is much worse. The difference (shifted to 3250) shows a small trend and there are small errors when the real irradiation is zero. The prediction error is about 10-20% when

there are no clouds on the sky. Having in mind the very simplified data input to these modules, as defined in the controller set-up, the forecasting can be adopted as satisfactorily. The real on-line tests (see below) showed that the controlled system does respond (T_i) slowly to abrupt weather changes allowing for such prediction errors. The situation will complicate if we will need to predict the ambient variables more steps ahead.

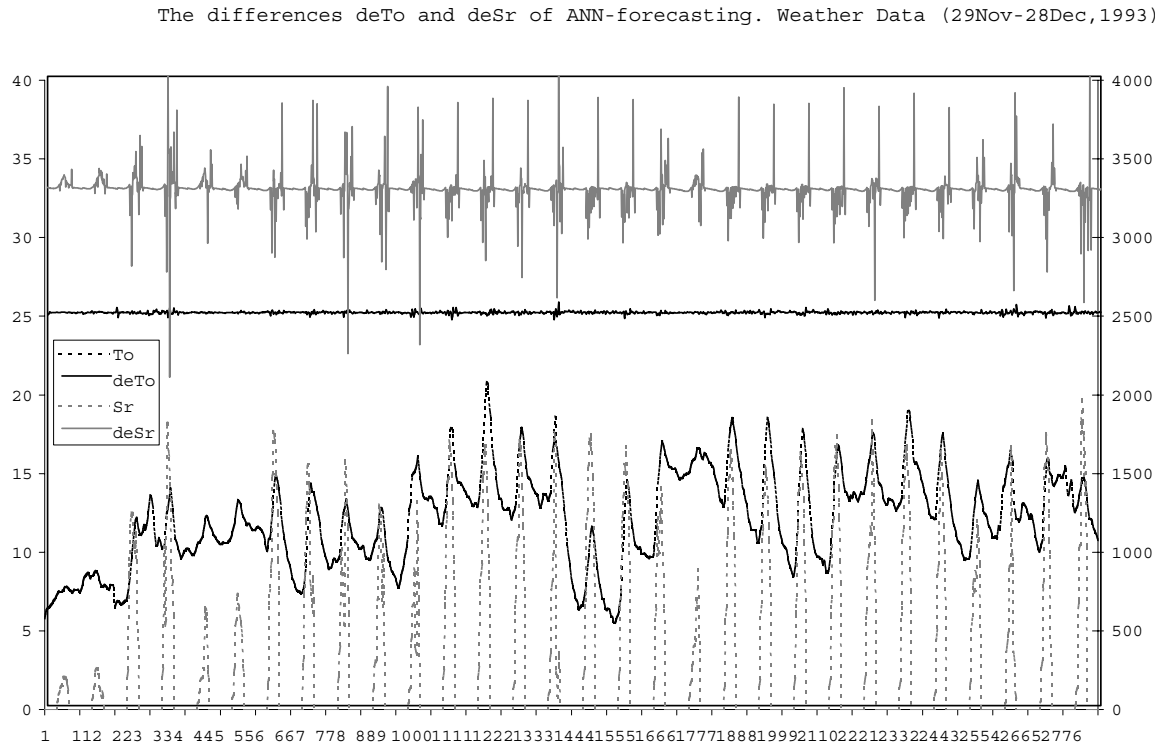


Figure 6.7. Online test results of the weather forecasting modules (ANN-controller for heating energy switch prediction). The differences between the forecasted and the real temperature (deTo) and solar irradiation (deSr) are shown artificially shifted.

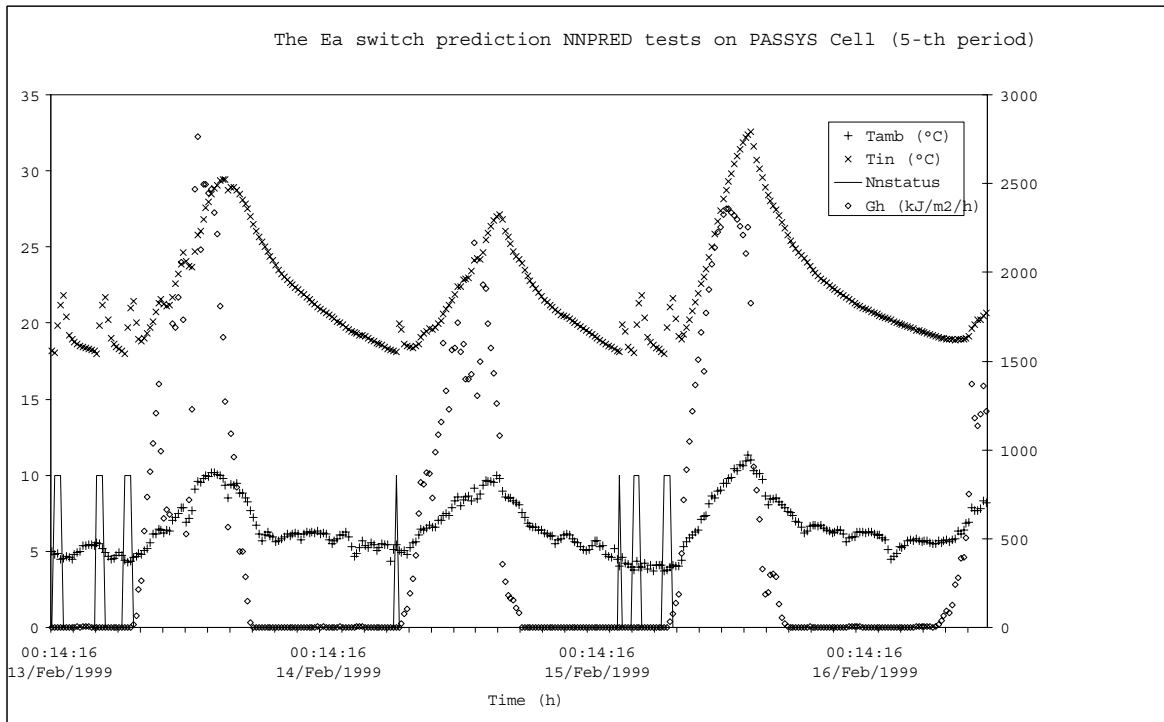
6.3.2 Heating energy switch predicting ANN-module (inverse model)

This module is implemented modifying the well investigated by us heating energy predictor (Bellas-Velidis et al., 1998). The used ANN has 35 input neurons, one hidden layer of 15 neurons and output layer of one neuron (**FF.i35h15o1**). The data set used to train/verify/test this ANN is prepared with TRNSYS model of the PASSYS Test Cell and weather data described above. This predictor is a modified version of the inverse model of the system. Here, the heating energy demand E_s parsed as input is defined by a simple logical rule taking into account the last T_i , T_s , and E_a . The inputs/outputs for this ANN module are listed in table 6.6.

Our first implementations for controller on-line tests in the PASSYS Cell included only this ANN-module. Part of the results from these tests is presented below (Figure 6.8). The **Nnstatus** variable shows the status of the heating system (10=on) for a given interval as set by the controller using for prediction the parameters from the last and six previous control intervals. The controller does not allow the system to fall below $T_i = 18^\circ C$ (as desired), but there is an overheating in up to two consecutive intervals. The analysis showed that the reason of this behaviour is hidden in the data set from TRNSYS model used to train the ANN. Nevertheless, this offline trained ANN-switch was found to be useful for first prediction of the heating demand in the final multi-module controller.

Table 6.6. Inputs and outputs for the ANN predicting the heating energy switch

Input	$N_h^{(0,-1,-2,-3,-4,-5,-6)}$	the last and six previous values of the (daily normalised) time
Input	$S_r^{(0,-1,-2,-3,-4,-5,-6)}$	the last and six previous values of the solar irradiation
Input	$T_o^{(0,-1,-2,-3,-4,-5,-6)}$	the last and six previous values of the outdoor temperature
Input	$T_i^{(0,-1,-2,-3,-4,-5,-6)}$	the last and six previous values of the indoor temperature
Input	$E_s^{(0,-1,-2,-3,-4,-5,-6)}$	the last and six previous values of the heating energy switch
Output	$\Delta S_r = S_r^{(+1)} - S_r^{(0)}$	the heating energy switch for the next interval

**Figure 6.8.** Online test results for the ANN-module for heating energy switch prediction

6.3.3 Indoor temperature defining ANN-module (internal model)

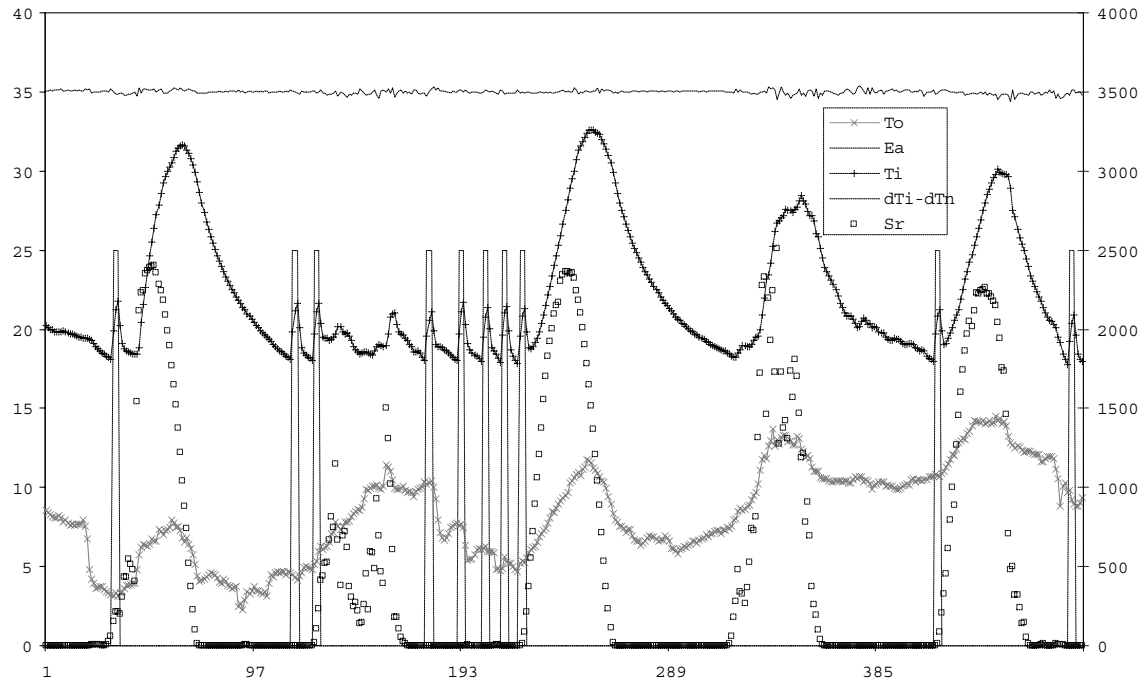
It is an internal model of the system, i.e. it gives us the internal state of the system (T_i) for a given time interval. For this, it uses the values of the external parameters (T_o , S_r , E_a) acting on the system for this and for previous intervals, as well as the previous internal state. The ANN used in this module has 12 input neurons, two hidden layers, the first of 12 and the second of 6 neurons, and one output neuron (**FF.i12h12h6o1**). As above, the data used to train/verify/test this ANN was taken from real experiments on the PASSYS Test Cell. For the ANN-based internal model the defined inputs & output are: listed in table 6.7. The offline tests showed very good performance of the ANN-based internal model. Using real data, the difference between the indoor temperature given by the ANN-module and the real one (see Figure 6.9, the temperature difference is artificially shifted to 35 °C) shows an error of about ± 0.2 °C.

In a real situation, using the multi-module controller, some of the input parameters to this ANN will be forecasted in advance by the other modules (Figure 6.5). The difference between the real and modelled indoor temperature is expected to increase because of the forecasting error propagation.

Table 6.7. Inputs and outputs for the indoor temperature defining ANN-module

Input	$S_r^{(+1)}$	the next (forecast) value of the solar irradiation
Input	$T_o^{(+1)}$	the next (forecast) value of the outdoor temperature
Input	$E_a^{(+1)}$	the next (predicted) value of the of the heating energy
Input	$\Delta S_r^{(+1)} = S_r^{(+1)} - S_r^{(0)}$	the predicted difference in the solar irradiation
Input	$\Delta T_o^{(+1)} = T_o^{(+1)} - T_o^{(0)}$	the predicted difference in the outdoor temperature
Input	$\Delta E_a^{(+1)} = E_a^{(+1)} - E_a^{(0)}$	the predicted difference in the heating energy
Input	$T_i^{(n=0, -1)}$	the last and the previous values of the indoor temperature
Input	$\Delta T_i^{(0)} = T_i^{(0)} - T_i^{(-1)}$	the last difference in the indoor temperature
Input	$\Delta S_r^{(0)} = S_r^{(0)} - S_r^{(-1)}$	the predicted difference in the solar irradiation
Input	$\Delta T_o^{(0)} = T_o^{(0)} - T_o^{(-1)}$	the predicted difference in the outdoor temperature
Input	$\Delta E_a^{(0)} = E_a^{(0)} - E_a^{(-1)}$	the predicted difference in the heating energy
Input	$E_s^{(0, -1, -2, -3, -4, -5, -6)}$	the last and six previous values of the heating energy switch
Output	$\Delta T_i = T_i^{(+1)} - T_i^{(0)}$	the indoor temperature difference for the next interval

The difference (deTi-deTnn) of ANN-model Prediction. PASSYS Cell Data (7Feb-11Feb, 1999)

**Figure 6.9.** Offline testing results of the ANN-module for the indoor temperature prediction

6.3.4 ANN-controller for online and simulation tests - *nnpred*

The modular ANN-based controller, described above, has been implemented as a standalone executable **nnpred.exe** created from a C-language program. The four ANN-modules, trained with SNNS were transformed to C functions, included in the program. This transformation was done with a particular tool of the SNNS software. The interface with the testing system is based on three ASCII files. The necessary input data are parsed by an input file (current state), created by the system, and by a buffer (history) file that is maintained by the controller itself. The defined control action is parsed back to the system by a proper output file. Additionally, the controller maintains a log-file for all the testing period. The execution of one control action on a Pentium PC takes less than second.

Simulation tests and initial on-line tests of the **nnpred** were carried out. This allowed us to improve (to adapt offline the ANN-modules) the controller for the final on-line run on the PASSYS Cell of NOA (see Sections 6.5 and 6.6). The final results (Section 6.7) showed that this modular ANN-controller performs quite well for the set-up task. The indoor temperature was maintained stable within the desired interval. In all the cases the overheating was due only to weather conditions.

6.3.5 ANN-modules development with MATLAB

It is necessary to include an adaptation of the ANN-modules in the final controller. But this is not applicable using the SNNS that is a stand-alone software system. Two alternative solutions were tried and tested. The one was using the Neural Networks Toolbox of the MATLAB software, and the other to create own C-program for ANN training. Implementing MATLAB functions for

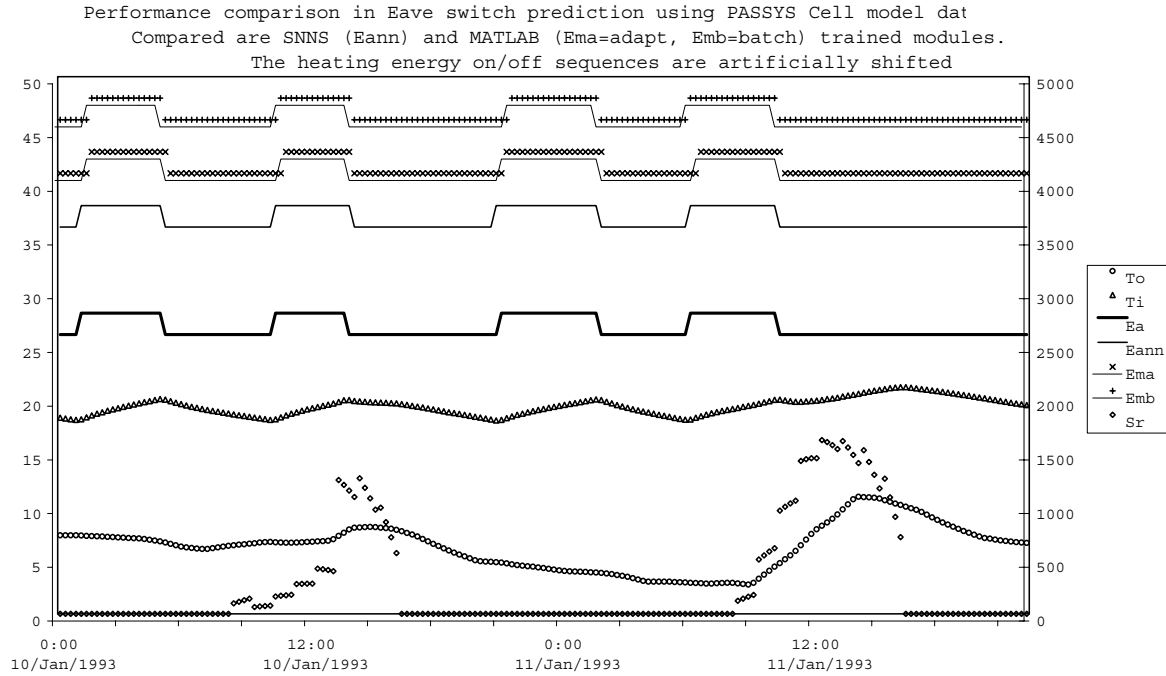


Figure 6.10. Performance comparison of the heating energy switch ANN-module trained with MATLAB (E_{ma} and E_{mb}) and with SNNS (E_{ann}) and the real data (E_a).

ANN learning/testing is quite easy using its scripting language (m-functions), but the final product

should be transformed to a C-function in order to be included in the real controller. All the four ANN-modules were recreated as M-functions and a set of training/verification/test procedures were carried out exactly as this was done with SNNS. Additionally, in adaptive training, a patterns random permutation was provided for better generalisation of the trained ANN, as it is included in SNNS. Exactly the same method (Back Propagation with Momentum Term) and the same training parameters values were used in the adaptive and the batch both MATLAB training and in SNNS.

The tests showed that MATLAB training procedures are too slow compared to SNNS (the latter runs on the same PC). In the weather forecasting, this is mainly due to the reach pool of data parsed for training and the data handling performed by MATLAB. Nevertheless, the training is significantly longer. Even more, all the modules showed worse performance (see for example the heating energy switch module results on Figure 6.10). Trials with increased number of training cycles and/or modified parameters did not improve the performance.

It seems possible to translate the m-functions to C using the MATLAB Compiler and C/C++ Math Library. But there will be a license problem with including such modules in the controller hardware. So well, because the MATLAB solutions are created toward solving many different problems, such modules include software parts unnecessary for our controller (arrays handling, different ANN models, etc.). This would lead to creating unnecessary large executables and to problems in code optimisation. **The final conclusion from these tests and the above remarks was that such M-functions are not suitable for use neither in a simulation environment nor in hardware implementation of the ANN-controller.**

6.3.6 ANN-modules development with own C-program *ann-learn*

We created our own training procedure, tightly coupled with the problem and the particular modules we are developing for the controller. We wrote a C-program **ann-learn.c**, with a very simple I/O interface, that can be run even under DOS. This allows its functions to be used for online adaptation in the real controller. The Feed Forward Back Propagation with Momentum Term and Flat Spot Elimination, in adaptive mode, and training patterns random permutation, is the only used learning algorithm. This is what the initial tests (see above) showed to be most suitable for our task, and this we have used in SNNS and MATLAB runs. We created, trained and tested all

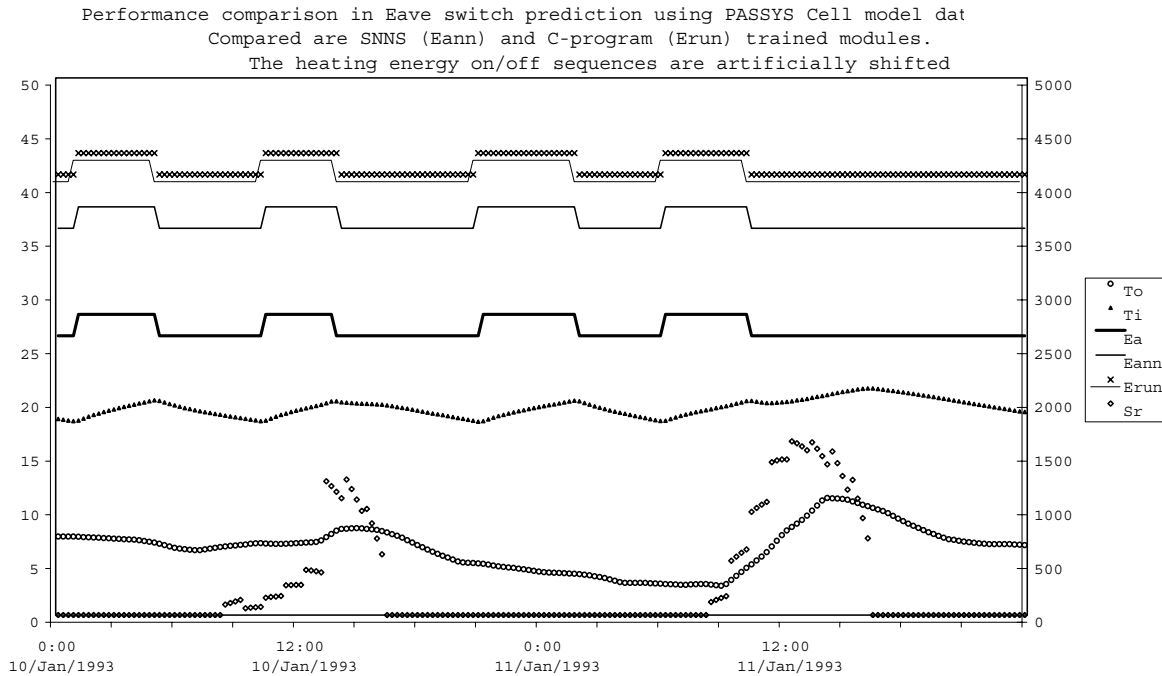


Figure 6.11. Performance comparison of heating energy switch ANN-module trained with the C-program *ann-learn* (E_{run}) and with the SNNS (E_{ann}).

the four ANN-modules using our C-program. The modules were exactly of the same architecture as these tested with SNNS and MATLAB. An example of the results is illustrated above (Figure 6.11). The tests showed very good performance of modules created with the **ann-learn** program. The learning is about as fast as in the SNNS. The final error in the E_a predicting module is smaller, whereas this for the T_i model ANN-module is about the same as the corresponding modules trained with SNNS. The situation with the weather forecasting modules is not so good, but their errors are smaller than in the MATLAB trained modules. **The conclusion is that the developed by us C-program is suitable for use in simulation (as MEX-file in SIMULINK or TRNSYS) and its training functions can be used for particular ANN-modules adaptation in the final hardware implementation of the controller.** The development of the ANN-based controller for $E_{on/off}$ and the results from its on-line testing are presented in a paper submitted for publication (Argirou, 1999 [ABVB99])

6.4 NOA ANN-Controller - final controller for T_{SUP}

The development of the final, ANN-based controller for the supply temperature of a hydronic heating system was carried out having in mind the final objectives. The inputs here are about the

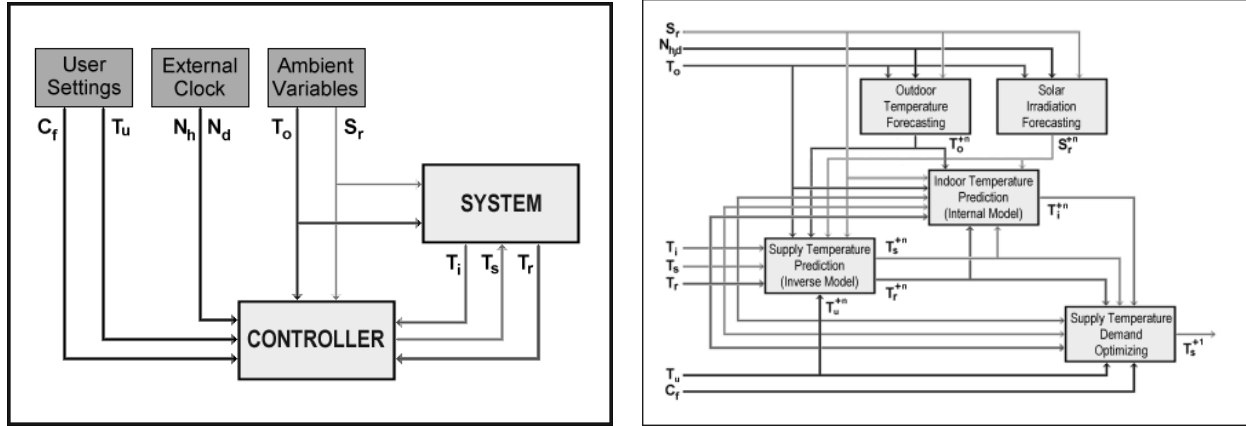


Figure 6.12. Solar house heating system controller set-up

same as for the heating switch controller: date and time (N_d, N_h), the outdoor temperature T_o and solar irradiation on south wall S_r , and the state of the controlled system, its indoor temperature T_i . Additionally, the previous supply temperature T_s and return temperature T_r of the heating system are used as input. The controller should optimally (e.g. based on some cost function C_f) maintain the T_i within the wished comfort zone (T_u) set by the user. But, the output parameter here is the supply temperature T_s of the heating system. So well, the return temperature T_r of the system should also be taken into account (Figure 6.12).

6.4.1 ANN-modules development with SNNS

This type of output makes the ANN-based controller's task much harder. Instead of heating energy on/off prediction E_a , the controlled output spans a wide range of T_s values in this controller. Nevertheless, the modular structure of the controller is generally the same as in the former case (see Section 6.3) and mainly the inverse and the internal models of the system are influenced. The data used to develop the Neural Networks were prepared using the ISFH-partner TRNSYS model. The set for $T_u = 20^\circ C$ was only used. The initial tests showed that it is necessary to provide more steps ahead prediction in all the models. Testing different ANN- modules performance and having in mind the ability to make an optimization, but still maintaining relatively simple Neural Networks it was fixed the ANN-modules to provide prediction up to four steps ahead. As the tests helped us to fix the optimal input/output configuration, they showed the necessity to include one more hidden layer in all the modules architecture and to increase the number of training cycles. The finally adopted modules, their inputs and outputs are described below (Table 6.8). The performance of the adopted ANN-modules was extensively tested off-line using one-year data. The results are shown in Table 6.9 below (in the Reference Models the last value of particular output parameter is used, instead of predicting it). **Undoubtedly, the ANN-modules perform better than reference ones in all the steps of prediction ahead and can be used in the developed controller.** The figures 6.13- 6.16 show the performance for particular set of cold days. Only in the case for solar irradiation the performance is still not good. Of course there is a physical reason. We are using only two weather variables for this forecast. These ANN-modules were included in the new **nnpred4** controller that is ready for simulation tests.

Table 6.8. The finally adopted ANN-modules input and output parameters for TSUP controller

S_r	FF. i18h32h32o4	Solar Irradiation Forecasting ANN-Module
Input	$N_h^{(0)}$	the (daily normalized) time value for the last interval
Input	$N_d^{(0)}$	the (yearly normalized) day number for the last interval
Input	$T_o^{(0, -1, -2, \dots, -7)}$	the last and eight previous values of the outdoor temperature
Input	$S_r^{(0, -1, -2, \dots, -7)}$	the last and three previous values of the solar irradiation
Output	$S_r^{(+1, +2, +3, +4)}$	the solar irradiation for the next four intervals
T_o	FF. i18h32h32o4	Outdoor Temperature Forecasting ANN-Module
Input	$N_h^{(0)}$	the (daily normalized) time value for the last interval
Input	$N_d^{(0)}$	the (yearly normalized) day number for the last interval
Input	$T_o^{(0, -1, -2, \dots, -7)}$	the last and eight previous values of the outdoor temperature
Input	$S_r^{(0, -1, -2, \dots, -7)}$	the last and three previous values of the solar irradiation
Output	$T_o^{(+1, +2, +3, +4)}$	the outdoor temperature for the next four intervals
T_s	FF. i52h32h32o12	Supply Temperature Predicting ANN-Module (inverse model)
Input	$T_o^{(0, -1, -2, \dots, -7)}$	the last and eight previous values of the outdoor temperature
Input	$S_r^{(0, -1, -2, \dots, -7)}$	the last and three previous values of the solar irradiation
Input	$T_i^{(0, -1, -2, \dots, -7)}$	the last and eight previous values of the indoor temperature
Input	$T_s^{(0, -1, -2, \dots, -7)}$	the last and eight previous values of the supply temperature
Input	$T_r^{(0, -1, -2, \dots, -7)}$	the last and eight previous values of the return temperature
Input	$T_o^{(+1, +2, +3, +4)}$	the outdoor temperature for the next four intervals
Input	$S_r^{(+1, +2, +3, +4)}$	the solar irradiation for the next four intervals
Input	$T_u^{(+1, +2, +3, +4)}$	the user set temperature for the next four intervals
Output	$T_s^{(+1, +2, +3, +4)}$	the supply temperature for the next four intervals
Output	$T_r^{(+1, +2, +3, +4)}$	the return temperature for the next four intervals
Output	$D_t^{(+1, +2, +3, +4)}$	the difference between the supply and the return temperature
T_i	FF. i52h32h32o4	Indoor Temperature Predicting ANN-Module (internal model)
Input	$T_o^{(0, -1, -2, \dots, -7)}$	the last and eight previous values of the outdoor temperature
Input	$S_r^{(0, -1, -2, \dots, -7)}$	the last and three previous values of the solar irradiation
Input	$T_i^{(0, -1, -2, \dots, -7)}$	the last and eight previous values of the indoor temperature
Input	$T_s^{(0, -1, -2, \dots, -7)}$	the last and eight previous values of the supply temperature
Input	$T_r^{(0, -1, -2, \dots, -7)}$	the last and eight previous values of the return temperature
Input	$T_o^{(+1, +2, +3, +4)}$	the outdoor temperature for the next four intervals
Input	$S_r^{(+1, +2, +3, +4)}$	the solar irradiation for the next four intervals
Input	$T_s^{(+1, +2, +3, +4)}$	the supply temperature for the next four intervals
Input	$T_r^{(+1, +2, +3, +4)}$	the return temperature for the next four intervals
Output	$T_i^{(+1, +2, +3, +4)}$	the indoor temperature for the next four intervals

Table 6.9. The performance (standard deviation of the difference between predicted and real values) of the ANN-modules compared to reference models

Module	S_r		T_o		T_s		T_i	
	Ref.Mod	ANN	Ref.Mod	ANN	Ref.Mod	ANN	Ref.Mod	ANN
Ahead								
+1	226	181	0.359	0.322	0.799	0.376	0.037	0.026
+2	333	251	0.579	0.475	1.067	0.416	0.059	0.027
+3	397	303	0.770	0.589	1.076	0.436	0.072	0.030
+4	434	328	0.956	0.692	1.251	0.491	0.086	0.031

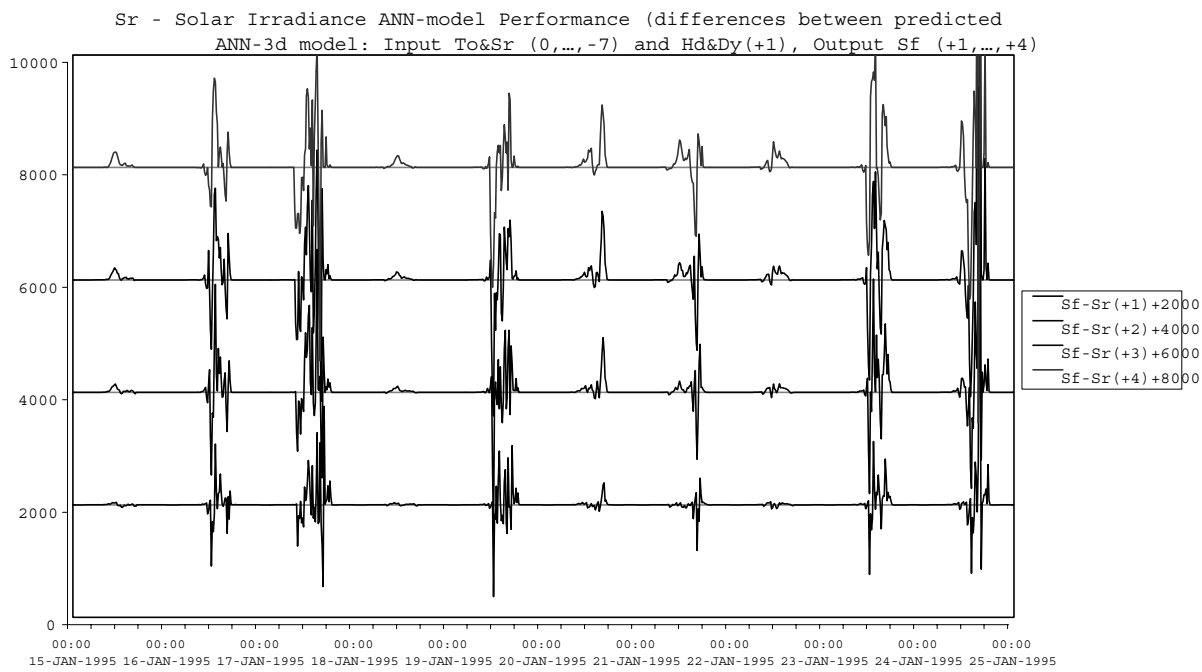


Figure 6.13. Solar irradiation ANN-module performance

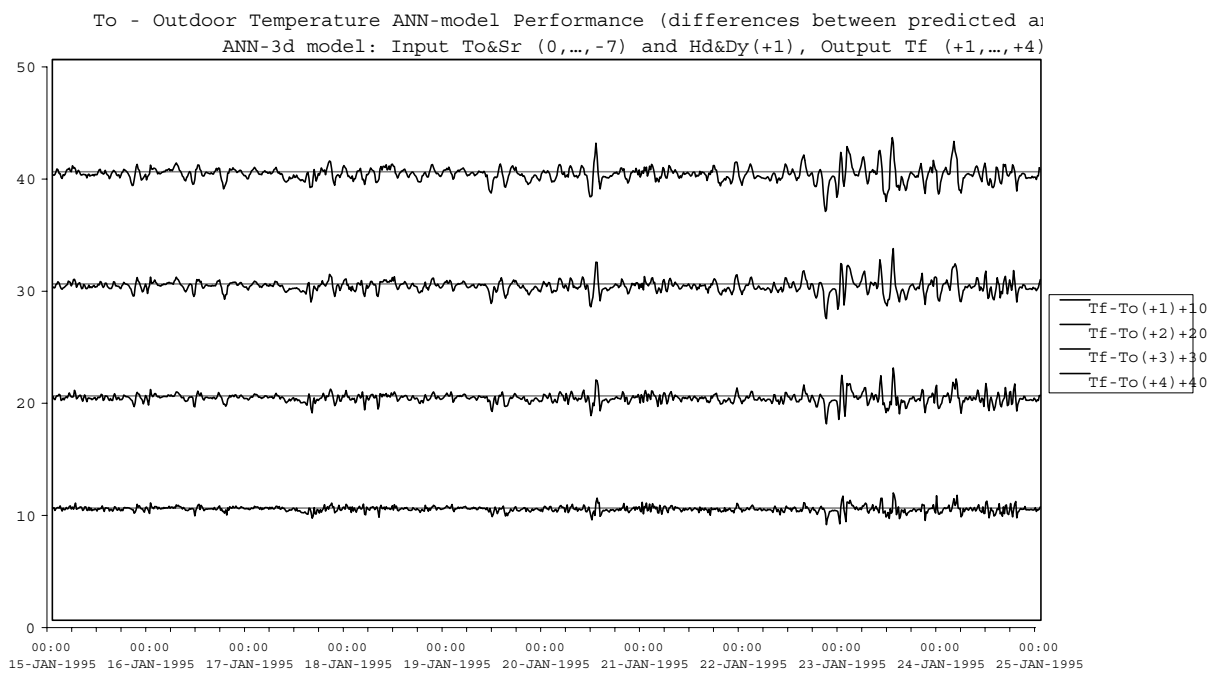


Figure 6.14. Outdoor temperature ANN-module performance

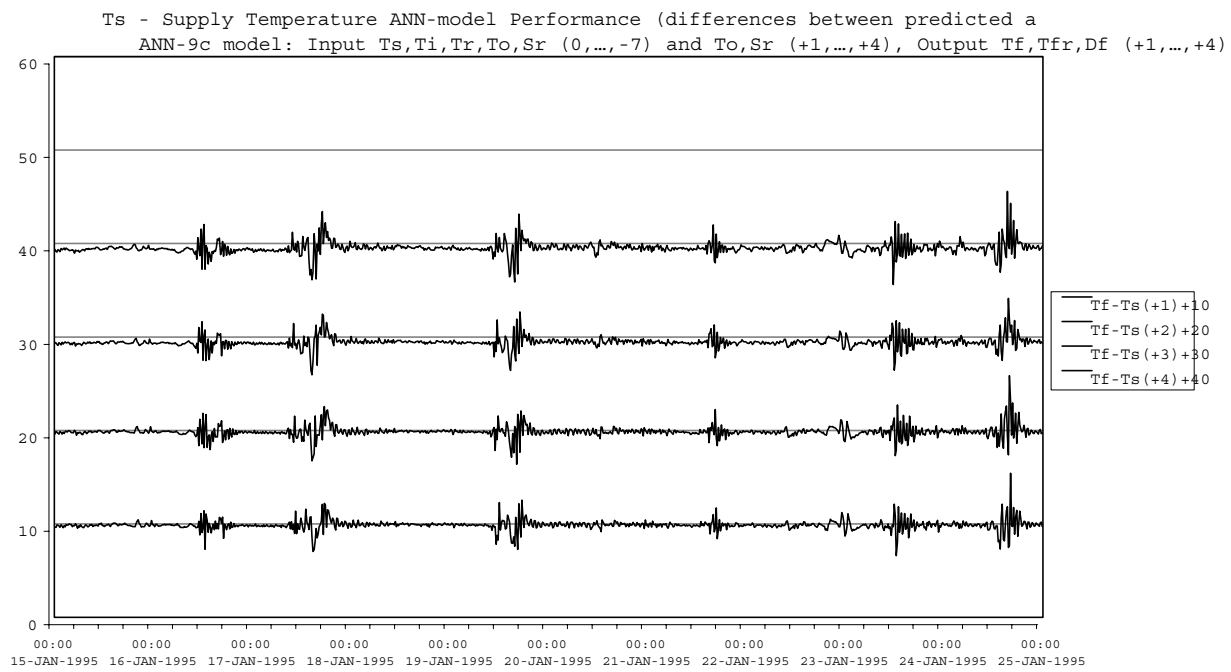


Figure 6.15. Supply temperature ANN-module performance

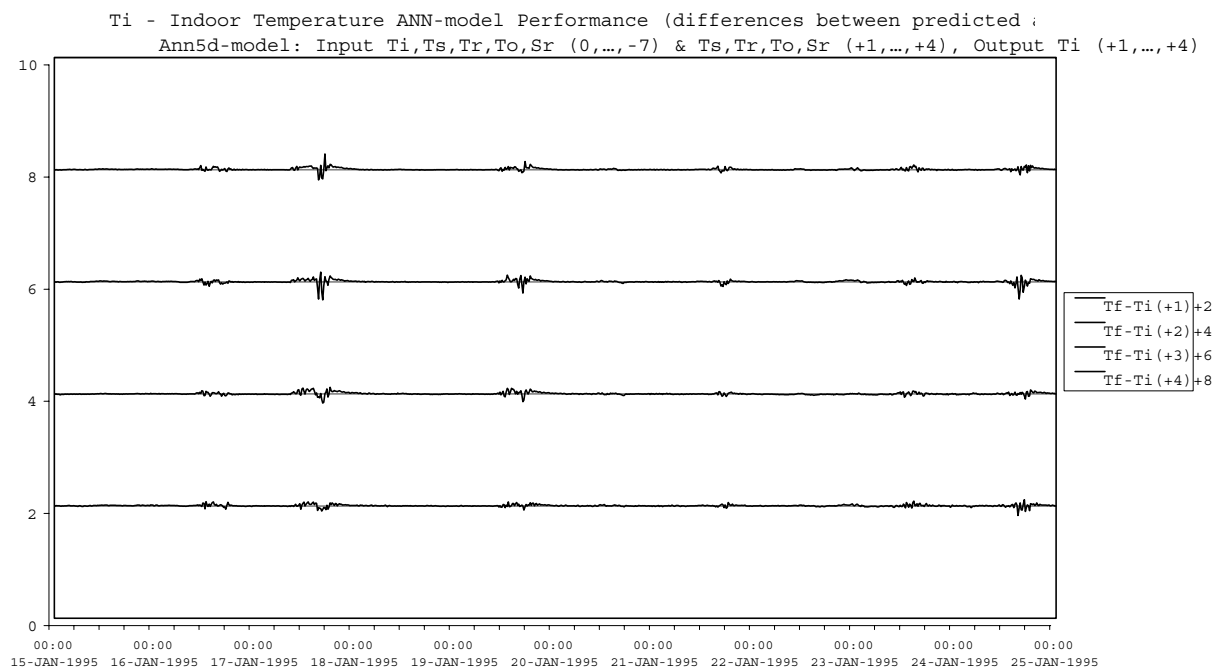


Figure 6.16. Indoor temperature ANN-module performance

As in the case of the energy switching (Section 6.3.6) a C-program **ann-learn4** was created to train the ANN-modules. Its has been extensively tested. Modules trained with it showed about the same performance as these developed with SNNS. This program is intended to be included in the real controller to adapt online its ANN-modules.

6.4.2 ANN-controllers for FUL and for ISFH buildings

Such ANN-modules, as described above, were used for the final controller. There were released two such controllers, one for the model (building and heating system) of FUL-partner and one for the model of ISFH-partner. Each controller's ANN-modules were trained, verified and tested using simulation data provided by the particular partner. The main difference from the above described training of the modules, was that the data sets now include simulation for two set points, $T_u=15\text{ }^{\circ}\text{C}$ and $T_u=21\text{ }^{\circ}\text{C}$ as it was decided during the last meeting of the project. This affected the "Inverse Model" and the "Internal Model" ANN-modules (Figure 6.12). Two-year data were used in the case of ISFH, whereas for the FUL controller the available data set included two heating seasons. The performance of the particular ANN-modules is close to this presented above (Figures 6.13 – 6.16). A small degradation in the weather forecasting modules was observed in the case of FUL. This is caused by the origin of the meteo-data set. The real data used for creating the simulation data had a 2-hour step. The set necessary for simulation was created by interpolation to 1-hour step and then repeating four times the hourly data to provide the final set (15-min step). The weather forecasting modules, trained with this data set provide a rather conservative prediction. The forecasted outdoor temperature and the solar irradiance are more close to their previous values. This of course influences the other modules as they use the predicted values as input. Nevertheless, the overall performance of the controller is quite good as shown by offline and online tests (see Section 6.10).

6.5 Experimental facility – PASSYS test cell of NOA

The prototype neural controller has been extensively tested in the PASSYS test cell, located at the premises of the National Observatory Athens in Pendeli. The facility is shown below (Figure 6.17). The photo on the left-hand side shows the cell from the outside, while on the right hand side the indoor of the test room of the cell is shown. The test room is heated via four electric resistances and a fan. In the actual mode the *EON/OFF* controller activates or deactivates these resistances.



Figure 6.17. The PASSYS Test Cell

The data acquisition system used is the Hewlett-Packard 38512A, controlled by a PC clone Pentium 133 Hz. The following sensors are connected to it:

- Seven Pt 100 platinum resistance thermometers measuring the indoor temperature at various points inside the test room.
- One Pt 100 thermometer measuring the ambient temperature. All these thermometers are shielded against radiation.
- A CM3 Kipp & Zonen pyranometer, measuring the global horizontal solar radiation on top of the test cell.

For the needs of the experimental testing the data acquisition system controls also the heating system. This function was implemented in such a way in order to allow testing of other controller algorithms also and not only of that developed by NOA. All sensors are interrogated every minute and 15-minute averages are stored and provided to the neural controller. The controller then decides whether or not the heating system should be activated or not. The data acquisition system records also the controller decision, the status of the switch that activates the heating system and also the energy consumed by the heating system. The acquisition of all these parameters allows the early detection of possible failure of the hardware to follow the instructions of the controller.

It should be noted that although the PASSYS cell is particularly well insulated, it has a very low thermal mass. In order to increase the thermal mass and better approximate the thermal behavior of the slow responding solar houses, two water tanks of 500 lt each were introduced into the test room. The effective thermal mass added this way was determined via the CTLSM ver. 2.6 identification method (Madsen & Holst, 1995 [MH95]).

6.6 Controller implementation in PASSYS test cell of NOA

The data acquisition system is programmed for the above-described tasks, using the VEE object oriented programming software. This software allows the user to implement other applications

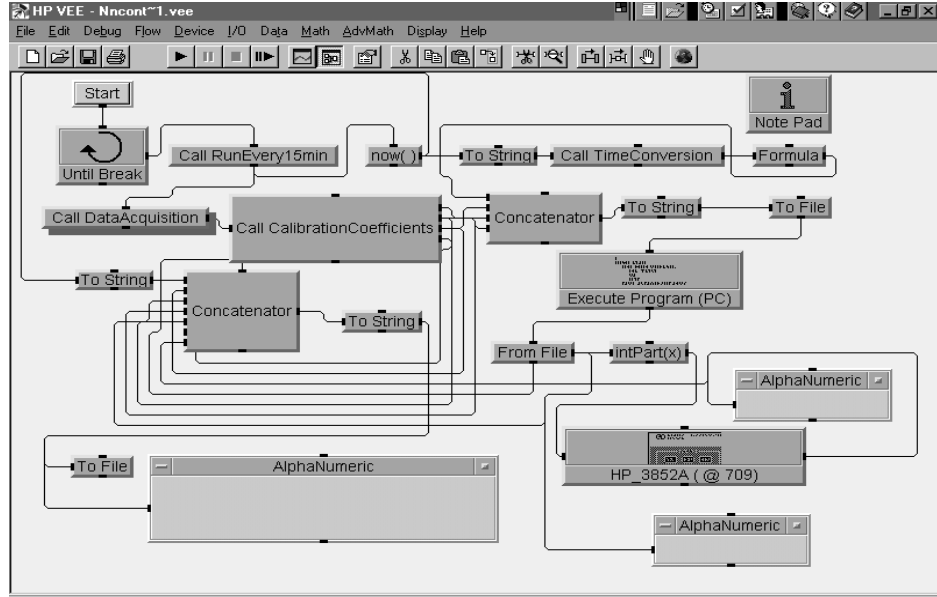


Figure 6.18. VEE-based testing environment of the controller in PASSYS Test Cell

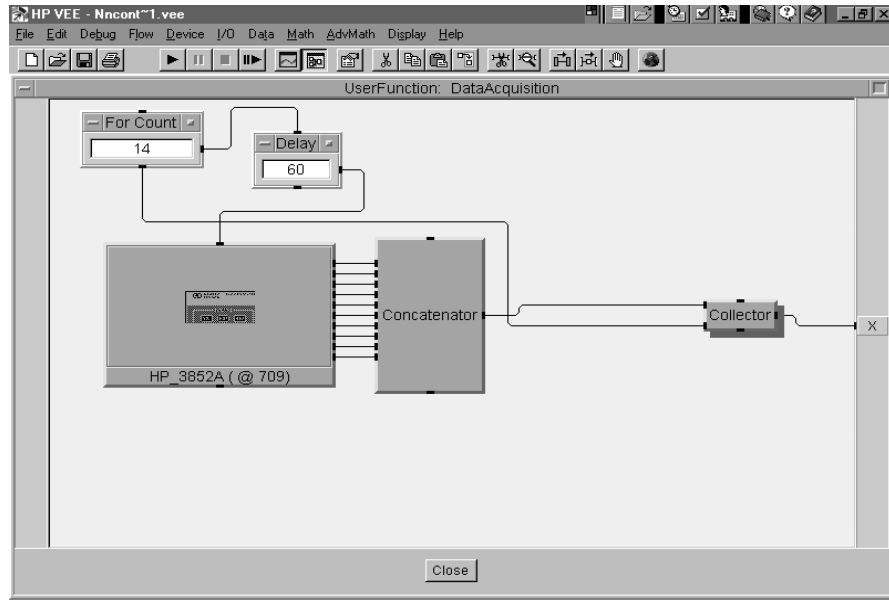


Figure 6.19. Example with opened the VEE Data Acquisition block

in a very easy way. When testing the neural controller, the algorithm was translated into a C code, which was then compiled. The executable of this code was called by VEE every 15 minutes; the acquired data are provided as input and the result of the controller activated a particular switch, defining thus the status of the heating system. The front end of the software is shown in

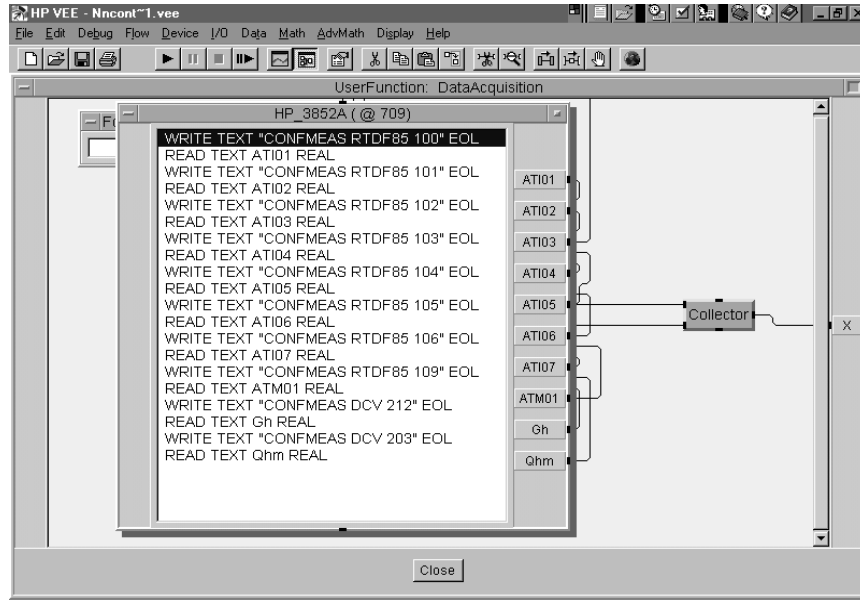


Figure 6.20. Example with the contents of the VEE block HP_3852A

Figure 6.18. Each one of the blocks of this front end, hide other information. An example is shown in Figure 6.19. Here the open form of the block labeled "Data Acquisition" is presented.

This block is responsible for the interrogation of the sensors. The delay of 60 seconds, is the interrogation period. In the following Figure 6.20, the contents of the block HP_3852A are shown. These are the instructions sent to the device for the interrogation of the sensors and the collection of the results.

The neural network controller program, named **nnpred**, is called in the block "Execute Program PC". Data are transmitted to and from the program via buffer files. The acquired data and the results of the neural network controller are stored in separate files. The nnpred program is an executable created from a C-language source code. All the described modules are written as C-programs that are called by a main program. Especially helpful for the case, is the ability of the SNNS to transfer the trained neural networks in the form of C-functions. The program, in addition to the use of buffer files for I/O, maintains a history stack of particular parameters six control intervals backward. So well, a log-file is continuously updated, saving all the I/O and some internal variables, necessary to monitor offline the particular module performance. Without applying any optimization of the code, the size of the executable is 233K. It executes almost instantly giving the necessary output. For the testing of the controller developed by Fondation Universitaire Luxembourg (FUL), the same principle was adopted. There are differences however since this controller was developed under Matlab. In order to avoid loss of time from converting the Matlab software into C, the "Execute Program" box of the data acquisition system is in this case launching Matlab; a special script launched together with Matlab, activates the controller software. No other significant changes were required, since all controllers tested in this project accept the same inputs.

6.7 NOA Online testing results - ANN-Controller for $E_{ON/OFF}$

The test of the neural control algorithms on the PASSYS test cell started relatively late, beginning of December 1998, since the weather was unseasonably warm until this time. The tests lasted until the end of March 1999; after this date the weather was such that did not allow any tests with the heating system. The collected data were analyzed almost everyday, in order to assess the behavior of the controller. The result of this analysis was a continuous improvement of the control algorithms. Each improvement was immediately implemented in the testing environment, without having to interrupt the operation of the experimental plant. Part of the obtained results

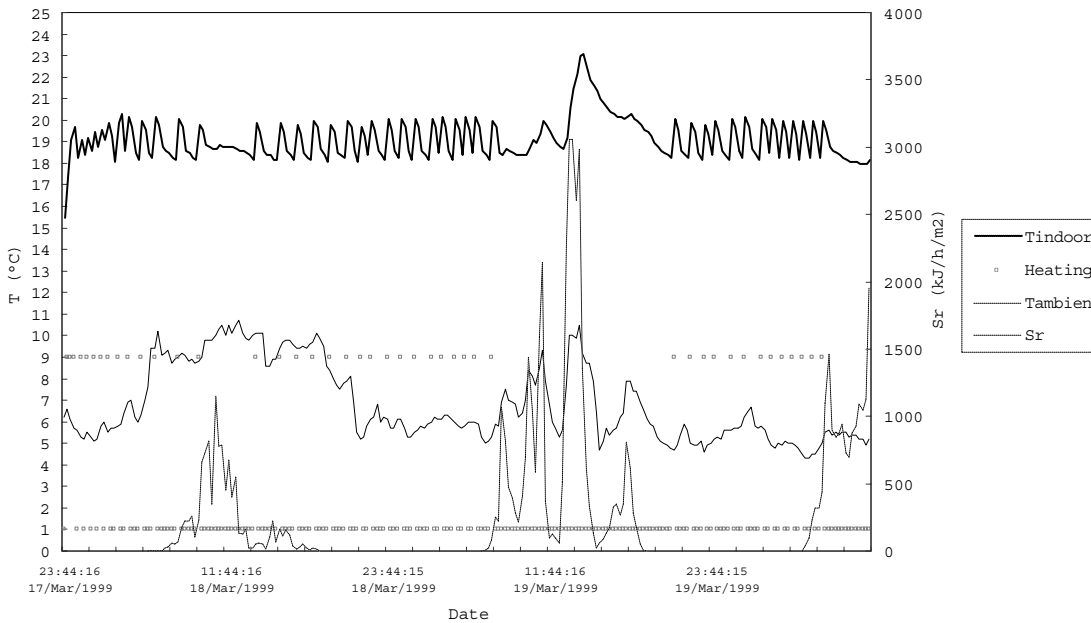


Figure 6.21. Results of the in-situ testing of the ANN controller (Heating System: 1=off, 9=on).

is shown in Figure 6.21. This figure shows the variation of the indoor and ambient temperature, solar irradiance and the status of the heating system ("9" indicates that the heating system is ON and "1" that the system is OFF). The desirable indoor temperature range was set at 18 to 20 °C. Accordingly, one can conclude that the developed controller maintains well the indoor temperature within the desired interval. Although the forecasts of the ambient temperature and solar radiation are not so accurate, as discussed in section refsec:NOAsec3, the impact on the overall performance of the controller is not significant. These results are presented in paper submitted for publication (Argiriou et al, 1999 [ALK⁹⁹]).

6.8 Off-line performances assessment – ANN-Controller for $E_{ON/OFF}$

The performance of the neural controller over a complete heating season and its comparison with a conventional controller was performed via numerical simulation. The thermal performance of the PASSYS test cell was simulated using the well known transient simulation code for solar systems and buildings, TRNSYS (Klein, 1994 [KB⁹⁴]). The advantage of TRNSYS is its modularity. It is therefore possible to create a new routine with the ANN controller algorithms and apply it to the heating system of the cell. The simulation time step is identical to the actuation interval of the controller (i.e. 15 minutes). The meteorological data used is the Typical Meteorological Year for

Athens, Greece (Argiriou et al., 1999 [ALK⁺99]). Two annual simulations were made: one assuming that the temperature inside the test cell has to be maintained within the range 18 to 20 °C by a conventional controller and a second during which the temperature is kept within the same range using the ANN controller. The goal of these simulations is to test whether the implementation of the ANN controller reduces the energy consumption, while maintaining the indoor temperature within the desirable range. Figure 6.22 shows the indoor temperature variation for the first four simulation days (solid black line) with the ANN controller. The dashed line shows the variation of the global solar irradiance on a horizontal plane and the gray line shows the status of the heating system of the cell ("0" indicates that the heating system is OFF and "25" that the system is ON). Figure 6.23 shows the corresponding data using the conventional controller for the simulation.

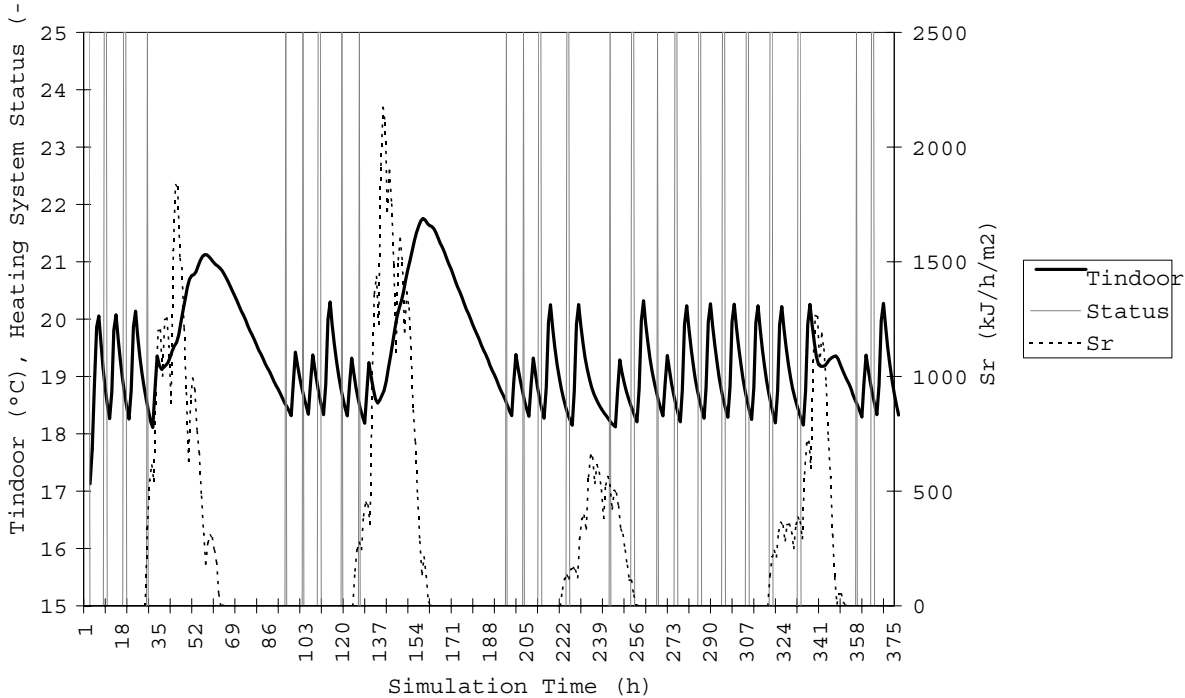


Figure 6.22. Results of the in-situ testing of the ANN controller (Test cell performance simulation with the ANN controller).

The comparison of the two figures leads to the following observations:

- In both cases the lower set point of 18 °C is well maintained.
- Although the conventional controller stops the heating system at 20 °C, the indoor temperature always exceeds this value. This is due to the fact that the conventional controller can not predict and therefore it does not take into account the thermal inertia of the test cell. In some cases, the indoor temperature exceeds 21 °C, even at times when solar irradiance is zero or very low. The neural controller switches-off the heating system at about 19 °C, when the solar irradiance is zero or very low, "knowing" that the temperature will increase to the upper set-point of 20 °C, due to the thermal inertia of the system. When the ANN controller forecasts also the increase of solar radiation, it might stop the heating system even at 18.6 °C.
- The conventional controller maintains the heating system on for about three time steps (i.e. 45 minutes in average), while the ANN controller does the same for about two time steps in average.

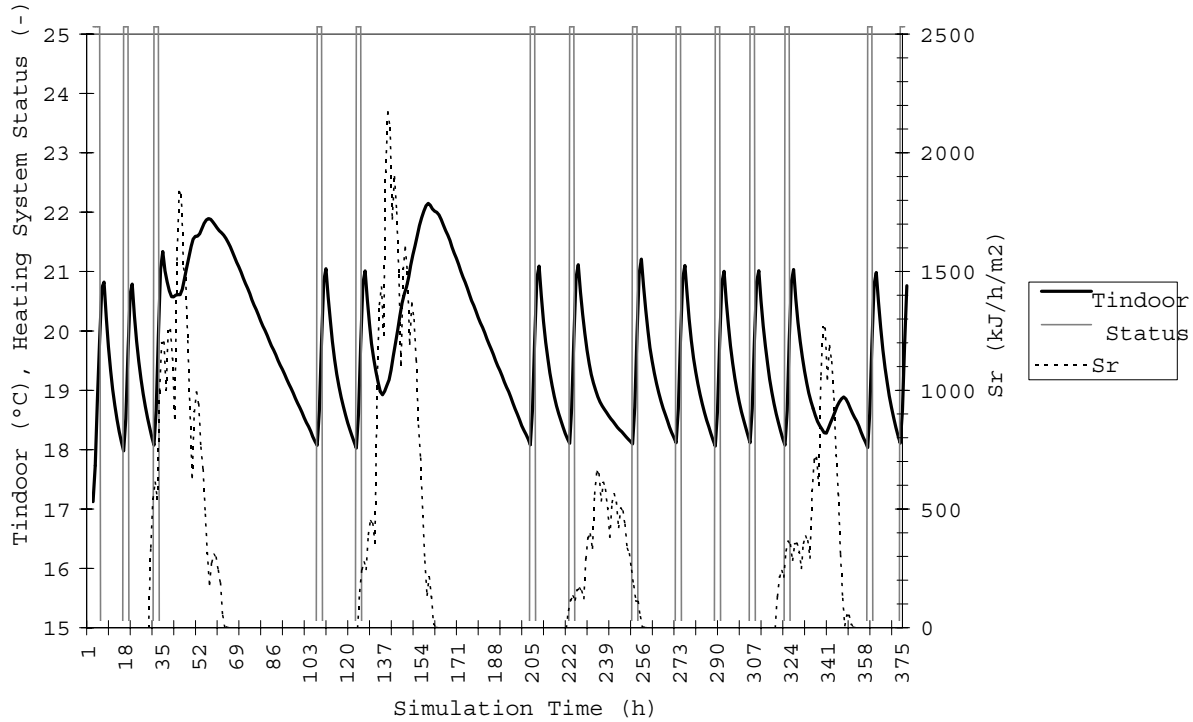


Figure 6.23. Results of the in-situ testing of the ANN controller (Test cell performance simulation with the conventional controller).

The above observations explain why the ANN controller can lead to a reduced heating energy consumption. Simulations showed that the total annual energy consumption of the test cell is 771 MJ with the conventional controller and 713 MJ with the ANN controller. Accordingly, the use of the neural controller can lead to a 7.5% decrease of the annual heating energy consumption of the PASSYS test cell.

6.9 Tests of the FUL partner $E_{ON/OFF}$ controller by NOA

. On December 1999, in the frame of the exchange of the various controller types, FUL adapted the format of inputs and outputs of its control algorithms to that of the data acquisition and control software used by NOA. The great difference between the original FUL controller and the adapted for this test is in the fact that there is a hydronic heating system in FUL building, whereas the PASSYS Cell uses an on/off air heating system.

The experimental testing lasted until the end of January 2000. The experimental results were delivered to FUL for the final assessment. They are presented in section 5.5.2, starting on page 88.

6.10 Tests of the NOA ANN-Controller for T_{SUP} at FUL

. The version of the ANN-controller **nnpred4** for T_{SUP} created for the FUL-partner system (see Section 6.4.2) was tested experimentally and in simulation by the partner. The "Shell for controllers exchange v 5.0", created by the FUL-partner was used for the simulation tests. The results from the simulations performed by FUL-partner are shown below (Table 6.10). Compared are: "Conventional" controller, the "Optimal" controller (FUL), the ANN-based controller (NOA) and the "Predictive" controller (ISFH). (Figure 6.24 and 6.25).

Table 6.10. The performance of different controllers tested in simulation by FUL-partner.

Comparing results for controllers (CompareSSBC V 1.00)													
Control	1	2	3	4	5	6	7	8	9	10	11	12	13
Control	Conv	Conv	Conv	Opti	Opti	Opti	Opti	ANN	ANN	Pred	Pred	Pred	Pred
CLD	0	0	0	4	5	6	7	0	0	8	8	9	9
NHSc	5	6	7	0	0	0	0	4	7	0	6	6	7
Temperature during occupation													
Min	19.76	20.12	20.57	19.59	20.16	20.17	20.23	17.62	19.45	15.72	19.17	19.92	20.65
Max	27.72	27.72	27.72	27.60	27.62	27.62	27.62	27.64	27.64	27.57	27.58	27.60	27.61
Avg	21.87	21.90	21.94	21.28	21.35	21.38	21.40	21.26	21.64	20.49	21.44	21.54	21.56
Avgabs	21.87	21.90	21.94	21.28	21.35	21.38	21.40	21.26	21.64	20.49	21.44	21.54	21.56
Stddev	1.19	1.17	1.16	1.13	1.11	1.10	1.10	1.40	1.21	1.74	1.20	1.15	1.15
Sacent	0.83	0.82	0.82	0.67	0.66	0.66	0.66	0.94	0.84	1.22	0.79	0.76	0.77
J_d during occupation (PPD-5)													
Min	0.000	0.000	0.000	0.000	0.000	0.000	0.000	0.000	0.000	0.000	0.000	0.000	0.000
Max	19.903	19.931	19.961	18.810	18.993	18.976	18.931	19.198	19.167	21.990	18.559	18.803	18.841
Avg	0.307	0.301	0.299	0.301	0.274	0.268	0.266	0.642	0.302	2.060	0.317	0.256	0.255
Avgabs	0.307	0.301	0.299	0.301	0.274	0.268	0.266	0.642	0.302	2.060	0.317	0.256	0.255
Stddev	1.796	1.799	1.805	1.593	1.613	1.613	1.610	1.895	1.651	3.640	1.586	1.608	1.614
Sacent	0.571	0.567	0.567	0.493	0.483	0.482	0.482	0.942	0.527	2.575	0.541	0.485	0.485
PMV during occupation													
Min	-0.2630	-0.1884	-0.0946	-0.2977	-0.1804	-0.1789	-0.1652	-0.7023	-0.3276	-1.0893	-0.3847	-0.2294	-0.0785
Max	1.0303	1.0311	1.0319	0.9986	1.0040	1.0035	1.0021	1.0099	1.0090	0.9890	0.9913	0.9984	0.9995
Avg	0.0177	0.0203	0.0226	-0.0123	-0.0013	0.0029	0.0056	-0.0490	0.0054	-0.1646	-0.0029	0.0155	0.0163
Avgabs	0.0295	0.0269	0.0248	0.0525	0.0421	0.0378	0.0351	0.0909	0.0379	0.2042	0.0432	0.0258	0.0250
Stddev	0.1237	0.1222	0.1213	0.1224	0.1178	0.1164	0.1159	0.1719	0.1233	0.2766	0.1262	0.1130	0.1126
Sacent	0.0451	0.0449	0.0448	0.0495	0.0417	0.0405	0.0402	0.0992	0.0427	0.2099	0.0430	0.0398	0.0398
Heating Consumption [kWh]													
	2768	2782	2807	2297	2320	2333	2346	2306	2492	2050	2435	2473	2522
Total Discomfort Cost [(%PPD-5)*h]													
	429.6	421.6	418.1	420.8	384.1	374.7	371.7	899.1	422.3	2883.4	443.9	358.7	357.0

The simulation tests showed that the ANN-controller gives smaller heating consumption, as compared to the conventional one, and is close to the predictive controller, but is worse than the optimal one. There is evident dependence of this performance on the heating schedule (NHSc) for the neural controller. Particular schedule leading to about 10% lower consumption gives rise to twice larger discomfort cost. A dummy-controller test was performed by the FUL-partner initially for the sake of I/O compatibility. The experimental, on-line testing started at FUL-building in February 3, 2000. A representative result for the ANN-controller performance is shown below

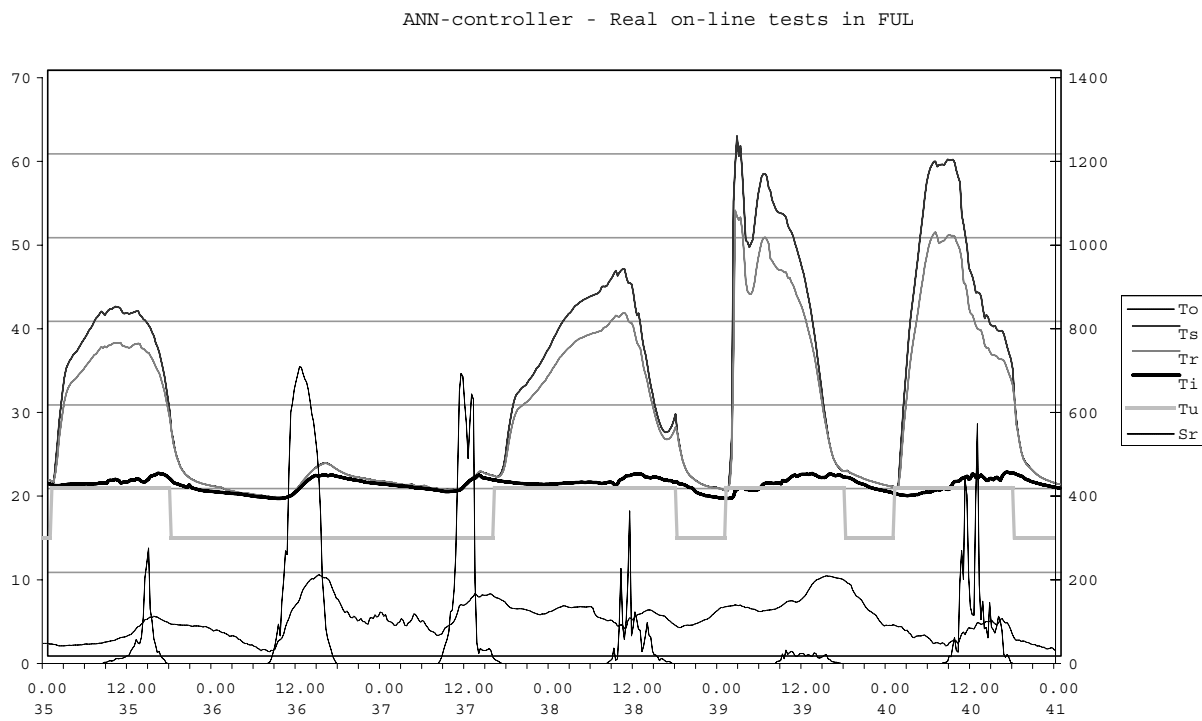


Figure 6.24. Results from online test of the ANN-controller for the FUL-building.

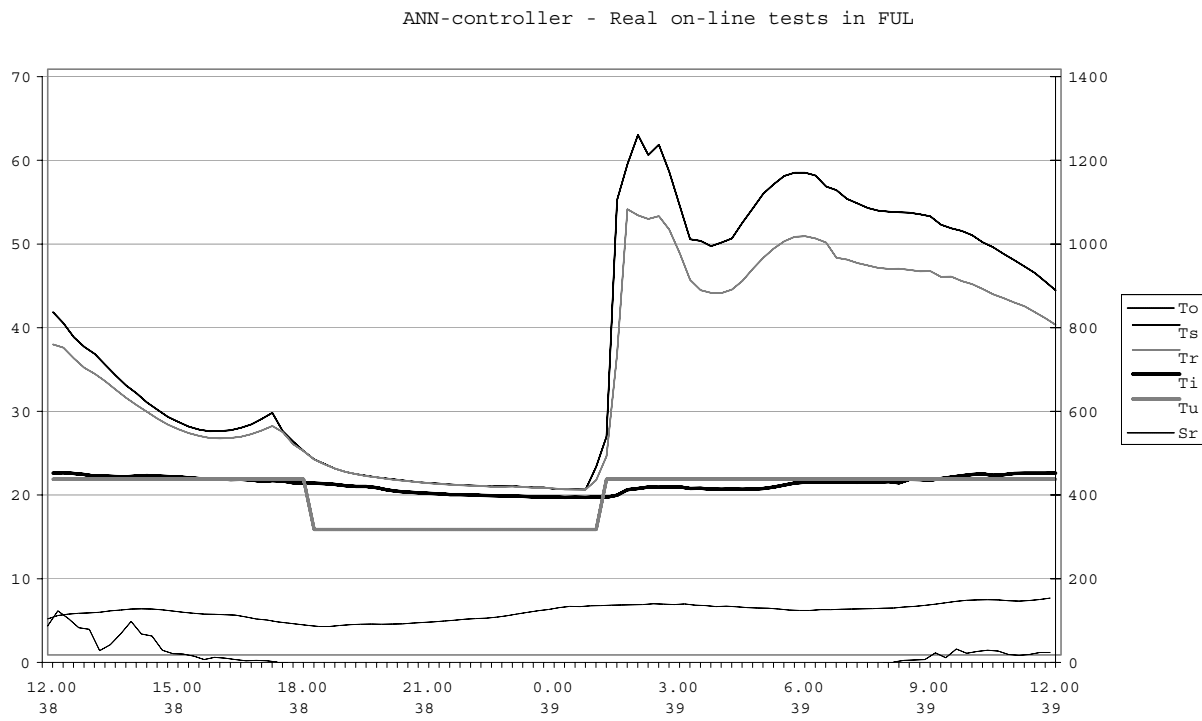


Figure 6.25. Results from online test of the ANN-controller for the FUL-building.

6.11 Conclusion

In the frame of the current project, the ability of the artificial neural networks to control the heating systems of individual solar houses was assessed. The controller was applied on two types of heating systems: an electrical one, where the ANN controller was acting as an on/off switch and a hydronic system, where the ANN controls the supply temperature to the radiators. Both cases were tested experimentally, but also under the TRNSYS simulation environment.

The initial development was related to the electrical heating system. It was found that the ANN controller can lead to a 7% of annual energy savings under the Hellenic weather conditions, when applied to the PASSYS test cell experimental facility. The controller of the hydronic system was based on this first development. This second type of controller was experimentally tested on the FUL building for a period of two weeks. During the tests, the controller operated generally as expected, based on the simulation results. Comparison with the other controllers tested on the same facility showed that this performs better than conventional controllers.

There are some issues however, which were not tested during this research project, mainly due to the lack of time available. These are:

1. The on-line adaptation possibility offered by ANN's. This was done only off-line for the electrical heating system of the PASSYS test cell. This feature can be added in future releases of the controller software. This requires only the addition of further instructions in the software code; the scientific basis of the related algorithms has been investigated. A drawback towards this direction is the performance of the microcontrollers used at this time, since the size of the software they can incorporate is limited. An adaptive controller requires much more memory space than the non-adaptive one.
2. The proposed ANN controller has been designed to perform optimally at specified thermostatic control values. In real applications however the set-points are frequently modified, even within the day. When the set-point is modified, this creates discontinuities for a certain period. These discontinuities are badly handled, it was not possible to obtain such data sets, either from experiments or simulation in order to train the ANN. It is believed however that an adaptive ANN controller can easily overcome this problem.

Finally it should be stated that the ANN software could not be implemented at this stage in the microcontroller proposed by the industrial partner of the project for the reason that the ANN algorithms require double precision operations, while the proposed microcontroller operates only in single precision. The off line tests we performed, training the ANN controller using double precision variables and then operating under a single precision environment reduces its capabilities substantially.

Summarizing, the work performed by the National Observatory of Athens showed that ANN's can be successfully used to control the heating plants of individual solar houses, leading to energy savings. There is however a small number of technical issues that need to be addressed prior to passing to the commercialization of the product.

Chapter 7

Work performed by INSA

Author: Pierre-Yves Glorennec

7.1 Introduction to INSA work

The project goal was to design and test smart controllers being able to save energy and assure comfort in solar buildings. Such a controller must:

- anticipate the building reactions faced with meteorological disturbances by increasing or decreasing heating in advance;
- provide the right energy: a controller has not to react to window opening, for example;
- allow the user to select a comfort level;
- manage the occupancy/unoccupancy periods.

Conventional controllers, based on outdoor or indoor temperature, can not achieve these goals. A control policy based on outdoor temperature allows to provide approximately the right energy, with two drawbacks:

- building inertia and dynamics are ignored and the thermal loads are computed according to instantaneous values of outdoor temperature;
- solar gains are not or badly taken into account.

This policy cannot avoid overheating and is clearly non-optimal. On the other hand, a control policy based on indoor temperature can cause energy waste when the thermostat reacts to window openings. Moreover these two policies are fixed and one-step ahead: they don't allow the determination of an optimal heating policy which is basically multi-step ahead.

7.2 INSA controller

7.2.1 General constraints

INSA wanted its controller to respect the constraints listed below. These constraints have a strong influence on our choice for the model and the different parts of the controller.

Genericity

Easy transposition from a building to another, with as less changes as possible.

Simplicity

As less understandable parameters as possible.

Robustness

Functioning possible even with badly tuned parameters.

Evolutivity

On-line self-learning capability, according to a protocol.

Small size

Optimized code for micro-controller applications.

Novelty

New concepts for building energy management.

7.2.2 Global architecture of INSA controller

The approach of INSA consists in computing a policy (i.e. a sequence of control actions over a sliding temporal window), with respect of comfort and energy requirements. For this purpose, three main components are necessary:

- a meteorological forecasting module,
- a model of the controlled building, in order to test different heating policies and to choose the best,
- a policy generator.

The model is necessarily either an open-loop model or an n-step ahead predictor, with order n large enough to validate the policy.

The architecture is described in Figure 7.2.2. The heating policy is evaluated using the model n-step ahead, with exclusively the successive evaluations of the simulated indoor temperature.

The controller inputs are:

- $H(t)$: hour of the day,
- $SG(t)$: solar gains at time step t ,
- $To(t)$: outdoor temperature,
- $Oc(t)$: occupancy index,
- $Tsp(t)$: set point temperature.
- $Ti(t)$: measured indoor temperature.

The output, $Tws(t)$, is the water supply temperature to radiators or heating floor. $Ti(t)$ is not an ordinary input. It is used:

- for model updates according to a protocol described in section 7.2.3,

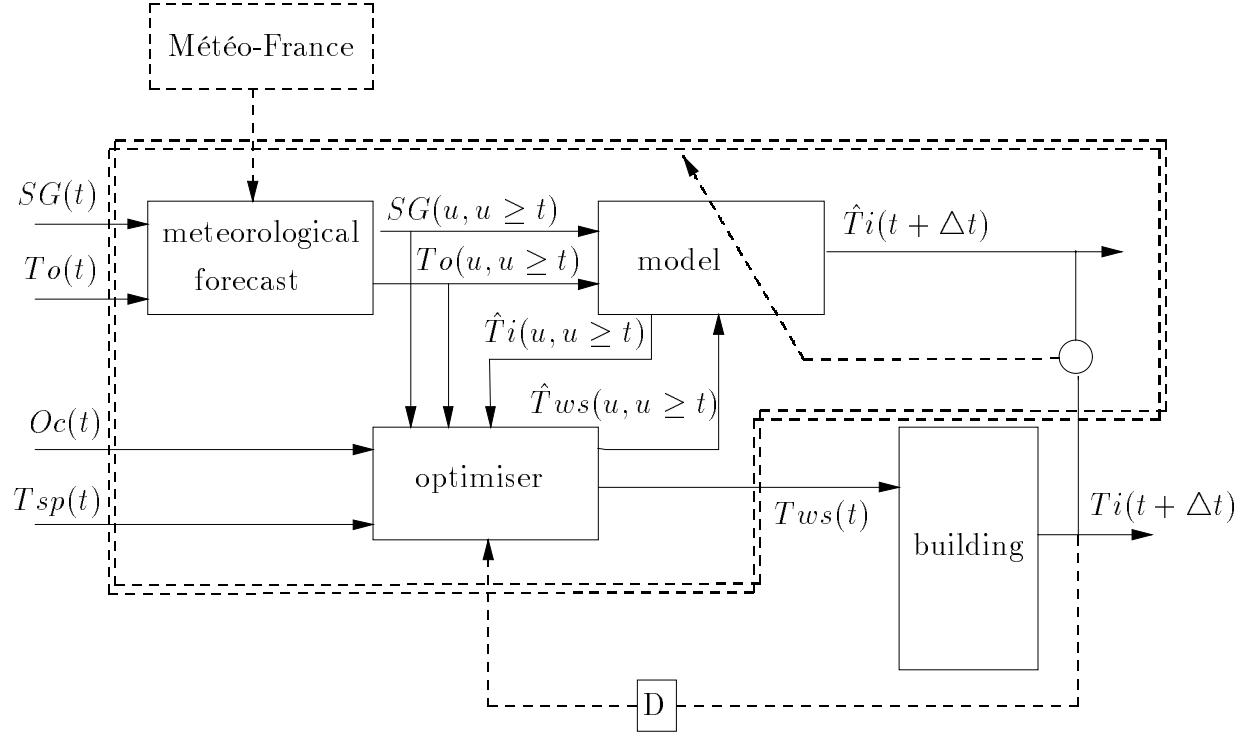


Figure 7.1. General architecture

- for research of the optimal start-up hour for the boiler, see section 7.3.2.

The controller computes internal intermediate values of \hat{SG} , \hat{To} , \hat{Tws} and \hat{Ti} , for time steps $t + \Delta t, \dots, t + n \Delta t$ (typically over three hours). Here, \hat{Ti} denotes the simulated indoor temperature given by the model, and \hat{Tws} is a candidate for control action.

For meteorological forecasts, INSA can use either Météo-France data server or an internal module using only local measures.

7.2.3 INSA Model of the building

The model of the controlled building plays a primordial role:

- it has to be sufficiently accurate to provide a reliable estimate of indoor temperature according to a given heating policy;
- it has to be sufficiently generic for easy transposition from a building to another, changing only some parameters.

Moreover, two constraints are added:

- on-line learning capability,
- small size for micro-controller applications.

INSA has chosen an identified model built using the structure of fuzzy Wiener models [Glo98, Glo99b]. Such a model is divided into a linear dynamic part followed by a static non-linear part.

- The linear dynamic part is a simple filter of the form:

$$Fx(t) = \alpha x(t) + (1 - \alpha) \times Fx(t - 1) \quad (7.1)$$

where $x()$ and $Fx()$ are the input and the output.

- The static non-linear part is a fuzzy inference system (FIS), more precisely a zero-order Takagi-Sugeno Fuzzy System. The architecture is described in Figure 7.2.3.

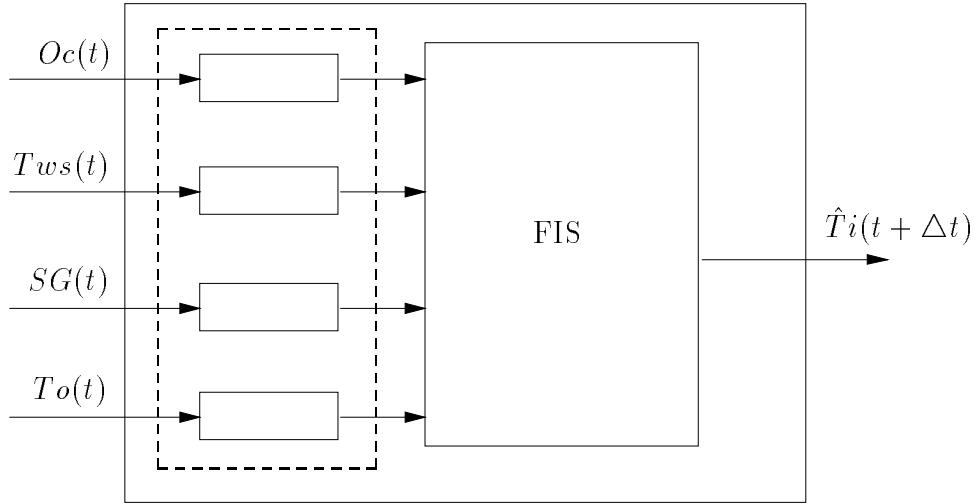


Figure 7.2. Fuzzy Wiener Model

The inputs of the model are the following:

- $Oc(t)$: occupancy index, defined by:

$$Oc(t) = \begin{cases} 1 & \text{if occupancy period} \\ 0 & \text{elsewhere} \end{cases} \quad (7.2)$$

- $TwS(t)$, $SG(t)$ and $To(t)$, as previously defined.

Let

$$\mathbf{x}(t) = (Oc(t), TwS(t), SG(t), To(t))^t \quad (7.3)$$

$$\mathbf{s}(t) = (FOc(t), FTwS(t), FSG(t), FTo(t))^t \quad (7.4)$$

We have the following state equations

$$\begin{cases} \mathbf{s}(t) = A\mathbf{x}(t) + B\mathbf{s}(t - 1) \\ \hat{T}i(t + \Delta t) = FIS(\mathbf{s}(t)) \end{cases} \quad (7.5)$$

where A and B are diagonal matrices and $FIS()$ is the input/output mapping performed by the FIS.

The output is an estimate of the indoor temperature under the current policy. We emphasize that the observed indoor temperature is not an input. Therefore, we have a pure open-loop model, built from real input/output data, using two identification algorithms.

- Filter coefficients are evaluated using a stochastic search (Solis and Wetts algorithm). The coefficients can be at hand initialized with simple rule of thumb, taking into account the time constant of the considered input. For example, let $FTws(t)$ be the filter output given by:

$$FTws(t) = \beta Tws(t) + (1 - \beta)FTws(t - 1) \quad (7.6)$$

An initial value for β can be:

$$\beta \approx \begin{cases} 0.1 & \text{for radiators} \\ 0.02 & \text{for a heating floor} \end{cases}$$

Clearly, this parameter is a function of inertia and time step.

- For the FIS, we impose the following structure:
 - triangular strong fuzzy partitions on each input domain;
 - two membership functions for input Oc , three for the other inputs.

This choice is not a real restriction but allows clarity in the rule base and easy tuning of FIS parameters. These parameters are tuned with a Fast Prototyping Algorithm, described in [Glo99a], according to the available input/output pairs.

Both filter and FIS parameters are settled off-line and the model can be immediately embedded into the controller.

A secondary on-line tuning process is allowed during the control period, each input/output pair being used only once. The conclusion of each rule is updated according to the difference between actual and simulated indoor temperature. Let C_k and TV_k respectively be the conclusion part and the truth value of rule k . The updating equation is:

$$\Delta C_k = -\epsilon(\hat{T}i - Ti)TV_k \quad (7.7)$$

where ϵ is a small learning rate (typical value: from 0.05 to 0.2).

This secondary tuning respects the following protocol:

- tuning is possible during the unoccupancy periods, presumably more representative of the real behavior of the building than the occupancy periods;
- tuning is allowed with a given probability, P , during the occupancy periods. By this way we attempt to limit introduction of noise in our model, because occupant's behavior is the origin of strong disturbances (door and window opening, usage of electrical devices,...). This secondary process is also used to compensate the simplicity of the model or the poorness of the training data. In our experiments, $P = 0.3$.

To summarize, the model is used under two modes:

- pure open-loop mode, in order to test a policy,
- pseudo-stochastic closed-loop, in order to track the actual indoor temperature.

7.2.4 Meteorological forecasts

INSA has experimented two approaches. The first used the meteorological data server of Météo-France. Values of temperature, humidity, cloudiness, wind velocity and direction, etc, are available 36 hours ahead, with updates all three hours. This approach gives good results and is obviously a way with future [GG98]. Unfortunately, such a data server is not available in all European countries. Therefore INSA has developed a second approach based on local informations, with continuous updates. We present only this second approach.

7.2.4.1 Temperature forecasts

For temperature forecasts we use a linear filter on the form:

$$To(t+6) = a_1To(t) + a_2To(t-6) + a_3To(t-12) + a_4To(t-18) + a_5To(t-24) \quad (7.8)$$

where the unit is one hour. This filter captures the periodic variations of outdoor temperatures. We have improved this method by adding two available informations:

- the difference between the actual temperature and the estimated value given by the filter six hour before;
- the good correlation between the errors at time t and $t + 2$ hours.

The temperature predictor has been tested with data from Rennes and Arlon (FUL building). In Figure 7.3, the curves represent the mean of cumulative errors, using the temperature of the previous day (solid line) and the forecasted temperature (dashed line), with FUL data in November. The mean of cumulative errors is defined by:

$$err(t) = \frac{1}{24} \sum_{j=1}^{24} (FTo(t+j) - To(t+j)) \quad (7.9)$$

where FTo stands for forecasted outdoor temperature. We have corresponding equation for temperatures of the previous day. More precisely, we call Today Like Yesterday (TLY) the method using the data of the previous day. This gives the following results:

policy	mean	standard dev.
TLY	0.004	2.48
FTo	0.23	1.10

7.2.4.2 Solar gains forecasts

Forecasting solar gains with a time step of 15 minutes is a very difficult task. The results of the INSA approach are not very good but nevertheless can be used in simulations. The main idea is to compare the actual and previous days at each time step, with sliding windows:

- if the correspondence is good enough, we can re-use the irradiations of the previous day,
- otherwise, we modify it according to the sign of the difference between the two sliding windows.

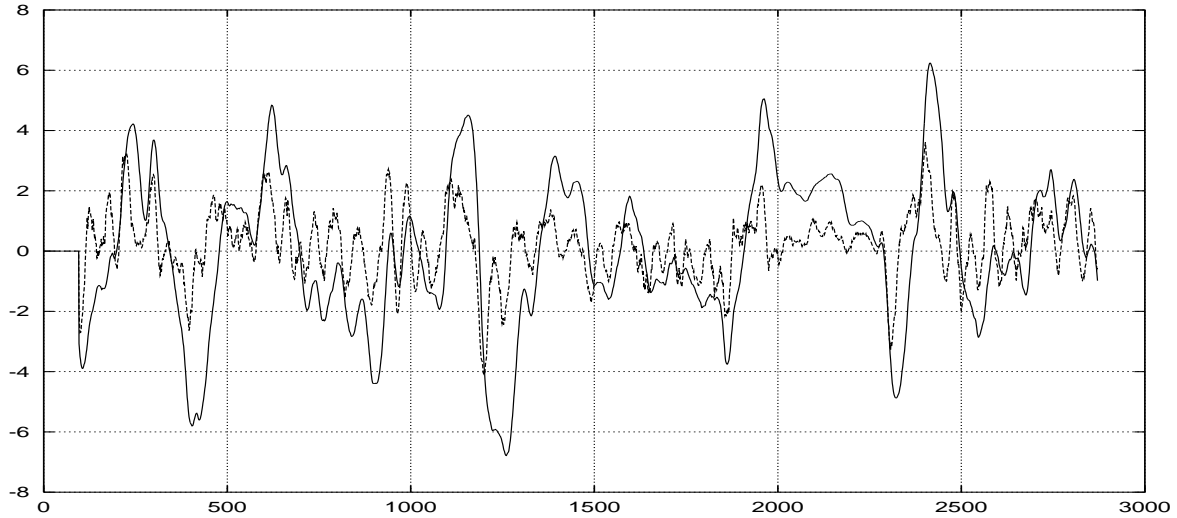


Figure 7.3. Temperatures of the previous day vs forecasted temperatures (solid line: TLY; broken line: FTo).

Of course, the method is very empirical and rough, but it gives some improvements in comparison with TLY. Forecasts on the basis of two hours ahead are made. The Figure 7.4 shows the difference between the mean cumulative errors for two hours ahead forecasts, using either TLY (solid line) or our method. The summary is given in Figure 7.4 and the following table:

policy	mean	standard dev.
TLY	39.01	175.98
FSG	21.79	74.81

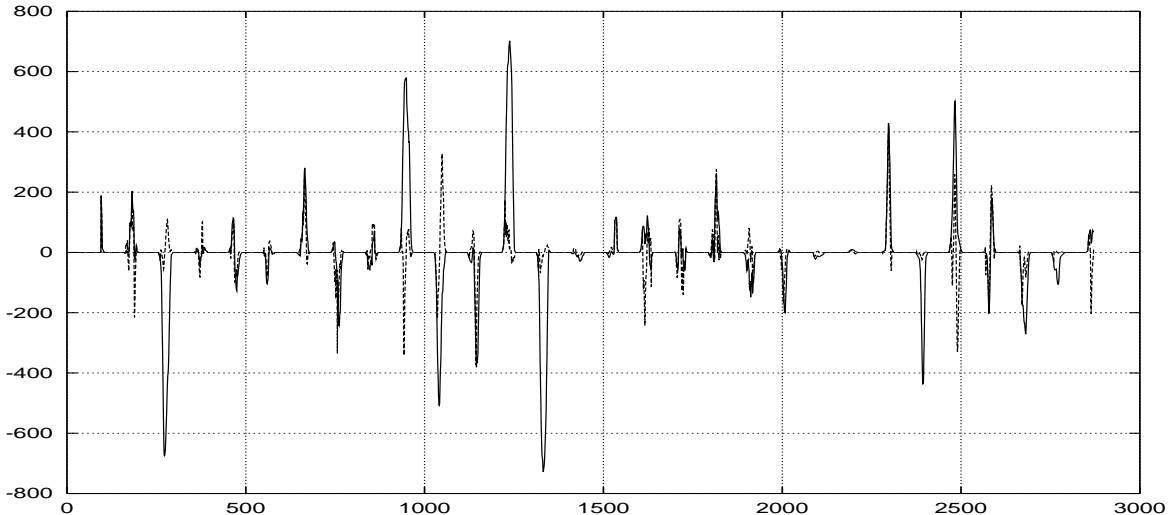


Figure 7.4. Solar gains of the previous day vs forecasted ones (solid line: TLY; broken line: FSG).

7.3 Optimization module

INSA treats the case of intermittent heating, where the boiler is cut off in unoccupancy periods. Four cases have to be distinguished:

- stopping periods (a part of nights and week-ends),
- search for optimal start-up hour for the boiler, before occupancy periods,
- starting-up periods,
- occupancy periods.

Therefore the controller has four modes: idle, research for start-up hour, starting-up and regulation.

7.3.1 Idle mode

In this mode, the boiler is stopped and indoor temperature evolves freely unless it falls under some fixed limit (e.g. 14°C): in this case the regulation mode is activated with a low set-point temperature.

7.3.2 Research for starting-up hour

To try to prevent untimely start-up, this research has two steps: finding a licit temporal window and computing the exact duration of pre-heating.

Licit temporal window A FIS gives the approximative duration of pre-heating, according to the observed internal temperature, T_i , and the forecasted mean value of outdoor temperature before the occupancy period, \bar{T}_o . The rule base is the following:

\bar{T}_o	T_i	cold	warm
cold	A	B	
warm	C	D	

with A = number of hours approximatively needed to reach the set-point temperature when T_i is cold (about 16°C) and \bar{T}_o is cold (about -2°C), B = number of hours approximatively needed to reach the set-point temperature when T_i is warm (about 19°C) and \bar{T}_o is cold, and so on. The values A, B, C and D are automatically computed given a model of the building.

Let t_{occ} be the beginning of occupancy period and h the output of the fuzzy system given T_i and \bar{T}_o . The licit temporal window is $[t_{occ} - h, t_{occ}]$.

Exact duration The exact duration of the pre-heating period is then computed using the model and meteorological forecasts. The controller can decide if either or not the boiler has to be activated, using the decision rule:

```
if set-point temperature is reached before 8 AM when starting-up is now
    then wait else start-up
```

7.3.3 Pre-heating period

The heating policy to shorten the pre-heating period with minimum energy consumption is to take the maximum value of \hat{T}_{ws} . This policy is proven to be the optimal one for energy saving. It is followed up to one hour before the occupancy hour, t_{occ} , in order to avoid overshoots.

7.3.4 Regulation mode

In this mode, the goal is to test a policy before applying it. There are four steps :

Test of a heating policy

At each time step, t , the controller tests a heating policy, $\hat{T}_{ws}(t), \dots, \hat{T}_{ws}(t + n \Delta t)$, using only the model and meteorological forecasts. The initial policy is generated using the heating curve, at the beginning of the occupancy period.

Internal PI control

Each value of $\hat{T}_{ws}(u), u \geq t$ is modified by an internal PI-like fuzzy controller, according to the difference between the simulated indoor temperature and the set point temperature, e , and its variation, ce :

$$e = T_{\text{model}} - T_{\text{set-point}} \quad (7.10)$$

$$ce = T_{\text{model}}(t) - T_{\text{model}}(t-1) \quad (7.11)$$

The output is the change in \hat{T}_{ws} , $\Delta \hat{T}_{ws}$. The membership functions for e and ce are described in Figure 7.3.4 and the rule base in Table 7.1.

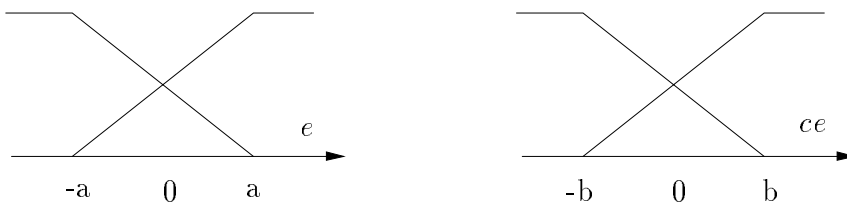


Figure 7.5. Membership functions for e and ce

ce	e	N	P
N		P	Z
P		Z	$-P$

Table 7.1. Rule base for the PI-like fuzzy controller

Only three interpretable parameters, a , b and P , are needed to define this internal controller. P is the maximum value of $\Delta \hat{T}_{ws}$ and is easily found, a and b define the operative range of the internal controller.

Optimized output

The sequence $\hat{T}_i(t), \dots, \hat{T}_i(t + K \Delta t)$ is analyzed: when an overheating is detected k step-ahead, $0 < k \leq n \leq K$, where n depends on the degree of confidence in forecasted data (n

corresponds to one hour and half in these tests), Tsp is reduced (see section 7.4) and the proposed values $\hat{Tws}(t), \dots, \hat{Tws}(t + k \Delta t)$ are decreased.

The mean of the two first values of the sequence is applied to the real system:

$$Tws(t) \leftarrow \frac{1}{2}\{\hat{Tws}(t) + \hat{Tws}(t + \Delta t)\}$$

By this way we introduce a complementary anticipative effect.

Preparing the next step

The sequence $(\hat{Tws}(u))_{u>t}$ is shifted towards the left and a new value for $\hat{Tws}(t + n \Delta t)$ is added. The actual values of Tws , To , SG and Ti are provided to the internal model in order to allow

- an update of the state (filter outputs),
- a probabilistic update of the fuzzy rules.

This process is illustrated in Table 7.2. As one can see, the largest part of the sequence, $\hat{Tws}(t + \Delta t), \dots, \hat{Tws}(t + K \Delta t)$ is re-used from a step to another. Therefore, there are successive improvements of the heating policy and the design of the internal PI-like fuzzy controller is not crucial: only the successive adjustments of \hat{Tws} must be "in the right sense".

$t = 13h00$	$\hat{Tws}(13.00) \quad \hat{Tws}(13.15) \quad \hat{Tws}(13.30) \dots \hat{Tws}(15.45)$
$t = 13h15$	$\hat{Tws}(13.25) \quad \hat{Tws}(13.30) \dots \hat{Tws}(15.45) \quad \hat{Tws}(16.00)$
$t = 13h30$	$\hat{Tws}(13.30) \dots \hat{Tws}(15.45) \quad \hat{Tws}(16.00) \quad \hat{Tws}(16.15)$

Table 7.2. Policy evaluation from 13h to 13h30

7.4 Comfort level

Saving energy can have negative influence on the comfort level and reciprocally. The user has to solve this dilemma by choosing a comfort level index between "maximum comfort" and "maximum energy saving". The simplest and more understandable way, in our opinion, is to allow the user to fix:

- the set point temperature, Tsp ,
- a tolerance, tol , around Tsp : the smaller the tolerance is, the higher the comfort is.

This tolerance is used in three circumstances to modulate the effective set point, denoted by Tsp_eff :

1. At the beginning of the occupancy period, it is sometimes difficult to reach T_{sp} , when To is low and if the boiler suffers from a lack of overpower. Let t_{occ} be the hour for the beginning, we have:

$$T_{sp_eff}(t_{occ}) = T_{sp} - tol$$

2. One hour before the end of the occupancy period, T_{sp} can be slowly decreased. Let t_{end} be the hour of the end of the occupancy period, we have:

$$T_{sp_eff}(t_{end}) = T_{sp} - tol$$

3. Before forecasted overheating, T_{sp} is also reduced.

7.5 Tests performed by INSA

The controller has been tested

- in simulation, using data from Rennes, Hameln (ISFH building) and Arlon (FUL building),
- in our experimental site.

7.5.1 Tests in simulation with FUL data

7.5.1.1 Model of FUL building

The data file from FUL building gives the following informations : day-of-the-year, hour, SG , To , Tws , Tr , Ti and Q , where Tr is the return temperature from the radiators and Q is the water flow rate.

The information about the flow rate and selected parts of the data file with $Q \approx 100$ was not used. Tws as the only estimate of the energy provided to the building should be used.

The data from day number 306 at 14h30 to day number 337 at 12h15 were selected. From these 3000 data, 1500 were used for learning the model and 1500 for tests. One set of fuzzy rules covering all the period and giving the open-loop model $\dot{T}i = F(Oc, Tws, To, SG)$ is obtained.

The difference between actual and simulated temperatures are shown in Figures 7.6 and 7.7. In Figure 7.6, the model is used in pure open-loop mode, without any update: the simulated temperature is deduced using only the inputs Oc , Tws , SG and To .

In Figure 7.7, a zoom is shown over the last week (from Sunday to Thursday) with the pseudo-stochastic updates of equation 7.7. These data were not used for learning. The model shows its tracking capabilities, and the improvements for both standard deviation (sd) and mean squared error (MSE) are about 20%. The results are summarized in Table 7.3 for the whole data set (31 days).

7.5.1.2 Control of FUL building

The model is used without any changes by the controller (in real situations, the model can be updated with a given probability, as previously said). In figures 7.8 and 7.10, we have selected two days (Monday and Tuesday of the last week) where real and simulated data were in good concordance. Therefore we can compare the real policy used at FUL and our policy. Figure 7.8

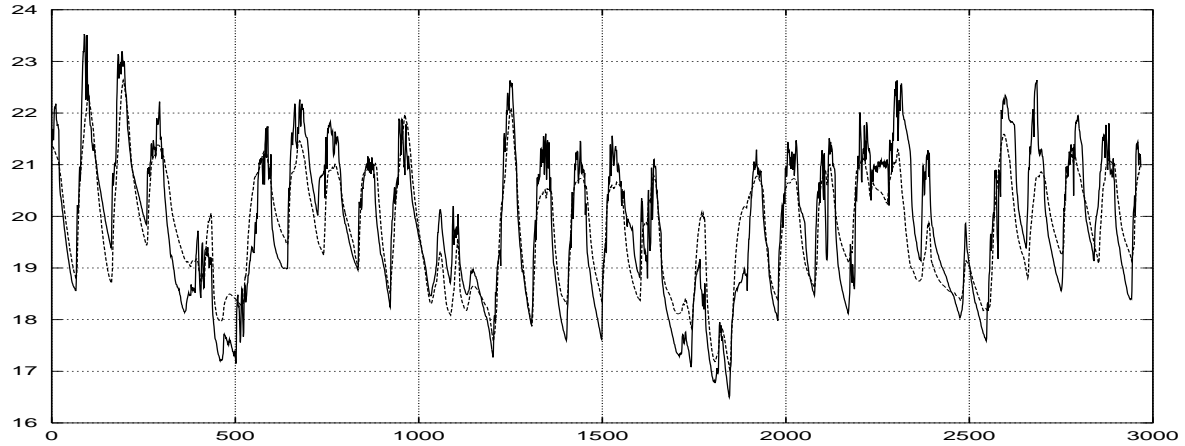


Figure 7.6. Actual vs simulated temperatures for FUL building, in open-loop mode (solid line: actual T_i ; broken line: simulated).

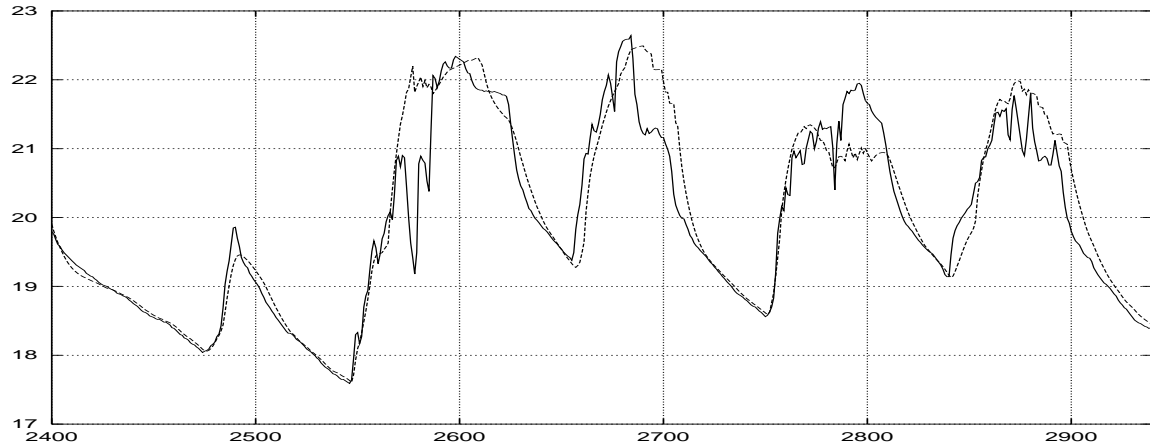


Figure 7.7. Actual vs simulated temperatures for FUL building, in tracking mode (solid line: actual T_i ; broken line: simulated).

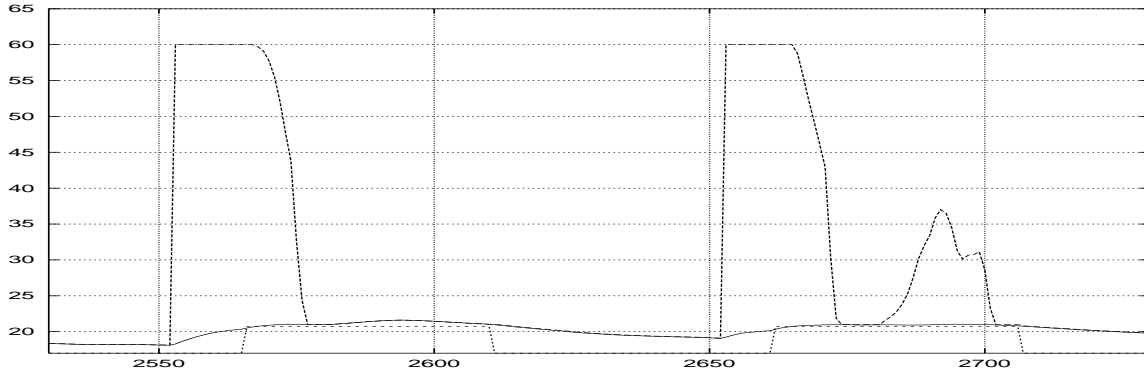
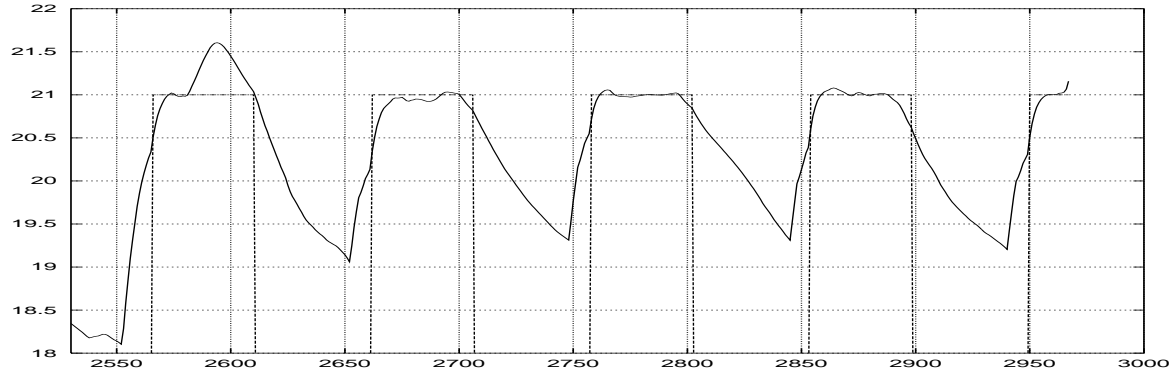
shows our control results which are realistic whereas Figure 7.10 shows the corresponding control period with FUL controller. As we can see in Figure 7.8, our controller gives an initial energy load, then stops because the solar and internal gains are taken into account. The second day, the controller has a small boost at the end of the occupancy period to compensate the solar gains that are decreasing. For this test, we have the following parameters:

- $T_{sp} = 21^\circ\text{C}$,
- $tol = 0.3^\circ\text{C}$

In both figures, the solid line represents T_i , the broken one represents T_{ws} and the dotted one the occupancy index.

Finally, in Figure 7.9, we show the results of our controller the last week. As we can see, the chosen value of tol allows to reach the set point in time.

	open-loop	pseudo-stochastic learning	
		$\epsilon = 0.1$	$\epsilon = 0.2$
m	-0.05	-0.02	-0.003
sd	0.67	0.53	0.47
MSE	0.45	0.28	0.22

Table 7.3. Performances of the model for FUL building**Figure 7.8.** Insa controller for FUL building**Figure 7.9.** Last week with INSA controller for FUL building

7.5.2 INSA tests in simulation with ISFH data

ISFH data were available from first of January to 29 of February 2000, with a time step of 15 minutes. The value of T_{ws} is computed by a conventional controller. 5760 samples of the variables hour of the day, To , SG , T_{ws} , Ti and Oc are available. The first part was used for learning.

7.5.2.1 Model of ISFH building

The data file from ISFH presents some particularities:

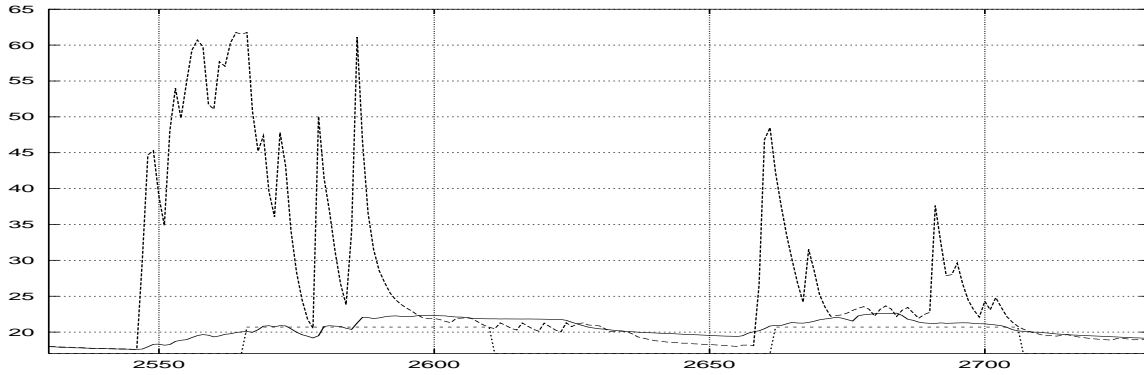


Figure 7.10. FUL controller for FUL building

- the occupancy period is from 9h to 17h, but the set point is $T_{sp} = 21^\circ\text{C}$ from 6h to 22h and $T_{sp} = 19^\circ\text{C}$ otherwise,
- the boiler is never stopped the week-ends.

Therefore, the data set is very poor because the indoor temperature do not decrease during the unoccupancy periods and its range is only from 18.7 to 21°C , with some peaks due to important solar gains.

In other words, we have a dynamical system with insufficient excitation for identification: if we can identify a model from the data, this model will suffer from lack of generalization property ¹.

Another way is to choose a model from a library and adapt it thanks to the pseudo-stochastic learning mode. This was proceeded as follows:

- the filter coefficients, FOc , $FTws$, FTo and FSG are extracted from ISFH data,
- the initial rule base is FUL rule base,
- FUL rule base is modified according to ISFH data with only one presentation of the data set, with a small learning rate ($\epsilon = 0.05$).

	learning with FUL rule base	open-loop with ISFH data	pseudo-stochastic learning
$\epsilon = 0.05$	$\epsilon = 0.0$	$\epsilon = 0.05$	
m	-0.01	0.07	0.02
sd	0.41	0.36	0.27
MSE	0.17	0.13	0.07

Table 7.4. Performances of ISFH model using FUL rule base

In Table 7.4, we have three results:

- in the first column, we have the performance of the initial rule base, extracted using FUL rule base with ISFH data;
- the second column shows the result of the model in open-loop;

¹This problem of poor data set can be solved using Simula, as explained in section 7.8.

- finally, we see that the tracking mode improves the performances.

We use the model extracted in the first step in open-loop. Figure 7.11 compares actual and simulated temperatures using ten days not used for learning.

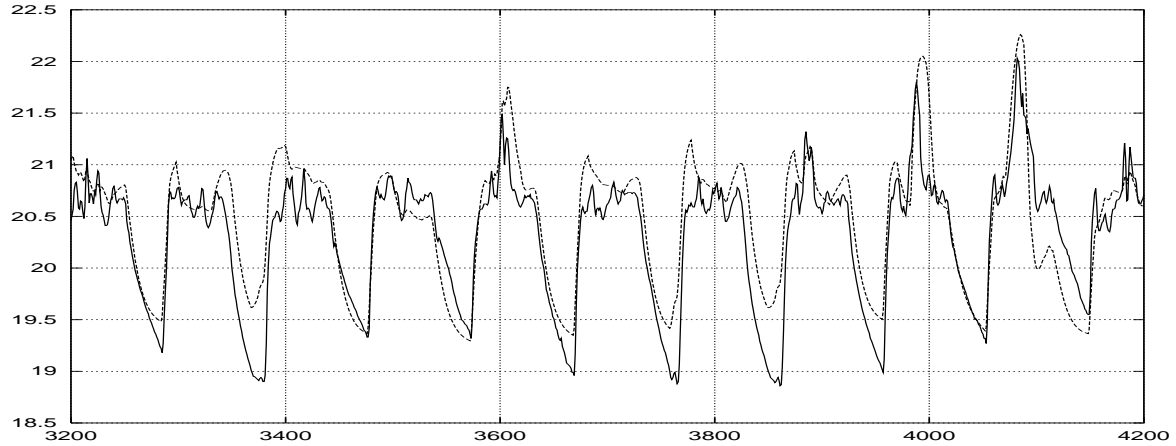


Figure 7.11. Actual vs simulated temperatures for ISFH building

7.5.2.2 Control of ISFH building

The INSA controller is used with the following parameters:

- $T_{sp} = 21^\circ\text{C}$, from 9h to 17h in occupancy period, the set point being free otherwise,
- $tol = 0.1^\circ\text{C}$

In Figure 7.12, the conventional controller was used from time step 3200 to 3500 (3rd to 6th of February) and our controller from time step 3500 to 4200 (seven days). The solid line represents T_i , the broken one represents T_{ws} and the dotted one represents the occupancy index Oc . In Figure 7.13, we represent only T_i and Oc in order to show in detail the behavior of the controller. Monday 7th and Friday 11th were sunny days in Hameln, therefore we see a small decrease in indoor temperature before the overheatings, because the set point was automatically decreased. The other days we respect the set point according to the given tolerance.

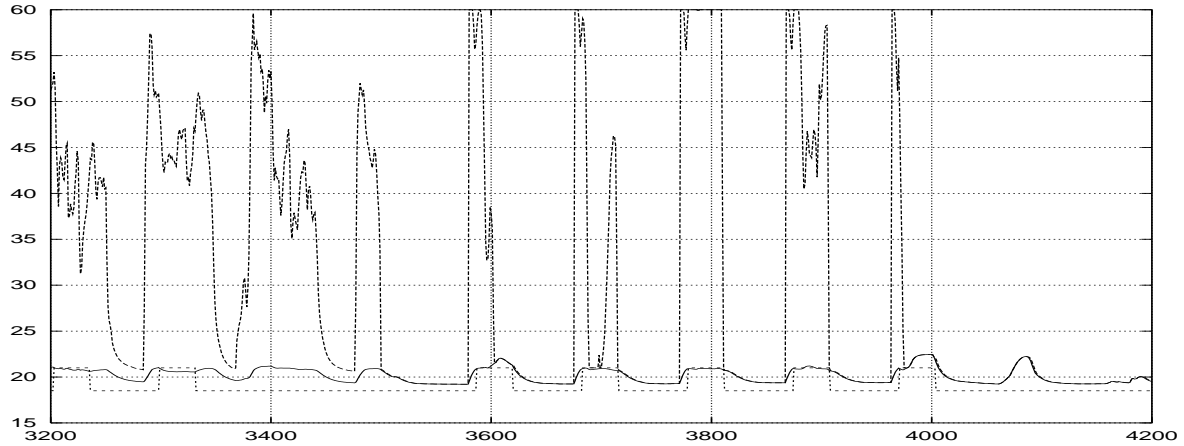


Figure 7.12. Conventional and smart control for ISFH building

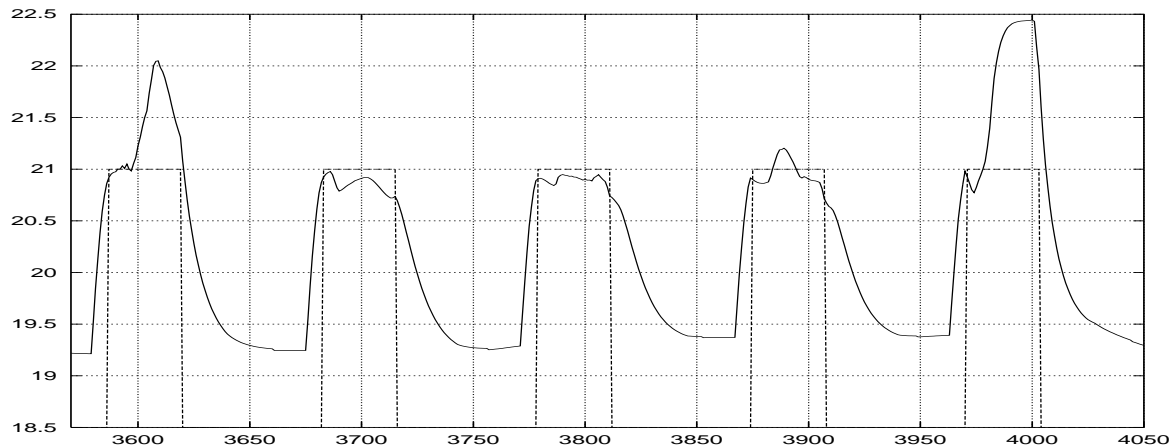


Figure 7.13. One week with INSA controller for ISFH building

7.5.3 Experiments in Rennes

The two previous tests were performed in simulation using real data from Arlon and Hameln. In this section, the experiments in the test building of INSA, a crèche in Rennes are reported. This building has a heating floor (with hot water) and electric radiators. We decide to control only T_{ws} for the heating floor. The radiators give extra heating considered as disturbances as well as occupant's behavior.

7.5.3.1 Model of Rennes building

The model for Rennes has the same structure that for Arlon or Hameln, with, of course, different parameters. The differences between real and simulated indoor temperature in open-loop mode are given in figure 7.14.

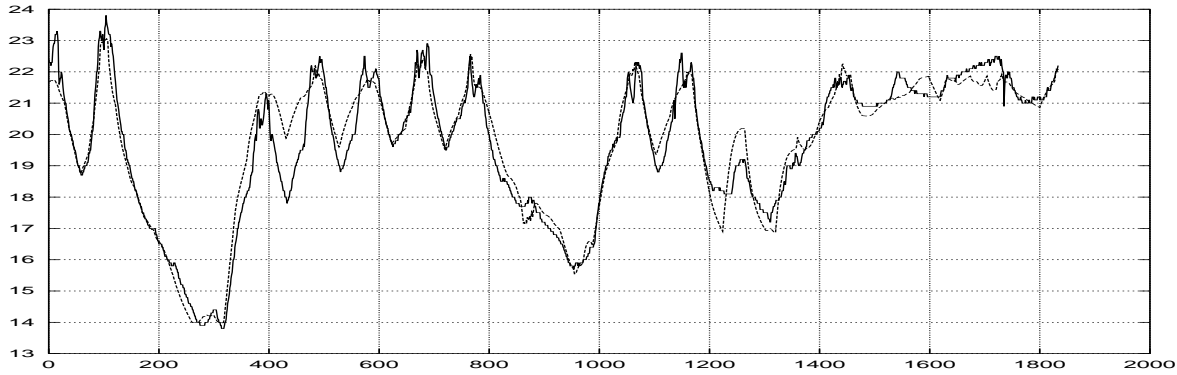


Figure 7.14. Actual vs simulated temperatures for INSA building

	open-loop	pseudo-stochastic learning		
		$\epsilon = 0.1$	$\epsilon = 0.2$	
	m	0.07	0.01	-0.02
	sd	0.58	0.45	0.40
	MSE	0.35	0.20	0.17

Table 7.5. Performances of the model for INSA building

7.5.3.2 Control of Rennes building

The previously described control policy was applied to the boiler. In figure 7.16, we see :

- real indoor temperature (solid line),
- our control policy, T_{ws} .

Knowing the heating curve of the conventional controller and the model of the building, we can simulate the behavior of the conventional controller with the same weather data. The simulated curves are in Figure 7.15, with:

- the simulated indoor temperature if the conventional controller had been used,
- T_{ws} proposed (but not applied) by the conventional controller, based on its heating curve.

The improvements of the predictive control policy can be seen. The boiler is stopped at the beginning of the occupancy period, with sometimes a small boost at the end. Overheatings are avoided or reduced.

7.5.3.3 Evaluation of energy saving

It is possible to make a rough evaluation of energy savings. The conventional takes only into account instantaneous values of outdoor temperature and computes T_{ws} from a heating curve: $T_{ws} = a \times T_o + b$, where $a = -1.13$ and $b = 38^\circ\text{C}$ are two building-dependent parameters.

In Rennes building, due to the strong inertia of the heating floor, the energy estimated at time t will be delivered with a delay of several time steps. Therefore, this energy can be added to solar energy and provoke overheatings, as we see in Figure 7.17.

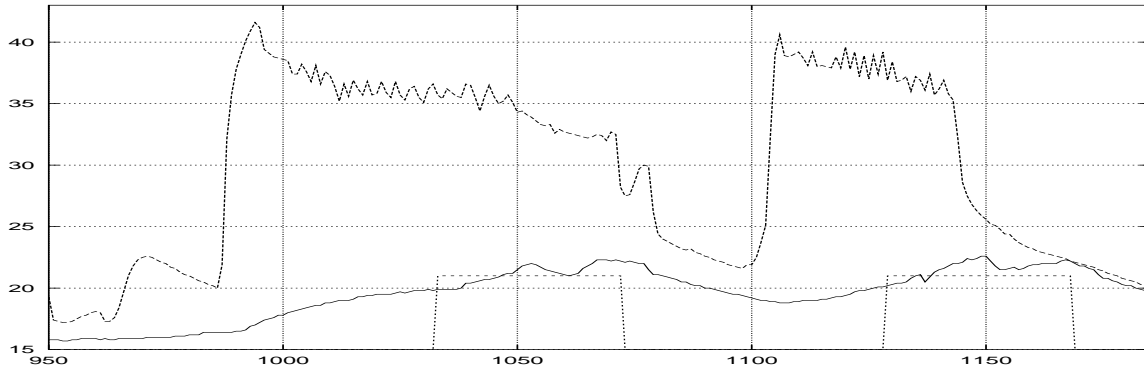


Figure 7.15. Conventional controller for INSA building

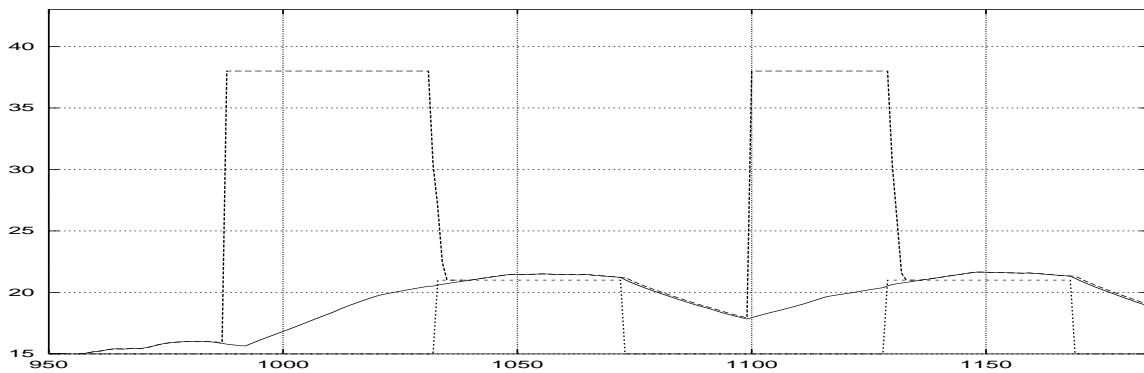


Figure 7.16. Smart controller for INSA building

As it is difficult to find two days with the same meteorological characteristics, we have chosen the following protocol:

- the conventional and the smart controller are compared with the same meteorological data, using the model; It is possible because the two policies are known;
- we take two consecutive days, Thursday 25 and Friday 26 of November 1999,
 - the first day has important solar gains and a mean outdoor temperature around 12-14°C,
 - the second is more cloudy and has a mean outdoor temperature around 9°C.

The results are summarized in Table 7.6 where \bar{T}_i is the mean value of T_i during the occupancy period, sd its standard deviation; the relative energy consumption is estimated by the mean value of $T_{ws} - \bar{T}_i$. The different curves are represented in Figures 7.17 and 7.18, with, from the bottom to the top of each figure: $SG/100$, To , Oc , T_i and T_{ws} .

In Figure 7.17, the boiler is always running in occupancy period. This causes discomfort and energy waste. In Figure 7.18, as solar gains are forecasted, T_{sp} is reduced with respect to the given tolerance and the boiler anticipates on internal and solar supplies.

Of course, the results in Table 7.6 have to be relativized: we don't proclaim that our controller reduces energy consumption of 53 percent with regard to a conventional one. Our goal is to highlight the advantage in considering both the dynamical aspects of a building and the forecasted disturbances. The situation of Thursday is characteristic of a day where a conventional controller

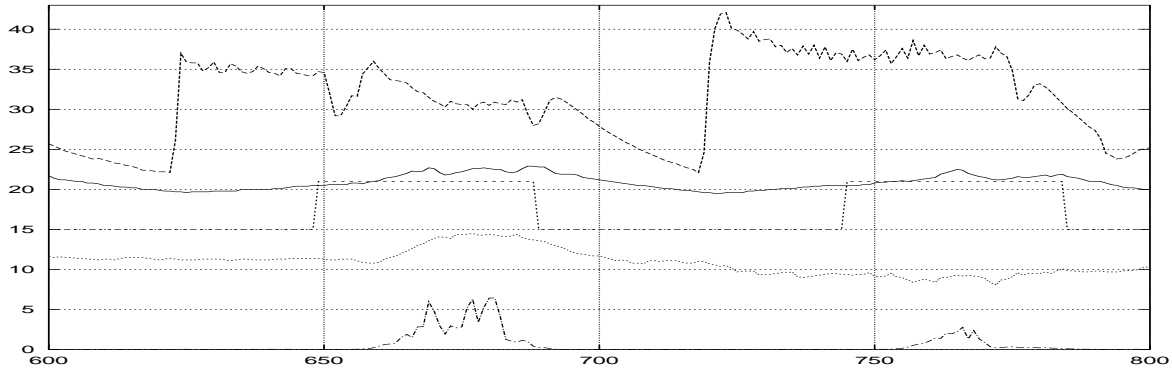


Figure 7.17. Conventional control based on outdoor temperature: solar gains creates overheatings.

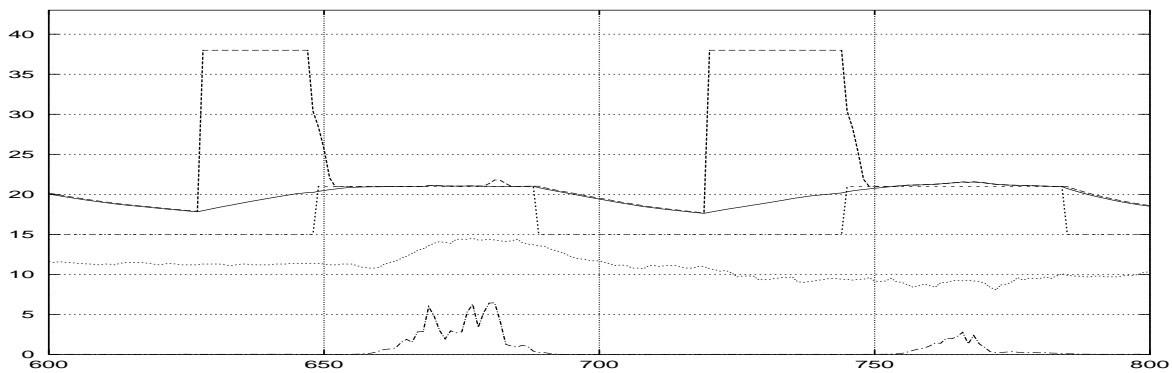


Figure 7.18. Predictive control: solar gains are integrated by the heating policy.

cannot optimize its policy, because it can't take into account the future solar gains. Moreover, a smart controller has another advantage because it can avoid overheatings thanks to its own estimation of indoor temperature.

7.6 Experimental hardware

The code for the controller, including the model and the meteorological module, has a size of about 30 kB. Therefore, we can incorporate it into a 8 bits micro-controller. Unfortunately, it was not possible to use INGA hardware. Therefore INSA has used our own 8051-based hardware. The system is described in Figure 7.19.

A data acquisition system was installed that is capable to acquire analog and digital data. Temperature sensors are available for the hot water supply and return, for the indoor temperatures in two playing rooms and for the outdoor temperature. For measuring the solar gain a pyranometer was placed on the roof of the building. Besides, three electric counters measure the energy consumption of the groups of electric radiators and deliver impulsions for the acquisition system. The acquisition is controlled by a PC. Data are digitalized and saved in memory as well as in data file by time steps of 15 minutes.

These data as well as the meteorological forecasts are sent to the 8051 controller card via a serial line. The controller performs the calculations to determine the desired value of hot water supply temperature for the heating floor. This value is sent back to the PC as an analog signal. The PC

	Thursday 25		Friday 26	
	conventional	smart	conventional	smart
T_i	21.80°C	20.94°C	21.38°C	21.10°C
sd	0.78°C	0.15°C	0.51°C	0.29°C
energy (%)	100	48	100	47
$T_i \geq 22^\circ\text{C}$	6h45	0h	1h	0h

Table 7.6. Elements of comparison (Thursday 25 and Friday 26 of November).

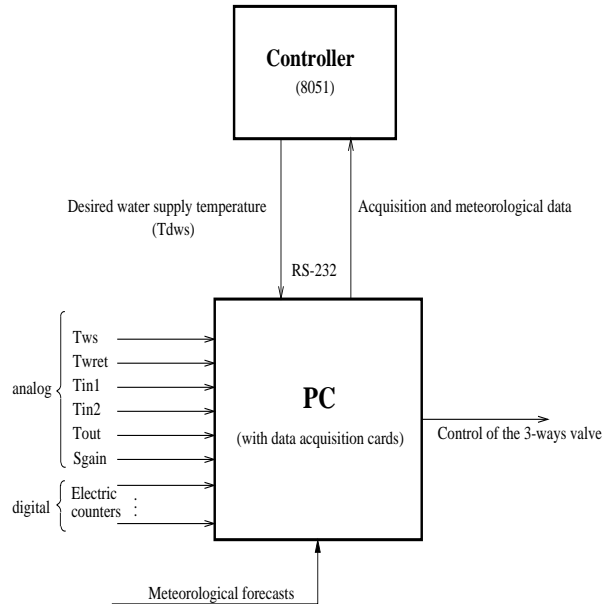


Figure 7.19. Experimental hardware.

controls the 3-way valve of the heating floor in order to assure that temperature.

The structure of the program in the 8051 controller is as follows:

1. reading the input variables delivered by the PC via the serial line,
2. calculation of desired hot water supply temperature: T_{ws} ,
3. returning this temperature to the PC,
4. waiting until the next time step (minimal value: 15 minutes).

In the PC a program is running for saving and transmitting data. It enables:

- writing data in file with time steps of 5 minutes,
- sending data on the serial line to the controller,
- controlling the 3-way valve according to the hot water supply temperature.

Although the algorithm was not implemented in the final hardware, the feasibility was shown. The actual board is shown in Figure 7.20. A complete board had to add a data acquisition system (with a Analogic to Digital Converter) and an analogue output to control the three-way valve.

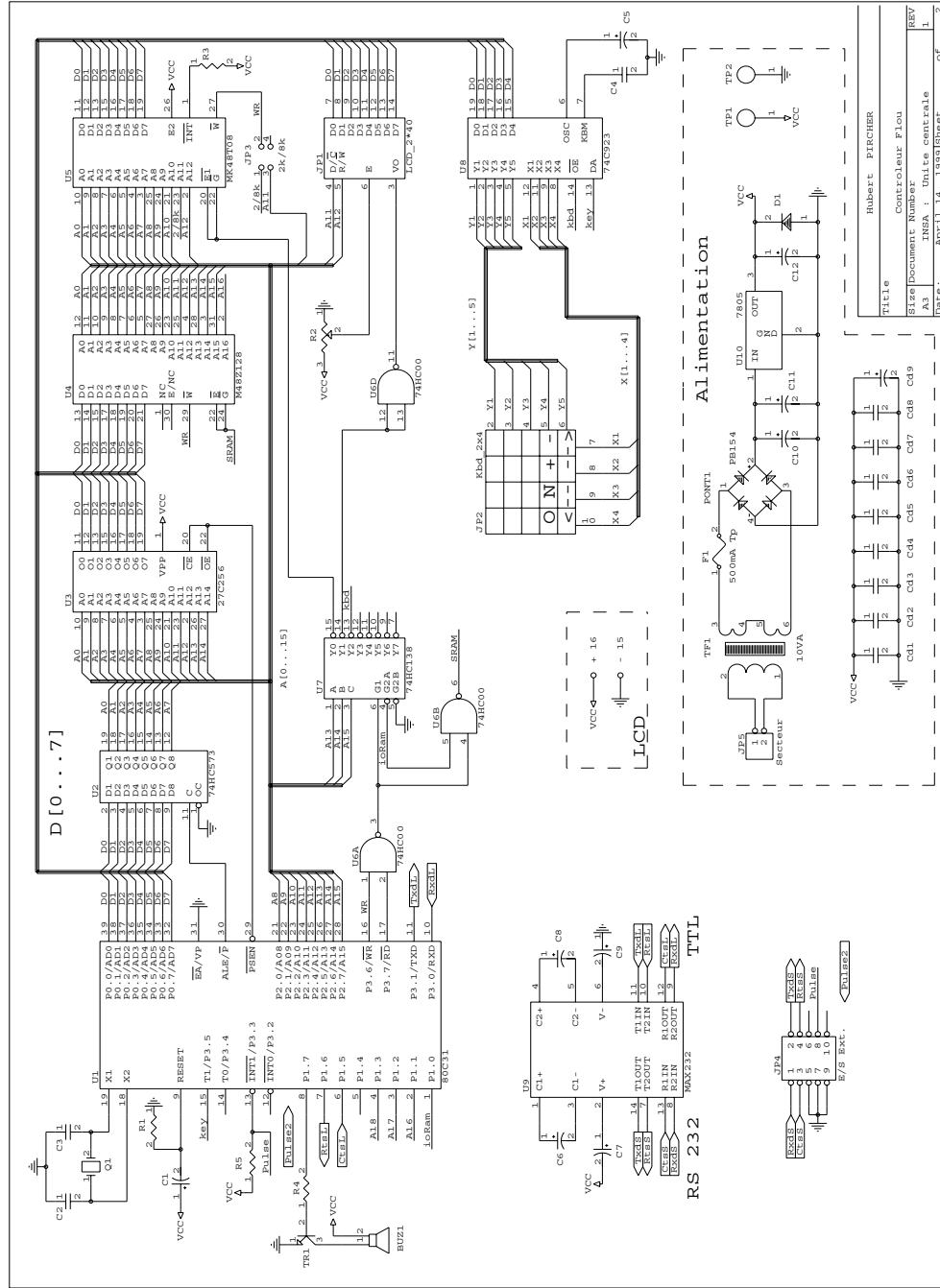


Figure 7.20. Hardware description

7.7 Limits of the INSA approach

7.7.1 Meteorological forecasts

The INSA controller needs approximative estimates of solar gains, each 15 min. It is obviously a very difficult task, because cloud movements are not foreseeable. Fortunately, a building acts like

a filter and softens small errors. Local informations about past measures are not sufficient and all informations about the next hours are necessary for optimization of the heating policy. A way with a future is the use of data server. In our opinion, accurate forecasts will be available in a few years in all European countries.

7.7.2 Training data

The INSA controller needs an accurate model of the building to evaluate a control policy. Thus, the availability of training data is another bottleneck if the controller should be used for any building. The training period can be reduced by one-line learning, as explained in section 7.2.3, but the goal is the design of a dedicated controller for a given building directly from the blueprints.

Such a controller must be able to react correctly faced with:

- all types of meteorological data: temperature and solar irradiation, but humidity and wind velocity can also be considered in the future;
- all types of situations or policies.

The corresponding training base would be huge and would need a long time to be built. The proposed method consists in:

- firstly, determining an initial controller using simulated data for all possible cases,
- secondly, updating the controller, on-line, with the pseudo-stochastic mode.

INSA is working with a team of CERMA (Nantes University) for this task and is adapting their software SIMULA.

7.8 Simula: a thermal simulation tool

In order to develop an intelligent predictive thermal controller applied to a solar building, it is necessary to have a sufficient and precise knowledge of its thermal behavior. Elsewhere, the micro-controller must contain very few information and must be able to self-adjustments to real buildings, each one having its own thermal characteristics. Therefore, the use of a simulation tool is twofold :

- firstly, to simulate and design the building, optimizing its thermal performance in terms of economy savings and comfort level; the tool is used in a design process.
- secondly, to help for designing the controller, using an identified model.

In this case, its role is to enable to define parameters of the controller, in a learning process, based on a series of daily sequences (in relation with type climatic conditions and user's scenario). The numerous simulations carried out constitute the input for the design process of the controller. At its turn, the thermal behavior of the controller (as a process command) can be verified on realistic climatic conditions. The proposed system is then iterative.

These objectives require a high performance tool that could easily model the physical properties and thermal links of buildings, taking into account unsteady conditions. The very few available operational simulation tools have complicated the problem. The very tractable tools have generally

poor thermal performance, working only in steady state, whereas sophisticated tools are difficult to use. Two software seemed interesting to consider, in a first look, TRNSYS and SIMULA.

The first one, TRNSYS was developed as a complete and general structure to resolve physical and thermal problems. Not dedicated especially to solar buildings, it offers an open framework to develop its own code. However, its use, generally convenient for research organisms, does not suit well to the operational work of thermal engineers. Moreover, the way the solar issue is taken into account in the simulation implied further numerical development and needed a theoretical investment, mainly to integrate the geometrical aspects of the buildings.

The Simula software, developed from 1990 by the Cerma Laboratory, is really dedicated to operational applications. Its design was elaborated with the French engineer association (CICF) in order to make available to practitioners dynamic procedures in the thermal analysis of buildings. The solar aspect, important parameter when it is necessary to consider the building in unsteady conditions, was integrated in the simulation due to the geometrical data provided for the building.

So, Simula software was chosen because it seemed better suit the requirements of the project. It is an operational tool for engineers and architects and can be diffused easily; it works in a multi-zone basis and uses a resolution method that gives rapidly results over time for air temperature and heat power to install. Inertia and solar gains, essential when considering solar buildings and thermal regulation, are considered with convenient procedures.

Simula was written in C language, enabling to modify it for adjusting to this specific type of use. The main tasks carried out to integrate Simula in the thermal design process of solar buildings with their own regulation controller can be listed as follows :

- elaboration of a new user interface for helping to model the buildings in thermal zones; the environment is a multi-windows system written in Visual C++ for PC
- transformation of the data in an object language structure
- constitution of libraries of components
- interface of calculation modules with the new structure of data
- integration of a batch procedure for carrying out the simulations in an iterative and repetitive way (after the interactive phase of thermal modeling)
- output in Ascii files with specific format in order to be processed by the learning tool for the design of the controller
- definition of several types of meteorological sequences.

The re-designed tool Simula is organized in two modules. The first one deals with the thermal modeling of the building and it is very interactive taking into account the 3D morphology of the building. The second enables the thermal simulation and results analysis, either in an interactive way, either in batch procedures; enabling the use of Simula, in a conventional way for professional engineers who have to design the thermal performance of their buildings, but also for the specific regulation application, in the framework of that European project, integrating Simula in a general process to define and design thermal controller.

A first beta version of the new Simula could be available soon and will be send to the project's partners.

These tasks imposed in fact almost a total re-writing of Simula and have required specific equipment and an engineer specialist in computer.

7.9 Available softwares from INSA

Three softwares are available, allowing to build a model from training data, using the model with on-line capability and controlling a building.

7.9.1 Design of the model

The training set must contain the following informations : hour, occupancy index, To , SG , Tws and Ti . The user has to define:

- the extremum values for To , Tws and SG ,
- initial values for filter coefficients,
- some learning parameters (default values are proposed).

The software creates a file which will be used by the controller.

7.9.2 The model

The model can be used either separately or as an internal model for the controller. The inputs are Oc , Tws , To and SG . The output is an estimation of Ti . The user has to define

- the name of the file giving the FIS structure,
- a learning rate for on-line updates.

7.9.3 The controller

The software loads two files for configurations:

- one file for FIS parameters,
- another for general parameters: maximum value of Tws , coefficients of the PI-like fuzzy controller,...

For example, the parameter file used for Rennes controller is given below.

```
# coefficients of the PI-like fuzzy controller
-0.5 0.5 -0.5 0.5
# set point temperature
21.0
# maximum value of Tws
38.0
# hour of end of occupancy period
18.0
# tolerance
0.2
```

A user manual will be available soon.

7.10 Conclusion

7.10.1 What is new ?

The smart controller developed by INSA has some new characteristics summarized as follows:

A novel building model

The fuzzy Wiener model is understandable and generic. The knowledge about the behavior of the building is embedded into fuzzy rules. For example, the three following rules corresponds to a starting-up of the boiler in unoccupancy period in Rennes building, when the mean value of outdoor temperature is 5°C:

1. $(0, 20, 5, 0) \rightarrow 17^\circ\text{C}$
2. $(0, 30, 5, 0) \rightarrow 19^\circ\text{C}$
3. $(0, 40, 5, 0) \rightarrow 21^\circ\text{C}$

For clarity, a rule is written " $(a, b, c, d) \rightarrow \text{conclusion}$ ", where a, b, c and d are the modal values of fuzzy sets. In this example, thanks to the time constant introduced by the coefficient of T_{ws} in the filter, these rules are successively applied over a temporal period.

The model parameters are identified off-line and/or on-line, and a large training set is not necessary.

Use of meteorological forecasts

A heating curve-based conventional controller only takes into account the instantaneous values of outdoor temperature. Therefore, it reacts with some delay. On the contrary, our controller "looks ahead" and modifies its policy in consequence.

With a meteorological data server, it is possible to find the optimal policy given some cost function. Nevertheless, with only local observations, looking one hour ahead gives some useful adjustments.

Optimal starting-up

Most of controllers for intermittent heating use a clock for starting-up. Our controller computes exactly the right hour, taking into account the building history and its thermal/physical characteristics.

Variable set-point temperature

A variable set-point temperature is automatically adjusted as a function of the user-defined set point, the desired comfort level and the foreseeable behavior of the building. For example, if important solar gains are forecasted, our controller decreases the set-point in advance.

7.10.2 Future work

The proposed controller is a prototype. Some improvements are necessary. Three tasks can be defined:

- firstly, a detailed inspection of the C code, in order to track down possible hidden bugs and improve the readability;
- secondly, design of a monitoring system to store historical data and analyze the behavior of the controller;
- thirdly, integrate SIMULA into the design chain.

Chapter 8

Work performed by UNN

Authors: Michaël Kummert, Ian Williamson and Dr. Sean Danaher

8.1 Introduction

This document reports on the simulation tests performed with the FUL passive solar ("Academic") building model and the last version of the simulation shell. Important parts of this reports have been created with the support of partner FUL.

Five controllers are compared :

- Conventional controller
- Fictitious thermostatic controller
- FUL optimal controller
- NOA ANN controller
- ISFH predictive controller

The simulated period includes one entire heating season. It uses real meteorological data measured in Uccle (Brussels) from Saturday 28th of September 1985 to Sunday 25th of April 1986. Real data was preferred to a typical reference year (TRY) in this case to allow a full testing of forecasting features of some controllers.

8.2 Simulation environment

The simulation environment, described Fig. 1, includes the following components :

Building model: TRNSYS TYPE 56. This model has been validated versus other simulation programs and versus experimental data in IEA research projects [L⁺94]. The parameters of FUL academic building have been computed from material data and some of them have been adapted taking measurements into account. It gives a reasonable accuracy, in the range of 15% for energy consumption. However, we can expect that the difference between two controllers performance using this model would be reproduced more accurately than the absolute performance. This point has been confirmed in previous studies for design changes [L⁺94]. The "measured" temperature is the operative temperature of the reference thermal zone (*Top*).

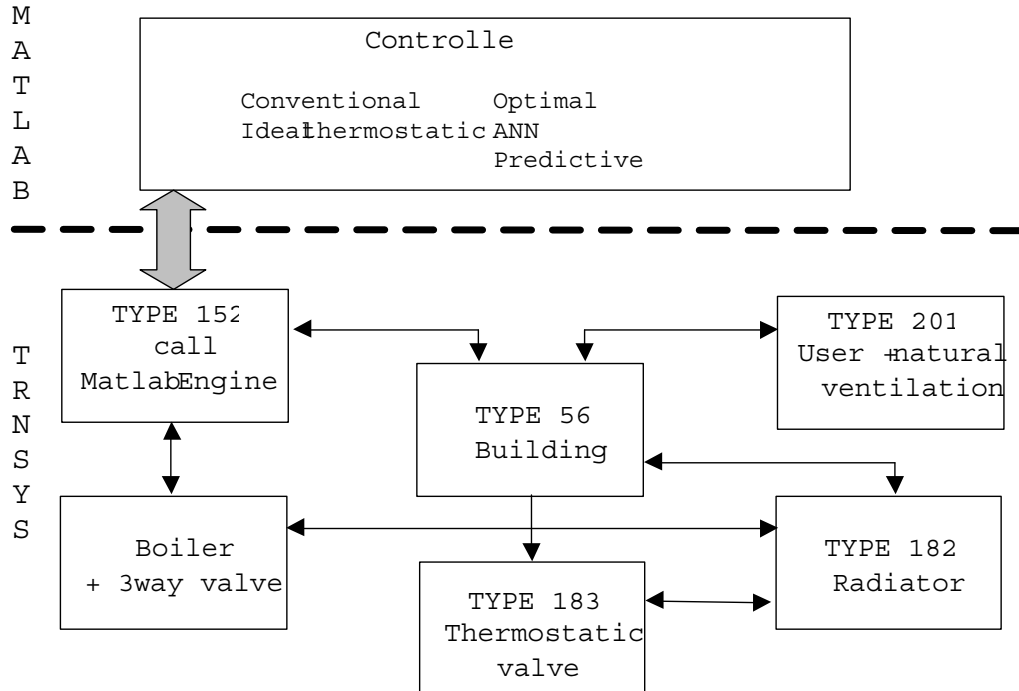


Figure 8.1. Simulation scheme

Radiator and thermostatic valve: (TRNSYS TYPES 182 & 183) The model used is based on IEA annex 10 models [IEA88]. They have been adapted by FUL to allow a 0.25h simulation time step, which had been retained in this project. Both components are modelled using first order representations. A non-linear expression is used to compute the heat flux from the radiator.

Boiler and 3-way valve: the boiler is supposed to have a constant setpoint (70°C). This temperature is the maximum value for water supply temperature (T_{ws}). The 3-way valve can adjust the water supply temperature between two bounds. The lower bound is fixed by the return water temperature (T_{wr}), since no cooling mean is present. The upper bound is fixed by the maximum boiler power : if all available power is used, the boiler cannot reach its setpoint and the maximum supply temperature is reduced. These constraints are taken into account by simple equations. The circulating pump is assumed to run continuously, as it is common in office-type buildings.

User behaviour and natural ventilation: (TRNSYS TYPE 201) The building presents windows that can be opened by occupants. A variable air infiltration rate is introduced in TYPE 56 to account for wind and windows position influence. The user behaviour concerning windows opening is modelled as follows :

- If the temperature exceeds the upper comfort limit, occupants open the window.
- If the temperature is colder than the lower comfort limit, they close the window.
- If the temperature is in the comfort range, they leave the window in current position.
- Occupants always close the windows when they leave the building for the night.

Controller call: (TRNSYS TYPE 152) All controllers are implemented in Matlab. For the controllers for which an executable program is available, the file data transfer and the call to executable routine are also realised in Matlab. The TYPE 152 was developed by FUL in

order to allow an efficient communication between TRNSYS and Matlab through the use of "Matlab Engine Library" [KA98c].

8.3 Performance assessment

The performance of different controllers is measured in terms of comfort and energy. Chosen indices are described in details in [KA98b]. Variable names are briefly summarised in the next paragraph.

Jd is the discomfort cost and is computed as $PPD'[\%]-5$ on 15 min values (PPD is Fanger's Predicted Percentage of Dissatisfied computed with variable clothing). PMV' is Fanger's Predicted Mean Vote computed in the same way. These indices are computed using the zone operative temperature (Top) and default values for other parameters.

Je is the energy cost, which is simply the energy consumption expressed in kWh.

8.4 Controllers parameters

The retained thermal comfort definition implies the day setpoint of operative temperature, which is the zone where the discomfort cost is zero (i.e. from 21°C to 24°C). It should be stressed here that the controllers do not really have to maintain a setpoint but rather have to maintain the temperature in the desired zone. Outside this zone, the penalty is computed by the cost function Jd which has a non-linear shape. Small deviations from this zone will cause very small discomfort cost, while the discomfort will become very important if the temperature goes far from the comfort range.

The only retained parameter for advanced controllers, once the comfort zone is defined, is the desired comfort level (CL). This comfort level is an integer number in the range [0;9] describing the importance that occupants give to comfort in comparison with energy. The value "none" will be used to describe any comfort level in the case the controller does not consider this parameter. Conventional and ideal controller are in this situation. Note that the current implementation of ANN controller does not take this parameter into account.

Other simulation parameters are :

- Thermostatic valve setting ($TsetV$) for the conventional controller. For all other controllers, the valve is supposed to be fully opened (referred to as $TsetV=open$) .
- The heating schedule. This parameter is described in the next section.

8.5 Schedules

8.5.1 Occupancy schedule

The occupancy profile was chosen to allow the study of heating start problems. The building is supposed to be occupied from 8 AM to 6 PM (Monday to Friday). No occupants are present during the week-end. A low value was chosen for the night setpoint temperature (15°C), while the "day" setpoint was determined by the comfort computation described here under. The comfort range, where the discomfort cost is zero, is [21-24°C].

8.5.2 Heating fixed schedule

Building heating is very often controlled using a fixed schedule, to start the heating early enough to obtain the desired temperature when occupants enter the building. The conventional and Ideal controllers use a fixed schedule, since it is the most common solution on existing buildings. The optimal controller anticipates the building behaviour with a long time horizon (more than 16 hours) and does not require the use of a fixed heating schedule. Indeed, it is able to heat up the building up to 16 hours in advance, which is sufficient for this building. The current version of ANN controller is not optimised to cope with setpoint changes and requires the use of a fixed heating schedule to obtain the comfort conditions when occupants arrive. The situation of predictive controller is more complex. This controller anticipates the building behaviour, but the weight of future values decreases when the desired comfort level increases. This results in a stronger anticipation for lower comfort level and almost no anticipation for very high comfort levels. Therefore, the use of a heating schedule starting the heating before real occupancy is needed for high comfort levels.

For all controllers, the used heating schedule has a strong influence on the comfort and energy performance. If the heating is started too late, the discomfort is high during the beginning of occupancy period, due to under-heating. On the other hand, if the heating is started too early, energy is wasted and the overheating risk is more important in the afternoon, since the building structure will be warmer. Seven different heating schedules were compared during the simulation tests. They will be referred to as $NHSc = 1..7$ in the following. $NHSc = \text{none}$ will be used to denote the absence of any heating schedule (the real occupancy profile is used). The time at which heating is stopped is always 6 PM. The start time of heating for different schedules is described in table 8.1.

Table 8.1. Heating start time for different schedules

Heating schedule	Start time (Sunday)	Start time (Monday)	Start time (Tu - Fri)
$NHSc = \text{none}$	/	8	8
$NHSc = 0$	/	6	7
$NHSc = 1$	/	5	6
$NHSc = 2$	/	4	6
$NHSc = 3$	/	2	5
$NHSc = 4$	/	2	4
$NHSc = 5$	/	0	3
$NHSc = 6$	21	0	2
$NHSc = 7$	16	0	1

8.6 Compared controllers

8.6.1 Conventional controller

This controller is based on a heating curve and thermostatic valves.

Two heating curves are used for "day" (occupied building) and "night". The heating curve gives the value of Tws as a function of the ambient temperature, $Tamb$. The value of Tws for a certain $Tamb$ is computed using the static properties of the building. The desired temperature in the reference zone (15°C for night, 21°C for day) should be maintained if the building was submitted to the given ambient temperature for a long period, without any solar radiation. In common practice, the "day" heating curve is slightly overestimated in order to allow a quicker warm-up of the building, while the "night" heating curve can be slightly underestimated to take dynamic behaviour into account (the initial building temperature is always higher than the desired value)

Thermostatic valves are traditionally combined with heating curves. These valves can reduce the flowrate in the radiators to prevent overheating. They have a very important role since no internal gains nor solar radiation are taken into account by the heating curve. Modelled thermostatic valves have a proportional band of 2°C and a hysteresis of 0.5°C , which is representative of commercially available models. They are supposed to be maintained at the desired setpoint (21°C) all the time. Fig. 8.2 presents the behaviour of the thermostatic valve for a setpoint temperature of 21°C . Note that the valve temperature depends on the zone temperature but also on the water supply and radiator temperatures. This problem is taken into account by the model used in these simulations.

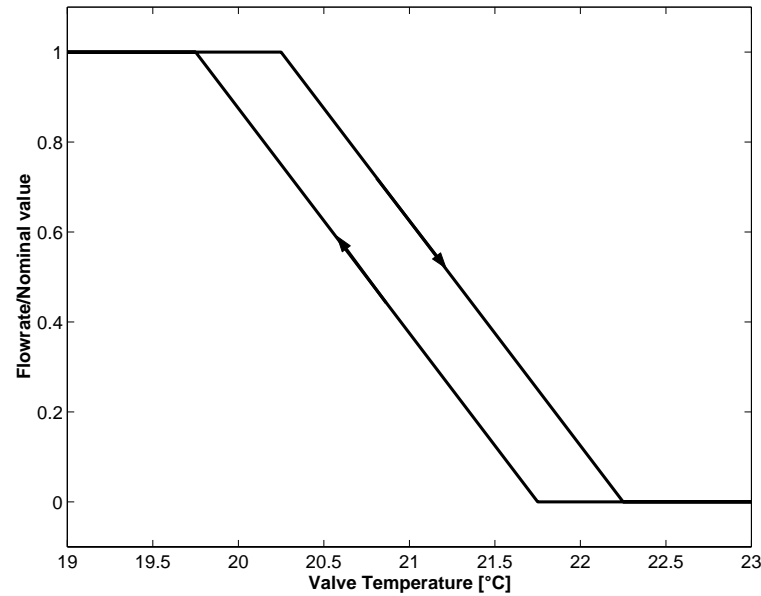


Figure 8.2. Thermostatic valve behaviour

8.6.2 Ideal thermostatic controller

A PID controller acting on the water supply temperature to maintain the zone temperature at the desired setpoint. The essential differences between this ideal controller and the conventional one are:

- No proportional band. The heating power is reduced as soon as the temperature approaches the setpoint and not when the temperature is already above this setpoint, as it is the case for thermostatic valves (see Fig. 8.2).
- Efficient night setback. For systems where the circulating pump is working continuously, a "full" night set back cannot be obtained by the here-above mentioned conventional controller. Indeed, the water supply temperature is computed to maintain the night setpoint in static conditions and the thermostatic valves do not close as they keep the "day" setpoint. The resulting heating power is almost always too high as the building is actually coming from a warmer state. In this respect, the "ideal" controller presents a behaviour close to "electronic thermostatic valves". These valves can have a programmable setpoint, e.g. 21°C during day and 15°C during night. This allows an efficient night setback as well.

8.6.3 Optimal controller

This controller was developed by FUL following the principles of optimal and predictive control theory. It can be noted that this controller was first developed for the building used in these simulations. Its internal parameters (prediction horizon, model order,...) are very well adapted to this building. However, its experimental application to Passys testcell showed that the used algorithm was also suitable for very different buildings. The parameters of the internal model are identified online, but realistic initial values are needed, which implies a good knowledge of the building.

8.6.4 ANN controller

NOA developed this controller using Artificial Neural Networks technique. The controller used in these simulation is the second version produced by NOA. It controls the water supply temperature, as all other controllers in this study. This controller was also tested on the FUL real building, as described chapter 5. This controller was adapted to cope with two setpoints (day and night) but is not optimised to change quickly between these two setpoints. This controller was trained using simulation data obtained on the same TRNSYS model with a different meteo data set.

8.6.5 Predictive controller

This controller was developed by ISFH using predictive and adaptive control theory. It is the only controller that uses no a priori knowledge of the building. The structure of the internal model has been adapted to ISFH and FUL buildings, but no initial values are needed for parameter identification.

8.7 Tested cases

Different controllers were tested with different simulation parameters.

For the conventional controller, different thermostatic valve settings were tested in combination with different heating schedules. This controller does not take the comfort level into account:

CL = None

NHSc = 5 & 7 (lower NHSc give poor performance)

TsetV = from 20°C to 22°C with 0.25°C steps

Extra cases:

CL=none, NHSc=7 and TsetV=19.75

CL=none, NHSc=6 and TsetV=21.00

For the ideal thermostatic controller, the thermostatic valve is fully open. All heating schedules were tested. This controller does not take the comfort level into account:

CL = none

NHSc = 0..7

TsetV = open

For the optimal controller, no heating schedule is needed. The thermostatic valve is fully open. The whole range of comfort level was tested:

CL = 0..9

NHSc = none

TsetV = open

For the ANN controller, the thermostatic valve is fully open. All heating schedules were tested. This controller does not take the comfort level into account:

CL = none

NHSc = 3..7 (lower NHSc give poor performance)

TsetV = open

For the predictive controller, the thermostatic valve is fully open. All heating schedules were tested.

The whole range of comfort level was tested:

CL = 0..9

NHSc = 5..7 (lower NHSc give poor performance)

TsetV = open

Extra cases:

CL=5..9, NHSc=4 and TsetV=open

CL=8..9, NHSc=3 and TsetV=open

CL=9, NHSc=2 and TsetV=open

CL=9, NHSc=1 and TsetV=open

CL=8..9, NHSc=0 and TsetV=open

The total number of cases is 84: 20 cases for conventional controller, 8 for ideal controller, 10 for optimal controller, 5 for ANN controller and 41 for predictive controller.

8.8 Results

8.8.1 Global performance

Tables given in annex present global results for all tested cases.

The total energy consumption and some comfort parameters are given.

Top: Operative temperature of the reference zone. Min, max and average values are given for the occupation period only.

PMV': Predicted Mean Vote computed as described here above. Min, max and average values are given (occupation period only).

Jd: Discomfort cost. It is $PPD' \cdot 5\%$, the predicted percentage of dissatisfied computed as described here above [%]. Min, max and average values are given (occupation period only).

$\int Je$: Energy consumption on the entire heating season [kWh].

$\int Jd$: Sum of discomfort cost on the entire heating season [% $PPD' \cdot h$]. Cost is zero when building is unoccupied.

Fig. 8.3 gives an overview of global performance of all tested cases. The Energy consumption over the entire heating season is plotted versus the total discomfort cost. In this graph, "good controllers" would be in the lower left corner (low energy consumption, low discomfort). It can first

be noted that for the same discomfort cost, very different energy consumption can be attained by different controllers on the same period for the same building. Maximum savings are in the order of 20%.

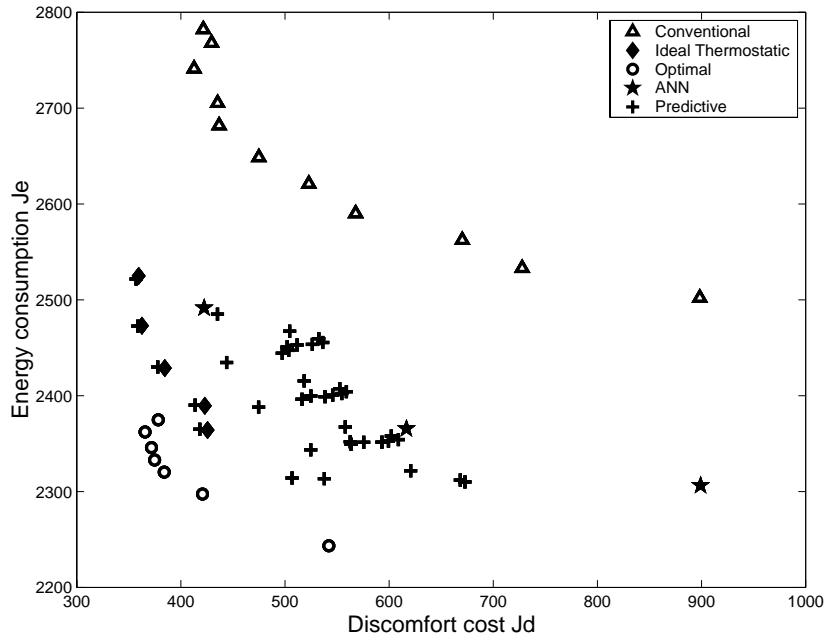


Figure 8.3. Controllers global performance

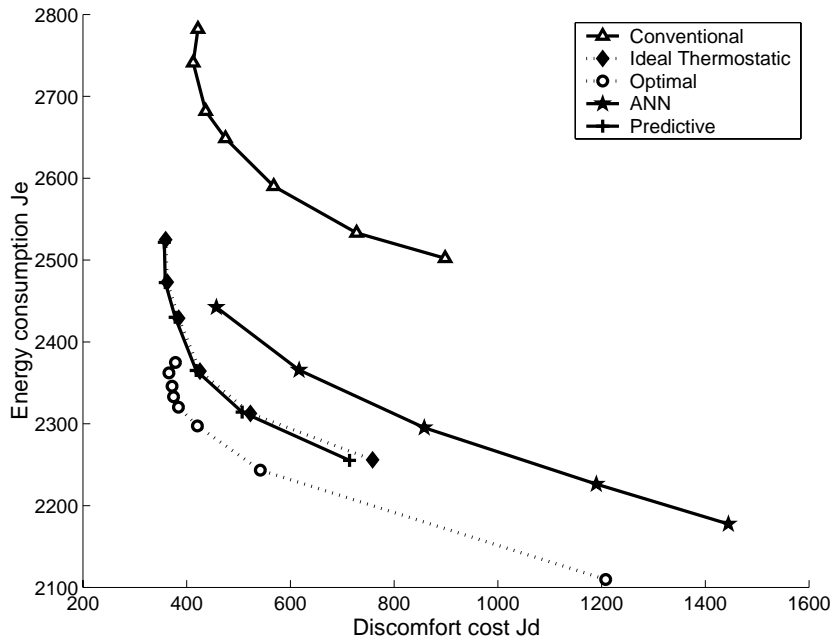


Figure 8.4. Controllers "trajectory" in (Jd, Je) plane

Furthermore, different settings of the same controller can lead to very different behaviour. This is obvious for the conventional controller, where the thermostatic valve setting plays an important role, but it is also the case for other controllers, where different heating schedules and different comfort level settings will cause different behaviours.

The general shape of all best-achievable solutions is a hyperbolic-like curve, which can be translated in words by : "if the discomfort cost is decreased, the energy consumption will increase". However, a more refined analysis will show that in some cases an energy consumption increase can lead to discomfort cost increase as well.

At the first glance, the "worst" performance is given by the conventional controller, while the "best" performance is given by the optimal controller, for the given building and the given simulation hypotheses.

Fig. 8.4 shows the same results where only the best cases of each controller are kept, and joined by a line to make the interpretation easier. The points on one line of the plot represent the trajectory of the controller global performance when some settings are changed.

It can be seen that the general "hyperbolic-like" curve is obtained by all controllers. The only "setting" of ANN controller was the heating schedule, for which only a limited number of cases were studied. This explains the small number of points and the absence of the "vertical" part of the curve.

8.8.2 Parameters influence

Fig. 8.5 shows the influence of the heating schedule and the thermostatic valve setting on the conventional controller's performance.

It can be seen that different thermostatic valve settings allow to obtain different performance. The influence of different heating schedule is small as far as they stay in the "acceptable" range. Heating schedules offering too short pre-heating periods were not retained, since the comfort performance is severely reduced.

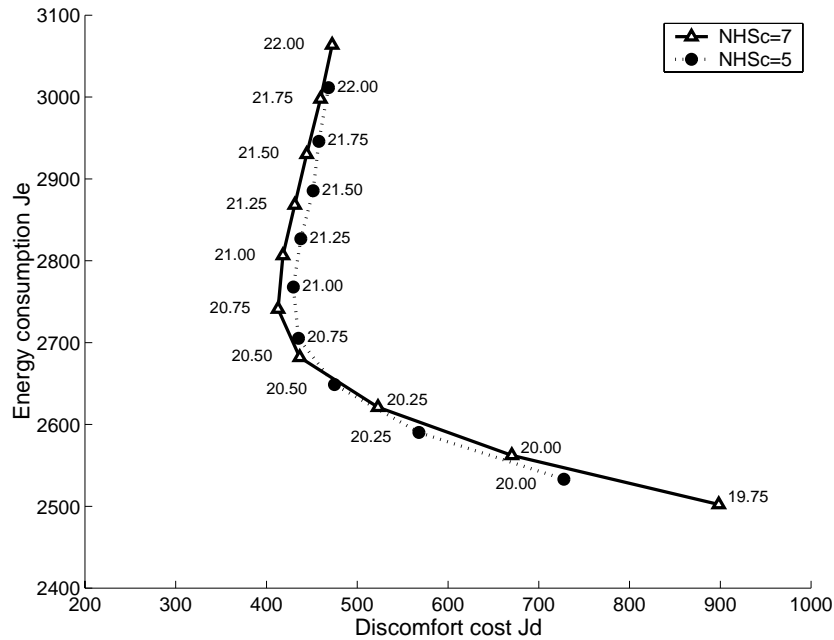


Figure 8.5. Influence of heating schedule (NHSc) and Thermostatic valve setting on conventional controller performance. Points labels indicate the thermostatic valve position

Fig. 8.6 shows the influence of the comfort level (CL) on the optimal controller's performance. This parameter is the only user setting of this controller. Some internal settings have to be adapted to

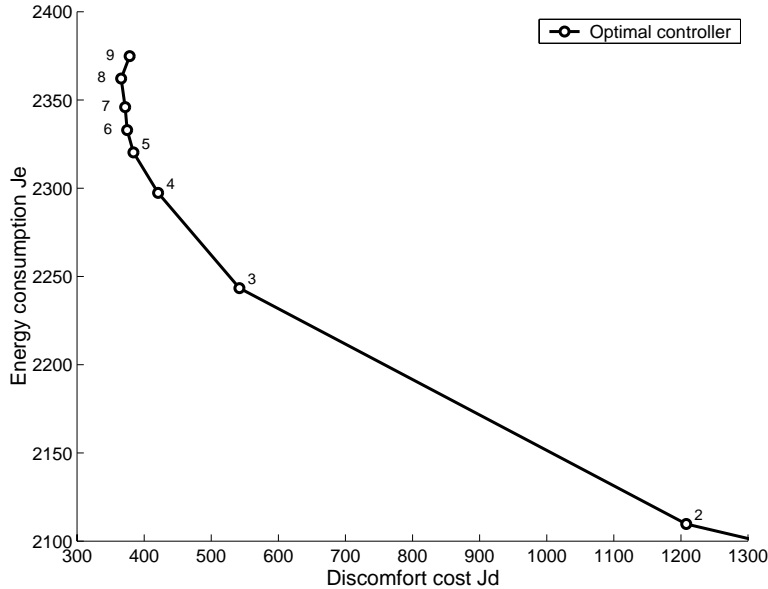


Figure 8.6. Influence of Comfort Level on optimal controller behaviour. Labels show the CL value

the building, but require an expert intervention. The figure presents obtained results for a well designed controller.

The CL parameter allows users to choose between high comfort and high energy savings. A commercial version should have a different scale to limit the CL value in the acceptable range (0 and 1 have been suppressed from this graph) and to offer a better repartition in (Je, Jd) plane.

Fig. 8.7 shows the influence of the heating schedule and CL parameter on the performance of the predictive controller. The shape of the curve for high CL values is close to the one obtained for other controllers, but the behaviour of the controller is different for lower CL values. The reason is that the anticipation of the predictive controller is stronger for these low CL values. The internal cost function gives more weight to future values, which allows a more efficient control of heating. This explains that the global performance obtained with $NHSc=7$ and $CL=0$ is better than the one obtained with the same heating schedule for $CL=7$.

Finally, Fig. 8.8 shows the influence of the heating schedule on the performance of ANN and Ideal controllers. $NHSc$ is the only adjustable parameter for these controllers. A more conservative heating schedule normally leads to higher energy consumption but better comfort, since "cold mornings" are suppressed. However, the overheating risk is also increased since the building structure is warmer. This explains the vertical part of the curve for the Ideal controller

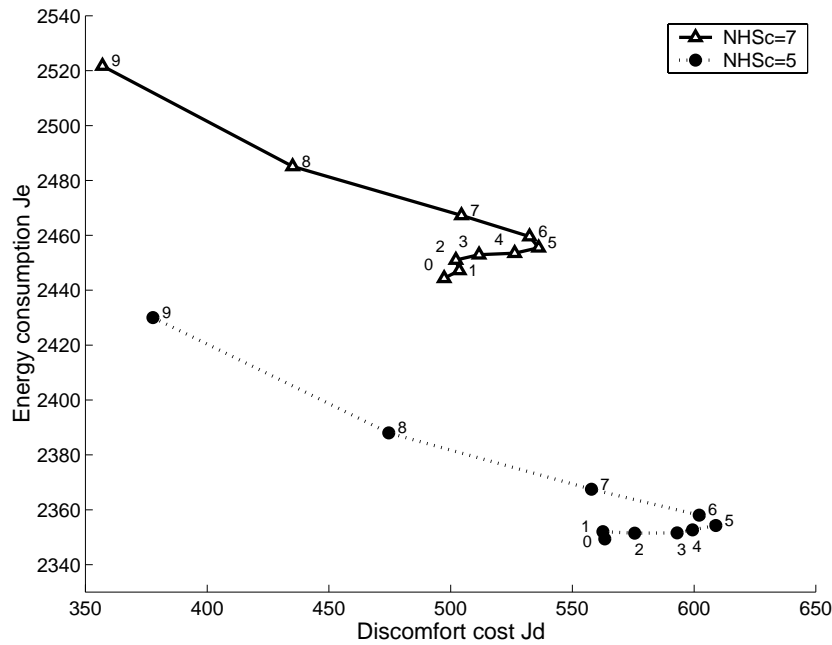


Figure 8.7. Influence of heating schedule (NHSc) and Comfort Level on Predictive controller performance. Labels show the CL value

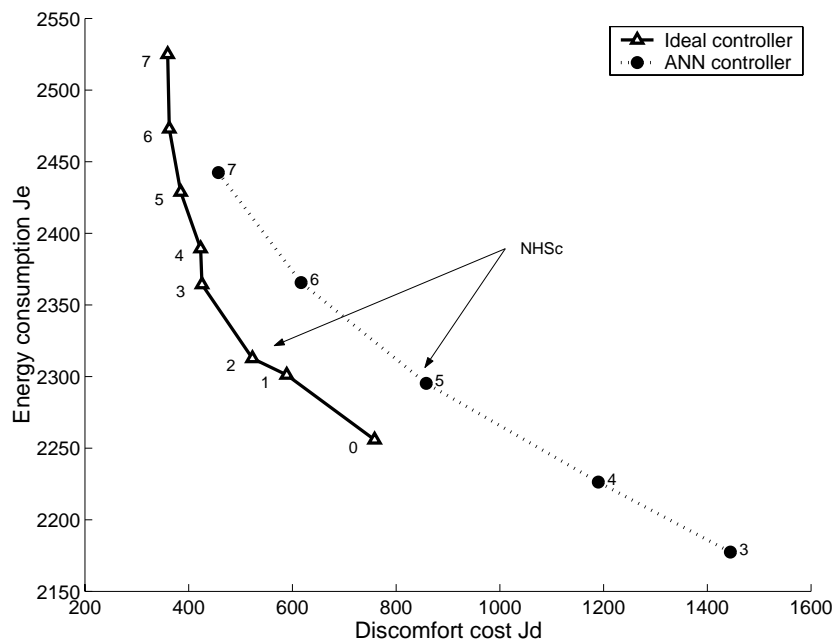


Figure 8.8. Influence of heating schedule (NHSc) on ANN and Ideal controller performance. Labels show the NHSc value

8.8.3 Typical profiles

8.8.3.1 Cold period

Fig. 8.10 to 8.14 present the behaviour of different controllers for a cold week (from Sunday January 5, 12:00 to Saturday January 11, 00:00). All graphs represent the same week and can be directly compared.

Grey zones in the graphs for *Top* (operative temperature in the reference zone) represent the comfort zone, during building occupancy. Light grey rectangles next to them represent the zone where the discomfort cost is not zero but is still very low (approximately 0.5°C below the lower comfort limit and 0.5°C above the upper comfort limit).

Fig. 8.9 presents the ambient temperature (*Tamb*) and the global solar radiation on a horizontal surface (*Gh*) for the considered week.

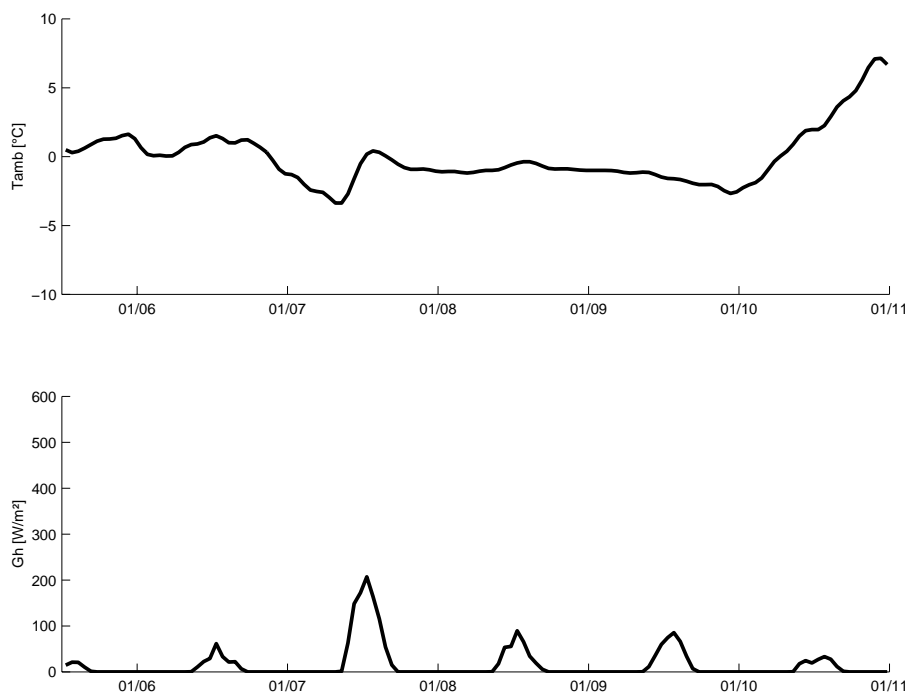


Figure 8.9. Meteorological variables, cold week

Fig. 8.10 presents the behaviour of the conventional controller for the cold week, for different heating schedules (NHSc) and different thermostatic valves settings (*TsetV*). Two major disadvantages can be seen :

1. The temperature during night is not so low as for other controllers (compare with Figs. 8.11 - 8.14). This is caused by the use of a heating curve, which is always designed to maintain the night setpoint (15°C) in static conditions
2. The proportional band of thermostatic valves makes that the heating power is decreased when the zone temperature reaches the setpoint, but the heating power is not zeroed.

Fig. 8.11 shows the same week for the Ideal thermostatic controller. It can be seen that the two major disadvantages of the conventional controller have been suppressed. This controller is still using a fixed heating schedule. Different NHSc are compared.

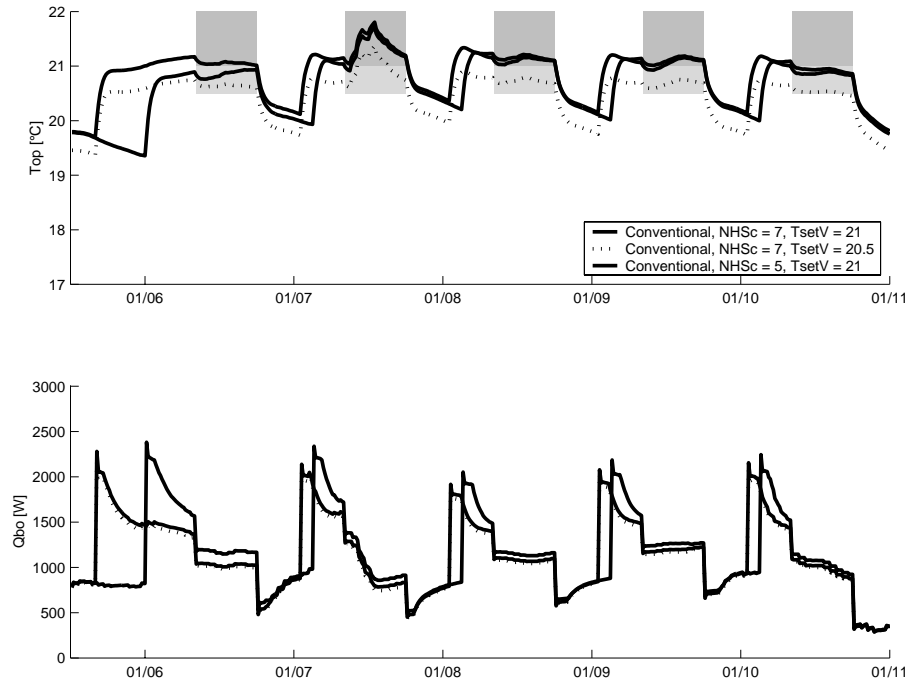


Figure 8.10. Conventional controller, cold week

It can be noted that the maximum available power (3000W) is used, while it was not the case for the conventional controller. This was due to 2 different factors:

1. The zone is never really cold for the conventional controller, which limits the power that can be emitted by the radiator (This power is roughly function of the temperature difference between the water supply temperature and the zone temperature)
2. Thermostatic valves are sensitive to the zone temperature but also to the water temperature. When this temperature is very high (e.g. at heating start), they would slightly close, preventing the maximum power to be reached.

Fig. 8.12 concerns the optimal controller. Different comfort level (CL) values are compared. It can be seen that the heating is started just in time in almost every case. For a high CL value, the zone temperature is very close to the lower limit of the comfort zone. For lower CL values, the controller gives a lower temperature during the day, but also reaches this temperature later and stops heating earlier.

Fig. 8.13 shows the temperature and power profile for the ANN controller. As mentioned here above, this controller is not optimised to change from one setpoint to the other and gives a very smooth temperature profile compared to other controllers. This slow response can lead to high discomfort on some mornings, as on the first day on the plot. This implies the use of rather conservative fixed schedules. On the other hand, it can be seen that the setpoint is very well maintained while the "switch" has been realised.

Finally, Fig. 8.14 shows the same week for the predictive controller.

For high CL values, the predictive controller maintains the setpoint (lower bound of the comfort zone in this case) almost perfectly, but requires the use of a fixed heating schedule. When CL is decreased, this controller shows a larger anticipation, which can be seen at the end of the day (heating is stopped one or two hours before the end of occupancy period).

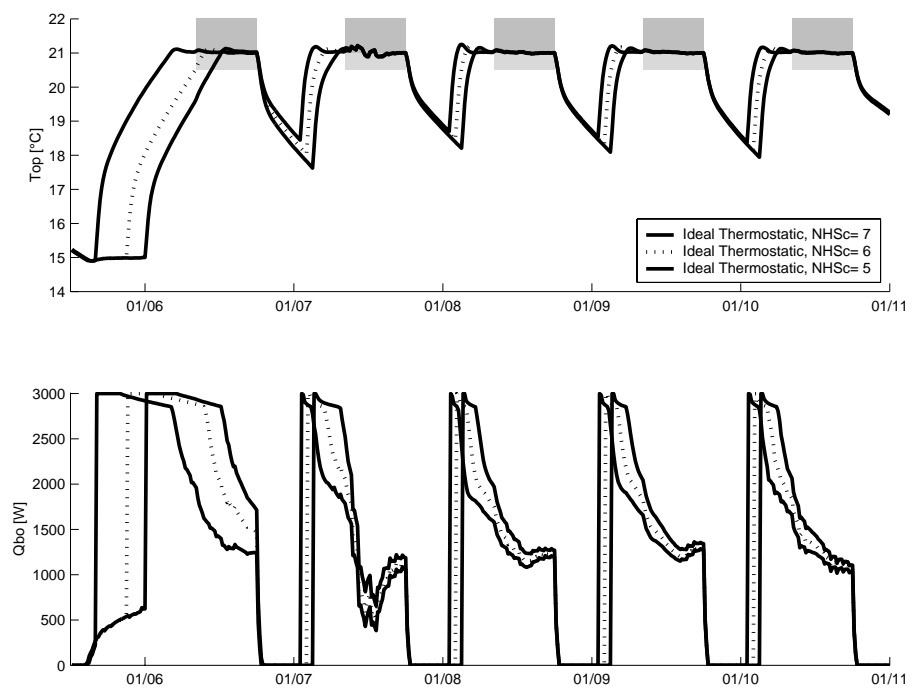


Figure 8.11. Ideal Thermostatic controller, cold week

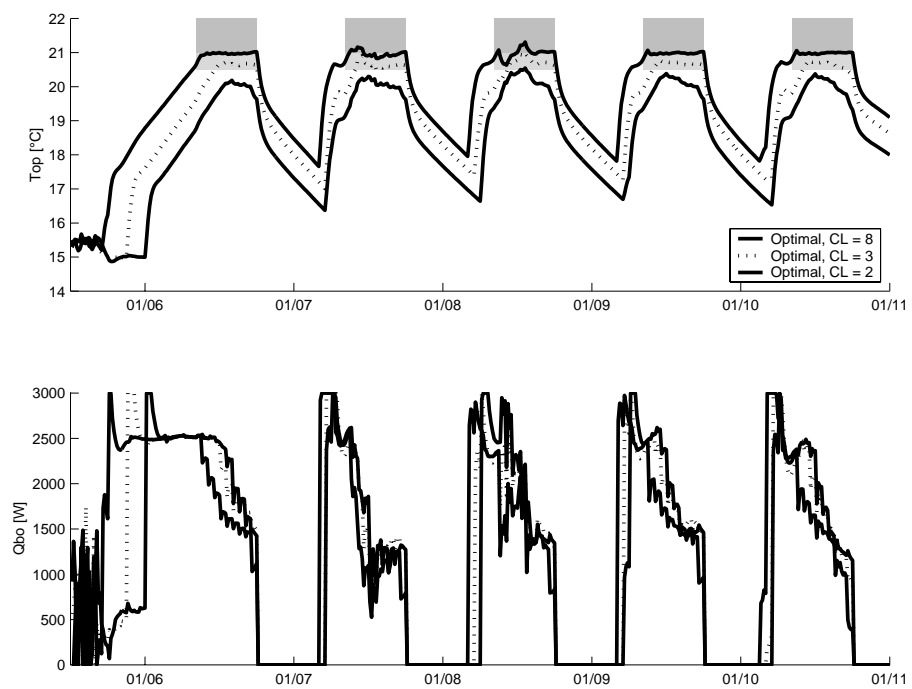


Figure 8.12. Optimal controller, cold week

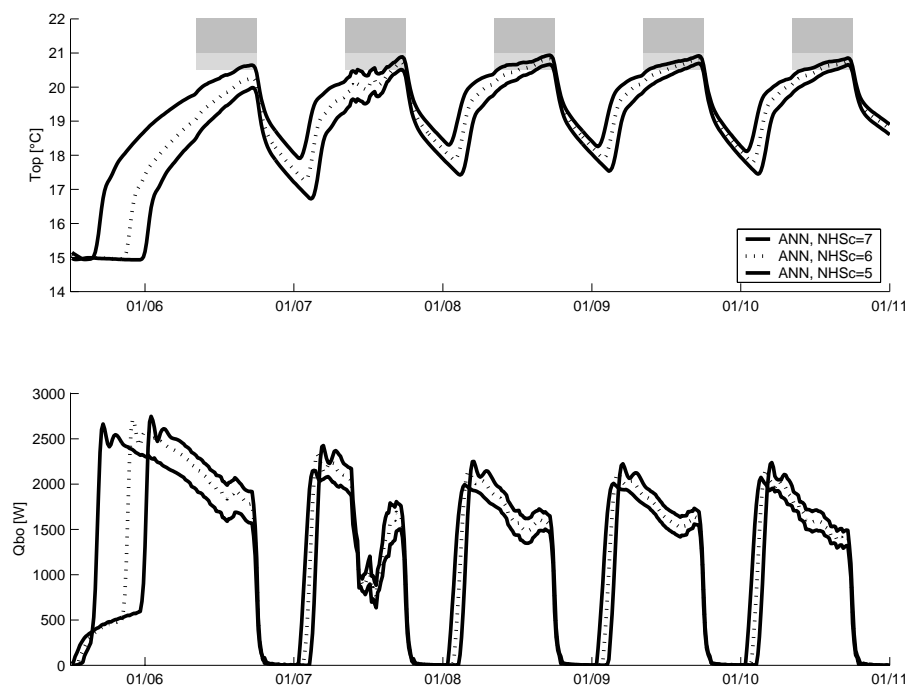


Figure 8.13. ANN controller, cold week

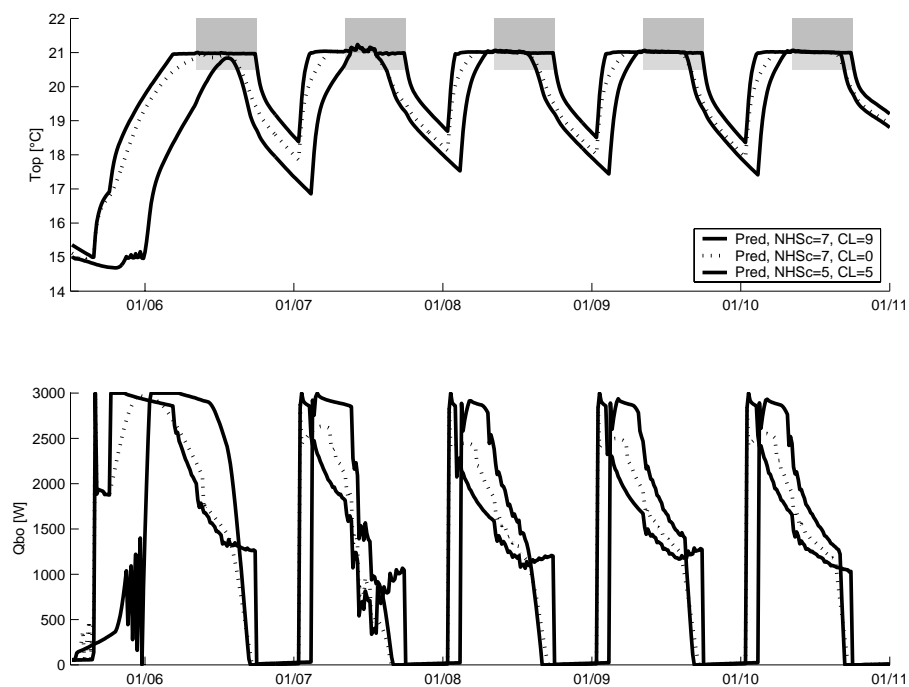


Figure 8.14. Predictive controller, cold week

8.8.3.2 Sunny mid-season period

Fig. 8.16 to 8.20 present the behaviour of different controllers for a sunny mid season week (from Sunday March 9, 12:00 to Saturday March 15, 00:00). All graphs represent the same week and can be directly compared.

Grey zones in the graphs for *Top* (operative temperature in the reference zone) represent the comfort zone, during building occupancy. Light grey rectangles next to them represent the zone where the discomfort cost is not zero but is still very low (approximately 0.5°C below the lower comfort limit and 0.5°C above the upper comfort limit).

Fig. 8.15 presents the ambient temperature (*Tamb*) and the global solar radiation on a horizontal surface (*Gh*) for the considered week.

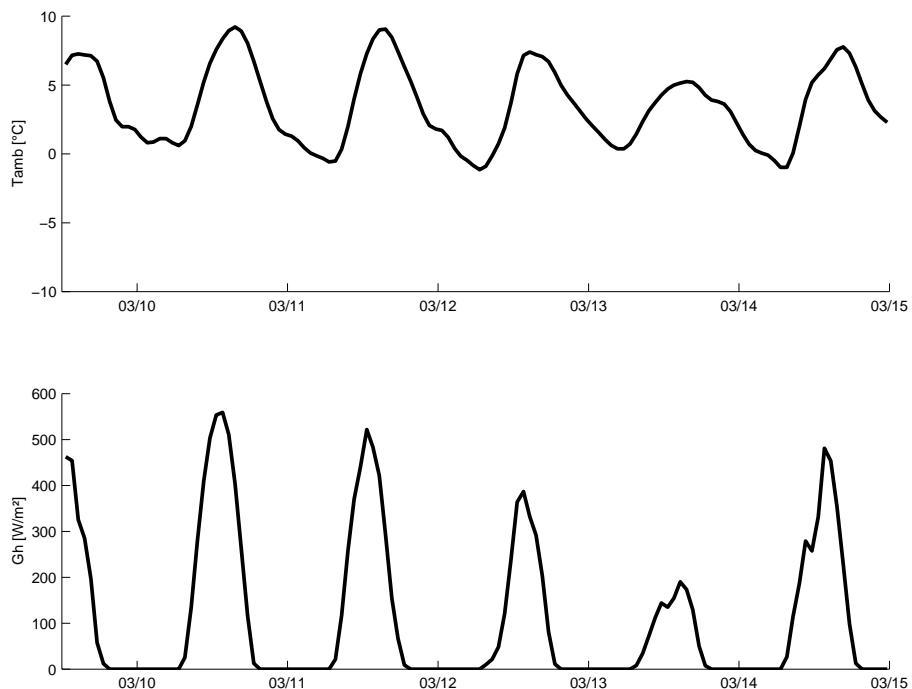


Figure 8.15. Meteorological variable, sunny mid-season week

Fig. 8.16 shows the temperature and heating power profile for the conventional controller during this week.

It can be noted that the building is significantly warmer with this controller than with other ones (see Fig 8.17 - 8.20). This is due again to the fact that thermostatic valves are supposed to keep their setpoint (*TsetV*) during the occupied but also the unoccupied periods. This situation always leads to unnecessary heating when the heating circulating pump is working continuously, which is very often the case in practice.

The use of a fixed heating schedule leads to a pre-heating of the building which is also unnecessary during this rather warm week. Energy is wasted and the overheating risk during the afternoon is more important.

Fig. 8.17 shows the same week for the Ideal thermostatic controller. The building is colder than for the conventional controller during the unoccupied periods, but the problems associated with the use of a fixed heating schedule are not suppressed.

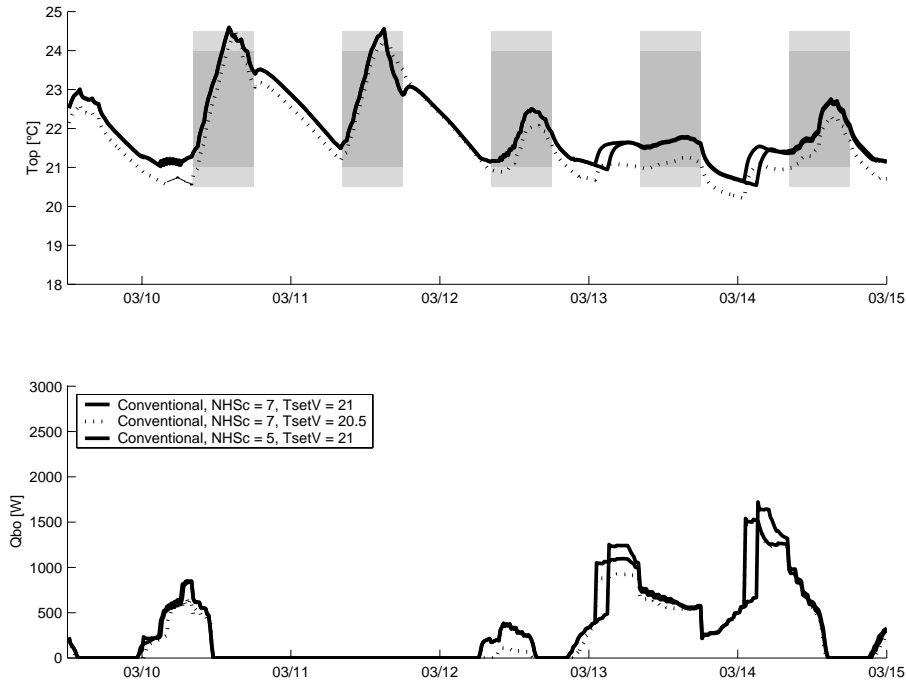


Figure 8.16. Conventional controller, sunny mid-season week

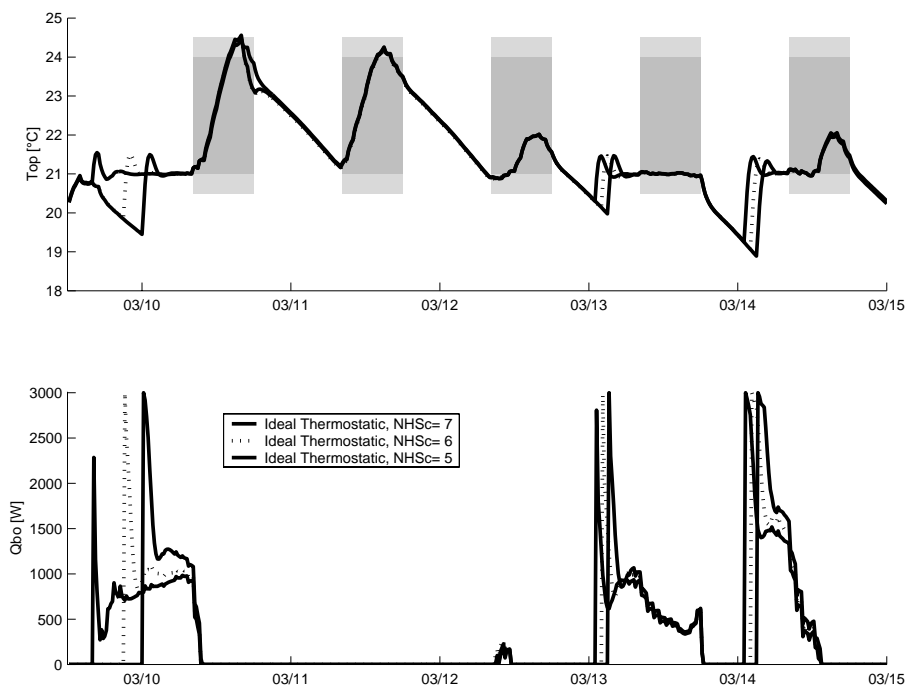


Figure 8.17. Ideal thermostatic controller, sunny mid-season week

Fig. 8.12 shows the optimal controller behaviour during the same sunny mid-season week. The controller is able to start the heating just in time but also to under-heat the building during the morning to prevent overheating in the afternoon.

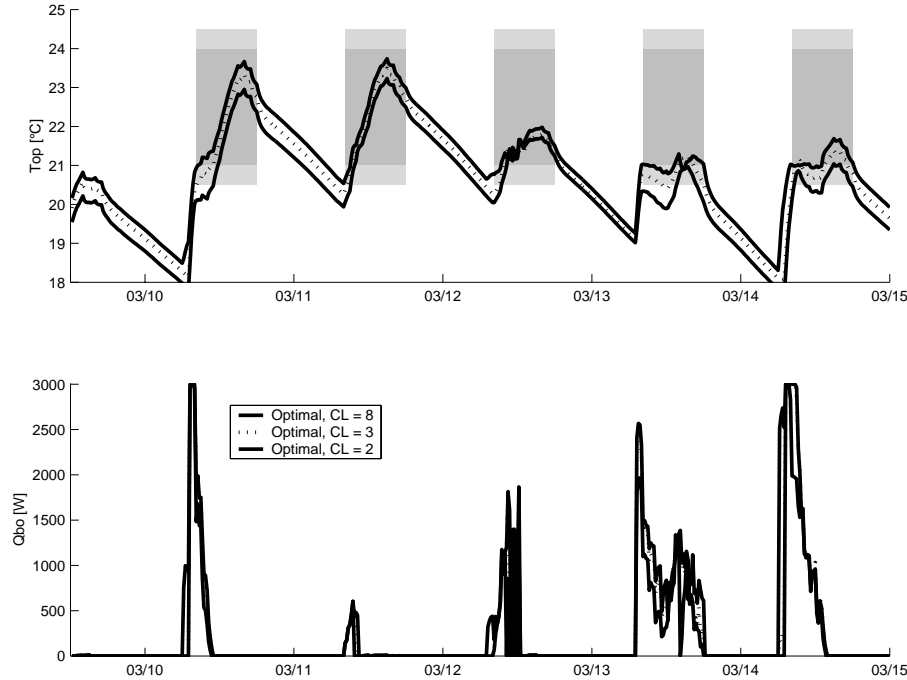


Figure 8.18. Optimal controller, sunny mid-season week

Fig. 8.19 presents the performance of ANN controller. It is clearly shown that the heating schedule 7 is too conservative for this period. The heating schedule 5 gives good performance. However, the same heating schedule cannot give good results during the whole heating season (compare with Fig. 8.13).

Finally, Fig. 8.20 shows the predictive controller temperature profile for the retained mid- season week. Here again, heating schedule 7 is not adapted to this period, while such large pre-heating times were required during the cold period (see Fig. 8.14).

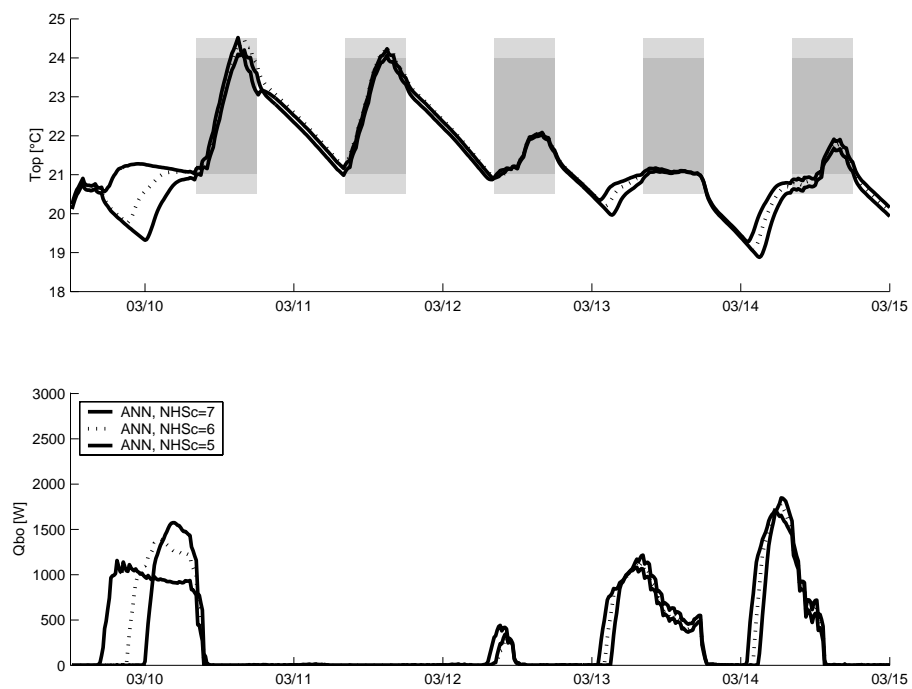


Figure 8.19. ANN controller, sunny mid-season week

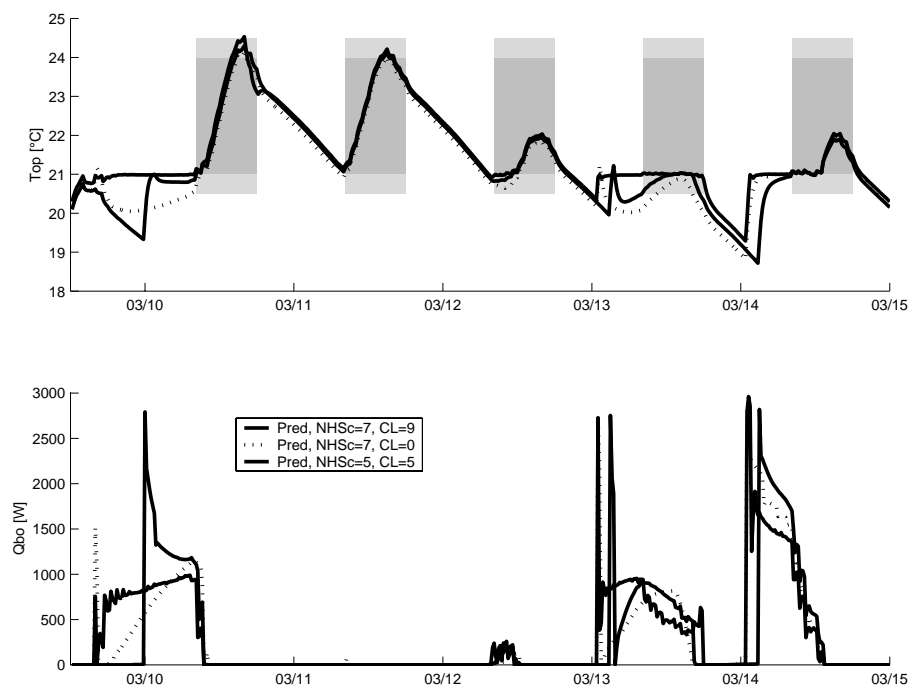


Figure 8.20. Predictive controller, sunny mid-season week

8.9 Conclusions

8.9.1 Energy - comfort performance

All controllers show an improvement of the performance compared to the conventional controller and they all offer the possibility to give more or less importance to comfort versus energy savings.¹

It must be reminded that this conclusion is based on the comfort definition using Fanger's PPD index, which takes overheating into account. If the occupants were supposed to accept overheating but not underheating, the best achievable performance would be very close to a perfect thermostatic control.

The highest energy savings for an equivalent discomfort cost are achieved by the optimal controller and reach 15%. This controller is also better than an Ideal thermostatic controller (the energy savings are reduced to 5% in this case). It can be noted that the experiments showed higher savings when the controllers were compared on short similar periods. Two reasons can explain this:

1. The conventional and Ideal controllers are perfectly tuned for the building and the weather conditions, since all possible parameters choices could be tried. This is also the case for the "advanced" controllers, but these controllers are sometimes easier to tune than a conventional controller (especially for their developers!). The user's behaviour model was also rather "energy and comfort conscious", which is not always the case in practice. Thermostatic valves are often open when the building is overheating and sometimes closed during a whole night, preventing any heating of the building before the occupants arrive.
2. secondly, higher energy savings can be achieved during cold and sunny periods, or during mid-season, since the overheating problem is more important. The global performance considered in this simulation study was computed for a whole heating season using real meteorological data and not a Typical Reference Year. Achieved energy savings can be far more important if shorter periods are considered, and are also likely to vary to some extent on a year-to-year basis. However, the used meteorological data is representative from the concerned location.

Comparison between advanced controllers

The optimal controller gives the best results for this building and the retained simulation hypotheses. It should be noted that this controller was developed on the simulated building and is perfectly adapted to this building. However, the application to the Passys testcell in Athens has proven that it can be adapted to very different buildings and meteorological conditions.

The ANN controller is currently not optimised to change from one setpoint to another, and this problem was reinforced by the very large inertia of the simulated building. However, this controller showed its ability to cope with the high overheating risk present in this building.

The predictive controller seems to offer a performance very close to the ideal thermostatic controller in the simulations. This can be explained by the need to use a rather conservative heating schedule. This controller seems more adapted to lower inertia buildings, or to "smoother" setpoint profiles. This is notably the case in residential buildings, where the night setback is usually less important and where the "Monday morning start" is not present.

8.9.2 Implementation aspects

The approaches of the three tested controllers are different. They can be summarised as follows:

¹The "comfort level" feature is not yet implemented in the ANN controller, but different behaviours can be obtained by using different heating schedules.

Optimal:

- Requires a good a priori knowledge of the building to obtain a physical model. A good quality model is required because of the long prediction horizon.
- Online identification of some parameters in a narrow range allowing to take into account real variations (e.g. air infiltration rate variable with windows opening). An adaptation to important changes in the building structure (windows size,...) would require an intervention.
- Complex optimisation algorithm offering a very high reliability (an optimum is always found) but implying a very important computational power compared to other algorithms.
- Anticipation of the building on a long horizon (16..24h), allowing optimal control strategies to start the heating "just in time" and afternoon overheating prevention. This requires reliable meteo and occupancy forecasting, but the use of previous day proved to be sufficient.
- The implementation in a low-cost micro-controller based on intel51 chip proved to be impossible within the time scale of this project. It would require a drastic simplification of the algorithm. This version of the controller is more suitable for implementation in a PC- like micro-controller or for PC-based solutions.

ANN controller:

- Completely black-box model of the building and heating plant. Requires a long period to train the model but no intervention is needed.
- Reasonable computational power is needed once the model is trained.
- The use of ANN's ensures the ability of the controller to adapt itself to building changes, but important changes would need a long period to be learned.
- Anticipation of building behaviour is limited to short-term in the current implementation
- An optimiser acting on higher level (i.e. managing the switch from one setpoint to another) can be realised using the same technique but would probably increase the required computational power.
- The implementation in a micro-controller of intel51 series was not fully realised but should be possible without important changes. A suitable trade-off between adaptability and memory requirements should be found.

Predictive controller:

- black-box model of the building with quick online adaptation of the parameters. The model currently implemented is probably limited to short or mid-term prediction horizon (1..6 hours)
- Small computational power compared with other advanced controllers.
- The use of a heating schedule is still required for high inertia buildings with intermittent occupancy and important night setback.
- This controller was successfully implemented in a low cost micro-controller of intel51 series, offering nearly the same controller performance as the PC version.

8.9.3 Summary of controllers characteristics

Table 8.2 shows a summary of the advantages/ disadvantages of different advanced controllers with respect to some selected criteria.

"+" , "0" and "-" indicate respectively a good, "neutral" , or bad performance for the given criterion. "X" indicates that the given criterion could not be evaluated for the considered controller.

Table 8.2. Summary of the advantages/ disadvantages of different advanced controllers. The energy/ comfort performance is based on the simulation test on FUL building only.

		Optimal		ANN		Predictive
Energy/ comfort performance	+	Best performance of the simulation test on FUL building	+	Improved performance compared to conventional	+	Good performance although stronger anticipation could improve it
Response to desired comfort level	+	CL reflects the relative importance of comfort and energy	X	Not implemented	-	Different behaviour for low and high CL values
Computational load	-	High computing power (flops) and rather important memory requirements	0	Low requirements for current version. Full version including online training and optimisation would have higher requirements	+	Low requirements for developed C code
Adaptation to different buildings	+	Adaptation is possible but requires expert knowledge	+	ANN must be trained for the building and meteo conditions	+	A model identification start "from nothing" is possible
Adaptation to building changes	0	on line identification in a restricted range	+	Inherent advantage of ANN	+	online identification with decreasing weighting of older measurements
Implemented into a Intel51 micro-controller	-	current implementation proved to be too complex. Best adapted to PC-like controllers	0	Re-coding work was not totally achieved but the current version is suitable for this implementation	+	successfully implemented

Chapter 9

Work performed by INGA

Authors: Horst Zacharias, Ingo Brauns, Ute Thron

The work of the industrial partner INGA (associated contractor of the ISFH) consisted of 4 parts:

- support for the scientific partners for the specification of necessary properties of the control algorithms to be developed,
- hardware and software development,
- market analysis,
- other activities.

9.1 General specifications

During Task 1, INGA was responsible for support of the scientific partners for the specification of necessary properties of the control algorithms to be developed. During all further tasks, INGA was responsible for the check of formulations concerning

- user friendliness of necessary operation
- keeping of the possible cost frame for the different applications
- contradictions to the laws in force
- applicability to typical HVAC-systems.

The points were discussed during the meetings and directly with the coordinator. Results are the general specifications, which are described in section 5. Furthermore, the specifications are reflected in the choice of the hardware described in the next section.

9.2 Hardware and software development by INGA

The hardware and software development was the main part of the industrial partner's work. Solutions are available for different applications:

- big buildings and housing schemes,

- small buildings (especially single family houses).

The solution for big buildings and housing schemes consists of the integration of the developed algorithms into a Software for building management developed by INGA (see figure 9.1. This

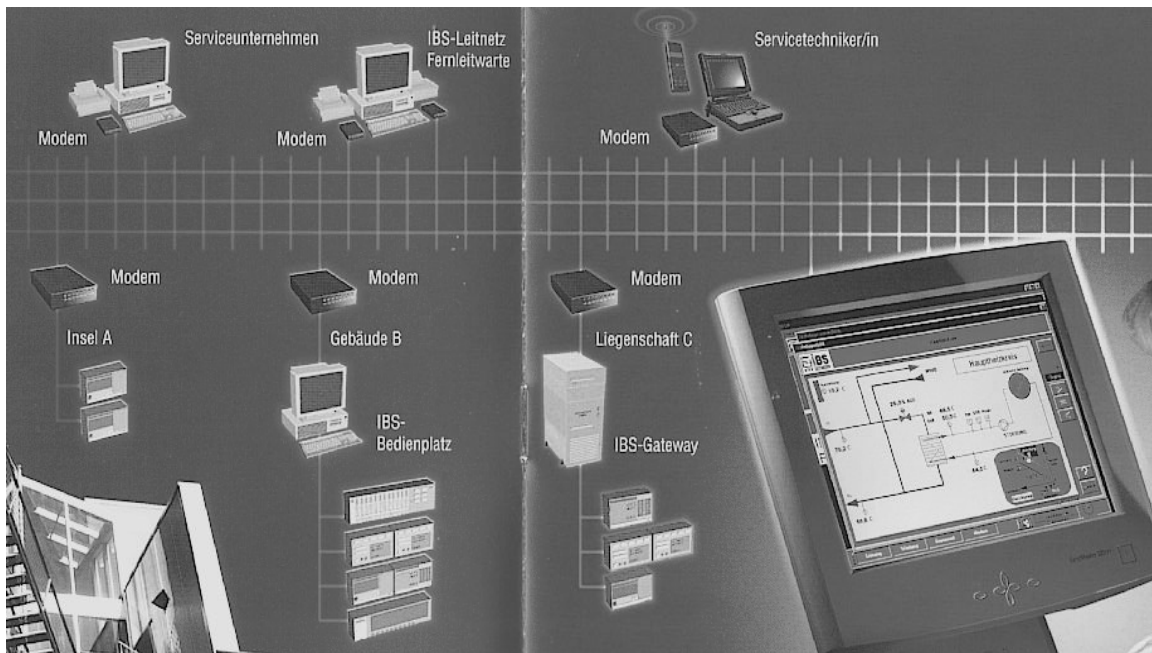


Figure 9.1. Application of the IBS Software developed by INGA

software is running on a PC. Since all algorithms have been tested on a PC, the implementation into the INGA software is straightforward. The INGA software is independent from the measuring and control system and the hardware. It is able to communicate with the protocols of many producers of measurement and control systems in building management. One requirement of the soft- and hardware to be developed was, that it should be applicable in a variety of buildings and heating systems. The INGA software is very suitable concerning this requirement. It is however concerning the costs too expensive for small family houses. Since the first development in this project was focussed to small family houses, another hardware and software was chosen for the standalone device.

The necessary properties of the hardware have been discussed intensively among all partners. Requirements concerned the:

- possibility of operation of the device by a layperson,
- computational power and memory,
- accuracy of sensors,
- installation and placement of the device,
- price and design.

The standalone device consists of a microcontroller delivered by the Brauns Control GmbH. The microcontroller takes over all tasks of input and output data handling, computing and user communication. Figure 9.2 shows a scheme of the microcontroller.

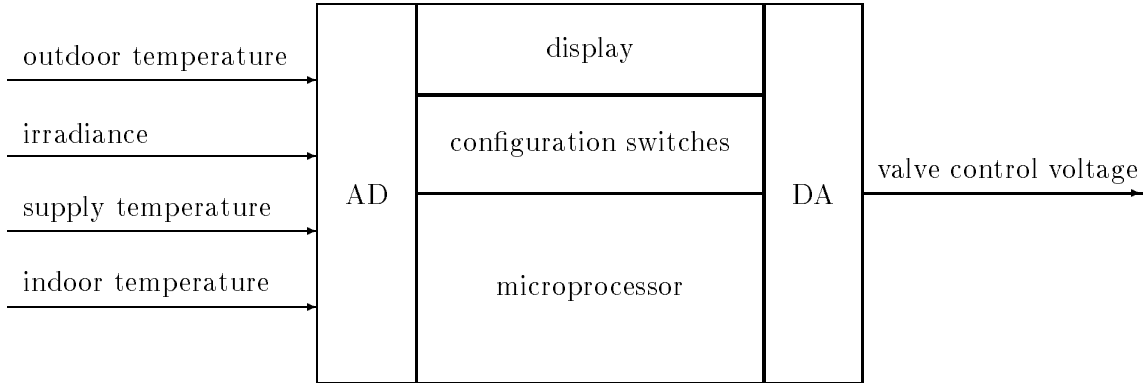


Figure 9.2. Scheme of the standalone device, AD: Analogue-digital conversion, DA: Digital-analogue conversion

Figure 9.3 shows a photograph of the device placed in the experimental houses of the ISFH.



Figure 9.3. View of the standalone device from outside

The chosen hardware consists of a small box which can be placed for example on the wall of the reference room (practically the room, where people stay most of the time). However any other room is possible too. The equipment inside the box consists of 2 parts: one circuit board for the connection of the cabling to sensors and actuators (figure 9.4) and the actual computer with processor, memory etc. (figure 9.5). A small display and 4 buttons are placed on the front side for the communication with the user. The partners agreed to limit the necessary user settings to 2 values: a time dependent indoor temperature set value (as usual) and a comfort parameter, which allows the user to switch between more comfort and more energy saving. The background is that more energy savings are expected when allowing a higher deviation from the set point.

The sensors that have been chosen are based on a temperature dependent current source for the temperature measurements. A temperature corrected solar cell was used as radiation sensor, because it had the best relation of price and precision from the sensors available on the market. The price of this sensor is considerably lower than the price of a pyranometer, but still relatively

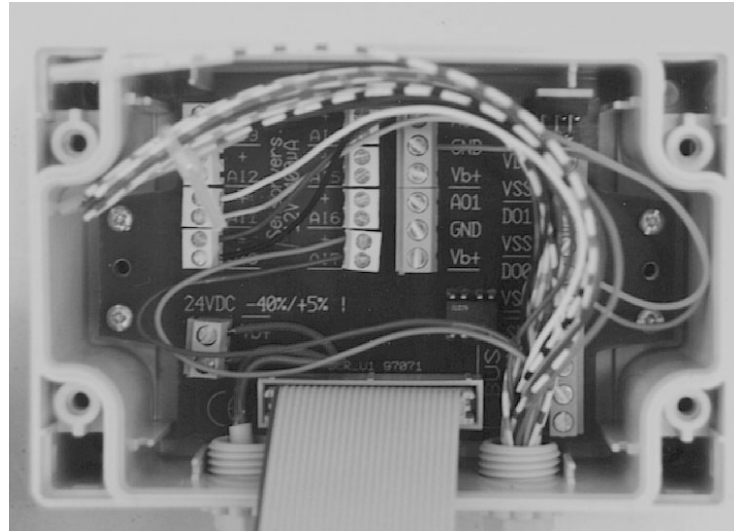


Figure 9.4. Sensor connection board of the standalone device

high in comparison to the total cost of the device. Since the controller device can accept many types of sensors, the effort was not put on searching the best sensor in the frame of the project. In case a better sensor will be available on the market, it can easily be integrated.

The hardware device can be coupled with a PC for a monitoring during the tests. Furthermore it is possible to change additional parameters during the tests. In case of a voltage cut-off a part of the controller's memory will be automatically rebuilt at restart. So, long adaptation phases can be avoided after any interrupt of the operation. For an adequate organisation of the available memory for the control program a survey has been done among the developing institutes. The survey concerned for example the length of the code and the number of variables or the necessary precision for measured values. The optimisation of the memory organisation concerns the size of the memory for code, variables, etc. to achieve the best computing power while keeping the restrictions of precision.

The device was already on the market for a conventional control. Therefore a software developed by the Brauns Control GmbH could be used to manage input and output data handling, computing and user communication. The calculation supply temperature via a heating curve has been replaced by the calculation of the optimal supply temperature with the algorithm developed by ISFH. However a number of adaptations were necessary to implement the relatively large code of the smart control:

- The memory model "large", which was used in the conventional controller of the Brauns Control GmbH was not sufficient to include the program modules using intensively mathematic floating point routines. Therefore it was necessary to select another suitable memory model. The complete code was transferred to the memory model "banked".
- The run time environment of the memory model "banked" contains a crucial software error in the floating point routines. This was found during the debugging of the code. The error leads to an underflow of very small negative numbers in the exponent in following multiplications. This has the consequence that the computer calculates with very large numbers instead of very small numbers (near zero). This error was discovered during the transfer of the developed code into the microcontroller. It aggravated the transfer considerably. The problem was caused by the producer of the microchip and the development environment and was difficult

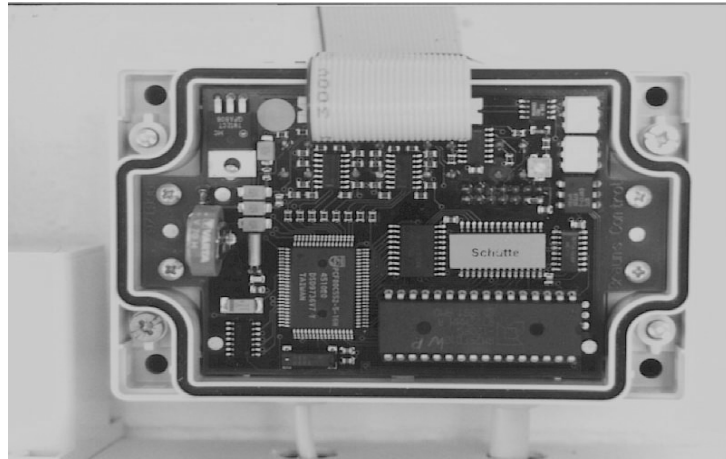


Figure 9.5. Computer board of the standalone device

to solve since they usually do not provide source code.

The Brauns Control GmbH supported ISFH during installation of the hardware and configuration of the software. Problems with imprecise measurements could be solved via an improved ground connection. The program of Brauns Control GmbH for the general process management has been optimized concerning calculation time. So, the calculation time of the smart algorithm in the first version for the microcontroller is about 50 s, and sufficient short already to run the control. The Brauns Control GmbH established proposals for a further optimisation especially of the matrix operation. It is expected, that with these optimisation in the framework of a series production the calculation time can be reduced again to 25%.

The planned procedure of implementing the smart controller code (sending the code by e-mail through the developing institutes, implementation at Brauns Control GmbH and sending the burned Flash memory per mail to the testing institutes) could not be realised. Due to the hidden errors in the run-time environment, it was necessary to debug the code in common sessions with the developer at the company Brauns Control GmbH. Therefore, only the ISFH algorithm could be implemented.

9.3 Market analysis performed by INGA

INGA carried out a market analysis to

- evaluate hardware components for the future prototype,
- check for other controllers using a weather forecast
- check for requirements to the hardware of future partners for a marketing

The evaluation of the market for suitable hardware components was carried out in the early stage of the project. Hardware components have been searched for as single components or as complete solutions. Some microchips which are mass products for cars or domestic appliances have

been checked. The investigation of available hardware was also important to define the limits of ressources for the programmers of the algorithm.

The market analysis for other controllers using a weather forecast gave the result that no other comparable controllers especially for the single family house application are available on the market yet.

Possible future partners for a common marketing have been looked for already. Contacts have been established to companies of the control branche as well as of industry for heating supply devices. The goal was, to know as early as possible the conditions for the marketing from the partner and the conditions of application in combination with another product. The results of this analysis was reflected in the specifications and their improvements.

A main experience was that the additional costs compared to the saved costs are the most important factor for marketing partners. In the hardware used, the radiation sensor causes the most additional costs for a single family house application. Further activities to reduce the hardware cost must therefore focus on the radiation sensor costs first. For big buildings and housing schemes, the additional cost for the radiation sensor and an external weather forecasting service are not important compared to the energy costs that can be saved and the total hardware costs.

The discussions with the possible marketing partners showed further, that a comfort improvement is difficult to "sell", and needs a special marketing strategy. Advantage for comfort are most aware to marketing partners in case of a floor heating system.

The market analysis was concentrated on the german market, because first marketing of the controller will take place there.

9.4 Other activities of INGA

Other activities of INGA in the framework of the project were:

- database and literature enquiries about possibilities of obtaining actual local weather data and the state of the art of control techniques for passive solar houses,
- investigation on the necessary interface of the controller to the other components of a home-automation system,
- investigations on patentability and similar products.

The enquiries about access to actual local weather data showed that there are in Germany 2 suppliers which are able to deliver the data in machine readable code. However, the time resolution is not very high. The German meteorological service (Deutscher Wetterdienst) offers 3 h interval forecasts with a local resolution of $10 \times 10 \text{ km}^2$. The solar radiation is forecasted only with a verbal description of the clouds degree in 4 levels (overcast, cloudy, lightly cloudy, sunny). A quantification of the expected insolation with this informations must remain very imprecise. The costs for the internet connection arising at present moreover are still relatively high in comparison with the savings to heating cost (114 Euro/month). It can however be expected, that better and cheaper services will be available in the near future.

The test of patentability showed that there are no relevant patents in Germany yet, however a mathematical procedure is not patentable. Any copyrights could be strived for for the software and the standalone hardware. A patent for a similar hard- and software exists in Switzerland. The device is available on the market for about 1500 Euro. Such price is regarded as too high for a single family house application.

INGA will continue establishing contacts with companies producing control devices and producers of heating systems to use their marketing structure for selling the soft- and hardware. A demonstration object is planned within the framework of the EXPO 2000, (Solar village near Hameln).

Bibliography

[ABVB99] Argiriou A., I. Bellas-Velidis, and C. Balaras. Development of a neural network heating controller for solar buildings (submitted). *Neural Networks*, 1999.

[ALK⁺99] A. Argiriou, S. Lykoudis, S. Kontoyannidis, C. Balaras, D. Asimakopoulos, M. Petrakis, and P. Kassomenos. Comparison of methodologies for try generation using 20 years data for athens greece. *Solar Energy*, 66:33–45, 1999.

[BVABK98] I. Bellas-Velidis, A. Argiriou, C. Balaras, and S. Kontoyanidis. Predicting energy demand of single solar houses using artificial neural networks. In *Proceedings of the 6th European Congress on Intelligent Technologies & Soft Computing EUFIT'98, Aachen, Germany*, volume 2, pages 873–877, September 7-10 1998.

[CGHC97] Daniel S. Clouse, C. Lee Giles, Bill G. Horne, and Garrison.W. Cottrell. Time-delay neural networks: Representation and induction of finite-state machines. *Transactions on neural networks*, 8(5):1065–1070, September 1997.

[Che97] Tsuhan (editor) Chen. The past, present, and future of neural networks for signal processing. *IEEE Signal Processing Magazine*, pages 28–48, 1997.

[CKB93] Peter S. Curtiss, Jan F. Kreider, and Michael J. Brandemuehl. Adaptive control of hvac processes using predictive neural networks. *ASHRAE Transactions*, 99(1):496–504, 1993.

[Cla94] D. Clarke. *Advances in Model-Based Predictive Control*. Oxford University Press, Oxford, 1994.

[CU93] A. Cihocki and R. Unbehauen. *Neural Networks for Optimization and Signal Processing*. John Wiley & Sons Ltd., New York, 1993.

[Fan72] P.O. Fanger. Thermal comfort analysis and application in environmental design, 1972. Mac Graw Hill.

[GG98] P.-Y. Glorennec and A. Gauthreau. Prévisions d'ensoleillement. In *Actes des journées LFA '98, Rennes, France*, November 1998.

[Glo98] P.-Y. Glorennec. Fuzzy modeling of building. In *Proceedings of the 6th European Congress on Intelligent Technologies & Soft Computing EUFIT'98, Aachen, Germany*, volume 2, pages 901–904, September 7-10 1998.

[Glo99a] P.-Y. Glorennec. *Algorithmes d'apprentissage pour systèmes d'inférence floue*. Ed. Hermès, 1999.

[Glo99b] P.-Y. Glorennec. A fuzzy wiener model. In *Proceedings of IAR Workshop on Intelligent Techniques for Information Processing, Nancy, France*, December 1999.

[Glo99c] P.-Y. Glorennec. Smart control of solar building: Insa progress report. Ec project periodic progress report, Institut National des Sciences Appliquées, Avenue des Buttes de Coësmes, January 1999.

[GMF] D. Groleau, C. Marenne, and F. Fragnaud. Simula, an unsteady-state thermal simulation tool applied to multi-zone buildings. Internal Report, Dec. 1999.

[Gra96] A. Grace. *Optimisation toolbox for use with MATLAB 5*. The MathWorks Inc., 24 Prime Park Way, Natick, MA 01760, Jun 1996.

[HSZG92] Kenneth. J. Hunt, Daniel Sbarbaro, Rafal Zbikowski, and Peter J. Gawthrop. Neural networks for control systems - a survey. *Automatica*, 28(6):1083–1112, 1992.

[HGXW⁺97] Yingduo Han, Lincheng Xiu, Zhonghong Wang, Qi Chen, and Shaohua Tan. Artificial neural networks controlled fast valving in a power generation plant. *IEEE Transactions on Neural Networks*, 8(2):373–389, 1997.

[IEA88] IEA. Building and community systems (bcs) programme, annex 10, system simulation. Technical report, International Energy Agency, <http://www.ecbcs.org/annex10.html>, 1988.

[Inc97] The MathWorks Inc. *Simulink 3.0*. The MathWorks Inc., 24 Prime Park Way, Natick, MA 01760, 1997.

[Jag] R. Jager. Rice: Routines for Implementation of C Expert systems. TNO Building and Construction Research, 1992.

[KA98a] S.A. Klein and F.L. Alvarado. *Engineering Equations Solver (EES) user's manual. F. chart software*. Madison, 1998.

[KA98b] M. Kummert and Ph. André. Proposal for a cost function to compare different controllers performance. Working document no. ful/980422/01, Fondation Universitaire Luxembourgeoise (FUL), 185, Avenue de Longwy, B-6700 Arlon, Belgium, April 1998.

[KA98c] M. Kummert and Ph. André. Software communication problems. example of trnsys and matlab. Working document no. ful/980430/01, Fondation Universitaire Luxembourgeoise (FUL), 185, Avenue de Longwy, B-6700 Arlon, Belgium, April 1998.

[KAGN98] M. Kummert, Ph. André, J. Guiot, and J. Nicolas. Short term weather forecasting for solar buildings optimal control: an application of neural network. In *Proceedings of the 6th European Congress on Intelligent Technologies & Soft Computing EUFIT'98, Aachen, Germany*, volume 2, pages 868–872, September 7-10 1998.

[KAN96] M. Kummert, Ph. André, and J. Nicolas. Development of simplified models for solar optimal building control. In *Eurosun'96 Freiburg, Germany*, 1996.

[KAN97] M. Kummert, Ph. André, and J. Nicolas. Optimal thermal zone controller for integration within a building energy management system. In *CLIMA'2000, Brussels*, 1997.

[KAN98] M. Kummert, Ph. André, and J. Nicolas. Heating optimal control applied to a passive solar commercial building. In *Proceedings EuroSun, Portoroz, Slovenia*, 1998.

[KAN99] M. Kummert, Ph. André, and J. Nicolas. Building and hvac optimal control simulation. application to an office building. In *Proceedings ISHVAC'99, Shenzhen, China*, 1999.

[KARL⁺97] Alireza Khotanzad, Reza Afkhami-Rohani, Tsun-Liang Lu, Alireza Abaye, Malcolm Davis, and Dominic J. Maratukulam. Anntslf—a neural-network-based electric load forecasting system. *IEEE Transactions on Neural Networks*, 8(4):835–846, 1997.

[KB⁺94] S. A. Klein, W. A. Beckman, et al. *TRNSYS, A transient system simulation program*. Solar Energy Laboratory, University of Wisconsin, Madison, WI 53706 USA, January 1994.

[Kre95] Jan F. Kreider. Neural networks applied to building energy. studies tutorial. In *Workshop on Parameters Identification*, pages 243–251. JRC Ispra., Bloem H., 1995.

[Kum99] M. Kummert. Description of the shell proposed for controllers exchange. Working document of ful, Fondation Universitaire Luxembourgeoise (FUL), 185, Avenue de Longwy, B-6700 Arlon, Belgium, 1999.

[L⁺94] K.J. Lomas et al. Empirical validation of thermal building simulation programs using test room data. Iea task 12 & annex 21 final report, International Energy Agency, 1994.

[Lju95] Lennart Ljung. *MATLAB System identification toolbox User's Guide*. The MathWorks Inc., 24 Prime Park Way, Natick, MA 01760, August 1995.

[Mas93] Timothy Masters. *Practical Neural Networks Recipes in C++*. Academic Press Inc., London, 1993.

[Mat96] The MathWorks Inc., 24 Prime Park Way, Natick, MA 01760. *MATLAB 5.2 Users guide*, Jun 1996.

[MH95] H. Madsen and J. Holst. Estimation of continuous-time models for the heat dynamics of a building. *Energy & Buildings*, 22:67–79, 1995.

[MR95] M. Morari and N. L. Ricker. *Model Predictive Control Toolbox for Use with MATLAB*. The MathWorks Inc., 24 Prime Park Way, Natick, MA 01760, April 1995.

[MZT96] P.M. Mills, A.Y. Zomaya, and M.O. Tade. *Neuro-adaptive Process Control. A Practical Approach*. John Wiley & Sons Ltd., New York, 1996.

[NF90] A. M. Nygård Ferguson. *Predictive thermal control of building systems, These No. 876*. PhD thesis, Ecole Polytechnique Federale de Lausanne, 1990.

[NI91] M. McCord Nelson and W.T. Illingworth. *A Practical Guide to Neural Nets*. Addison-Wesley, Reading, Massachusetts, 1991.

[RKE] Raab, Karcher, and Energieservice. sensonic. Herstellerprospekt.

[SAH89] J.E. Seem, P.R. Armstrong, and C.E. Hancock. Algorithms for predicting recovery time from night set-back. *ASHRAE Transactions*, 95(2):439–446, 1989.

[SC98] U. Schramm and D. Christoffers. New approaches in smart solar building control—a joint ec project. In *Proceedings of the 6th European Congress on Intelligent Technologies & Soft Computing EUFIT'98, Aachen, Germany*, volume 2, pages 860–862, September 7-10 1998.

[Sta95] Holger Stadtmann. Entwicklung einer vorausschauenden Verschattungsregelung für eine transparnt gedämmte Solarwand. Master's thesis, Technische Universität Braunschweig, Braunschweig, Oktober 1995.

[TC00a] U. Thron and D. Christoffers. Intelligente heizungsregelung f r solarh user, entwicklung test und implementierung in einen microcontroller. In *Internationales Sonnenforum 2000, Freiburg, Germany*, page to be published, July 6-7 2000.

[TC00b] U. Thron and D. Christoffers. Vorausschauende und selbstadaptierende heizungsregelung f r solarh user. In *10. Symposium Thermische Solarenergie, Kloster Banz*, page to be published, Mai 10-12 2000.

[VW94] Luk Vandaele and Peter Wouters. The passys services, eur 15113 en. Technical report, European Commission, DG XII, Brussels, 1994.

[WDC98] I.R. Williamson, S. Danaher, and C. Craggs. Optimisation of solar building control using predictive methodologies. In *Proceedings of the 6th European Congress on Intelligent Technologies & Soft Computing EUFIT'98, Aachen, Germany*, volume 2, pages 878–879, September 7-10 1998.

[Yal97] Karla Yale. Preparing the right data diet for training neural networks. *IEEE Spectrum*, pages 64–66, 1997.

[Z⁺96] A. Zell et al. *SNNS Stuttgart Neural Network Simulator, User Manual, Version 4.1*. SNNS Group, Institute for Parallel and Distributed High-Performance Systems, University of Stuttgart, Stuttgart, Germany, 1996.

Chapter 10

Comparison of initially planned objectives and work actually accomplished

The defined objectives to be achieved by the consortium during the project are listed in table 10.1:

Table 10.1. Achieved and stated objectives. Explanation for Status: **A**: achieved objective, **P**: partly achieved objective, **N**: not achieved objective

Task No.	Type	Description	Partner	Status
1	Preparation	Details fixed for effective cooperation	all	A
2	Software	Predictive adaptive control algorithm	ISFH	A
2	Software	Predictive optimal control algorithm	FUL	A
2	Software	Art. Neural Networks control algorithm	NOA	A
2	Software	Fuzzy logic Control algorithm	INSA	A
2	Software	Numerical environment for test	UNN, FUL	A
2	Hardware	Review of algorithms, first hardware choice	INGA	A
4	Hardware	Realisation of first stand-alone prototype	INGA	A
3, 5	Test results	Results of tests of algorithms in numerical simulation	UNN, FUL	P
3, 5	Test results	Experimental test results for algorithms in test cell	NOA	P
3, 5	Test results	Experimental test results for optimized algorithms in test building	ISFH	P
3, 5	Test results	Experimental test results for optimized algorithms in test building	FUL	P
3, 5	Test results	Experimental test results for optimized algorithms in test building	INSA	P
5	Test results	Experimental test results with microcontroller in test building	ISFH	A
6	Hardware	Realisation of final prototype	INGA	A

The specifications of Task 1 were made to create the basis for and exchange of controllers among the testing institutes and for an implementation into the final hardware. These specifications concerned the programming language, the requirements on additional hard- and software, the inputs and outputs of the controller.

Each of the developing institutes (ISFH, FUL, INSA, NOA) developed successfully a smart controller with the approaches mentioned in table 10.1. The algorithms showed considerable advantages compared to a conventional control in simulation and experiment. During the tests, all algorithms have been optimized by each partner.

A numerical environment for simulation tests has been successfully established by UNN and FUL. This tool has been extensively used by FUL and ISFH to optimize their controller before the implementation into a real occupied building. An optimizd version of the tool served for the comparison of different controllers in simulation.

The results of tests of algorithms in numerical simulation are only partly available due to several reasons:

- Delay in the development of the simulation environment
- Final controllers to be tested have been delivered with a delay
- INSA controller was not compatible with the simulation environment
- Due to severe adaptation problems, simulations could only be carried out with one set of weather data and one building model

The controllers have been successfully tested in the experimental facilities of the developing institutes. The exchange of controllers for an experimental testing was succesful in the case of the FUL controller, which was tested in the NOA PASSYS test cell. An experimental test for other controllers and other buildings could not be carried out due to the following reasons:

- severe adaptation problems with available hard- and software a the test sites
- special hardware in the NOA test site (no hydronic heating system) which required adaptation of algorithms
- for ISFH building it was found to be necessary to test both the same algorithm running on a PC and on the microcontroller to evaluate any quality differences coming from the hardware, therefore this building could not be used to test controllers from other partners
- necessary time consuming pre-training of some algorithms to match the building behaviour

In general, the time and effort necessary to adapt different controllers to the different hard- and software was underestimated at the beginning of the project. Although clear specifications concerning the exchange have been established and updated this could not prevent a number of adaptation problems arising from:

- differences in C-compilers leading to problems in memory allocation
- MATLAB use not practical for all algorithms
- pre-training necessary for some algorithms before they can be applied to a building.

The implementation of the ISFH algorithm into a microcontroller was successfully carried out but it was also more time consuming as expected. The reason was an error in the microcontroller development tool which occured only for the chosen memory model. The debugging required a close cooperation between the developer of the code and the industrial partner. The Microcontroller showed its ability to take over the control task in almost the same quality as the PC. Results and experiences with tests have been reported to the industrial partner to create the optimized final hardware.

Chapter 11

Conclusions

The report on hand presents the work carried out in the frame of the project "Development and Test of Modern Control Techniques Applied to Solar Buildings" funded by the European Commission. The aim was the development of algorithms for intelligent heating control in buildings with high solar gains. Four algorithms using different approaches have been developed by the partners FUL, INSA, NOA and ISFH. They have been investigated in a simulation environment and test buildings. Partner UNN was responsible for the comparative evaluation of the algorithms with the help of simulation tests. A special simulation environment has been developed by partner FUL and UNN in the frame of this project. Experimental tests have been carried out by the developing institutes each providing a test building. The buildings differ with regard to their use, climatic conditions and thermal properties.

The tests showed that all approaches are suitable in principle for an intelligent heating control leading to energy savings of up to 15% in the in-between season and comfort improvements compared to conventional controls. The investigations showed further, that an evaluation only on the basis of energy consumption and a comfort indicator is not sufficient to reflect the different properties necessary also for practical application. Table 11.1 gives an overview over the most important properties of the developed algorithms.

The energy and comfort evaluation can be directly compared for the controllers of FUL, NOA and ISFH. For the simulation test on the FUL building model, the FUL controller showed the best performance concerning these criteria. For the response to the desired comfort level, again, FUL controller shows the best performance. Due to the considerable effort necessary for training, the comfort level feature has not been implemented in the ANN controller, however the use of heating schedules allows to achieve a similar behaviour.

ISFH and INSA controller require the lowest computational load. The NOA controller also has a low demand for the current version, but it increases when the online- training and optimisation is included.

The adaptation to different buildings is best possible with the ISFH algorithm. The other algorithms require a pre-training before the application to a building, either on the basis of measured data or of information about the building structure. Adaptation to building changes is possible for the NOA and the ISFH controller.

Table 11.1. Summary of the advantages/ disadvantages of different advanced controllers. The energy/ comfort performance is based on the simulation test on FUL building only.

	Optimal (FUL)	ANN (NOA)	Predictive (ISFH)	Fuzzy (INSA)
Energy/ comfort performance	Best performance of the simulation test on FUL building	Improved performance compared to conventional	Good performance although stronger anticipation could improve it	Good performance tested on INSA building
Response to desired comfort level CL	CL reflects the relative importance of comfort and energy	Not implemented	Different behaviour for low and high CL values	Implemented
Computational load	High computing power and considerable memory requirements	Low requirements for current version. Full version including online training and optimisation would have higher requirements	Low requirements for developed C code	Low requirement
Adaptation to different buildings	Adaptation is possible but requires expert knowledge	ANN must be trained for the building and meteo conditions	A model identification start "from nothing" is possible	Requires pre-training with measured building data or information about building structure
Adaptation to building changes	Online identification in a restricted range	Inherent advantage of ANN	Online identification with decreasing weighting of older measurements	Pre-identification necessary
Implemented into a Intel51 microcontroller	Current implementation proved to be too complex. Best adapted to PC-like controllers	Re-coding work was not totally achieved but the current version is suitable for this implementation	Successfully implemented	Successfully implemented

The ISFH and the INSA algorithm both have been successfully implemented into a Intel 51 series microcontroller. The NOA algorithm needs to be re-coded to match memory and calculation power of a microcontroller but is suitable in principle. The current FUL controller implementation is best adapted to PC-like controllers. The ISFH algorithm was chosen for an implementation into the final hardware because it combines high control quality with the lowest computing requirements. The final hardware which was provided by the industrial partner INGA is a microcontroller which works as a stand-alone device.

Experimental tests on a real building showed that the newly developed PC controllers as well as the smart microcontroller met the high expectations formulated in the project programme. The hardware is now available for demonstration objects.

Appendix A

List of outcomes of the project

A.1 Publications and conference presentations

Argiriou A., I. Bellas-Velidis, and C. Balaras.

Development of a neural network heating controller for solar buildings (submitted). *Neural Networks*, 1999.

A. Argiriou, S. Lykoudis, S. Kontoyannidis, C. Balaras, D. Asimakopoulos, M. Petrakis, and P. Kas-somenos.

Comparison of methodologies for try generation using 20 years data for athens greece. *Solar Energy*, 66:33–45, 1999.

I. Bellas-Velidis, A. Argiriou, C. Balaras, and S. Kontoyanidis.

Predicting energy demand of single solar houses using artificial neural networks. In *Proceedings of the 6th European Congress on Intelligent Technologies & Soft Computing EUFIT'98, Aachen, Germany*, volume 2, pages 873–877, September 7-10 1998.

P.-Y. Glorennec and A. Gauthreau.

Prévisions d'ensoleillement. In *Actes des journées LFA '98, Rennes, France*, November 1998.

P.-Y. Glorennec.

Fuzzy modeling of building. In *Proceedings of the 6th European Congress on Intelligent Technologies & Soft Computing EUFIT'98, Aachen, Germany*, volume 2, pages 901–904, September 7-10 1998.

P.-Y. Glorennec.

A fuzzy wiener model. In *Proceedings of IAR Workshop on Intelligent Techniques for Information Processing, Nancy, France*, December 1999.

M. Kummert, Ph. André, J. Guiot, and J. Nicolas.

Short term weather forecasting for solar buildings optimal control: an application of neural network. In *Proceedings of the 6th European Congress on Intelligent Technologies & Soft Computing EUFIT'98, Aachen, Germany*, volume 2, pages 868–872, September 7-10 1998.

M. Kummert, Ph. André, and J. Nicolas.

Heating optimal control applied to a passive solar commercial building. In *Proceedings EuroSun, Portoroz, Slovenia*, 1998.

M. Kummert, Ph. André, and J. Nicolas.

Building and hvac optimal control simulation. application to an office building. In *Proceedings*

ISHVAC'99, Shenzhen, China, 1999.

U. Schramm and D. Christoffers.

New approaches in smart solar building control- a joint ec project. In *Proceedings of the 6th European Congress on Intelligent Technologies & Soft Computing EUFIT'98, Aachen, Germany*, volume 2, pages 860–862, September 7-10 1998.

U. Thron and D. Christoffers. Intelligente Heizungsregelung für Solarhäuser, Entwicklung, Test und Implementierung in einen Microcontroller. In *Internationales Sonnenforum 2000, Freiburg, Germany*, to be published, July 6-7 2000.

U. Thron and D. Christoffers.

Vorausschauende und Selbstadaptierende Heizungsregelung für Solarhäuser. In *10. Symposium Thermische Solarenergie, Kloster Banz*, to be published, Mai 10-12 2000.

I.R. Williamson, S. Danaher, and C. Craggs.

Optimisation of solar building control using predictive methodologies. In *Proceedings of the 6th European Congress on Intelligent Technologies & Soft Computing EUFIT'98, Aachen, Germany*, volume 2, pages 878–879, September 7-10 1998.

A.2 Internal Working Documents

M. Kummert and Ph. André.

Proposal for a cost function to compare different controllers performance. Working document no. ful/980422/01, Fondation Universitaire Luxembourgeoise (FUL), 185, Avenue de Longwy, B-6700 Arlon, Belgium, April 1998.

M. Kummert and Ph. André.

Software communication problems. example of trnsys and matlab. Working document no. ful/980430/01, Fondation Universitaire Luxembourgeoise (FUL), 185, Avenue de Longwy, B-6700 Arlon, Belgium, April 1998.

M. Kummert.

Description of the shell proposed for controllers exchange. Working document of ful, Fondation Universitaire Luxembourgeoise (FUL), 185, Avenue de Longwy, B-6700 Arlon, Belgium, 1999.

A.3 Doctoral thesis

The use of results of the project in a doctoral thesis is foreseen at partner FUL, UNN and ISFH.

A.4 Prototypes

A prototype of the final hardware has been created and is now ready for demonstration (see chapter 9).